

Towards New Thickeners Based on Inter-Polyelectrolyte Complexes

zur Erlangung des akademischen Grades eines
DOKTORS DER INGENIEURWISSENSCHAFTEN (Dr.-Ing.)

der Fakultät für Chemieingenieurwesen und Verfahrenstechnik der
Universität Fridericiana Karlsruhe (TH)

genehmigte
DISSERTATION

von
Msc. Yves Matter
aus Strasbourg, Frankreich

Referent: Prof. Dr. Norbert Willenbacher

Korreferent: Prof. Dr. Manfred Wilhelm

Tag der mündlichen Prüfung: 9. Juni 2009

INTRODUCTION	1
1. STATE OF THE ART	5
1.1. FREE RADICAL POLYMERIZATION	5
1.1.1 FREE RADICAL HOMOPOLYMERIZATION	5
1.1.2. FREE RADICAL COPOLYMERIZATION	6
1.1.3. FREE RADICAL TEMPLATE POLYMERIZATION	8
1.1.3.1. Mechanism	8
1.1.3.2. Influence of the template	9
1.2. POLYELECTROLYTES	10
1.2.1. CLASSIFICATION OF POLYELECTROLYTES	10
1.2.1.1. Positively and negatively charged polyelectrolytes	10
1.2.1.2. Weak and strong polyelectrolytes	11
1.2.1.3. Integral and pendant type	11
1.2.2. ORIGIN OF POLYELECTROLYTES	13
1.2.2.1. Polyelectrolytes in nature	13
1.2.2.2. Synthetic polyelectrolytes	15
1.3. ELECTROLYTES IN SOLUTION	16
1.3.1. BJERRUM LENGTH	16
1.3.2. DEBYE-HÜCKEL'S LAW	16
1.3.3. MANNING'S CONDENSATION	18
1.4. POLYELECTROLYTES BASED COMPLEXES	19
1.4.1. POLYELECTROLYTES AND SURFACTANTS	19
1.4.2. POLYELECTROLYTES AND CHARGED SURFACE	20
1.4.3. POLYELECTROLYTES AND DNA	22
1.4.4. OPPOSITELY CHARGED POLYELECTROLYTES	23
1.4.4.1. Formation of a complex	23
1.5. POLYMERIC NETWORKS	28
1.5.1. GELATION IN BIOPOLYMERS	29
1.5.2. GELATION IN HYDROPHOBICALLY MODIFIED POLYMERS	30
1.5.2.1. Hydrophobically modified cellulose	30
1.5.2.2. Hydrophobically modified alkali-soluble emulsion	31
1.5.2.3. Hydrophobically modified ethoxylated urethanes	33
1.5.3. GELATION IN POLYELECTROLYTES	34
1.5.3.1. Diblock polyelectrolytes	34
1.5.3.2. Triblock polyelectrolytes	34
1.5.3.3. Polyelectrolyte complexes	35
2. IN-SITU PREPARATION OF COLLOIDAL INTER-POLYELECTROLYTE COMPLEXES	38
2.1. INTRODUCTION	38
2.1.1. MOTIVATION	38
2.1.2. POTENTIAL MECHANISM OF FORMATION OF STABLE DISPERSIONS	39
2.1.3. EXPERIMENTAL CONDITIONS	40
2.1.3.1. Materials	41
2.1.3.2. Processing parameters	42
2.2. POLYMERIZATION	43
2.2.1. MATERIALS	43
2.2.2. EXPERIMENTAL PART	44
2.2.2.1 Synthesis of P(AETAC _{0.43} -co- Acrylamide _{0.57})	44
2.2.2.2. Synthesis of P(AETAC _{0.25} -co- Acrylamide _{0.75})	47
2.2.2.3. Synthesis of P(AETAC _{0.33} -co- Acrylamide _{0.67})	48

2.2.3. CONVERSION AND SIDE PRODUCTS	50
2.3. COMPLEXATION	53
2.3.1. POLY(ACRYLIC ACID) AS COMPLEXING AGENT	53
2.3.1.1. Synthetic work	53
2.3.1.2. Characterization by NMR	55
2.3.1.3. Characterization by cryo-TEM	57
2.3.2. PAMPS AS COMPLEXING AGENT	59
2.3.2.1. Synthetic work	59
2.3.2.2. Characterization by NMR	60
2.3.3. P(AA-CO-AMPS) AS COMPLEXING AGENT	61
2.3.3.1. Synthetic work	61
2.3.3.2. Characterization by NMR	62
2.3.3.3. Characterization by cryo-TEM	63
2.3.4. MOLAR MASS OF THE POLYMERS	64
2.3.5. DISCUSSION OF THE STABILITY OF THE DISPERSIONS	65
2.4. CONCLUSION	67
2.5. PERSPECTIVES	68
<u>3. RHEOLOGICAL PROPERTIES OF MIXTURES OF POSITIVELY CHARGED POLYELECTROLYTES WITH POLY(ACRYLIC ACID)</u>	<u>69</u>
3.1. INTRODUCTION	69
3.2. EXPERIMENTAL	70
3.2.1. MATERIALS	70
3.2.1.1. Polyanions	70
3.2.1.2. Polycation	71
3.2.2. METHODS	71
3.2.2.1. Sample Preparation	71
3.2.2.2. Measurements	72
3.3. RESULTS AND DISCUSSION	73
3.3.1. RHEOLOGY OF PURE POLYANIONS	73
3.3.2. RHEOLOGY OF MIXTURES OF PAA AND POLYCATION DEPENDING ON MIXING RATIO	77
3.3.2.1. Permanent polycation	77
3.3.2.2. Non permanent polycation	79
3.3.3. RHEOLOGY OF MIXTURES OF PAA AND P(VP-VI)	81
3.3.3.1. Mixtures at an overall concentration of 2wt%	81
3.3.3.2. Mixtures at an overall concentration of 1wt%	83
3.3.3.3. Mixtures at an overall concentration of 0.5wt%	85
3.3.3.4. Summary	87
3.3.4. INFLUENCE OF THE MOLAR MASS OF POLY(ACRYLIC ACID)	89
3.3.4.1. Mixtures of P(VP-VI) with PAA250	89
3.3.4.2. Mixtures of P(VP-VI) with PAA900	89
3.3.4.3. Mixtures of P(VP-VI) with PAA3300	93
3.4. CONCLUSION	96
<u>4. INFLUENCE OF THE NATURE OF THE NEGATIVE CHARGE</u>	<u>99</u>
4.1. INTRODUCTION	99
4.2. EXPERIMENTAL	100
4.2.1. MATERIALS AND METHODS	100
4.2.1.1. Polyanions	100
4.2.1.2. Polycation	100
4.2.1.3. Sample preparation	100
4.3. RESULTS AND DISCUSSIONS	101

4.3.1. RHEOLOGY OF PURE POLYANIONS	101
4.3.2. RHEOLOGY OF MIXTURES	103
4.3.2.1. P(AA _{0.8} -AMPS _{0.2}) + P(VP-VI)	103
4.3.2.2. P(AA _{0.6} -AMPS _{0.4}) + P(VP-VI)	106
4.3.3. THICKENING EFFICIENCY OF PAA, P(AA _{0.8} -AMPS _{0.2}) AND P(AA _{0.6} -AMPS _{0.4})	108
4.4. CONCLUSION	110
<hr/>	
5. BEHAVIOR OF MIXTURES OF OPPOSITELY CHARGED POLYELECTROLYTES UNDER EXTENSIONAL FLOW	112
<hr/>	
5.1. INTRODUCTION	112
5.2. EXTENSIONAL RHEOLOGY OF PURE POLYANIONS	114
5.2.1. POLY(ACRYLIC ACID)	114
5.2.2. POLY(ACRYLIC ACID-CO-2-ACRYLAMIDO-2-METHYL-1-PROPANESULFONIC ACID)	118
5.2.3. EXTENSIONAL RELAXATION TIMES OF PURE POLYANIONS	120
5.3 EXTENSIONAL RHEOLOGY OF MIXTURES OF POLYANIONS WITH P(VP-VI)	121
5.3.1. REPRODUCIBILITY OF THE MEASUREMENTS	121
5.3.2. POLY(ACRYLIC ACID) + P(VP-VI)	124
5.3.3. P(AA-CO-AMPS) + P(VP-VI)	129
5.3.4. EXTENSIONAL RELAXATION TIMES OF MIXTURES POLYANIONS+P(VP-VI)	135
5.4. CONCLUSION	137
<hr/>	
6. ORIGIN OF THE THICKENING MECHANISM	139
<hr/>	
6.1. INTRODUCTION	139
6.2. MICROSTRUCTURE OF MIXTURES OF POLYANIONS WITH P(VP-VI)	140
6.2.1. SHEAR VERSUS EXTENSIONAL RHEOLOGY OF PURE POLYANIONS	140
6.2.2. SHEAR VERSUS EXTENSIONAL RHEOLOGY OF MIXTURES OF POLYANIONS WITH P(VP-VI)	141
6.2.2.1. Mixtures at pH=7 and pH=8	141
6.2.2.2. Mixtures at pH=5.5 and pH=6	143
6.2.2.3. Possible microstructure of mixtures of polyanions with P(VP-VI)	144
6.3. ORIGIN OF COOPERATIVE INTERACTIONS	147
6.3.1. INTRODUCTION	147
6.3.2. RHEOLOGICAL BEHAVIOR OF MIXTURES POLYANIONS + PVP	148
6.3.3. BALANCE BETWEEN POSITIVE AND NEGATIVE CHARGES	150
6.4. CONCLUSION	153
6.5. PERSPECTIVES	154
<hr/>	
SUMMARY	157
<hr/>	
EXPERIMENTAL PART	161
<hr/>	
REFERENCES	168
<hr/>	
ACKNOWLEDGMENTS	176
<hr/>	

List of figures

Chapter 1

Figure 1-1: mechanism of free radical polymerization.	5
Figure 1-2: mechanism of initiation in free radical copolymerization.	6
Figure 1-3: mechanism of propagation in free radical copolymerization.	7
Figure 1-4: zip (a) and pick-up (b) mechanisms of template polymerization.	9
Figure 1-5: examples of integral type polyelectrolytes.	12
Figure 1-6: examples of pendant type polyelectrolytes.	12
Figure 1-7: chemical structure of alginate (a.) and hyaluronate (b).	13
Figure 1-8: chemical structure of chitosan.	14
Figure 1-9: compaction mechanism of DNA on histones.	15
Figure 1-10: pearl necklace structure of polyelectrolyte-surfactant complexes.	20
Figure 1-11: flexible (left hand side) or stiff (right hand side) polyelectrolyte-surfactant complexes.	20
Figure 1-12: principle of the layer-by-layer deposition technique.	21
Figure 1-13: rearrangement from “scrambled-egg” (random) to “ladder-type” (ordered) structures.	24
Figure 1-14: core-shell structure obtained by non-stoeichiometric mixing of polyanions with polycations.	26
Figure 1-15: influence of the titrant addition rate on the stability of IPEC.	28
Figure 1- 16: chemical structure of HMC and schematic representation of their gelation mechanism.	31
Figure 1-17: chemical structure of hydrophobically modified alkali-soluble emulsions.	31
Figure 1- 18: schematic representation of the gelation mechanism in HASE.	32
Figure 1-19: schematic representation of the gelation mechanism in HEUR.	33

Chapter 2

Figure 2-1: scheme of the steps leading to the formation of a stable dispersion	39
Figure 2-2: copolymerization pattern of AETAC and AM.	44
Figure 2-3: ¹ H-NMR of acrylamide in D ₂ O.	50
Figure 2- 4: ¹ H-NMR of AETAC in D ₂ O.	50
Figure 2- 5: ¹ H-NMR of S43I01 (a), S33I01 (b) and S25I01 (c) in D ₂ O.	51
Figure 2- 6: ¹ H-NMR of choline chloride in D ₂ O.	52
Figure 2-7: ¹ H-NMR of dispersion D11 in D ₂ O.	56
Figure 2-8: ¹ H-NMR of supernatant of dispersion D18 in D ₂ O.	56
Figure 2-9: cryo-TEM imaging of dispersion D14.	57
Figure 2-10: cryo-TEM imaging of dispersion D19.	58
Figure 2- 11: cryo-TEM imaging of dispersion D110.	58

Figure 2- 12: NMR spectra of dispersions D22, D23, D24 and D25 60
 Figure 2-13: NMR spectra of dispersions D31, D32, D33 and D35 63
 Figure 2-14: cryo-TEM imaging of dispersion D34 64
 Figure 2-15: cryo-TEM imaging of dispersion D42 64
 Figure 2-16: molar mass distribution of dispersions D15, D19, D110, D33, D34 and D42..... 65

Chapter 3

Figure 3-1: storage (full symbols) & loss (open symbols) moduli of PAA1600 at 2wt% (top left), 1wt% (top right), 0.5wt% (bottom left), 0.25wt% (bottom right). 74
 Figure 3-2: complex viscosity vs frequency of PAA1600 at 2wt% depending on pH. 75
 Figure 3-3: zero shear viscosity of PAA1600 as a function of pH and concentration. 76
 Figure 3-4: zero shear viscosity of mixtures of PAA1600 and P(VP_{0.7}-QVI_{0.3}) as a function of mixing ratio at 2wt% and pH=7. 77
 Figure 3-5: complex viscosity (), storage (closed symbols) and loss (open symbols) moduli of one to nine mixtures of PAA1600 with P(VP_{0.7}-QVI_{0.3}). 78
 Figure 3-6: complex viscosity of mixtures of PAA1600 with P(VP-VI) depending on mixing ratio. 80
 Figure 3-7: storage (closed symbols) and loss (open symbols) moduli of mixtures of PAA1600 with P(VP-VI) depending on mixing ratio. 80
 Figure 3-8: complex viscosity vs ω of mixtures of PAA1600 with P(VP-VI) at 2wt% depending on pH. 81
 Figure 3-9: storage (closed symbols) and loss (open symbols) moduli vs ω of mixtures of PAA1600 with P(VP-VI) at 2wt% depending on pH. 82
 Figure 3-10: complex viscosity vs ω of mixtures of PAA1600 with P(VP-VI) at 1wt% depending on pH. 84
 Figure 3-11: storage (closed symbols) and loss (open symbols) moduli vs ω of mixtures of PAA1600 with P(VP-VI) at 1wt% depending on pH. 84
 Figure 3-12: complex viscosity vs ω of mixtures of PAA1600 with P(VP-VI) at 0.5wt% depending on pH. 86
 Figure 3-13: storage (closed symbols) and loss (open symbols) moduli vs ω of mixtures of PAA1600 with P(VP-VI) at 0.5wt% depending on pH. 86
 Figure 3-14: viscosity enhancement for mixtures of PAA1600 with P(VP-VI) depending on concentration and pH. 88
 Figure 3-15: complex viscosity (left column), storage (closed symbols) and loss (open symbols) moduli (right column) vs ω for 1 :1 mixtures of P(VP-VI) + PAA900 at 2wt% (upper row), 1wt% (middle row) and 0.5wt% (lower row) depending on pH. 91
 Figure 3-16: viscosity enhancement for mixtures of PAA900 with P(VP-VI) depending on concentration and pH. 92

Figure 3-17: complex viscosity (left column), storage (closed symbols) and loss (open symbols) moduli (right column) vs ω for 1:1 mixtures of P(VP-VI) + PAA3300 at 2wt% (upper row) and 0.5wt% (lower row) depending on pH.....	94
Figure 3-18: viscosity enhancement for mixtures of PAA3300 with P(VP-VI) depending on concentration and pH.....	95
Figure 3-19: viscosity enhancement for mixtures of PAA with P(VP-VI) depending on concentration and pH.....	96
Figure 3-20: viscosity enhancement for mixtures of PAA and P(VP-VI) at SC=1%, depending on Mw of PAA and pH.....	97
 Chapter 4	
Figure 4-1: frequency dependence of storage (closed symbols) & loss (open symbols) moduli of P(AA _{0.8} -AMPS _{0.2}) (left hand side) and P(AA _{0.6} -AMPS _{0.4}) (right hand side) at 2wt% depending on pH	101
Figure 4-2: $ \eta^* _0$ of P(AA _{0.8} -AMPS _{0.2}) (left hand side) & P(AA _{0.6} -AMPS _{0.4}) (right hand side) depending on concentration and pH.	102
Figure 4-3: $ \eta^* _0$ (left hand side) & dynamic moduli (right hand side) of P(AA _{0.8} -AMPS _{0.2})+P(VP-VI) depending on pH at 2wt% (top row), 1wt% (middle row) and 0.5wt% (bottom row).....	105
Figure 4-4: $ \eta^* _0$ (left hand side) & dynamic moduli (right hand side) of P(AA _{0.6} -AMPS _{0.4})+P(VP-VI) depending on pH at 2wt% (top row), 1wt% (middle row) and 0.5wt% (bottom row).....	107
Figure 4-5: viscosity enhancement for mixtures of PAA, P(AA _{0.8} -AMPS _{0.2}), P(AA _{0.6} -AMPS _{0.4})+P(VP-VI) depending on concentration and pH.	108
Figure 4-6: viscosity enhancement for mixtures of PAA, P(AA _{0.8} -AMPS _{0.2}), P(AA _{0.6} -AMPS _{0.4})+P(VP-VI) depending on concentration and pH.	109
 Chapter 5	
Figure 5-1: brightness profile used for diameter calculation.	113
Figure 5-2: filament decay of PAA1600 at 2wt% pH=7.....	115
Figure 5-3: filament decay of PAA1600 at 2wt% depending on pH.	116
Figure 5-4: time-evolution (rows) of the filament formed by PAA at pH=6, pH=7 and pH=8 (columns).....	117
Figure 5-5: filament decay of P(AA _{0.8} -AMPS _{0.2}) at 2wt% depending on pH.....	118
Figure 5-6: time-evolution of the filament formed by P(AA _{0.8} -AMPS _{0.2}) at pH=6, pH=7 and pH=8.....	119
Figure 5-7: time-evolution of the filament formed by PAA+P(VP-VI) 2wt% pH=7.....	121
Figure 5-8: time-evolution of the filament formed by PAA+P(VP-VI) 2wt% pH=7.....	122
Figure 5-9: time-evolution of the filament formed by PAA+P(VP-VI) 2wt% pH=5.5.....	122

Figure 5-10: time-evolution of the filament formed by PAA+P(VP-VI) 2wt% pH=5.5.	123
Figure 5-11: time-evolution of normalized diameter of PAA+P(VP-VI) depending on pH.....	126
Figure 5-12: time-evolution of mixtures of PAA with P(VP-VI) at 2wt% depending on pH.	127
Figure 5-13: time-evolution of PAA+P(VP-VI) at 1wt%, pH=5.5 and pH=8 (first two columns respectively) and at 0.5wt%, pH=5.5 and pH=8 (third and fourth column respectively).	128
Figure 5-14: time-evolution of normalized diameter of P(AA _{0.8} -co-AMPS _{0.2})(1 st column) and of P(AA _{0.6} -co-AMPS _{0.4})(2d column)+P(VP-VI), a: 2wt% ; b: 1wt% ; c:0.5wt%, depending on pH.	130
Figure 5-15: time-evolution of P(AA _{0.8} -co-AMPS _{0.2})+ P(VP-VI) at 2wt% at depending on pH.	131
Figure 5-16: time-evolution of P(AA _{0.8} -co-AMPS _{0.2})+ P(VP-VI) at 1wt%, pH=5.5 and pH=8 (first two columns respectively) and at 0.5wt%, pH=5.5 and pH=8 (third and fourth column respectively).....	132
Figure 5-17: time-evolution of P(AA _{0.6} -co-AMPS _{0.4})+ P(VP-VI) at 2wt% depending on pH.	133
Figure 5-18: time-evolution of P(AA _{0.6} -co-AMPS _{0.4})+ P(VP-VI) at 1wt%, pH=5.5 and pH=8 (first two columns respectively) and at 0.5wt%, pH=5.5 and pH=8 (third and fourth column respectively).....	134
Figure 5-19: ratio extensional relaxation times of mixtures of polyanions with P(VP-VI)	136

Chapter 6

Figure 6-1: schematic representation of gels formed by mixtures of PSSNa with lysosomes.	145
Figure 6-2: dynamic moduli for mixtures of PAA, P(AA _{0.8} -AMPS _{0.2}) and P(AA _{0.6} - AMPS _{0.4}) (1st, 2d & 3rd rows respectively) with PVP at 2wt % & 1wt % (1 st & 2d column respectively) depending on pH.....	149
Figure 6-3: viscosity enhancement for mixtures of PA ⁻ and PVP depending on concentration and pH.....	150
Figure 6-4: preponderant species in a mixture of PAA with P(VP-VI) depending on pH.....	151
Figure 6-5: negative to positive charge ratio in a 1:1 mixture of PA ⁻ with P(VP-VI) depending on pH.	152

List of tables

Chapter 2

Table 2-1: suitable conditions for polymerization and complexation.....	40
Table 2-2: solubility and decomposition properties of V50 at 50°C in water.....	42
Table 2-3: solution copolymerization of 43% of AETAC and 57% of AM at 15wt%.....	45
Table 2-4: solution copolymerization of 43% of AETAC and 57% of AM in presence of sodium formate at 15wt%.....	46
Table 2-5: solution copolymerization of 43% of AETAC and 57% of AM at 5wt%.....	46
Table 2-6: solution copolymerization of 25% of AETAC and 75% of AM in presence of sodium formate at 15wt%.....	47
Table 2-7: solution copolymerization of 25% of AETAC and 75% of AM at 5wt%.....	48
Table 2-8: solution copolymerization of 33% of AETAC and 67% of AM at 5wt%.....	48
Table 2-9: copolymerization of 33% of AETAC and 67% of AM in presence of poly(acrylic acid).....	54
Table 2-10: copolymerization of 33% of AETAC and 67% of AM in presence of poly(acrylic acid) with Mw of 100kDa and 1500kDa.....	55
Table 2-11: copolymerization of 33% of AETAC and 67% of AM in presence of PAMPS.....	59
Table 2-12: copolymerization of 33% of AETAC and 67% of AM in presence of P(AA _{0.66} -co-AMPS _{0.33}).....	61
Table 2-13: copolymerization of 33% AETAC and 67% AM in presence of P(AA _{0.33} -AMPS _{0.66}).....	62

Chapter 3

Table 3-1: quantity of initiator and molar mass of synthesized PAA.....	71
Table 3-2: composition and molar mass of the polycations used in rheology investigations.....	71
Table 3-3: zero shear viscosity in Pa.s of PAA1600 as a function of pH and concentration.....	75
Table 3-4: zero shear viscosity and crossover frequency of mixtures of PAA1600 with P(VP-VI) depending on mixing ratio.....	79
Table 3-5: apparent molar mass of mixtures of PAA1600 with P(VP-VI) at 2wt% depending on pH.....	83
Table 3-6: viscosity enhancement for mixtures of PAA1600 with P(VP-VI) depending on concentration and pH.....	87
Table 3-7: zero shear viscosity in Pa.s of PAA900 depending on concentration and pH.....	89
Table 3-8: zero shear viscosity in Pa.s of PAA3300 depending on concentration and pH.....	93

Chapter 4

Table 4-1: $|\eta^*|_0$ of P(AA_{0.8}-AMPS_{0.2}) & P(AA_{0.6}-AMPS_{0.4}) depending on concentration and pH. 102

Table 4-2: viscosity enhancement of P(AA_{0.8}-AMPS_{0.2})+P(VP-VI) depending on concentration and pH..... 104

Table 4-3: viscosity enhancement of P(AA_{0.6}-AMPS_{0.4})+P(VP-VI) depending on concentration and pH..... 106

Table 4-4: summary of typical behavior observed for mixtures of PA⁻+P(VP-VI) depending on concentration..... 110

Chapter 5

Table 5-1: relaxation features of pure PA⁻ depending on pH and concentration. 120

Table 5-2: relaxation features for mixtures of PA⁻+P(VP-VI) at pH=7 & 8 depending on concentration. 135

Table 5-3: filament lifetimes for mixtures of PA⁻+ P(VP-VI) at pH=5.5 & 6 depending on concentration. 136

Chapter 6

Table 6-1: relaxation features of polyanions at pH=7 and 8 at 1wt% and 2wt%..... 140

Table 6-2: relaxation features of mixtures of PA⁻+ P(VP-VI) at pH=7 & 8 depending on concentration. 141

Table 6-3: filaments lifetime of mixtures of PA⁻ with P(VP-VI) at pH=5.5 & 6 depending on concentration..... 143

Table 6-4: relaxation features for mixtures of PA⁻ with P(VP-VI) depending on pH and concentration. 144

List of abbreviations and symbols

Chemicals

AA	Acrylic acid
AETAC	[2-(Acryloyloxy)ethyl]trimethylammonium chloride
AM	Acrylamide
AMPS	2-acrylamido-2-methyl-1-propanesulfonic acid
CC	Choline chloride
D ₂ O	Deuterium oxide
NaNO ₃	Sodium nitrate
NaOH	Sodium hydroxide
P(AA-co-AMPS) (also P(AA-AMPS))	Poly(acrylic acid-co-2-acrylamido-2-methyl-1-propanesulfonic acid)
P(VP-co-VI) (also P(VP-VI))	Poly(vinyl pyrrolidone-co-vinyl imidazole)
PAA _x	Poly(acrylic acid) with M _w =x
PQVI	Poly(quaternized vinyl imidazole)
PVI	Poly(vinyl imidazole)
V50	2,2'-azobis (2-amidinopropane) dihydrochloride

General

CA	Complexing agent
CD	Charge density
CaBER	Capillary Break-up Extensional Rheology
CRU	Constitutive repeating unit
FFF	Field flow fractionation
IPEC	Inter-polyelectrolyte complexes
NMR (also ¹ H-NMR)	Proton Nuclear Magnetic Resonance spectroscopy
PA ⁻	Polyanions
PAV	Piezo-driven axial vibrator
PC ⁺	Polycations

PEC	Polyelectrolyte complexes
SC	Solids content (weight concentration)
TEM	Transmission electron microscopy

Symbols

δ	Loss angle
d	Gap height in piezo-driven axial vibrator
D	Diameter of the filament in CaBER experiments
D_0	Initial diameter of the filament in CaBER experiments
D_c	Diameter of the CaBER plates
D_x	Dispersion number x
$\dot{\gamma}$	Shear rate
γ	Strain
G'	Storage modulus
G''	Loss modulus
G^*	Complex modulus
I	Ionic strength
K^*	Complex squeeze stiffness
κ^{-1}	Debye length
l_B	Bjerrum length
λ_D	Debye length
λ_E	Extensional relaxation time
λ_S	Shear relaxation time
L_{final}	Final gap in CaBER measurements
L_{initial}	Initial gap in CaBER measurements
M_n	Number average molecular weight
M_w	Weight average molecular weight
$M_{w,\text{app}}$	Apparent molecular weight
n	Degree of polymerization
η^*	Complex viscosity

η^*_0	Zero shear viscosity
r_x	Copolymerization parameter of comonomer x
S_x	Solution number x
t	Time
t_0	Initial time in CaBER measurements
τ	Shear stress
t_F	Filament lifetime in CaBER experiments
ω	Frequency
ξ	Manning parameter

Introduction

Polymers are omnipresent in our daily life, from the objects which surround us to the building blocks of our body (proteins, DNA...). Human beings discovered polymers and their unique properties empirically thousands of years ago (traces in Egypt 1200 BC). At that time, these natural polymers were extracted directly from plants. After this early discovery, the major breakthrough in the field of polymer science occurred less than a century ago, when chemists figured out ways to synthesize these very peculiar molecules (Staudinger 1920): the era of the industrial development of polymers/plastics had started.

Polymers have remarkable properties which gave rise to a large variety of applications, both as solid objects or in solution. Indeed, solutions of polymers (in a good solvent) exhibit flow properties dramatically different from the pure solvent. From Newtonian, the behavior usually becomes viscoelastic. This specific property of polymers is utilized in many industrial formulations to control or model their flow properties. Polymers, either natural or synthetic, are specifically used in this purpose: they are referred to as rheology control agents, rheology modifiers or more simply thickeners. With new environmental laws and general concerns, most solvent based formulation will be in the near future replaced by water based formulations. In this respect, thickeners used in aqueous solutions are of first importance. A particular class of polymers has proven to be very water soluble and is therefore widely used in waterborne systems: polyelectrolytes (PE).

These macromolecules, as indicated by their name, carry charges. A lot of natural polymers, DNA and proteins amongst them, are charged. The former, because of its phosphate backbone is negatively charged while the latter can be either positively or negatively charged, or both at the same time. These three kinds of polyelectrolytes are called respectively polyanions, polycations and polyampholytes. Besides the fact that it makes them very soluble in aqueous media, the presence of charges induces other unique properties. Many fundamental studies have been carried out on polyelectrolytes, either pure or mixed with other molecules. The behavior of pure polyelectrolytes is interesting since the presence of charges usually leads to more stretched conformation compared to neutral polymers but also gives birth to more exotic structures like pearl necklaces. Their sensitivity to ionic strength, temperature, pH etc has also been studied extensively. Regarding pH, the sensitivity depends greatly on whether the charges on the polymer are permanent or not, i.e. whether the polyacid/polybase is strong or not. In the case of weak polyacids or bases the degree of ionization can be tuned through pH from one (polymer

fully charged) to zero (neutral polymer): properties can be modified greatly using the pH as a simple tool. Mixtures of polyelectrolytes with various “objects” and molecules have also attracted a lot of interest, especially when they carry opposite charges. For example, mixtures of polyelectrolytes with inorganic particles, with proteins, with surfactants have been studied extensively. All these systems are interesting from a fundamental point of view, but also from an industrial one. Examples of applications of the three aforementioned systems are, amongst others, waste water treatment by flocculation, biotechnologies (from diagnostic to targeted drug delivery) and personal care products (all shampoo contain surfactants and oppositely charged polymers). The discovery and development of the layer by layer (LbL) deposition technique in the 90’s, in which positively and negatively charged polyelectrolytes are deposited alternatively on a substrate (generally surfaces or particles) has renewed the interest on complexes between polymers, called inter-polyelectrolyte complexes (IPEC).

Indeed, when two macromolecules carrying opposite charges are brought in the vicinity one to each other, they can interact electrostatically. This phenomenon first been studied by Michaels in the late 60’s has since then attracted a lot of attention. Kabanov, Tsuchida or more recently Dautzenberg can be cited as major contributors to this field. From the considerable number of systems studied, they concluded that IPEC can only exist under three forms:

- **Soluble IPEC**, i.e. macroscopically homogeneous systems containing small PEC aggregates.
- **Turbid colloidal systems** with suspended PEC particles in the transition range to phase separation.
- **Two-phase systems** of supernatant liquid and precipitated PEC which is readily separated and isolated as a solid after washing and drying.

Whether one or the other system is formed depends primarily on the charge matching, i.e. on the ratio between the two polymers considered and in the case of weak polyelectrolytes on pH. To form stable systems, an excess of charge is necessary to ensure electrostatic repulsion between the aggregates, hence their stability.

However, this is only true at low concentration, as most studies are carried out under dilute conditions (~0.1%), for which polymers with a medium molar mass are not entangled. At higher concentration, the aggregation phenomena are more difficult to control and even charge mismatching does not ensure to obtain stable systems, as Dautzenberg for example has recently shown (Dautzenberg 2002).

In the work described in the second chapter of this manuscript, I have tried to synthesize stable systems/dispersions based on IPEC at 5wt%, a concentration significantly higher than the ones

most published works refer to. In addition to the high concentration used, the work reported here is unique as the dispersions are not obtained by classical mixing experiments but by the in-situ free radical polymerization of positively charged monomers in the presence of a negatively charged polymer. The potential advantage of this process is, beside its simplicity inherent to a “one pot process”, the fact that the polycation which is synthesized can interact with the polyanion during polymerization, thus directly forming stable particles. The major drawback of this approach lies in the number of parameters which have to be taken into account. Indeed, not only should the complexation step be controlled, but an efficient polymerization of the cationic monomers is a must. To simplify the study, my choice was to fix all parameters except one: the ratio polycation/polyanion. For the positively charged monomer to be polymerized, [2-(acryloyloxy)ethyl] trimethylammonium chloride (AETAC) was chosen. To reduce the charge density of the synthesized polycation, AETAC is copolymerized with acrylamide (AM) in a ratio one to two: resulting copolymers are known to be almost statistical. For the polyanions, poly(acrylic acid) (PAA), a weak polyelectrolyte with a pKa of 4.6, poly(2-acrylamido-2-methyl-1-propanesulfonic acid) (PAMPS), a strong polyelectrolyte, as well as P(AA-co-AMPS) have been used. Resulting systems have been analyzed using mainly NMR spectroscopy and cryo-TEM.

Keeping in mind a potential use of these systems as rheology control agents, a study under technically relevant conditions, i.e. lower concentrations and higher pH, has also been carried out. Because of degradation problems encountered with AETAC, a one to one copolymer of vinyl pyrrolidone (VP) and vinyl imidazole (VI) was used. This polymer, besides its stability, has the advantage that VI being a weak base, its charge density can be tuned by changing the pH.

In chapter 3, mixtures of P(VP-VI) with PAA have been analyzed using a cone-plate rheometer, under small amplitude oscillatory shear experiments. Measuring the storage and loss moduli versus frequency gives insight on the microstructure of the mixtures and on changes occurring when pH or concentration are changed. In chapter 4, the importance of the nature of the negative charge has been assessed by studying mixtures of P(VP-VI) with P(AA_{0.8}-co-AMPS_{0.2}) and P(AA_{0.6}-co-AMPS_{0.4}). In both chapters, the results obtained for mixtures are compared with the ones obtained for pure polyanions, in order to quantify the discrepancies observed.

In many technical applications, not only is the behavior under shear important but the behavior under extensional flow also plays a major part. Therefore, in chapter 5, the same mixtures which have been analyzed using a rotational rheometer were analyzed under extensional flow

using a capillary break-up extensional rheometer (CaBER). A filament lifetime, which can be related in some cases to the extensional relaxation time of the macromolecules, can be measured. Pictures taken during the experiment also give valuable information about the decay pattern of the filaments which are formed.

Finally, in chapter 6, the results from chapters 3, 4 and 5 are brought together and by comparing the results obtained under shear and extensional flow, a tentative microstructure of the mixtures of oppositely charged polyelectrolytes depending on pH and concentration is proposed.

1. State of the Art

1.1. Free radical polymerization

The polymerization of unsaturated monomers typically involves a chain reaction (Vollmert 1988). The carbon-carbon double bond is, because of its relatively low stability, particularly susceptible to attack by a free radical. Many vinyl monomers are therefore polymerized using free radicals as active centers: this process is called free radical polymerization. Historically, free radical chain polymerizations are by far the method most commonly used in industry to produce polymers. Polyethylene, polystyrene, poly(vinyl chloride) – the three polymer of major economic importance- as well as poly(vinyl acetate), poly(methyl methacrylate), poly(acrylonitrile) and many other homo/copolymers can be manufactured by this type of polymerization.

1.1.1 Free radical homopolymerization

Schematically, free radical polymerization is usually described as successive steps leading to the formation of a “dead” macromolecule, each step being characterized by a rate constant k , as summarized in **Figure 1-1**.

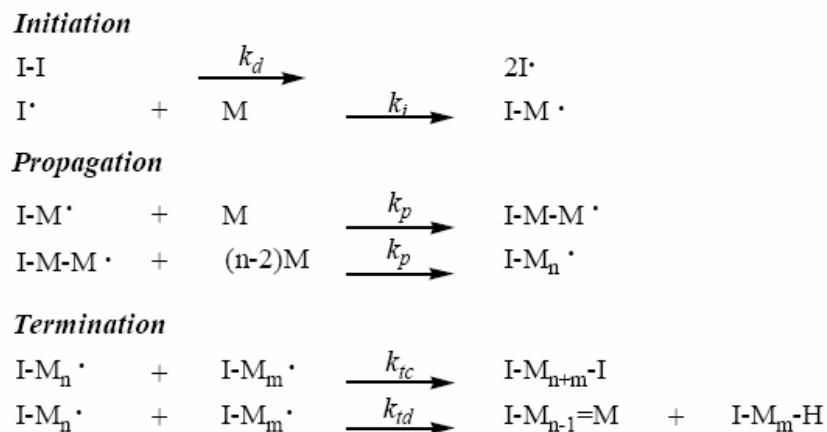


Figure 1-1: mechanism of free radical polymerization.

- **Initiation**

The propagating site is a free radical which is usually generated by the decomposition of an initiator. The initiation can be separated into 2 distinct steps; first, the actual decomposition of the initiator I-I to form the free radicals $\text{I}\cdot$. This can be done in a number of ways, including thermal decomposition or photo decomposition of organic peroxides and hydroperoxides

(Mageli 1968) or azo and diazo compounds (Zand 1965). High energy radiations (Dole 1972), oxidation-reduction reactions, electro-chemical reactions are other methods which can be used to generate unpaired electrons, as reviewed in the 60's (Bevington 1961, O'Driscoll 1969). Once free radicals are formed, they can react on carbon-carbon double bonds to form new radical species which can further react with additional monomers.

- **Propagation**

A free radical polymerization involves many successive steps of growth. In each of them a monomer molecule is added to a growing chain, whereby the radical site is reformed on the newly attached last unit of the chain: the reactive center propagates on the forming macromolecule. Usually it can be assumed that the propagation rates i.e. k_p are, within certain limits, independent of the chain length of the growing polymer.

- **Termination**

Propagation would continue until all the monomer supply was exhausted were it not for the strong tendency of radicals to react in pairs to form a covalent bond with loss of radical activity. The radicals can interact in 2 ways: either by coupling (recombination), in which a bond is formed by pairing the single electrons of the free radical sites of 2 growing chains. Or by disproportionation, in which a hydrogen atom is transferred from a chain to another one, giving birth to 2 dead chains.

1.1.2. Free radical copolymerization

Different monomers can also be copolymerized by free radical polymerization. The general polymerization mechanism is similar to the one described in the case of homopolymerization. Because the reactivity of the different monomers, hence their polymerization rate may not be the same, copolymerizations are usually not statistical.

Initiation

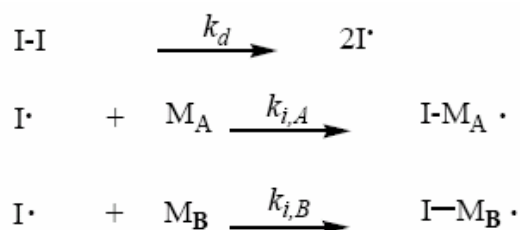


Figure 1-2: mechanism of initiation in free radical copolymerization.

If 2 monomers M_A and M_B are considered, M_A^\bullet and M_B^\bullet being the corresponding free radicals, there are 4 possible ways in which monomers can add:

Propagation

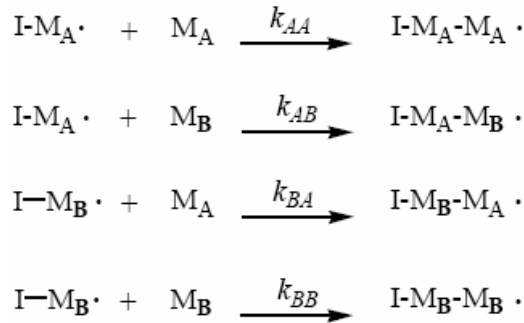


Figure 1-3: mechanism of propagation in free radical copolymerization.

The kinetics of copolymerization was fully elucidated in 1944 by Alfrey, Mayo, Simha and Wall. They assumed that all radical species are in a steady state. Thus, the rate of conversion of M_A^\bullet to M_B^\bullet must be equal to the rate of conversion of M_B^\bullet to M_A^\bullet .

$$k_{BA} \cdot [M_B^\bullet] \cdot [M_A] = k_{AB} \cdot [M_A^\bullet] \cdot [M_B] \quad (1-1)$$

The rates of disappearance of the 2 types of monomers are given by:

$$\text{For } M_A: -\frac{d[M_A]}{dt} = k_{AA} \cdot [M_A^\bullet] \cdot [M_A] + k_{BA} \cdot [M_B^\bullet] \cdot [M_A] \quad (1-2)$$

$$\text{For } M_B: -\frac{d[M_B]}{dt} = k_{AB} \cdot [M_A^\bullet] \cdot [M_B] + k_{BB} \cdot [M_B^\bullet] \cdot [M_B] \quad (1-3)$$

By defining $r_1 = \frac{k_{AA}}{k_{AB}}$ and $r_2 = \frac{k_{BB}}{k_{BA}}$ and combining them, it can be shown that the composition of a copolymer formed at any instant is given by the ‘‘copolymer equation’’ (Tirrell 1989, Rempp 1986):

$$\frac{d[M_A]}{d[M_B]} = \frac{[M_A]}{[M_B]} \cdot \frac{r_1[M_A] + [M_B]}{[M_A] + r_2[M_B]} \quad (1-4)$$

The monomer ratios r_1 and r_2 are the ratios of the rate constant for a given radical adding its own monomer to the rate constant for adding the other monomer. Thus $r_1 > 1$ means that M_A^\bullet

prefers to add to M_A . On the contrary, $r_1 < 1$ means that M_A^\bullet prefers to add to M_B . Same is true for r_2 . Knowing r_1 and r_2 , it is therefore possible to predict if a copolymerization will be statistical or if a drift in composition will occur.

1.1.3. Free radical template polymerization

Template polymerization, also known as replica or more commonly matrix polymerization was first described by Szwarc (1954). It refers to a one-phase polymerization process in which the monomers units are organized by interactions with a preexisting macromolecule present in the reaction medium. The organization can take place thanks to hydrogen bonds, electrostatic interactions or covalent bonds. Template effect has been reported for ionic polymerization, polycondensation and even ring-opening polymerization. But radical matrix polymerization remains by far the most common process.

The presence of the template usually affects the reaction by either modifying its kinetics or changing the properties of the polymer synthesized (degree of polymerization, polydispersity, etc).

1.1.3.1. Mechanism

Most studies carried out on template polymerization have been focusing on determining either its exact mechanism or its kinetic. Concerning the mechanism of reaction, several studies (Polowinski 1994, 1997; Tan 1987, 1989; 1994) have shown that the matrix effect can occur in 2 different ways:

- **Zip Mechanism**

This mechanism is characterized by the fact that all monomers interact with the matrix before the polymerization starts (cf. **Figure 1-4**), i.e. the rate of complexation of the monomers on the template is higher than the rate of polymerization. This mechanism occurs only if the monomers and the matrix can exchange high-energy interactions like electrostatic interactions, strong hydrogen or covalent bonds.

- **Pick-up Mechanism**

The zip mechanism can only occur if every available site on the template is occupied. Often, the coverage of the template is not full and the polymerization starts in the solution. This is known as pick-up mechanism. It occurs when the rate of polymerization is roughly the same as the rate of complexation of the polymer and when both are higher than the rate of complexation of the

monomer. In this mechanism, the monomer is free in the beginning and the polymerization starts in the solution. When the growing polymer chains reach a critical length, they bond to the template and the propagation proceeds along the matrix by addition of monomer molecules from the surrounding solution. If the critical molecular weight necessary for complexation is high, only the pick-up mechanism occurs.

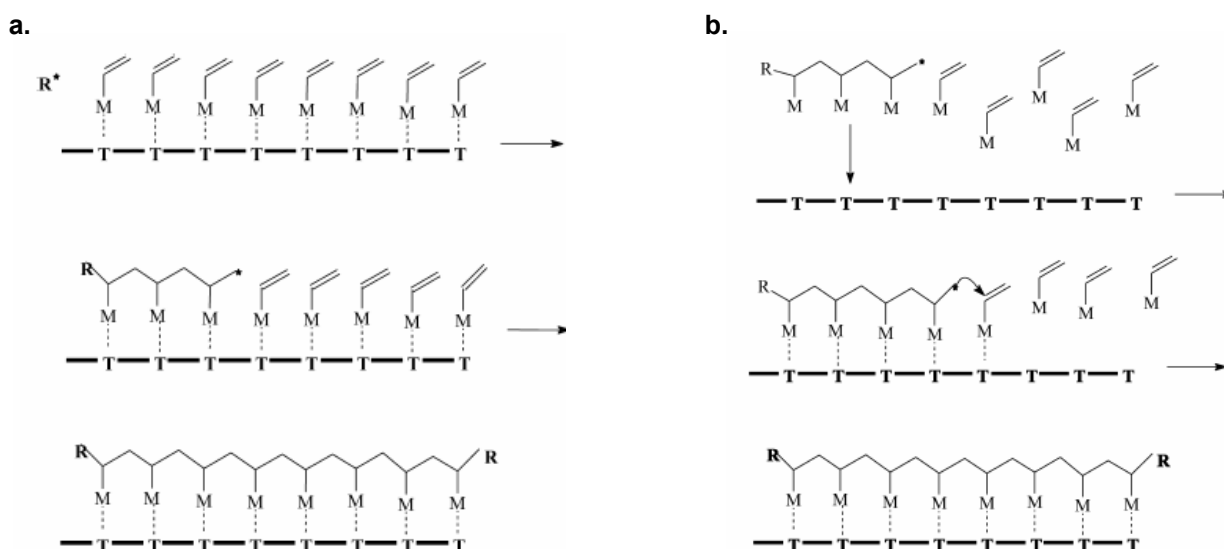


Figure 1-4: zip (a) and pick-up (b) mechanisms of template polymerization.

1.1.3.2. Influence of the template

The presence of the template influences mainly the kinetics of the polymerization and the morphology of the synthesized polymer.

In most cases, the organization/alignment induced by the template results in an increase of the polymerization rate. The evolution of this increase with template concentration depends on the mechanism:

- With the zip mechanism, the polymerization rate increases until $[\text{Template}]/[\text{Monomer}]=1$ and then decreases.
- With the pick-up mechanism, the polymerization rate increases until $[\text{Template}]/[\text{Monomer}]=1$ and then remains constant.

This difference is often used to determine which mechanism occurs with specific systems (Polowinski 2002). Some systems exhibit a decrease in polymerization rate, because of the reduced freedom of the macro-radicals which are bound to the template. However, such decreases are only observed for systems following the pick-up mechanism.

The presence of a template can also modify the reactivity of some monomers. For example, the polymerization of acrylic acid is notoriously difficult at high pH because of the electrostatic repulsion between monomers. By using a positively charged matrix, this effect can be overcome and the polymerization can proceed. Tsuchida and Osada (1975) studied the polymerization of acrylic acid in presence of poly(N,N,N',N'-tetramethyl-N-p-xylylene-ethylenediammonium dichloride). They showed that electrostatic repulsion could be fully suppressed by an effective complexation. Similar phenomenon was observed by Blumstein and Kakivaya (1977) when styrene sulfonic acid is polymerized in the presence of ionenes.

The template can also influence the morphology of the synthesized polymer. It has been shown that, provided that the polymerization follows the zip mechanism, the molar mass and polydispersity of the latter can be correlated with the molar mass and polydispersity of the former (Ferguson 1983).

The morphology of the inter-polyelectrolyte complexes obtained by template polymerization of one of the polyelectrolyte in the presence of the other one can be significantly different than the complexes obtained by simply mixing 2 interacting polymers. Thanks to template polymerization, it is possible to synthesize complexes which are closer to the ladder-like type described in the paragraph 1.4.4. This was explained by the “ordering” effect of the template due to concerted phenomena. Several groups have reported this phenomenon [Cerrai 1994, 1996; Baranovsky 1984; Kabanov 1981) and their observations all show a higher ordering and structures closer to the thermodynamically stable product.

1.2. Polyelectrolytes

By definition, polymers which bear ionized or ionizable groups are called “polyelectrolytes” (PE). The variety of existing polyelectrolytes is enormous; some of their specific properties and potential applications are summarized in this section.

1.2.1. Classification of polyelectrolytes

1.2.1.1. Positively and negatively charged polyelectrolytes

Similar to smaller electrolytes like salt or organic molecules, polyelectrolytes can carry:

- **Negative charges:** a polymer composed of anionic or anionogenic monomers is referred to as anionic polyelectrolyte or polyanion if the charges are dissociated. In this case, positively charged counter-ions are released in the solution.
- **Positive charges:** a polymer composed of cationic or cationogenic monomers is referred to as cationic polyelectrolyte or polycation if the charges are dissociated. In this case, negative counter-ions are released.
- **Both:** macromolecules carrying at the same time anionic and cationic moieties are called amphoteric. These molecules can show an interesting pH dependency as the molecule can be only positively charged, only negatively charged or both depending on the pK_a of the ionizable groups.

It is rather common that not all the repeating units of a polyelectrolyte are ionized or ionizable; the fraction of ionizable monomers in the polymer is called α . When all ionizable groups are dissociated, the charge density (CD) on the polymer is maximum.

1.2.1.2. Weak and strong polyelectrolytes

Depending on the nature of the charge present in a polymer, it is possible to distinguish:

- **Weak polyelectrolytes:** refers to PE which are not permanently charged. The apparition of charges on such polymers can be due either to the capture of a free charge or to the dissociation of a polarized covalent bond. The charged and uncharged forms are in equilibrium. The degree of dissociation can be estimated using Hendersen- Hasselbach equation:

$$pH = pK_a + \log \frac{[A^-]}{[AH]} \quad (1.5)$$

The dissociation can be favored or hampered by external factors like coordinated interactions or Manning condensation (cf. Paragraph 1.3.3.)

- **Strong polyelectrolytes:** refers to PE which charge density does not depend on external factors. It is for example the case of molecules baring quaternized atoms (like nitrogen atoms) and of strong acids which are deprotonated in aqueous media. However, Manning condensation can still occur and reduce the actual charge density.

1.2.1.3. Integral and pendant type

Two polyelectrolytes can differ chemically as described above but they can also differ in their morphology. Again, it is possible to distinguish two types of polyelectrolytes:

- **Integral type:** the charges are in the main chain. Integral polyelectrolytes have usually more rigid backbones, due to the electrostatic repulsion between adjacent charges, which leads to a “stretching” of the macromolecules.

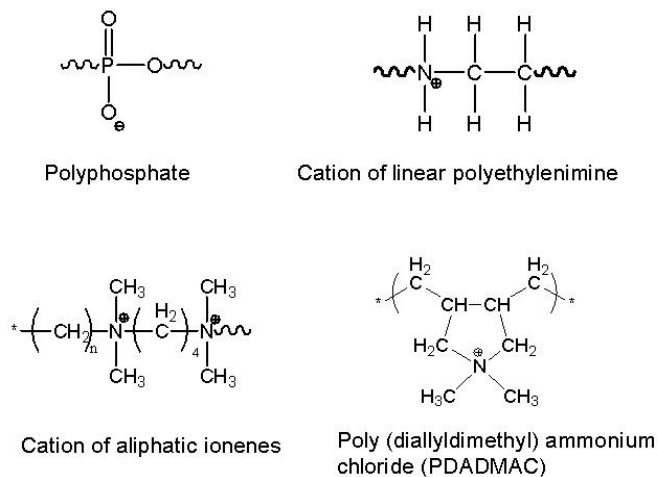


Figure 1-5: examples of integral type polyelectrolytes.

- **Pendant type:** the charges are on side chains. These chains can differ in length, flexibility and density of charge, inducing various behaviors for the corresponding macromolecules.

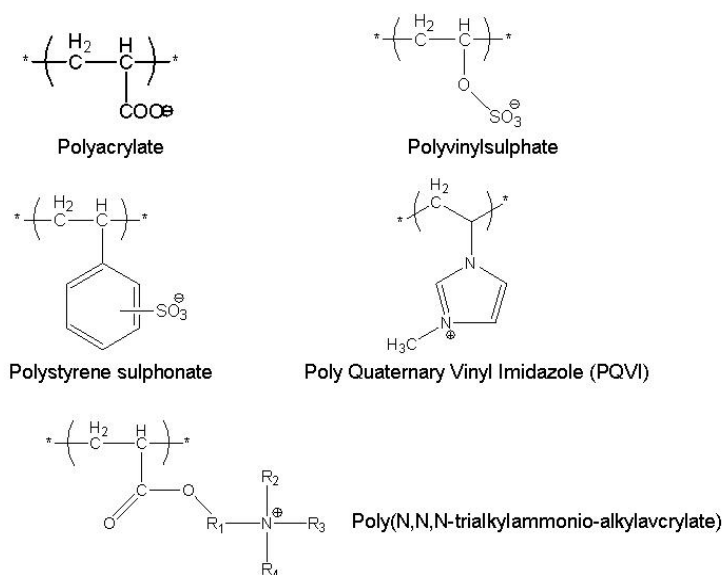


Figure 1-6: examples of pendant type polyelectrolytes.

Regarding interactions with oppositely charged species, like surfactants or other charged polymers, integral polyelectrolytes are less reactive and exhibit deviation from ideal stoichiometry because their charges are more sterically hindered (Philipp 1989).

1.2.2. Origin of Polyelectrolytes

1.2.2.1. Polyelectrolytes in nature

In nature, most living-beings have the same source of energy: glucides. The simplest one, resulting from photosynthesis is glucose. Glucides can bind to form macromolecules, called polysaccharides. Some of them are uncharged species, like cellulose and starch, but most polysaccharides are carrying either positive or negative charges, making them natural polyelectrolytes.

As examples of negatively charged polysaccharides, alginate and hyaluronate can be cited (Alberts 1998). The former one can be extracted from brown algae. Chemically, it is a copolymer of β -D-mannuronate and α -L-guluronate. It is largely used in food industry as gelifing or thickening agent as it has the property to gel in the presence of divalent ions like Ca^{2+} . The latter is a linear copolymer of glucuronate disaccharidiques and N-acetylglucosamine (Meyer 1934). Distributed throughout connective, epithelial, and neural tissues, it is one of the components of the extracellular matrix, and contributes significantly to cell proliferation and migration. In the articulations, like knee or elbow, it participates to lubricification.

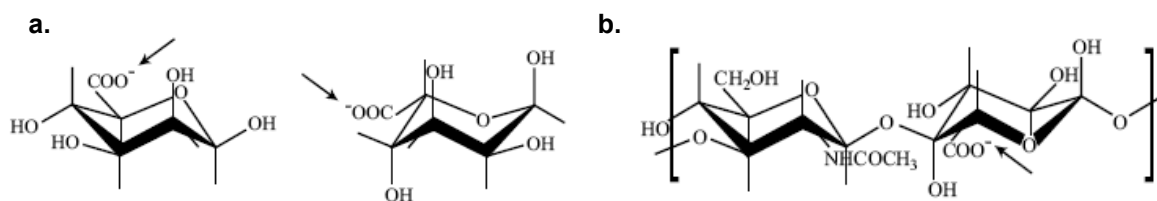


Figure 1-7: chemical structure of alginate (a.) and hyaluronate (b).

The most common cationic polyelectrolyte is chitosan. It is a linear polysaccharide composed of randomly distributed β -(1-4)-linked D-glucosamine (deacetylated unit) and N-acetyl-D-glucosamine (acetylated unit). It is produced industrially by the deacetylation of chitin (Roberts 1992), which is extracted from the exoskeleton of crustaceans. The degree of deacetylation varies typically between 60 and 90 percent for commercially available products. Chitosan is a biocompatible and biodegradable polymer and is used preferentially in biomedical applications.

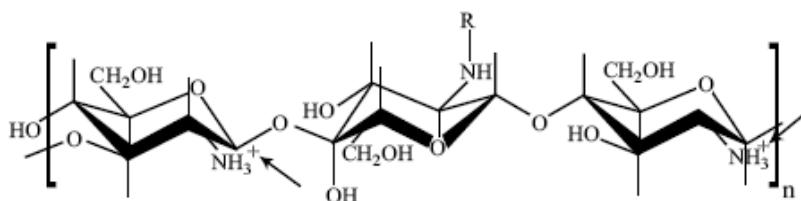


Figure 1-8: chemical structure of chitosan.

Amino-acids are small molecules which bear both an amino moiety and a carboxylic acid moiety. Thus, two amino acids are able to bind by dehydration as the carboxylic group of one molecule reacts with the amino group of an other one to give birth to an amid function. When many amino acids bind, the product is called polypeptide or protein. The former usually refers to molecules having a molecular weight below 10kDa, while the latter refers to macromolecules having a higher molar mass.

Polypeptides contain only one free amino and one free carboxyl group each at one end of the molecule. Nevertheless, these two groups may not be the only ones charged within the polypeptide since six proteinogenic amino acids out of twenty carry ionisable groups: depending on pH, a protein can be positively charged, negatively charged or neutral.

DesoxyriboNucleic Acid (DNA), carrying the genetic information in the nucleus of cells, is a long polymer composed of nucleotides. The backbone of the DNA strand is made of alternating phosphate and sugar residues, and is negatively charged. This feature is of first importance in the compaction mechanism which leads to the formation of chromosomes: DNA is a 1.8m long stiff molecule but thanks to electrostatic interactions with histones (cationic proteins) it can be compacted 50,000 times to form chromatines and subsequently chromosomes (Netz 1999, Kunze 2000). The packing of DNA around histones is a good example of complexation between oppositely charged molecules, phenomenon described in further details in paragraph 1.4.

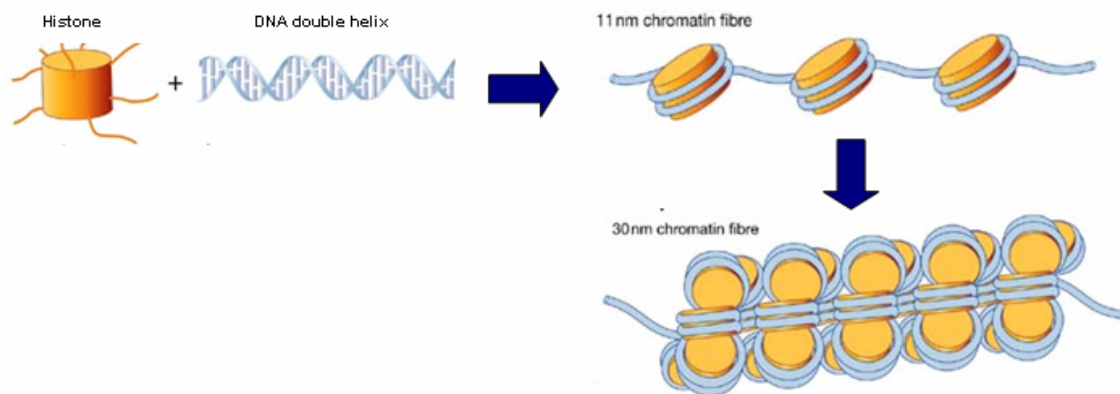


Figure 1-9: compaction mechanism of DNA on histones.

1.2.2.2. Synthetic polyelectrolytes

The amounts of natural polyelectrolytes available are considerable (like cellulose and chitosan). However, their extraction and purification is difficult; thus, so far, their use has been confined in “niche” markets. Most commodity polyelectrolytes used today are synthetic.

There are two basic routes to synthesize polyelectrolytes. The first one consists in directly polymerizing charged monomers. With this technique, because of repulsion between monomers, conversion and molar masses are often low. The other method of choice is to polymerize a neutral monomer and induce the apparition of charges afterwards by chemical modifications. In this case, the major drawback is that the charge distribution is less controlled. Similar to neutral polymers, potential applications of polyelectrolytes depend on their chemical properties (functional groups, charge density, solubility in water, molar mass etc). Of first importance is whether they are synthesized as crosslinked or non crosslinked polymers. When polyelectrolytes are crosslinked, provided that their degree of crosslinking is high enough, their behavior is strongly altered: they lose one of their basic features, which is that they are highly water soluble. Nevertheless, they do not lose their hydrophilicity and this means that if put into water, a crosslinked polyelectrolyte can swell considerably. This property is used in superabsorbents: they are crosslinked polyelectrolytes that have the property to absorb and retain massive amounts of water. Slightly crosslinked PE are also used as thickeners. Again, the fact that these molecules swell in water is responsible for their properties. Non-crosslinked polyelectrolytes are widely used in industry. Amongst the biggest fields of applications, one can cite the stabilization of colloidal dispersions, both organic and mineral as well as the stabilization of foams for cosmetics and mining industries. They are also used in wastewater

treatment for their capacity to flocculate charged impurities. Finally, the rheological features of many formulations like paints, coatings, paper, inks and even food is controlled by the addition of polyelectrolytes. A new family of hydrophobically modified polyelectrolytes has been developed in this respect, as discussed in paragraph 1.5.2.

1.3. Electrolytes in solution

1.3.1. Bjerrum length

In general, the physics of charged systems is governed by two major laws. The first one is the condition of electroneutrality, stating that each charge must be balanced by an oppositely charged counterpart. The second one is the coulombic potential. Let's consider two charges at a distance r one from each other in a homogeneous medium having a dielectric constant ϵ . The value of the first charge is $Z_A e$ and the value of second one $Z_B e$. The coulombic energy U between them is then:

$$U(r) = \frac{Z_A Z_B e^2}{4\pi\epsilon\epsilon_0 r} \quad (1.6)$$

To compare this energy to the thermal energy, one can write:

$$\frac{U(r)}{kT} = \frac{Z_A Z_B e^2}{4\pi\epsilon\epsilon_0 kT r} \quad \text{or} \quad \frac{U(r)}{kT} = \frac{Z_A Z_B l_b}{r} \quad (1.7)$$

$$\text{where } l_b \text{ is the Bjerrum length: } l_b = \frac{e^2}{4\pi\epsilon\epsilon_0 kT} \quad (1.8)$$

The Bjerrum length defines the distance at which the electrostatic interaction and the thermal energy are equal. In water at 25°C, it is 0.713nm.

1.3.2. Debye-Hückel's law

The electrostatic potential $\psi(r)$ around a single point I carrying a charge $Z_i e$ in a uniform medium with a dielectric permittivity ϵ is:

$$\psi_i(r) = \frac{Z_i e}{4\pi\epsilon\epsilon_0 r} \quad (1.9)$$

As soon as other charges are present in the medium, this potential is modified. Indeed, the electrostatic interactions either lead to attraction between charges of opposite sign or repulsion when the charges are identical.

Around the central charge i , the Poisson equation is then written:

$$\Delta \psi_i(r) = -\frac{\rho_e(r)}{\varepsilon_0 \varepsilon} = -\frac{e}{\varepsilon_0 \varepsilon} \sum_j Z_j n_j(r) \quad (1.10)$$

With $\rho_e(r)$ is the local charge density and $n_j(r)$ is the local density of the specie j . By definition of the pair distribution function, it is possible to write: $n_j(r) = \rho_j g_{i,j}(r)$. The sum above refers to all the ions present in the solution. In their approach, Debye and Hückel assumed that:

$$g_{i,j}(r) = e^{-\frac{Z_j e \psi_i(r)}{kT}} \quad (1.11)$$

The boundary conditions impose that the potential is equal to zero at infinite distance of the central charge because of the screening due to the other charges present in the medium. This rough assumption considering an average field implies that there is no correlation between neighboring ions. The combination of the previous equations leads to the Poisson Boltzmann equation:

$$\Delta \varphi_i(r) = -4\pi l_b \sum_j \rho_j Z_j e^{-Z_j e \varphi_i(r)} \quad \text{with} \quad \varphi_i = \frac{e \psi_i}{kT} \quad (1.12)$$

Where φ_i is the potential and l_b the Bjerrum length defined above.

After linearization of the exponentials factors, the the Poisson Boltzmann equation becomes:

$$\Delta \varphi_i(r) = \kappa^2 \varphi_i(r) \quad \text{with} \quad \kappa = \sqrt{4\pi l_b \sum_j \rho_j Z_j^2} \quad (1.13)$$

This is the famous Debye-Hückel equation.

The electroneutrality conditions states that
$$\sum_j \rho_j Z_j = 0 \quad (1.14)$$

Therefore, the solution to the Debye-Hückel equation is:

$$\varphi_i(r) = \frac{Z_i l_b}{r} e^{-\kappa r} \quad (1.15)$$

In a nutshell, the presence of many ionic species in a medium leads to faster drop of the electrostatic potential according to a law in $e^{-\kappa r}/r$ instead of $1/r$ for an isolated ion. This

phenomenon is called electrostatic screening with κ being the screening constant. The inverse of this constant is called Debye length λ_D and is defined as the distance after which the potential comes back to zero i.e. the distance after which a charge is fully screened.

When ions are placed into a medium, they contribute to increase the so called ionic strength I which depends on the concentration and valence of the ions as follows:

$$I = \frac{1}{2} \sum_j \rho_j Z_j^2 \quad (1.16)$$

The Debye length is directly related to the ionic strength as more ions in a solution means a better screening effect:

$$\lambda_D = (4\pi l_b I)^{-1/2} \quad (1.17)$$

1.3.3. Manning's condensation

Manning's parameter is defined as the ratio between the Bjerrum length and the distance b between two adjacent ionic sites on the polymer backbone:

$$\zeta = \frac{l_b}{b} \quad (1.18)$$

Whether the counter ions are free to move faraway from the chain or on the contrary are bound to it is directly linked to the value of ζ .

The condensation mechanism proposed by Manning and Oosawa is valid for a rigid chain which is characterized by its contour length L_c and the size of one unit of monomer a . Moreover, this chain is partially charged and the monovalent ionic sites are separated by a distance b . So to simplify the calculation, the macromolecule is treated as an infinite thread bearing a uniform charge density.

The electrostatic potential around this macromolecule at a distance r is:

$$\varphi(r) = \left(\frac{e}{4\pi\epsilon_0 \epsilon b} \right) \ln(r) = \left(\frac{2kTl_b}{eb} \right) \ln(r) \quad (1.19)$$

The counter ions distribution is following a Poisson-Boltzmann distribution and can be written:

$$n(r) = n_0 \exp(-\varphi(r)) \approx r^{-2l_b/b} \quad (1.20)$$

The number of counter ions around the chain which are closer than r is therefore:

$$p(r) = \int_0^r 2\pi r' n(r') dr' = 2\pi n_0 \int_0^r r'^{(1-2l_b/b)} dr' \quad (1.21)$$

with n_0 the average density of counter ions

The last integer is converging to a finite value only when the power of r is bigger than -1 , i.e. if $b > l_b$. If this condition is fulfilled, condensation is not occurring. On the contrary, if $b < l_b$ the integer diverges. In this case, free ions condensate on the chain and a new effective value b_{eff} appears, so that $b_{\text{eff}} > l_b$. Physically, the Bjerrum length is the minimum distance between two charges on a polyelectrolyte. If some charges are closer than l_b , Manning condensation occurs. This explains why the effective charge density is difficult to control on polyelectrolytes. Taking poly(acrylic acid) ($\text{pKa}=4.6$) as an example, at $\text{pH} \gg 4.6$ all carboxylic groups should dissociate. But because of Manning condensation, some groups always remain protonated.

1.4. Polyelectrolytes based complexes

1.4.1. Polyelectrolytes and surfactants

The interactions between synthetic polymers and surfactants are highly interesting both from an academic and industrial point of view. They lead to the formation of surfactant-polyelectrolyte complexes (SPEC). In the presence of polyelectrolytes, micelles are stabilised, inducing the lowering of the critical micellar concentration (CMC) of surfactants: this is referred to as a cooperative binding of the surfactant to the polyelectrolyte. The general picture emerging from the studies carried out on SPEC is that micelle-like surfactant clusters bind to the polymer chains so that the charged segments are neutralised by the oppositely charged head groups of the surfactant. The majority of the investigations directed towards the structure of polyelectrolyte/surfactant complexes have focussed on the properties of the surfactant aggregates, notably their aggregation numbers N_{agg} . General conclusions were that N_{agg} is essentially independent of the concentration of the bound surfactant (Hansson and Almgren 1994, 1995; Anthony and Zana 1996). The N_{agg} values for polyelectrolyte-bound aggregates increase with the surfactant chain length as in polymer-free systems (Almgren 1992), but decrease with temperature (Hansson 1995) and are independent of the nature of the surfactant counterion (Hansson 1994) and of the added electrolyte (Hansson 1995).

Depending on the molar mass of the polyelectrolyte, and on the size of the surfactant micelles, two conformations are frequently described. With long polymers, pearl-necklace structures can

be formed (Cabane 1987), in which the polyelectrolyte wraps around small surfactant aggregates to shield their hydrophobic tails from surrounding water (Koetz 2001).

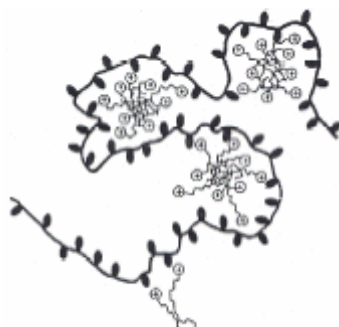


Figure 1-10: pearl necklace structure of polyelectrolyte-surfactant complexes.

When polymers are short, one chain can only bind to one surfactant aggregate. This case has been studied widely using numerical and analytical approaches (Wallin 1996, Netz 1999, Chodanowski 2001). The major conclusion is that the conformation of the polyelectrolyte chains depends mostly on their stiffness. Flexible chains wrap around micelles while stiff ones have only few contact points with the micelles (cf. **Figure 1-11**).

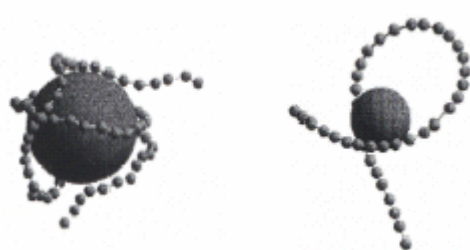


Figure 1-11: flexible (left hand side) or stiff (right hand side) polyelectrolyte-surfactant complexes.

Regarding industrial applications, SPEC are used in personal care industry: the interactions between anionic surfactants which are the foaming and washing agents and cationic polyelectrolytes ensure the quality and durability of the foam of shampoos and soaps.

1.4.2. Polyelectrolytes and charged surface

Interactions between polyelectrolytes and oppositely charged surfaces are highly relevant in industry in surface modification and sorption processes. From an academic point of view, the field has gained new interest since Decher introduced the layer-by-layer deposition technique (LBL) (Decher 1997, Loesche 1998). In this method, a charged substrate is dipped into a solution of polyelectrolyte of opposite charge: a layer of this polyelectrolyte adsorbs then

irreversibly on the substrate. After the adsorption of the polymer, the net charge is the opposite of what it was originally. This operation can be reproduced many times by dipping the substrate alternatively in oppositely charged polyelectrolyte solutions, the sample being washed after each dipping in order to remove the unbound polyelectrolyte. The result is a nanostructured object consisting of alternated layers of polyelectrolytes (**Figure 1-12** from Decher 1997).

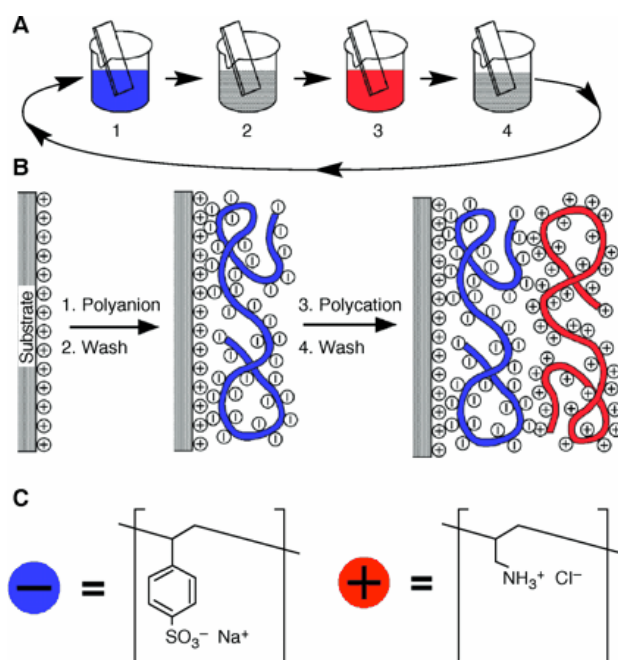


Figure 1-12: principle of the layer-by-layer deposition technique.

Such “nanocomposites” are very promising in several fields of applications:

- **Cell encapsulation:** most cells are negatively charged; therefore, it is possible to protect them by adsorbing a layer of polycations at their surface (Diaspro 2002). To improve the protection, a multilayered nanostructure obtained by LBL with a proper cationic surface can also be used. Encapsulated this way, cells can keep their activity and be used subsequently (Tong 2005, Chanana 2005).
- **Hollow capsules:** the LBL technique can be applied to charged spheres instead of plane surfaces (Donath 1998, Berth 2002, Kohler 2002). Thus spherical multilayered nanoobjects can be produced. If the core is chosen so as to be removable (by pH modification for instance), hollow spheres can be synthesized. Such containers could eventually be used for drug delivery (Volodkin 2007).

- **Structured surfaces:** if the surface which is used for the deposition of the polyelectrolytes is not uniformly charged, it is possible to use the LBL technique to structure the surface based on a charged pattern. By this means, it is possible to grow the pattern in the third dimension (Jiang 2000). This is potentially promising for building new chips and electronic devices.

1.4.3. Polyelectrolytes and DNA

Gene therapy is at the time one of the most promising way for the treatment of both genetic and acquired diseases. In this type of therapy, sick genes are replaced by healthy ones or new genes that encode for a protein curing the targeted disease are added. Efficient delivery of the gene into target cells and maintenance of its functional activity therein constitute the most important condition of successful gene therapy. So far, the use of retroviruses or adenoviruses as DNA/RNA carrier had been the method of choice as transfection (i.e. the introduction of foreign material into an eukaryotic cell) is very efficient using this method. But problems of immune responses may arise, as the body does not accept the virus and non-viral based transfection agents had to be developed. The complexation of DNA with cationic polymers to form neutral complexes has also been studied extensively in recent years. A large number of positively charged polymers have been used. As examples, one can cite:

- **Polyethyleneimines (PEI):** thanks to its high charge density, linear or branched PEI is very efficient to complex DNA (Ferrari 1997, Goula 1998, Demeneix 1998). However, because of the high positive charge density, decomplexation can be difficult which can lead to moderate transfection efficiency (Boussif 1995). PEI has the other drawback that it is not fully biocompatible: it can be grafted with alginate blocks to lower its potential cytotoxicity (Patnaik 2006) and yield carriers that are more efficient.
- **Chitosan:** being a natural polymer, chitosan has beneficial qualities such as low toxicity, low immunogenicity, excellent biodegradability and biocompatibility (Shu 2002, Lee 2005). However, the transfection efficiency is acceptable only above a critical molar mass as well as a critical degree of deacetylation,

Besides PEI and chitosan, other cationic polymers can be used, like poly-l-lysine (Moriguchi 2005), poly((2-hydroxypropyl)methacrylamide-b-(dimethylamino)propylmethacrylamide) (Romoren 2004), polyamidoamine (Tsutsumi 2007) etc. Independent of the polymer used, complexes formed by DNA/RNA with cationic polymers have to be shielded from undesirable interactions with impertinent surroundings. This is usually done by PEGylation i.e. that the

polycation is coupled with a polyethylene oxide block, which forms a protective shell around the polyplexes (Choi 1998, Oupicky 2000, Harada-Shiba 2002).

1.4.4. Oppositely Charged Polyelectrolytes

The discovery of the electrostatic nature of the interactions between two charged natural macromolecules took place in 1896 (Kossel 1896). After this empirical finding, the preparation of well defined “polysalts” (precipitated polyelectrolyte complexes) with a 1 to 1 stoichiometry was successfully carried out only 60 years later by Michaels (1961, 1968). Since then, a lot of work has been done in the field of inter-polyelectrolyte complexes (IPEC), emphasizing mostly on determining the stoichiometry of complexes obtained with a wide variety of polymers; the structure of these complexes has also been studied intensively.

1.4.4.1. Formation of a complex

When a polycation and a polyanion are mixed under suitable conditions, a complex can be formed. The driving forces leading to the formation of such a complex are similar to the ones driving the formation of SPEC:

- Coulombic interactions between opposite charges.
- Entropy gain due to the release of small counter ions in the solution.
- Hydrophobic interactions between uncharged portions of the macromolecules.

The entropy gain due to the release of the counter-ions and the water around the charged groups is usually the most powerful driving force (Kriz 2001).

Concerning the morphology of the complexes, it results from the balance between thermodynamically controlled associations and kinetically controlled ones (Tsuchida 1974, Koetz 1986, Thuenemann 2004), respectively:

- **Ladder-type** structures resulting from the stretching and ordering of the polymer chains during complexation coupled with cooperative effects. This lead to regular structures in which the charges are ideally neutralized.
- **“Scrambled eggs”** structures resulting from the random meeting of opposite charges. This leads to random and only partial charge neutralization: the stoichiometry differs from the ideal 1 to1 situation.

If rearrangements are possible, the kinetically formed structures can reorganize to yield the thermodynamically stable ones, as schemed in **Figure 1-13** (from Tsuchida 1994).

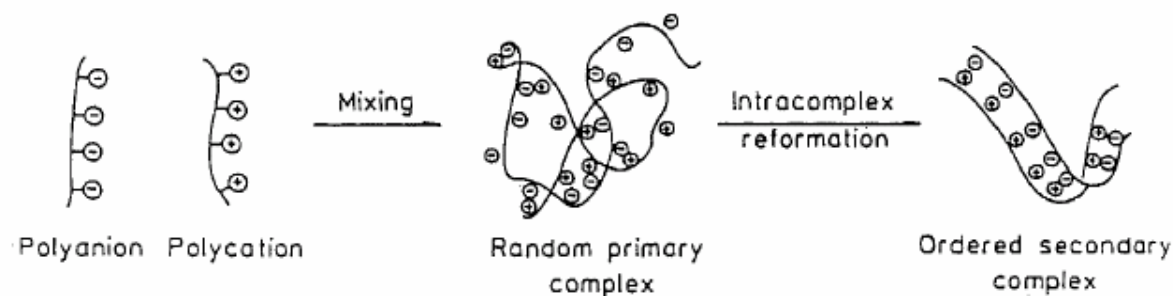


Figure 1-13: rearrangement from “scrambled-egg” (random) to “ladder-type” (ordered) structures.

High temperatures can favor such conformational changes; if the electrostatic interactions are strong, however, such processes may still be very slow or even impossible. Steric hindrance may also hinder rearrangements.

Macroscopically, depending on the chemical structure of the polymers, on the concentration, on the solvent quality, on the mixing conditions etc, several systems can be obtained (Philipp 1989):

- **Two-phase system:** also referred to as polysalt, the system separates into a solid phase which precipitates and a clear supernatant.
- **Soluble complexes:** macroscopically the system is transparent but it contains small polyelectrolyte aggregates, which are fully soluble in water.
- **Colloidal complexes:** macroscopically the system is milky and looks similar to waterborne latexes. It is formed by small particles or aggregates, which are usually only kinetically stable.

The formation of one or another system depends on many factors as already mentioned. They can be split into two major categories:

The first one concerns the characteristics of the individual components: whether the PE are strong or weak acids / bases, potentially their pKa, the position of the ionic sites (pendant or integral type), the charge density, the rigidity of the polymer backbone, etc.

The second ones concern the physicochemical environment: the nature and quality of the solvent, the ionic strength, the valence of co-ions, the pH, the temperature, etc.

Some of these parameters are interdependent. Therefore, it is difficult to give general rules, which enable to predict the behavior when two oppositely charged polymers are mixed: empirical trials are still the best way to determine how a particular system behaves.

1.4.4.1.1. Precipitated complexes

In their classical work, Bungenberg de Jong and Dekker (1936) studied polysalts obtained from gelatin plant gum and by elemental analysis determined a 1:1 charge stoichiometry in the precipitated phase. Most of the work carried out afterwards emphasized again on determining the stoichiometry of the complexed formed. Kikushi's work based on natural polyelectrolytes like dextran derivatives, gelatin and chitosan showed unpredictable results for the stoichiometry depending on the ratio between component and preparing methods (Kikushi 1985). Kabanov (1984) and Philipp (1989) centered their work on synthetic polymers and obtained reliable results showing that the charge ratio in the precipitated phase is always close to 1:1. Nevertheless, deviation from this ideal stoichiometry can occur due mainly to:

- Misfit of the charge repartition on the backbone of the polymer making a strict neutralization impossible.
- Steric hindrance of the ionic site, especially true for non linear and integral type polymers.

Regarding applications, polysalts can be used either in the swollen state, thus taking advantage of their relatively high affinity towards water or in the dry state. In the former case, swollen complexes are primarily used for slow release. The complexes are then considered as physically crosslinked hydrogels, and the release can be triggered by changes in pH, ionic strength or temperature. In the latter case, highly selective membranes can be obtained by an appropriate choice of the polyelectrolytes mixed as well as their mixing ratio.

1.4.4.1.2. Soluble complexes

Tsuchida (1972) started to investigate the importance of the charge balance in the formation of soluble complexes by studying the interactions between polystyrene sulphonate and various ionenes. His first conclusions were that macroscopically homogeneous systems could be obtained when the positive and negative charges are added in non-stoichiometric ratios. This work was completed by Nakajima (1972) working on cationically and anionically modified poly(vinyl alcohol) and Tsuruta (1978) working on poly(vinyl alcohol) sulfate and ionenes. Both similarly pointed out the importance of the charge mismatch in the stability of polyelectrolyte mixtures.

Kabanov (1984) was amongst the first ones to investigate the influence of the molar mass of the components on the stability of polyelectrolyte complexes. He showed that a guest-host system formed by two polyelectrolytes having very different molar masses is an efficient approach to form soluble complexes. Studying many systems based on polyacrylates, polyphosphates and

heparin complexed with ionenes, quaternized poly(vinyl pyridine) or bovine serum albumine, he was able to show that a ratio between the molar mass of the two complexed polyelectrolytes of three to one is required to achieve solubility. Kabanov also investigated systematically the influence of the degree of quaternization in weak polyelectrolytes system, like poly(methacrylic acid) mixed with partially quaternized poly(vinyl pyridine). Using luminescence methods, he showed that the degree of complexation increases when the degree of quaternization decreases. This phenomenon was explained as an increase of mobility of the chains when they are less charged. As the weak polyelectrolyte becomes more densely charged, the structure evolves from a looped complex to a more ladder-like structure in which the charge matching is not perfect anymore.

The concentration is also a key point in the stability of PEC. c^* is usually lower for polyelectrolytes compared to non-charged polymers because of the stretched conformation induced by electrostatic repulsions. Therefore, most studies have been carried out at very low concentration in order to remain in the dilute regime. When the concentration is increased Philipp (1989) showed that the molar mass of the aggregate increases in parallel. More recently, Dautzenberg (1997) established that for mixtures of poly(styrene sulfonate) with poly(diallyldimethylammonium chloride), the size of the aggregates a_g increases with the concentration c following the power law: $a_g \sim c^{0.82}$.

1.4.4.1.3. Colloidal complexes

Polyelectrolyte complexes can also be formed as colloidal complexes. The polymers aggregate to form dispersed particles which are bigger than in the case of purely soluble PEC: a milky dispersion is obtained. The stability of such dispersions is usually kinetic and is ensured by an excess of either positive or negative charges in the system. The morphology of the particles is core-shell, the core being formed by the electroneutral complex and the shell by the charged polymer in excess (cf **Figure 1-14**).

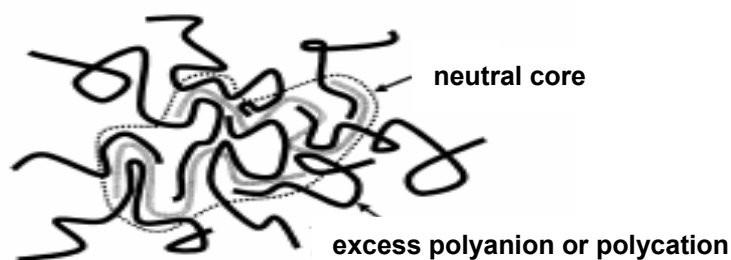


Figure 1-14: core-shell structure obtained by non-stoichiometric mixing of polyanions with polycations.

The first studies on colloidal PEC was carried out by Fuoss and Sadek (1949), by mixing poly(4-N-butyl-pyridinium) with sodium polyacrylates and sodium polystyrene. Michaels (1961) studied the stoichiometry of various systems using turbidimetry and proved that sedimentation occurs at 1:1 molar charge ratio. The most recent studies in this field draw the same conclusions as Michaels did more than 40 years ago, i.e. that a charge imbalance is necessary for stabilization; such complexes agglomerate near the isoelectric point. Scattering methods and optical density measurements are still preferred to study such agglomeration processes.

For example, Buchhammer studied systems based on poly(maleic acid-co-propene) or poly(arylamide-co-sodium acrylate) mixed with poly(diallyldimethylammonium chloride) (PDADMAC) (2003) and poly(maleic acid-co-propene) mixed with poly(ethyleneimine) hydrochloride (2004) to show the importance of the mixing procedure. In particular, he pointed out that the isoelectric point should not be crossed during addition of the titrants, this leading to loss of stability.

Dragan also explored the relationship between stoichiometry, addition of titrants and stability of PEC dispersions. She studied successively PEC formed by Poly(acrylic acid) and copolymers of acrylic acid and itaconic acid or maleic acid mixed with N,N-dimethyl-2-hydroxypropylenammonium chloride based polycations (1996, 1998), Poly(styrene sulfonate) mixed with the same polycation (2001), poly(sodium 2-acrylamido-2-methylpropanesulfonate) (PAMPS) mixed with PDADMAC (2004), random copolymers of AMPS, and either *t*-butylacrylamide (TBA) or methyl methacrylate (MM) mixed with poly(diallyldimethylammonium chloride). Dragan pointed out the aggregation at the isoelectric point and also showed that stable aggregates are easier to form at faster mixing rates. The explanation for this is the kinetic “trapping” of the titrants which form a protective shell around neutralized polymers (cf. **Figure 1-15**).

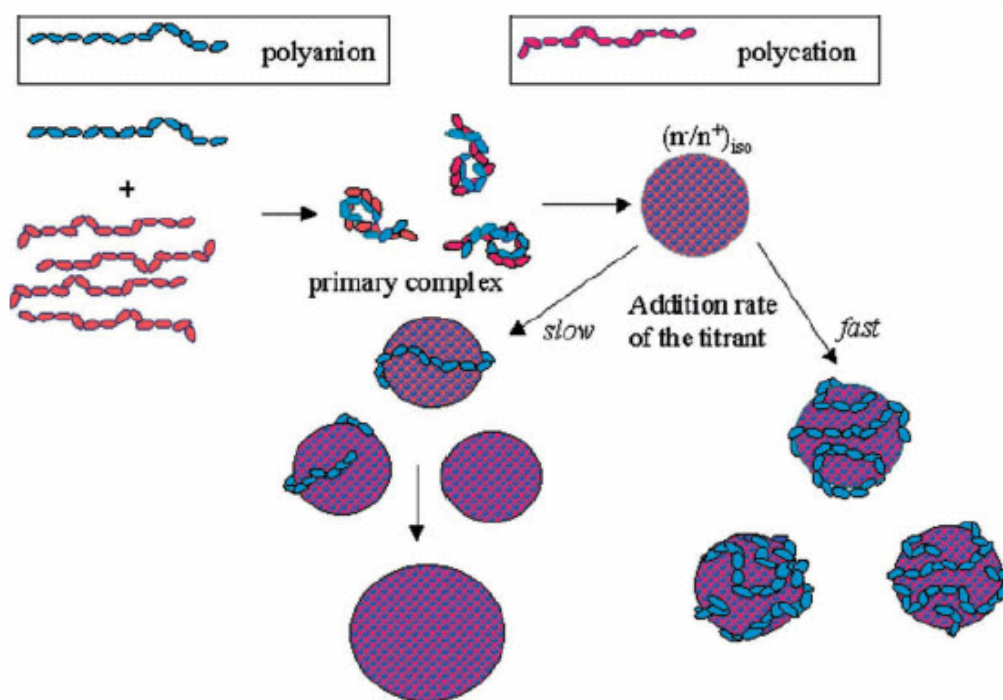


Figure 1-15: influence of the titrant addition rate on the stability of IPEC.

During the last decade, Dautzenberg studied extensively the influence of salt on mixtures of a strong, polyanion poly(styrene sulfonate) and a weak polyanion, poly(methacrylic acid) with PDADMAC (Dautzenberg 1999, 2000, 2002, 2003). Different results are obtained depending on the strength of the polyanion: with weak ones addition of salt usually leads to the separation of the aggregates into smaller subunits and finally to break-up; with strong ones, the complex may be salted-out and its precipitation is favoured. However, these are not general rules and may not apply to other systems.

1.5. Polymeric networks

Most polymeric networks result from the chemical crosslinking of macromolecules. Thus, in 1839, Goodyear synthesized the first permanently elastic rubber by “vulcanizing” i.e. crosslinking natural rubber using sulphur. The first completely synthetic polymer material was a network based on phenol-formaldehyde obtained in 1905 and called Bakelite. From this period on, most work has emphasized on chemically crosslinked gels; but from a technological as well as scientific point of view, physically crosslinked materials are attracting more and

more attention. The fact that, in such materials, the junction points are not permanent gives rise to new interesting properties.

For example, the strength of physically crosslinked gels depends on the nature of the crosslinks. Whether hydrophobic interactions, hydrogen bonds or electrostatic interactions are responsible for the building-up of the gel has a strong influence on its behavior. It is possible to distinguish strong and weak physical gels. Under large deformation, the former have a tendency to rupture and can be reformed only by heating and crossing an order/disorder temperature. The latter are structured fluids and therefore have a liquid-like behavior under strain, meaning that they will flow rather than fail. The difference is mostly due to binding energies: typically, weak gels have binding energies of only a few kT while it is significantly higher for strong ones.

1.5.1. Gelation in biopolymers

Most work on physical gels has been carried out on systems formed by only one polymer which can undergo a phase transition. Such systems are numerous in nature and often involve protein denaturation, usually induced by heat. This is what happens when ovalbumin (egg protein), serum albumins, chymotrypsin, soy proteins, bovine or milk globulin are heated: the spatial conformation of these proteins is modified leading to gelation. X-ray data showed that in such transitions, the proteins conformation is only slightly modified keeping an overall globular shape: the exposition of few hydrophobic parts leads to the formation of intermolecular β -sheets instead of intramolecular ones. Denaturation can be induced by other means like pH modification, addition of a non-solvent or enzymatic phenomenon. For example, in food industry, the enzyme driven gelation of milk casein is how yoghurt and cheese are produced.

Another gelation mechanism in biopolymers is the formation of helical structures. Gelatin is a polypeptide obtained by the hydrolytic degradation of collagen which exhibits such behavior. Above 40°C , gelatin dissolves and the polypeptides exist as flexible single coils. Upon cooling, transparent gels are formed consisting of extended physical junction zones characterized by triple-helical collagen-like sequences. The same behavior is observed for some polysaccharides extracted from seaweed like carrageenan and alginates. It was shown that upon heating-cooling cycles, they undergo a transition from disordered molecules to double stranded helices.

1.5.2. Gelation in Hydrophobically modified polymers

Hydrophobically modified water-soluble polymers (HMP) are formed by a hydrophilic backbone onto which hydrophobic groups are chemically attached. In industry, they are also referred to as associative thickeners (Strauss 1989). The hydrophobic tails behave similarly to free surfactant, forming micelles under appropriate conditions. This phenomenon gives rise to unique solubility and rheology features which are widely used for industrial applications. In the 80's, Landoll (1982) was the first one to describe the use of HMP as rheology modifiers for water borne paints. In his study, he used hydrophobically modified hydroxyethyl-cellulose (HMC). This type of HMP is still one of the most widely used in formulations, along with hydrophobically modified alkali-soluble emulsions (HASE) and hydrophobically modified ethoxylated urethanes (HEUR).

1.5.2.1. Hydrophobically modified cellulose

Cellulose is one of the most common polymers in nature. In its native state, it forms large crystalline regions and is not soluble in water. To prevent crystallization and make cellulose water soluble, side chains are grafted on the cellulose backbone, forming so called hydrophobically modified cellulose (HMC). The side chains are usually aliphatic having a number of carbon atoms typically between 10 and 20. Their repartition is random. The degree of hydrophobization is low, typically around 1% in moles (Thuresson 1995), which is sufficient to modify the rheological properties significantly but low enough to ensure that the water solubility is still good. In water, the hydrophobic pendant chains have a tendency to aggregate. The association mechanism is comparable to self-association of surfactants. The hydrophobic groups form a micelle-like structure which surface is covered by the hydrophilic polymer backbone. At low concentration, the aggregation process can be mainly intramolecular, and the viscosity is lower compared to the one of non-modified polymer (Bock 1989, Tanaka 1990, Gelman 1987, Aubry 1994, Tam 1998). When the polymer concentration reaches a critical value (critical aggregation concentration CAC), intermolecular interactions occur, giving rise to a network structure (cf. **Figure 1-16**). The strength of this network depends mostly on the degree of hydrophobization, the length of the hydrophobic groups R and the distribution of these groups along the chain.

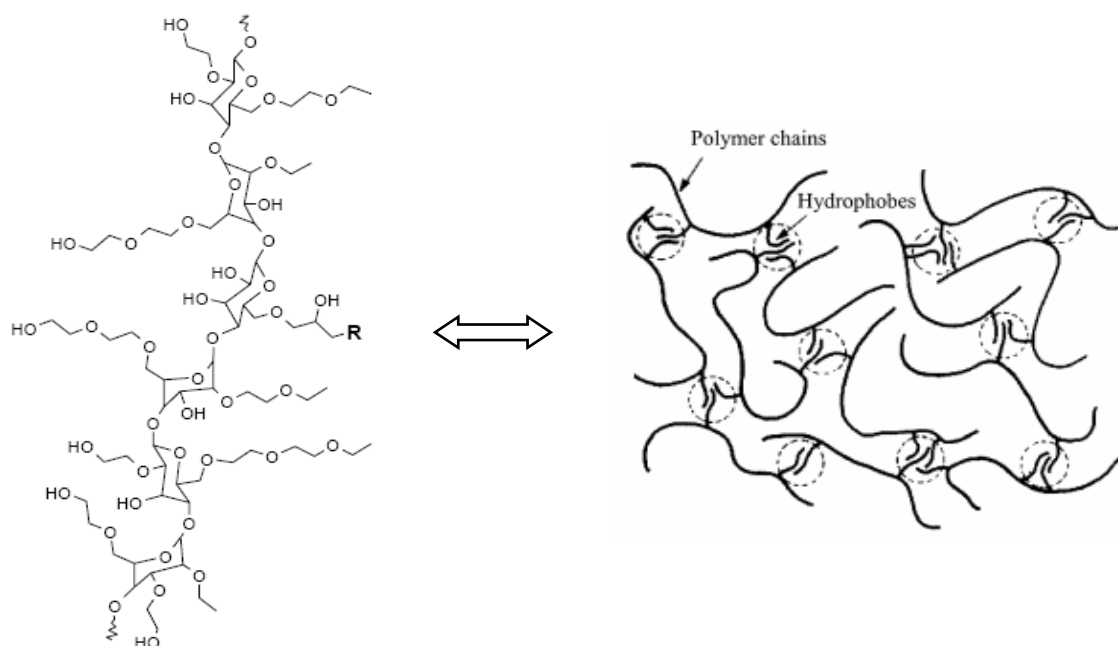


Figure 1- 16: chemical structure of HMC and schematic representation of their gelation mechanism.

1.5.2.2. Hydrophobically modified alkali-soluble emulsion

The hydrophobically modified alkali-soluble emulsions (HASE) are classified as hydrophobically modified associative polymers with charged backbones. They are based on acrylic or methacrylic monomers, which provide the ionic sites. These acrylic monomers are copolymerized with hydrophobic monomers, usually composed of a polyethylene oxide chain, providing flexibility to which an aliphatic chain is grafted, providing the hydrophobic character. Ethyl acrylate can also be incorporated into the chain to enhance hydrophobic interactions. The general structure is schematized in **Figure 1-17** (Seng 2000, Tam 2000, Dai 2001).

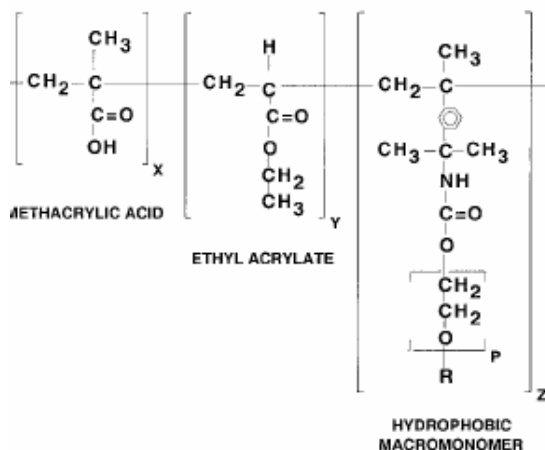


Figure 1-17: chemical structure of hydrophobically modified alkali-soluble emulsions.

Typically, the molar content of hydrophobic macromonomers in the chain is close to 1%. The ratio between methacrylic acid and ethyl acrylate is roughly equimolar in industrial products. This family of polymers is called alkali-soluble as they are soluble in water only above a critical pH value. Under acidic conditions, the carboxylic acid groups are not charged and the chains are collapsed. The hydrophobic groups are forming intramolecular aggregates. Upon neutralization, the acid groups become negatively charged and repulse each other. Thus, the chains expand and their solubility in water is greatly increased. The hydrophobic macromonomers end units from one chain can interact with the hydrophobic units of other chains, forming a transient network: the viscosity of the emulsion increases typically by several orders of magnitude. The gelation mechanism is essentially similar to the one observed for hydrophobically modified cellulose except that additional hydrophobic interaction result from the aggregation between short ethyl acrylate blocks (Tan 2000).

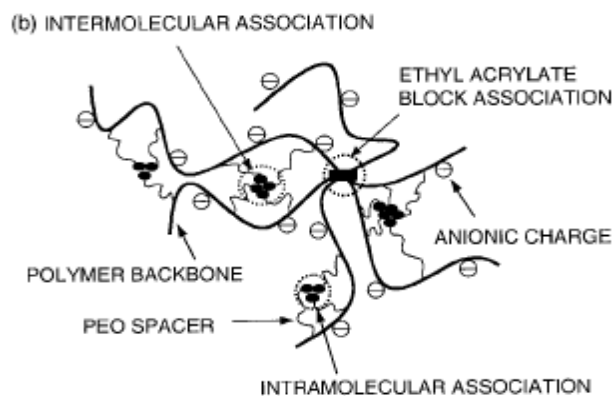


Figure 1- 18: schematic representation of the gelation mechanism in HASE.

HMC and HASE are the most common comb-like hydrophobically modified polymers. However, a large variety of other monomers can be copolymerized with small quantities of hydrophobes, yielding other comb-like HMP. For example, polyacrylamide based backbones have been studied (Xie 1996, McCormick 1988, Jenkins 1991, Hwang 1995, Hill 1991, Kästner 1994) as well as natural polymers like guar (Aubry 1994), pullulan (Akiyoshi 1992), alginates (Sinquin 1993) or chitosan (Desbrières 1997). The hydrophobic tails are mostly aliphatic but it has been shown that aromatic groups (Yekta 1993, Hu 1990, Duhamel 1992, Uemura 1995) or fluorinated chains (Kästner 1994) lead to similar rheological properties.

1.5.2.3. Hydrophobically modified ethoxylated urethanes

Contrary to HMC and HASE in which hydrophobized polymers have a comb like structure, hydrophobically modified ethoxylated urethanes (HEUR) are examples of end-capped polymers. They have a block structure, formed by a hydrophilic polyethylene glycol in the middle and two hydrophobic parts at each end (Annable 1993, Yekta 1993, Semenov 1995a, Tanaka 1992). Their molar mass is low with regard to typical polymers used as thickeners, typically between 15kDa and 50kDa (Glass 2001). The commercial approach to produce HEUR is to first react polyethylene glycol with a slight excess of diisocyanate. These diisocyanate end-functionalized chains are reacted with long chain alcohols to yield the final polymers, which have an ABA structure.

The hydrophobic groups can interact but following a different mechanism from the one described for HMC and HASE. Under dilute conditions, the ABA polymer chains are free; above the critical micellar concentration (CMC), they aggregate in isolated flower-like micelles (Wang 1990, Semenov 1995b). As concentration is increased, these micelles tend to agglomerate into clusters as some molecules have one hydrophobic part in one micelle and the other hydrophobic part in another micelle. If the concentration is further increased, the bridging between clusters leads to the formation of a 3D network (Yekta 1993, Tam 1998).

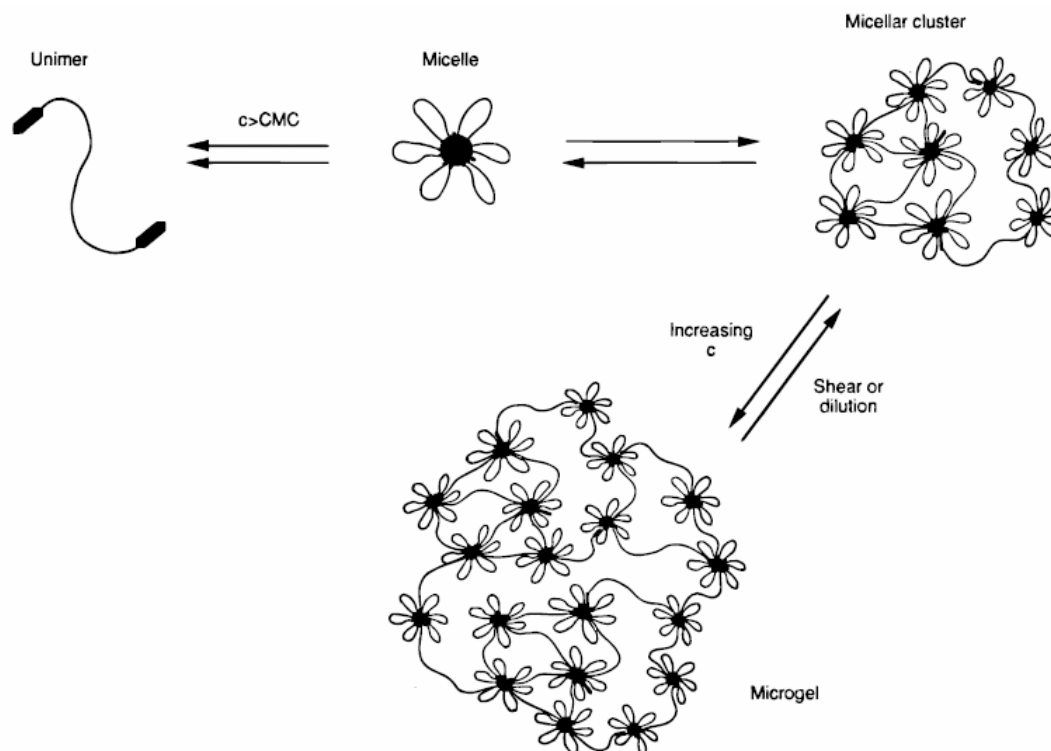


Figure 1-19: schematic representation of the gelation mechanism in HEUR

1.5.3. Gelation in polyelectrolytes

1.5.3.1. Diblock polyelectrolytes

The most widely studied diblock polyelectrolytes are those based on poly(styrene-*b*-acrylic acid). Because of the poor water solubility of the polystyrene block, these molecules can form micelle-like structures in aqueous solutions. A core formed by the polystyrene blocks is surrounded by a swollen poly(acrylic acid) shell. Other morphologies like rods, lamellae and vesicles have been observed (Cameron 1999, Zhang 1995) but will not be discussed further.

The micellar systems have been widely studied by Korobko (2005) at concentration ranging from 0.45wt% to 4.4wt% and at a neutralization degree of 50%. He showed that when the concentration is increased, the rheological behavior of the solution evolves from a Newtonian behavior to gel-like behavior. The building of the gel is due to the interpenetration of the poly(acrylic acid) blocks from the corona of the micelles. Since poly(acrylic acid) is a weak polyelectrolyte, the behavior of the micelles can be modified by changing the ionic strength or the pH: an addition of salt to such a system leads to a decrease in viscosity because of the shrinkage of the poly(acrylic acid) chains and therefore the reduction of overlap between micelles (Bhatia 2001) while addition of sodium hydroxide leads to an increase in viscosity due to the expansion of the poly(acrylic acid) chains (Ballauff 2003).

1.5.3.2. Triblock polyelectrolytes

Triblock polymers have structures similar to end-capped polymers. They differ only in the fact that at least one of their blocks is ionizable. Tsitsilianis has carried out an extensive study on telechelic ionizable polymers formed by a central poly(acrylic acid) block and two hydrophobic end blocks (Tsitsilianis 2000a, 2000b, 2002). In aqueous solutions, such polymers form micelle-like structures. Above a critical concentration, a gel is formed. The presence of an ionizable group in the polymer enables to fine tune the rheological properties of the system. When the pH is increased, the carboxylic groups dissociate; this leads to a stretching of the central block of the macromolecules. In such an extended conformation, the probability to form loops is lowered and the probability to form bridges is enhanced. Therefore, the critical gelling concentration is lowered when pH is increased. Similarly, at a given concentration, the gel becomes stronger when pH is increased. Thus, the rheological properties of ABA terpolymers can be modified by changing both the concentration and the pH.

Katsampas and Tsitsilianis also studied (ABC) triblocks formed of poly-(styrene-*b*-sodium acrylate-*b*-*n*-butyl methacrylate) (Katsampas 2005). Styrene and *n*-butyl methacrylate are not compatible; this means that depending on the conditions, it is possible to form micelles with two different hydrophobic cores. Thus, the probability of bridging is enhanced and the critical concentration is decreased compared to an ABA polymer.

Finally, he and his coworkers studied the rheological behavior of the triblock polyampholyte poly(acrylic acid-*b*-2-vinylpyridine-*b*-acrylic acid) (Sfika 2003, Bossard 2005). This polymer differs from the ones studied previously as it does not have a hydrophobic part. Nevertheless, at a proper pH value (fixed at 3.4 in this study), a network is formed despite the lack of hydrophobic associating groups. The transition from isolated species to a transient network was clearly visible as the elastic modulus changed from being frequency dependent to being frequency independent (cf. next paragraph). The structure of such gels has not yet been elucidated.

1.5.3.3. Polyelectrolyte complexes

As detailed in paragraph 1.4, most work undergone on inter-polyelectrolyte complexes concerns the determination of their phase diagram, their stability, their stoichiometry etc. Besides hydrophobically modified systems, very few studies focus on the rheological behavior of IPEC. The major reason for this is that the large majority of studies deal either with very diluted systems, which have a viscosity close to water or with more concentrated systems which macroscopically phase separate into a solid complex and a water-like supernatant. Hereafter, works dealing with purely hydrophilic based polyelectrolyte complexes are summarized.

Tsitsilianis et al. studied the rheological characteristics of the triblock polyampholyte poly(acrylic acid-*b*-2-vinylpyridine-*b*-acrylic acid) (PAA-P2VP-PAA). It was found that PAA-P2VP-PAA self-assembled into a network structure despite the lack of hydrophobic associating units. Above the percolation concentration c_g , a transient network formed due to interchain attractions, and above the transition concentration c' , a three-dimensional network formed. The solution viscosity increased with concentration, and the zero-shear viscosity displayed three different regimes of concentration dependence. At semi-dilute concentrations ($c < c_g$), the viscosity was Newtonian for all shears and $\eta_0 \sim c^{0.58}$, close to the predicted dependence for unentangled polyelectrolytes. At higher concentrations, the viscosity had a slight thickening and then thinning with increasing shear. The zero shear viscosity in the intermediate regime ($c_g < c < c'$) had a greater dependence on the concentration than in the concentrated regime. At

concentrations above c_g , a hysteresis loop was observed, with the zero-shear viscosity matching in the concentrated regime ($c > c'$), but not matching in the intermediate regime. These different response regimes were due to the associations formed in solution, with intramolecular attraction occurring at low concentrations and an intermolecular network forming above c_g . Dynamic shear experiments found that the solution was a viscoelastic fluid in the intermediate regime, with G' and G'' both dependent on ω and a crossover from $G'' > G'$ to $G' > G''$ seen at the lowest frequencies. Above c' , the moduli were almost independent of the frequency and $G' > G''$, so the triblock solution was an elastic gel.

Liu et al. (2001, 2003) studied mixtures of a rigid cationic cellulose ether with polyanions. This work was focused on hydrophobically modified polyanions but mixtures of cellulose with poly(2-acrylamido-2-methylpropanesulfonate) have also been investigated. Even though PAMPS does not carry any hydrophobic groups, it also acts as a viscosity enhancer when added in small amount to a cellulose solution. A static rheological investigation of this system was undertaken: the zero shear viscosity of mixed systems is enhanced by several orders of magnitude, compared to the viscosity of a cellulose solution, and the viscosity enhancement increases with increasing polyanion concentration. This pattern was taken as an indication of an increasingly higher level of polyanion cross-links between entangled polycation chains. The viscosity profiles of all polyanion-poor mixed systems display shear thinning characteristics with no evidence of shear thickening: below a critical shear rate (γ_{thin}), viscosity is independent of shear rate (Newtonian regime), and above γ_{thin} , it rapidly decreases with increasing shear rate. The value of γ_{thin} shows a marked dependence on the fluid composition, decreasing with increasing polyanion content. In all mixed systems, γ_{thin} is lower than the value recorded for a cellulose solution, which is weakly shear thinning but only under high shear rate. Using Carreau-Yasuda model, Liu et al. determined the relaxation time, equal to the inverse of the critical shear rate γ_{thin} . The relaxation times of the fluids increase with increasing polyanion concentration from 0.02s (pure cellulose) to 0.80s (8wt% of polyanion in mixture), reflecting an increase in the size and/or number of cross-linking points between polymer chains as more polyanions are added to the system. If more polyanion is added to cellulose, the system macroscopically phase separates.

Recently, the rheological behavior of chitosan/alginate solutions was investigated in relation to gelation and polyelectrolyte complex formation by Shon et al.(2007). The viscoelastic gel state of chitosan/alginate complex solutions was mainly determined according to the criteria that $G' > G''$, and that $\tan\delta$ increases with the frequency. The sol–gel state was significantly affected

by the solution concentration. Studying mixtures at 1wt%, 2wt% and 3wt%, they established that gelation is more pronounced at lower concentration and that a transition towards a sol-state is observed as concentration increases. Their explanation for this phenomenon is that the PEC formation was relatively weak and slow, taking place mostly at the interface of the two solutions at 1wt%: domains are entrapped by the PEC which were found to be highly elastic gel-aggregates, leaving the solution in a viscoelastic gel state. Meanwhile, at a higher concentration, the conversion of chitosan/alginate into PEC precipitates was more active in reducing the number and size of the gel domains, resulting in a viscoelastic sol state. The PEC precipitate formed in the chitosan/alginate solutions had the shape of a fiber with a microfibrillar structure. Their conclusions suffer the major drawback that the homogeneity of the sample is not taken into account: using a concentric cylinder rheometer, it is difficult to compare data obtained for mostly liquid samples with data obtained for mostly precipitated ones...

Zhang and Huang studied the interactions of carboxymethyl-cellulose with poly(acrylamide-co-dimethyldiallylammonium chloride) at various ratios and in the concentration range 0.7wt% to 1wt%. They determined that the viscosity of such mixtures is significantly higher than expected for non-interacting materials and conclude that, although there are other parameters determining the degree of viscosity enhancement, it was mainly dependent on the development of homogeneous intermacromolecular complexation between the two oppositely charged polyelectrolytes in aqueous solution. Maximum viscosity enhancement, corresponding to an increase of viscosity of 20 times compared to the pure polyanion used as a reference, was observed for the complex solution having a poly(acrylamide-co-dimethyldiallylammonium chloride) content of 67wt%. These complex solutions behave as a typical non-Newtonian shear-thinning fluid.

2. In-situ preparation of colloidal inter-polyelectrolyte complexes

2.1. Introduction

2.1.1. Motivation

Polyelectrolytes are used in industry in many formulations. As examples, flocculating agents or thickeners can be mentioned (Glass 1986, Jenkins 1990, Annable 1993, Dautzenberg 1994). These two applications represent an already large but still developing market. In both cases, the polyelectrolytes used have to be of high molar mass to be efficient. The problem when handling long polymer chains is that they lead to high viscosities when dispersed in a good solvent. Most polyelectrolytes are fully or at least partly water-soluble. This means that a solution of these polymers in water usually has a high viscosity and is therefore difficult to handle. To circumvent this problem, most high molar mass polyelectrolytes for industrial purposes are delivered as powders or as dispersions in organic solvents. These so-called water-in-oil (w/o) dispersions have become undesirable from an environmental point of view and will have to be replaced by solvent free formulations in coming years. Powders are the most effective formulations for polymers regarding shipping costs and storage but have the drawback that the redispersion of a high molar mass dry polymer can be long and uneasy. Thus, one of the big challenges in the near future is to produce, in a cost effective way, easy to use and to handle waterborne formulations containing hydrophilic polymers. To do so, the peculiar properties of polyelectrolytes can be used.

The aim of the work presented in this second chapter is to prove that new formulations of high molar mass hydrophilic polyelectrolytes, completely free of organic solvents, can be developed. The used concept is based on the phenomenon explained in paragraph 1.4, stipulating that colloidal IPEC can be obtained when two hydrophilic polymers interact one with each other. However, the approach exposed here differs significantly from the work done so far in this field. While most studies up to now focus on building complexes via mixing experiments at low concentrations, the work described in this chapter aims at producing stable dispersions at significantly higher concentrations by using an in-situ inter-polyelectrolyte complexation.

To the best of our knowledge, no work has been so far published on this particular approach. Therefore, this work focuses on determining the reaction conditions which are suitable for the preparation of stable dispersions under industrially relevant conditions.

2.1.2. Potential mechanism of formation of stable dispersions

The principle of the experiments described hereafter is to polymerize a positively charged monomer in the presence of a negatively charged polymer. This process is sometimes referred to as “template polymerization” even though the term may be usurped, as there is no evidence of a selective interaction of the monomer with the polymer prior to polymerization.

To be able to determine proper conditions for synthesizing stable dispersions, the reaction mechanism is assessed, in order to point out relevant parameters.

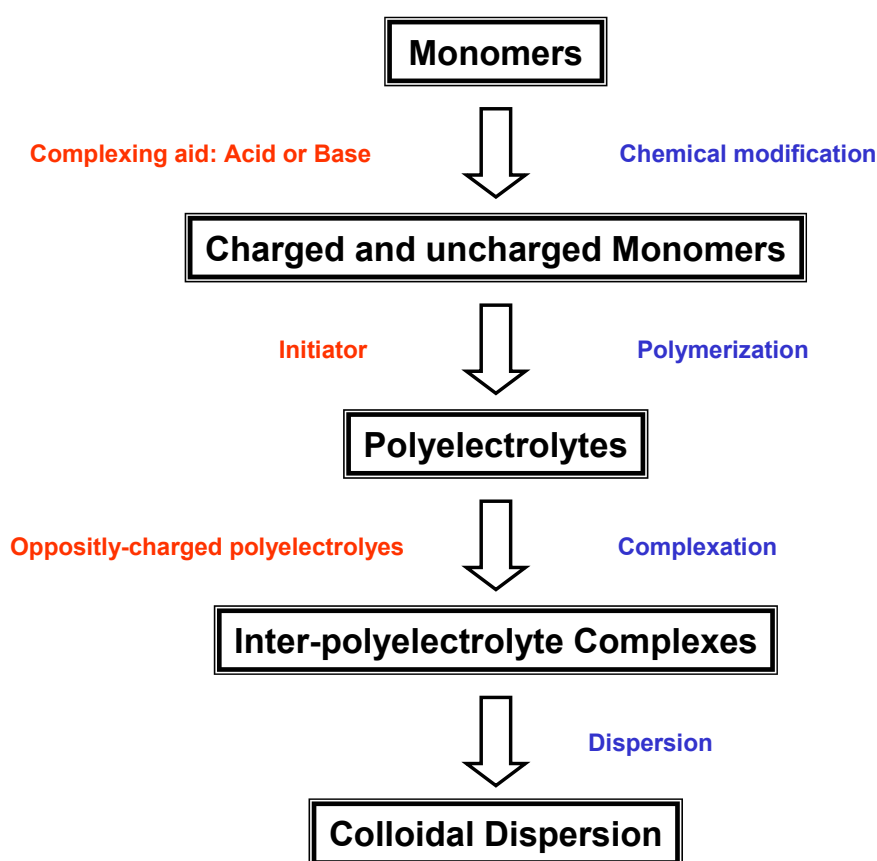


Figure 2-1: scheme of the steps leading to the formation of a stable dispersion.

Figure 2-1 represents a potential reaction scheme which could lead to the formation of a colloidal dispersion. The three colors present in the scheme represent: in black, the resulting

products of each step; in red, the chemical or reagent necessary to obtain this product; in blue, the chemical or physical process taking place within the system.

The process can be separated into three main steps:

- **Polymerization:** the cationic/catiogenic monomers are polymerized or copolymerized using a radical initiator.
- **Complexation:** the positively charged polymers start to interact with negatively charged chains, referred to as complexing agent (CA). Several chains of each type can interact with each other, until equilibrium is reached.
- **Dispersion:** if the ratio between the two oppositely charged polymers, the temperature, the pH etc are suitable, stable particles may be formed. In this case, the final product is a stable colloidal dispersion.

It is important to keep in mind that even if the process is described as a succession of clearly separated steps, all these steps occur simultaneously. For the sake of clarity, each one is considered and discussed separately in the upcoming paragraphs.

2.1.3. Experimental conditions

Each of the 3 steps mentioned in the previous paragraph requires specific conditions summarized in **Table 2-1**. It is assumed that the conditions required for initiation and polymerization are the same.

Table 2-1: suitable conditions for polymerization and complexation.

Step	1. Atmosphere	2. Stirring	3. Process	4. Temperature	5. pH	6. Time
Polymerization	Inert	RPM(P)	Monomer Feed	Suitable T_p	pH_p	t_p
Complexation	Ambient	RPM(C)	CA Feed	Suitable T_c	pH_c	t_c

Amongst these six parameters, it is important to first determine which ones are the most critical and second to find conditions under which both polymerization and complexation can occur effectively. This depends on the chemistry of the system under investigation.

2.1.3.1. Materials

The choice of the system is related to potential future applications. This requires that the polymers, monomers initiator etc used are commercially available and easy to react under standard conditions of pressure, temperature and atmosphere.

- **Complexing agents**

As complexing agent, the polyanion used in the first trials is poly(acrylic acid) (PAA). It is a weak polyacid with a pKa value of 4.6 (Spencer 1962).

Poly(2-acrylamido-2-methyl-1-propanesulfonic acid) (PAMPS) is tried next. AMPS is a strong acid and therefore the corresponding polymer is permanently and fully charged.

Copolymers of acrylic acid and 2-acrylamido-2-methyl-1-propanesulfonic acid are also tested. Examples of recipes for the synthesis of these polymers are given in the experimental section.

- **Monomers**

The monomers which are to be polymerized in the presence of a polyanion have to fulfil some prerequisite. They have to be commercially available, easy to handle and to react. The final polymer has to carry positive charges but it is not necessary that it is fully charged. Therefore a cationic monomer can be copolymerized with a neutral monomer.

[2-(acryloyloxy)ethyl]-trimethylammonium chloride (AETAC) is a permanent cationic monomer which is often used in industry. For instance, AETAC based polymers are used in paper chemicals as retention aids, in water treatment as flocculation agents and in cosmetics as thickeners or conditioners in shampoos. This cationic monomer polymerizes easily with acrylamide (Cabestany 1981, Griebel 1992, Rio 2007).

Recent experiments have shown that the copolymerization parameters, determined by automatic continuous online monitoring (ACOMP) of polymerization reactions, are respectively $r_1 = 0.47$ and $r_2 = 1.10$ for AETAC and AM (Gonzalez Garcia 2008). In this study, opposite trends in composition drift and final molar mass were found; low starting percentage of AETAC led to low composition drift and high molar mass, whereas the opposite was found at high starting percentage of AETAC. For a better control of the reaction and more statistical repartition of both monomers, parallel feed is the method of choice.

- **Initiator**

[2-(acryloyloxy)ethyl]-trimethylammonium chloride is a cationic acrylic monomer and this kind of monomers suffers the disadvantage that during polymerization in aqueous solutions, they might undergo hydrolysis which can lead to a reduction in the cationic nature of the

resulting polymer. In order to overcome this problem, polymerization is usually carried out in the pH range between two and five. Persulfates or redox system catalysts do not give satisfactory results under such conditions. Viscosity on storage is reduced due to the degradation of the polymer in the presence of residual persulfates. With redox system initiators, it is difficult to achieve polymerization at such low pH values.

Therefore, amongst redox, persulfates and azonitrile initiators, the last ones seem to be the best choice. Another advantage of this class of initiators is that their hydrophilicity/solubility depends on their structure and can be chosen according to the solvent and pH conditions used to carry out the reaction.

All these parameters taken into consideration, the choice of a specific initiator is essentially driven by two factors: the temperature and the duration of the reaction. Actually, these three parameters are intertwined and choosing one has consequences on the choice of the others. The choice was made to set the temperature of the reaction at fifty degrees (easy to reach and to maintain) and the reaction time at five hours.

2,2'-azobis (2-amidinopropane) dihydrochloride (V50) is a azonitrile compound very soluble in acidic aqueous solutions which shows high activity at moderate temperature (**Table 2-2**). It is used hereafter for the copolymerization of AETAC and acrylamide (AM).

Table 2-2: *solubility and decomposition properties of V50 at 50°C in water.*

Solubility (g/100g)	Half Life time (Min)	Constant of decomposition (s ⁻¹)
35.3	1100	8,3.10 ⁴

2.1.3.2. Processing parameters

- **Stirring**

The major role of stirring is to ensure a quick mixing of the fed reagents and an efficient homogenization of the reacting media. The stirring should not be too slow, otherwise this double requirement is not fulfilled. But on the other hand, it should not be too vigorous as some preliminary tests have shown that fouling and appearance of coagulate is favored by a vigorous stirring. The possible stirring range with the set up used varies between 0 and 300 rpm (rotations per minute). All experiments are carried out with a stirring speed lying just in the middle of this range, i.e. at one 150 rpm. At this speed, the homogenization is good and the formation of coagulates does not seem to be favored.

- **Reactive atmosphere**

As mentioned in **Table 2-1**, the free radical polymerization requires to work under inert atmosphere to ensure the efficiency of the initiator. Gaseous nitrogen is bubbled in the reactor during the entire duration of the experiment and the initial feed is deoxygenated for 30 minutes before initiator is introduced.

- **Feeding strategy**

There are four charges which have to be introduced into the vessel: the complexing agent, two monomers and the initiator. Concerning the initiator, feeding it during a free radical polymerization is recommended both to obtain a narrow distribution of the molecular weights and to ensure full conversion of the monomers (O'dian 2004). Concerning the complexing agent and monomers, the two charges are fed in parallel (at the same speed). This helps to ensure a constant polycation/polyanion ratio in the reactor and possibly to get a better reproducibility regarding the stoichiometry of the formed complexes.

2.2. Polymerization

Prior to attempting to form dispersions, proper conditions for the copolymerization of AETAC with AM are determined. The goal of the work described in this paragraph is to produce solutions of poly(AETAC-co-AM) with a viscosity around 20Pa.s. A polyanion will subsequently be added to the recipe of this solution to try to form dispersions and reduce this viscosity.

2.2.1. Materials

AETAC is provided by BASF (transparent liquid >98%). Acrylamide is purchased from Fluka (powder >98%). Both monomers are used as received without further purification.

Reacting conditions are as described in the previous paragraph: 150 rpm, 50°C under Nitrogen atmosphere.

The initiator, 2,2'-azobis(2-amidinopropane) dihydrochloride purchased from Fluka (powder, >99%) is used as received.

Initiator and monomers diluted to a concentration of either 30wt% or 10wt% using distilled water and are fed over two hours in three separate dropping funnels.

The detailed reaction pattern is described in the experimental section.

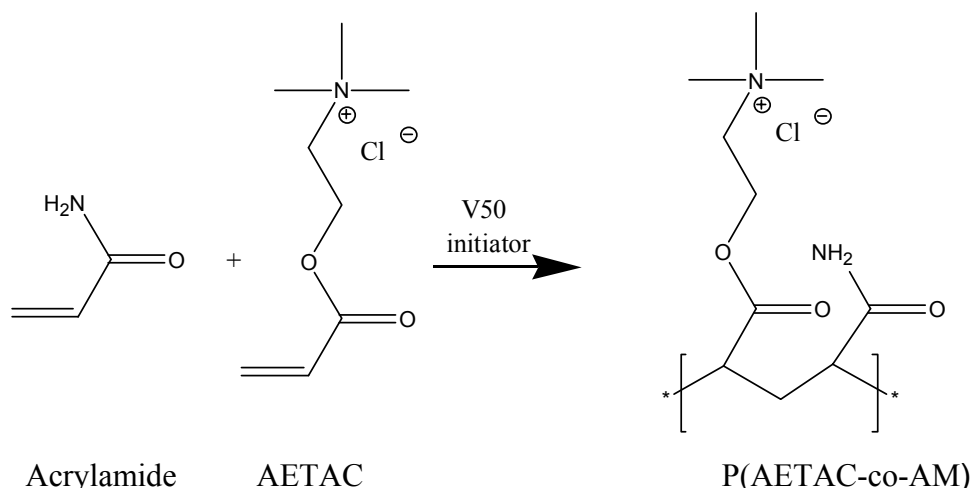


Figure 2-2: copolymerization pattern of AETAC and AM.

Three different ratios of AETAC to AM are tested. The amount of AETAC in the copolymer corresponds to the charge density (CD) of the polymer. The charge densities tested are: 25, 35 and 43 percent.

2.2.2. Experimental part

2.2.2.1 Synthesis of P(AETAC_{0.43}-co- Acrylamide_{0.57})

2.2.2.1.1. Solution polymerization at 15wt%

As mentioned earlier, the molar mass of the synthesized polymer depends on the rate of initiation of the polymerization process, which depends on the temperature and on the type and quantity of initiator that is used. The molecular weight of the polymer is directly influencing the viscosity of the final product. Therefore, the quantity of initiator necessary to reach full monomer conversion while the viscosity of the solution remains acceptable (i.e. around 20 Pa.s) has to be assessed.

Five concentrations of initiator are tested: 0,1%, 0,2%, 0,5%, 1% and 2%. These percentages are expressed as molar fraction of the constitutional repeating unit (CRU) which is a theoretical unit composed in this case of 43% of AETAC and 57% of AM. The CRU used in the coming paragraphs always corresponds to a theoretical monomer composed of x mole percent of AETAC and 1-x percent of AM. The results obtained for five concentrations of initiator are gathered in **Table 2-3**.

Table 2-3: solution copolymerization of 43% of AETAC and 57% of AM at 15wt%.

Product	mol % of V50 by mole CRU	Brookfield viscosity 15 wt % (Pa.s)	pH
S43I01	0.1	>1000	3.5
S43I02	0.2	>1000	3.4
S43I05	0.5	>1000	3.8
S43I1	1	112	3.6
S43I2	2	21	3.7

Except for S43I2, the viscosity of all solutions is much higher than the targeted value. Such high viscosity solutions can not be handled easily. To reduce the viscosity without further increasing the quantity of initiator in the recipe, two approaches can be considered:

- A convenient chain transfer agent can be used to reduce the molecular weight of the polymer synthesized. For example, sodium formate could be suitable to diminish the molar mass of poly(acrylamide) in solution polymerization.
- The solids content can be diminished. This has the additional advantage that the recipe remains very simple as only three reagents are used.

2.2.2.1.2. Solution polymerization at 15wt% using a chain transfer agent

The chain transfer agent, sodium formate, will be used in proportions ranging between 0.5% and 6% by weight of acrylamide. Different quantities of initiator and chain transfer agent are tested.

Table 2-4: solution copolymerization of 43% of AETAC and 57% of AM in presence of sodium formate at 15wt%.

Product	mol % of V50 by mole CRU	wt % of sodium formate to AM	Brookfield Viscosity (Pa.s)	pH
S43I01F0.5	0.1	0.5	>1000	3.7
S43I01F2	0.1	2	32.3	4.1
S43I01F3	0.1	3	18.4	4.3
S43I01F4.6	0.1	4.3	16.9	4.7
S43I02F3	0.2	3	12.4	4.2
S43I02F4.3	0.2	4.3	15.3	4.5
S43I02F4.3	0.3	3	12.3	4.6
S43I04F3	0.4	3	9.1	4.7
S43I1F6	1	6	1.6	5.1

A clear decrease in viscosity is observed when sodium formate is added except in product S43I01F0.5 in which the amount is not sufficient to have a visible effect. This strategy seems efficient to decrease the viscosity of the synthesized solutions but has the drawback that pH is slightly increased as sodium formate is a weak base. This could be prejudicial as the ester group on AETAC can undergo hydrolysis when pH is increased (Euranto 1969).

2.2.2.1.3. Solution polymerization at 5%

The other option to decrease the viscosity consists in reducing the total solids content drastically to 5wt% instead of 15wt%. All the other parameters remain similar to the ones used to synthesize the dispersion S43I01 etc.

Table 2-5: solution copolymerization of 43% of AETAC and 57% of AM at 5wt%.

Product	mol % of V50 by mole CRU	Brookfield viscosity 5 wt % (Pa.s)	pH
S43I01'	0.1	27.2	3.8
S43I02'	0.2	19.2	3.6
S43I05'	0.5	14.7	3.8
S43I1'	1	11.1	3.4
S43I2'	2	2.3	3.7

The decrease of solids content influences the viscosity of the final product dramatically. When working at a solids content of 5wt%, the viscosities of the solutions are more in accordance with the values targeted, lower than 20Pa.s when the concentration of initiator is equal to or higher than 0.2%.

The values of pH are also significantly lower compared to what is measured when sodium formate is added. Regarding the chemical stability of the polymer, pH < 4 are preferable and this approach might be more promising in this respect.

2.2.2.2. Synthesis of P(AETAC_{0.25} –co- Acrylamide_{0.75})

It is clear that solution polymerizations carried out at 15 wt % without addition of chain transfer agent lead to very high viscosities. A similar approach as in the previous paragraph is used to synthesize a copolymer containing three quarters of acrylamide. The first set of experiments is carried out at 15wt% with addition of increasing amounts of sodium formate (**Table 2-6**) while the second set is carried out at 5wt % using only initiator and AETAC+AM as monomers(**Table 2-7**).

Table 2-6: solution copolymerization of 25% of AETAC and 75% of AM in presence of sodium formate at 15wt%.

Product	mol % of V50 by mole CRU	wt % of sodium formate to AM	Brookfield Viscosity (Pa.s)	pH
S25I01F2	0.1	2	-	-
S25I02F2	0.2	2	-	4.8
S25I02F3	0.2	3	36.0	5.0
S25I02F3.8	0.2	3.8	19.1	5.1
S25I02F4.3	0.2	4.3	13.3	5.2
S25I04F3	0.4	3	11.1	4.8

Table 2-7: solution copolymerization of 25% of AETAC and 75% of AM at 5wt%.

Product	mol % of V50 by mole CRU	Brookfield Viscosity (Pa.s)	pH
S25I01	0.1	34.8	3.7
S25I02	0.2	19.3	3.2
S25I05	0.5	13.2	3.6
S25I1	1	11.7	3.3

Table 2-6 and **Table 2-7** show the same global trend as observed previously: the more initiator and/or transfer agent is added, the lower the viscosity. The products are slightly more viscous compared to the serie S43 because of the higher proportion of AM which usually yields higher molar masses (Gonzalez Garcia 2008). Again, when sodium formate is added, pH values are too high to ensure a proper stability of the polymer.

2.2.2.3. Synthesis of P(AETAC_{0.33} –co- Acrylamide_{0.67})

A last set of experiments is carried out in order to produce copolymers containing one third of AETAC and two third of AM. Only reactions at a total solids content of 5wt% without addition of sodium formate are carried out.

Table 2-8: solution copolymerization of 33% of AETAC and 67% of AM at 5wt%.

Product	mol % of V50 by mole CRU	Brookfield viscosity (Pa.s)	pH
S33I01	0.1	28.4	3.1
S33I02	0.2	22.3	3.3
S33I05	0.5	17.3	3.5
S33I1	1	13.2	3.6
S33I2	2	3.9	3.6

Table 2-8 shows that the viscosities as well as pH values for a 5wt% solution are in the appropriate range for initiator concentrations higher than 0.1%. pH values are identical to what has been measured so far under similar conditions.

At a concentration of 15wt%, the copolymerization of AETAC and AM yields very high viscosity whatever the ratio between the two monomers. The two approaches tested to reduce this viscosity, either using a chain transfer agent or reducing the solids content, are equally efficient. To keep the recipe as simple as possible in this “proof of concept” study, the second approach is privileged. Therefore, in the next paragraphs, all experiments realized in the presence of a complexing agent are carried out at a total solids content of 5wt%.

2.2.3. Conversion and side products

The sharp increase in viscosity observed during polymerizations indicates that polymer chains are formed quickly. To confirm this visual observation, $^1\text{H-NMR}$ spectra of samples S43I01, S33I01 and S25I01 are measured in D_2O . It is assumed that if conversion is total for these samples in which 0.1% of initiator is used, it is also total for the ones in which more initiator is initiating the polymerization.

As a reference, NMR spectra of the pure monomers AETAC and AM are measured first and plotted (**Figure 2-3** and **Figure 2-4**).

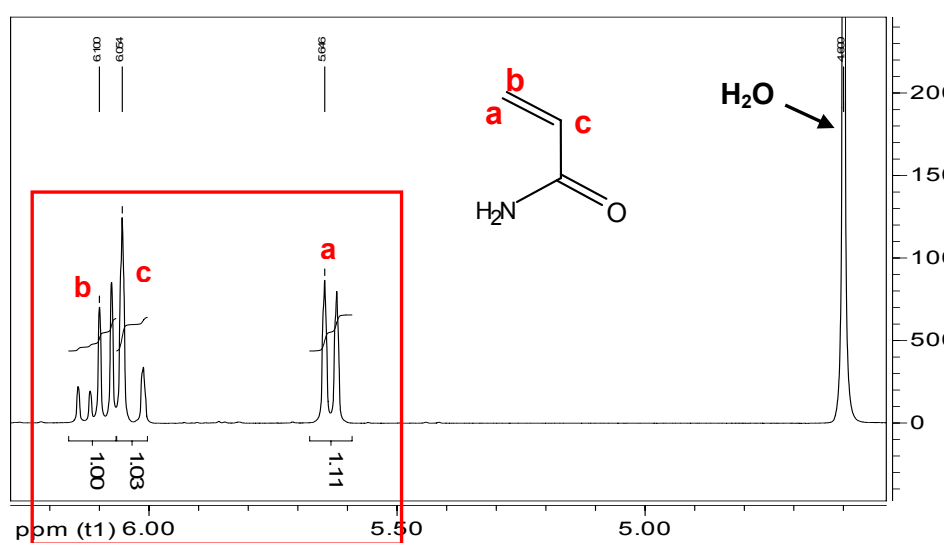


Figure 2-3: $^1\text{H-NMR}$ of acrylamide in D_2O .

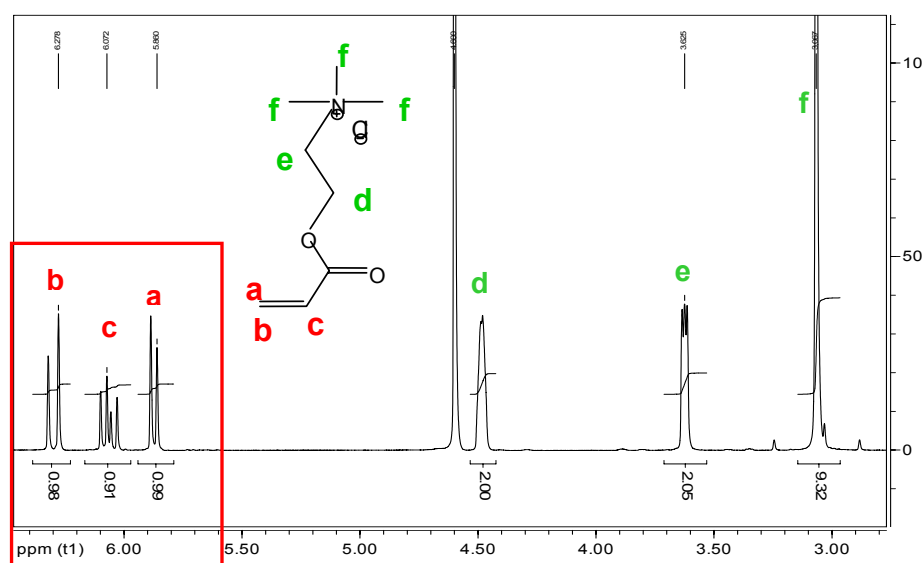


Figure 2-4: $^1\text{H-NMR}$ of AETAC in D_2O .

In these two spectra, the protons a, b and c corresponding to the double bond appear at a chemical shift higher than 5ppm which is typical for vinylic monomers (Ito 1966, Hatada 2002). Other peaks assigned to AETAC appear at the following chemical displacements: $\delta = 4.49$ (d, $-\text{COO}-\underline{\text{CH}}_2-\text{CH}_2-\text{N}^+(\text{CH}_3)_3$, 2H), 3.62 (e, $-\text{COO}-\text{CH}_2-\underline{\text{CH}}_2-\text{N}^+(\text{CH}_3)_3$, 2H), 3.05 (f, $-\text{COO}-\text{CH}_2-\text{CH}_2-\text{N}^+(\underline{\text{C}}\text{H}_3)_3$, 9H)

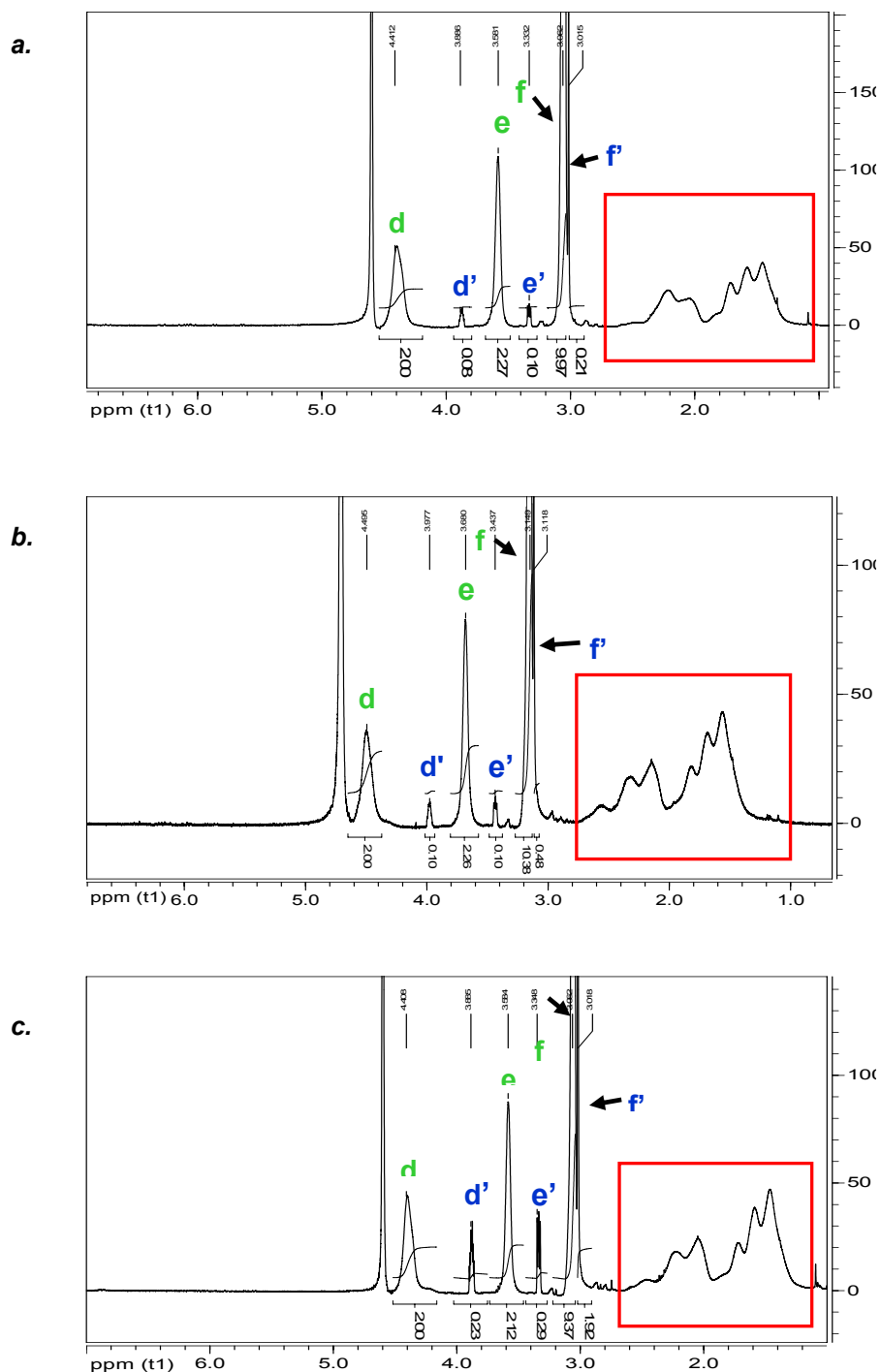


Figure 2- 5: $^1\text{H-NMR}$ of S43I01 (a), S33I01 (b) and S25I01 (c) in D_2O

In **Figure 2-5**, no peaks appear in the region above 5ppm corresponding to the double-bond of the vinylic monomers. But new peaks appear in the region below 2.5ppm. These peaks are not assigned one by one but correspond to the protons present on the backbone of the polymers. This proves that conversion is close to one for all the experiments. The amount of initiator and the temperature are suitable for efficiently copolymerizing AETAC and AM. As mentioned in the introduction, because of the small dissimilarity in copolymerization parameters ($r_{\text{AETAC}}=0.47$ and $r_{\text{AM}}=1.10$) conjugated with the parallel feed strategy leading to a low and comparable concentration of monomers in the reactor at any time of the reaction, the copolymerization is considered to be statistical and a potential drift in composition is not further investigated.

Beside the shift of the vinylic peaks to lower displacement, a new set of peaks are visible in **Figure 2-5**. Indeed, peaks d', e' and f' ($\delta \sim 3.9, 3.35$ and 3.05 respectively) do not appear in **Figure 2-4** and are not assigned. Keeping in mind that AETAC can undergo hydrolysis, a supplementary species can be present in the reacting medium resulting from the degradation of the ester bond: choline chloride.

Figure 2-6 shows the $^1\text{H-NMR}$ spectrum of choline chloride (Aldrich, >99%): $\delta = 3.88$ (d', HO- $\text{CH}_2\text{-CH}_2\text{-N}^+(\text{CH}_3)_3$, 2H), 3.33 (e', HO- $\text{CH}_2\text{-CH}_2\text{-N}^+(\text{CH}_3)_3$, 2H), 3.02 (f', HO- $\text{CH}_2\text{-CH}_2\text{-N}^+(\text{CH}_3)_3$, 9H). Peaks d', e' and f' correspond perfectly to the unassigned peaks in **Figure 2-5**.

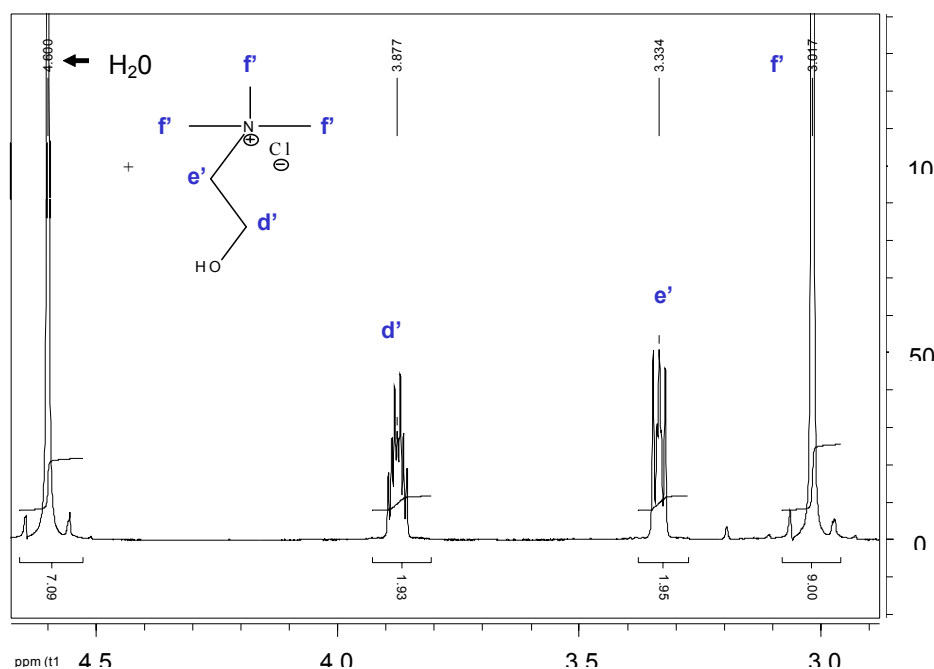


Figure 2- 6: $^1\text{H-NMR}$ of choline chloride in D_2O

At 50°C, using 0.1% of initiator (with respect to moles of CRU), NMR measurements show that AETAC and AM fully copolymerize in 5 hours. This copolymerization is considered as statistical. Apparition of new peaks proves that AETAC undergoes non negligible hydrolysis under studied reaction conditions.

2.3. Complexation

The recipe used to produce the solution S33I02 is used as a reference for the synthesis of dispersions. Thus, in addition to the reagents used in this recipe, a negatively charged polymer which can react with the polycation synthesized in-situ is added. The polyanion is fed in parallel with the two monomers and the initiator. The amount of template is the only variable in the recipe.

This chapter is divided into 3 subchapters, each one corresponding to a different chemistry of the polyanion. To start with, poly(acrylic acid), which is one of the cheapest and the most widely used negatively charged polymer is tested. Poly(2-acrylamido-2-methyl-1-propanesulfonic acid) (PAMPS), a strong polyanion is tested next. The last trials are realized with 2 copolymers of acrylic acid and AMPS, the first one containing 2/3 of AA, the second one only 1/3. The initiator and monomers used are the same as in the first paragraphs of this chapter.

The goal of this study is to determine suitable ratios polycation/polyanion permitting the formation of stable low viscosity dispersions. Abusively, all products obtained in the coming paragraphs are called “dispersions”, even if no real dispersion is actually obtained.

2.3.1. Poly(acrylic acid) as complexing agent

2.3.1.1. Synthetic work

Poly(acrylic acid) is provided by BASF as a 35wt% solution in water. Average molar mass determined by Field Flow Fractionation is 250kDa. The stock solution is diluted to the required concentration using distilled water.

PAA is a weak polyelectrolyte with a pK_a value of 4.6. This means that the pH inside the vessel determines the degree of dissociation of the complexing agent and therefore its efficiency. The experiments reported in the previous paragraphs show that the polymerization of the monomers without any complexing agent is carried out efficiently at pH values around 3.5. At such pH,

only a minority of the acid groups are dissociated and therefore the actual charge density of PAA is low.

In each experiment, 0.06 moles of AETAC are copolymerized with 0.12 moles of AM. The amount of complexing agent is varied from 0.01 to 0.12 moles of CRU (carboxylic groups in this case). It is important to note that it is not the number of polymer molecules which is varied, only the number of constitutive repeating units.

For each experiment, the pH and the Brookfield viscosity are measured and the visual appearance of the product is monitored.

Table 2-9 shows the results obtained for 8 amounts of PAA, from 0.01 to 0.15 moles of complexing agent.

Table 2-9: *copolymerization of 33% of AETAC and 67% of AM in presence of poly(acrylic acid).*

Dispersion	Moles CA	Viscosity (Pa.s)	pH	Aspect
D11	0.01	10.1	4.6	Transparent liquid
D12	0.03	7.3	4.2	Whitish liquid
D13	0.045	6.2	3.7	Whitish liquid
D14	0.06	3.4	3.2	Milky dispersion
D15	0.075	2.7	3.3	Milky dispersion
D16	0.09	1.9	2.6	Milky dispersion
D17	0.12	-	2.1	Coagulate+Supernatant
D18	0.15	-	2.2	Coagulate+Supernatant

Concerning the aspect of the products, an evolution from a transparent liquid towards a two phase system is observed when more and more complexing agent is added. Three successive regimes can be distinguished:

- “**Solution regime**” for D11, D12, D13: the products are transparent or close to transparent and their viscosity is rather high.
- “**Dispersion regime**” for D14, D15, D16: the product looks similar to latexes obtained by classical water in oil polymerization (i.e. milky dispersions). Nevertheless, viscosities are significantly higher than that of typical latex dispersions.
- “**Precipitation regime**” for D17, D18: stability is lost and the system phase separates into a solid coagulum and a transparent, water-like supernatant.

To obtain a stable dispersion, a minimum of 0.06moles of PAA have to be used. Compared to the 0.18 moles of cationic CRU, the ratio is one to three; however, the ratio of catiogenic to anionic groups is 1 to 1. It is difficult to evaluate precisely the charge compensation as the

degree of dissociation of the acid groups is not known accurately. Assessing that half of the acid groups are present as carboxylates (it should be less at pH=3.2), only half of the positive charges would be neutralized.

To check the influence of the molecular weight on the aspect and viscosity of the final dispersions synthesized, two experiments are carried out using exactly the recipe of D15 but with two PAA having a molar mass of respectively 1500kDa for D19 and 100kDa for D110. The first PAA is synthesized according to the recipe in the experimental section, the second one is provided by BASF as a 35wt% solution in water.

Table 2-10: copolymerization of 33% of AETAC and 67% of AM in presence of poly(acrylic acid) with Mw of 100kDa and 1500kDa.

Dispersion	Moles CA	pH	Viscosity (Pa.s)	Aspect
D19	0.075	4.4	4.5	Milky dispersion
D110	0.075	4.1	2.3	Milky dispersion

D19 and D110 are stable dispersions which have a milky appearance similar to D15. The viscosity of D19 is slightly higher: this is due to the molar mass of the complexing agent which is significantly higher and the uncomplexed CA accounts for the substantially higher viscosity.

2.3.1.2. Characterization by NMR

NMR spectroscopy is particularly useful regarding two aspects. First, it allows to determine if full conversion is reached, thanks to the disappearing of the peaks corresponding to vinylic protons near $\delta=6$ ppm. Second, in the region $2.5\text{ppm}<\delta<4.5\text{ppm}$, by comparing peaks d, e and f with d', e' and f', it is possible to get information about the degree of hydrolysis of the AETAC leading to the apparition of choline chloride.

Figure 2-7 and **Figure 2-8** present NMR spectra of products D11 and of the supernatant of product D18 in a narrow chemical shift region, from 2.5 to 4.5 ppm. Full spectrum shows that conversion is total, so only the ppm range where hydrolysis can be quantified is displayed.

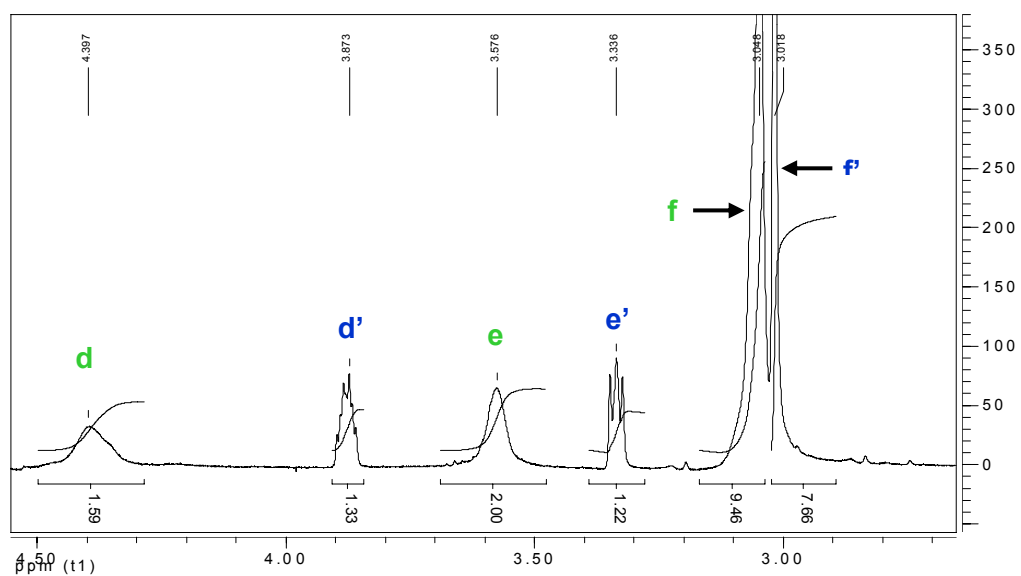


Figure 2-7: $^1\text{H-NMR}$ of dispersion D11 in D_2O .

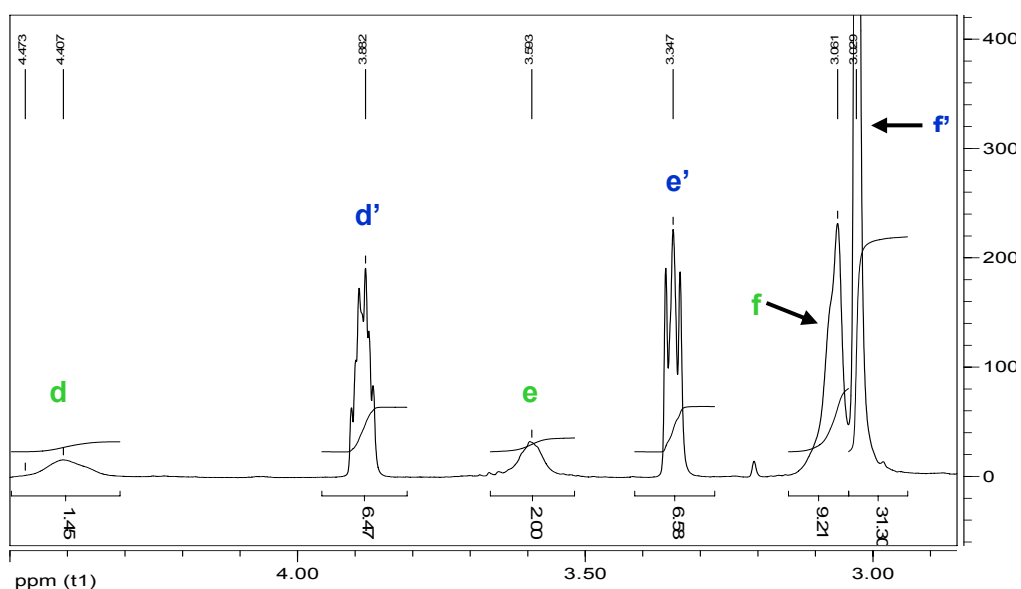


Figure 2-8: $^1\text{H-NMR}$ of supernatant of dispersion D18 in D_2O .

The spectra of both dispersions is similar to what has already been observed in **Figure 2-5** and **Figure 2-6** and correspond respectively to AETAC repeating units for d, e and f and to choline chloride for d', e' and f'.

It is difficult to determine absolute concentrations using only NMR as there is no reference to compare to. Nevertheless, integration of the peaks reveals that both AETAC and CC are roughly present in the same proportions. One can conclude that hydrolysis of the polymer is not negligible; this is due to the pH which is slightly higher than 4 and favours the breaking of the ester bond.

In the supernatant of “dispersion” D18, the peaks corresponding to the polymer are small. Peaks d', e' and f' corresponding to choline chloride are preponderant: AETAC is clearly the species in default in the supernatant. This observation can mean two things: first hypothesis is that a large majority of ester groups of AETAC is hydrolysed. But the rather low pH value is not favourable for the breaking of the ester bonds. The second hypothesis is that all the polymer which is not hydrolysed is present in the coagulate. To confirm this assumption the solids content of D11, D14 and the supernatant of D18 is measured yielding values of 4.9%, 5% and 0.9% respectively. This shows that the supernatant of D18 contains only little polymer as most of it is in the coagulum: complexation is very efficient under these conditions.

2.3.1.3. Characterization by cryo-TEM

Trials using dynamic light scattering did not provide reliable data concerning the size of the particles present in stable products, i.e. D14, D15 and D16. But these particles can be observed directly using cryo-TEM imaging. The major limitation of this technique is that the samples have to be highly diluted before freezing and therefore the size of the particles may vary compared to their actual size in a 5wt% dispersion.

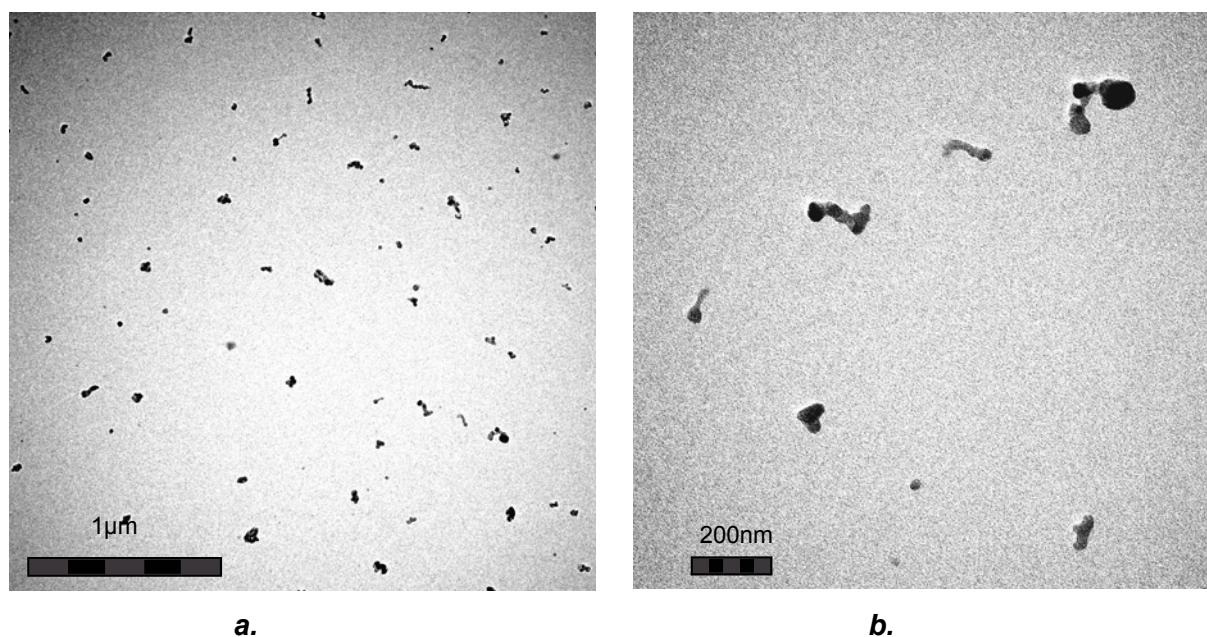


Figure 2-9: cryo-TEM imaging of dispersion D14.

Figure 2-9 a. shows that both the size and the shape of the particles are very heterogeneous. The smallest particles are barely visible and have a size in the range of ten nanometres. The biggest particles have a size of several hundred nanometres. In **Figure 2-9 b.**, at higher magnification, the structure of the aggregates seems to result from the aggregation of many small particles.

This mechanism of aggregation seems to be a constant and all “big” particles are formed by smaller ones coming together. The degree of aggregation and the way packing occurs is not reproducible and this explains the variety observed in the size and shapes.

The same kind of non reproducible/random packing is observed for D19 and D110 (**Figure 2-10** and **Figure 2-11** respectively). The cryo-TEM pictures seem to show that the size and shape of the aggregates are similar to the ones observed in D14.

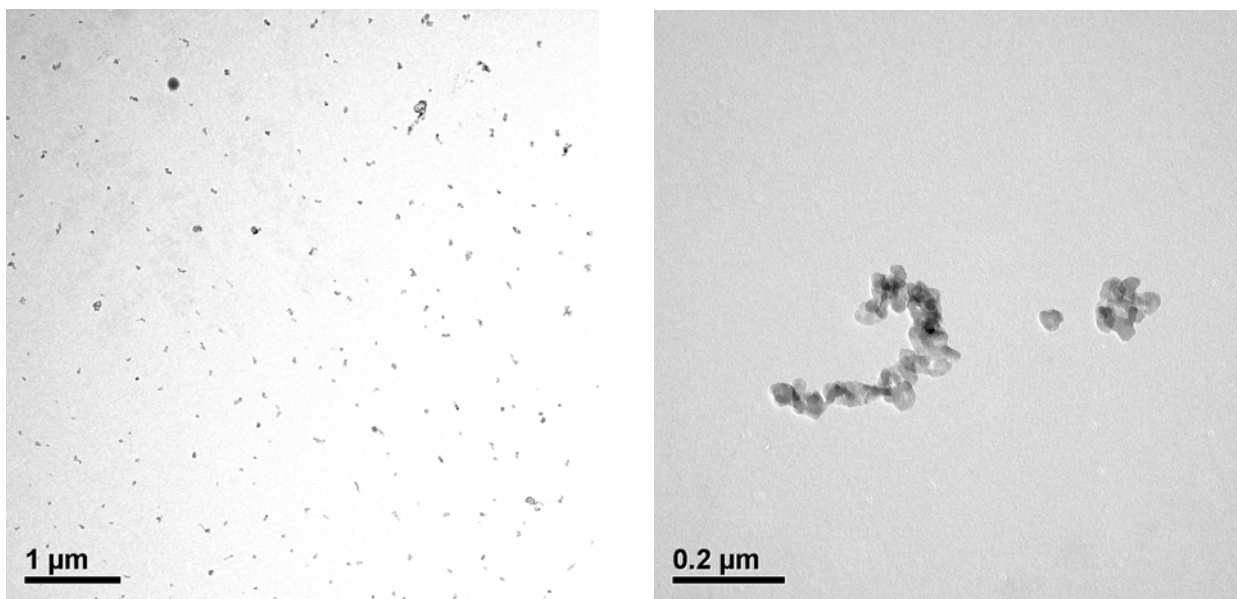


Figure 2-10: cryo-TEM imaging of dispersion D19.

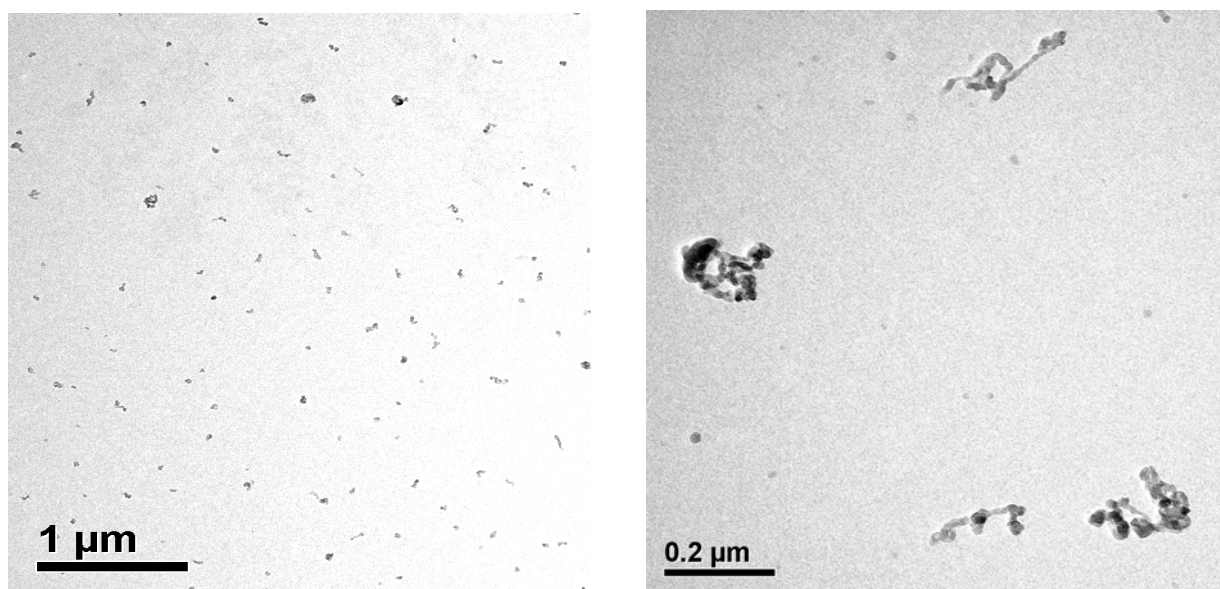


Figure 2- 11: cryo-TEM imaging of dispersion D110.

2.3.2. PAMPS as complexing agent

The amount of poly(acrylic acid) necessary to complex enough polymer to form stable particles is 0.06moles for 0.18moles of positively charged CRU. The quantity of complexing agent required might be diminished by using a polyanion which is more efficient i.e. carrying more potentially complexing groups. Using a weak polyanion, this means increasing the pH which is not desirable for the stability of AETAC. Another approach is to use a polyanion which is permanently charged, like PAMPS.

2.3.2.1. Synthetic work

Same approach as before is used to determine the amount of polyanion necessary to yield stable dispersions. As the actual charge density is higher on PAMPS compared to PAA (PAMPS is fully charged under all pH), the amounts of complexing agent tested in the first place are significantly lower in this case.

Table 2-11: copolymerization of 33% of AETAC and 67% of AM in presence of PAMPS.

	Moles CA	η (Pa.s)	pH	Solids content (%)	Aspect
D21	0.003	11.2	2.7	4.9	Transparent Matrix + Coagulate
D22	0.005	9.3	2.3	4.7	Idem
D23	0.01	3.8	1.9	3.8	Idem
D24	0.03	0.6	1.7	2.1	Idem
D25	0.05	-	1.8	1.1	Idem

The results gathered in **Table 2-11** show that contrary to the previous study, using homo PAMPS does not permit to obtain stable dispersions under the conditions investigated. The system always phase separates into a solid coagulate which sinks to the bottom of the reactor or sticks to its wall and a transparent supernatant. The viscosity of the supernatant decreases with increasing amount of PAMPS added. In parallel to this decrease in viscosity, a drop of solids content of the supernatant occurs, confirming that encapsulation efficiency is enhanced.

2.3.2.2. Characterization by NMR

Again NMR spectra show that monomer conversion is complete and only the range $2.5\text{ppm} < \delta < 4.5\text{ppm}$ is displayed in **Figure 2-12**, showing the spectra of the supernatants of dispersions D22, D23, D24 and D25. Two regimes can be distinguished:

- In spectra of the supernatants D22 and D23, the peaks d' and e' are negligible compared to d and e: there is almost no choline chloride in the continuous phase compared to the copolymer.
- For D24 and D25, the ratio choline chloride to copolymer is much higher. Taken into account that hydrolysis is not favored because of the low pH due to the use of a strong acid, the straightforward conclusion is again that the amount of polymer in the supernatant is low. This assumption is in good agreement with the evolution of the viscosity and of the solids content which indicate that there is less polymer in the supernatant for samples D24 and D25.

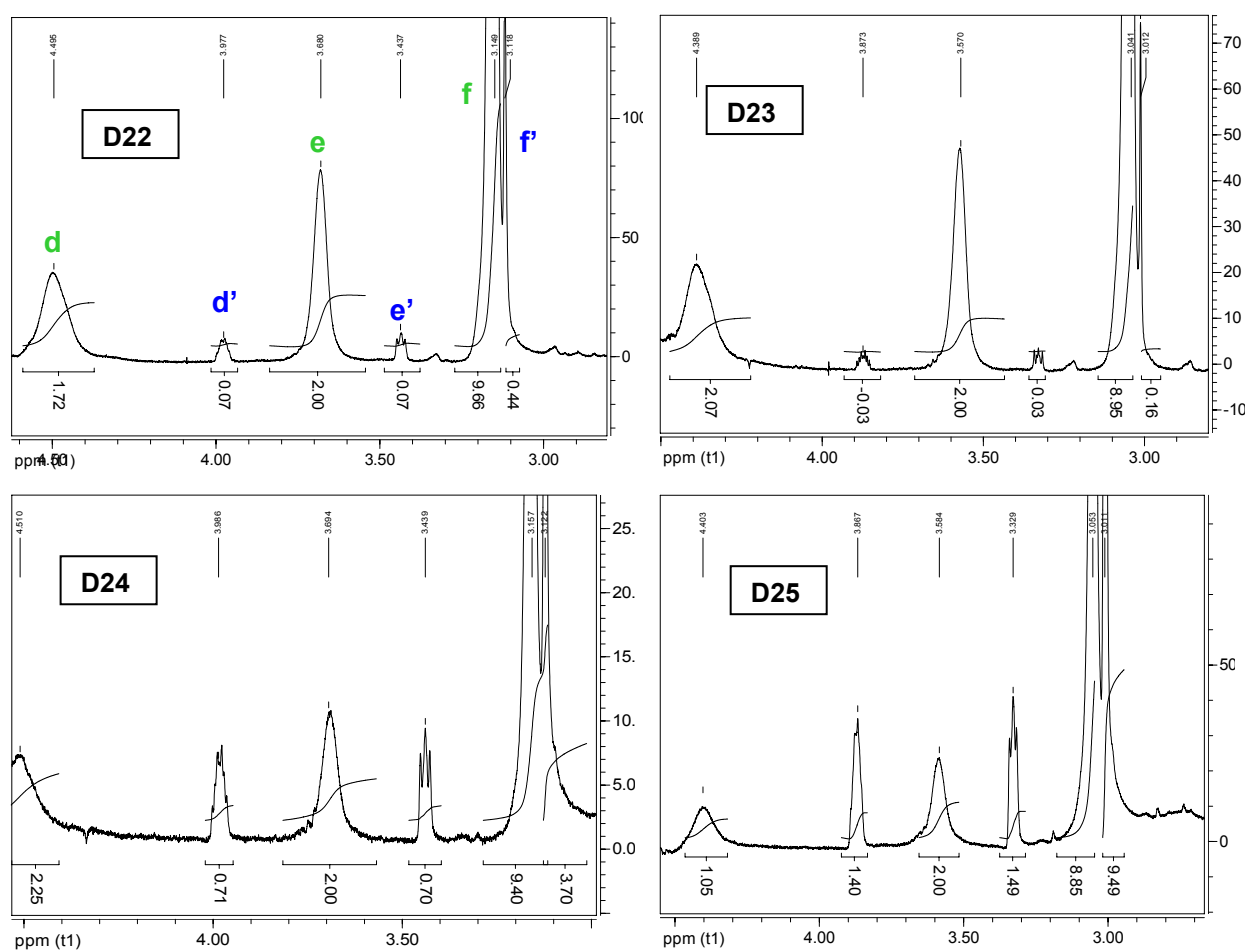


Figure 2-12: NMR spectra of dispersions D22, D23, D24 and D25.

PAMPS is very efficient to complex P(AETAC-co-AM): only 0.03moles are enough to complex almost all the positively charged copolymer. However, the interactions seem to be too strong to allow the formation of a stable dispersion and using PAMPS as CA always results in macroscopic phase separation.

The use of strong polyanions as complexing agent is not suitable to produce stable dispersions under the conditions of the study.

2.3.3. P(AA-co-AMPS) as complexing agent

In a last set of experiments, copolymers of AA and AMPS are used as complexing agents. Such copolymers combine weak and strong charges. If the ratio between the two is appropriate, efficiency of complexation should be increased and stable dispersions possible to obtain. Two copolymers are tested: P(AA_{0.66}-co-AMPS_{0.33}) and P(AA_{0.33}-co-AMPS_{0.66}).

2.3.3.1. Synthetic work

Synthesis of the two copolymers is realized according to the recipe described in the experimental section. Molar masses determined by FFF are respectively 450kDa and 370 for P(AA_{0.66}-co-AMPS_{0.33}) and P(AA_{0.33}-co-AMPS_{0.66}).

As previously, increasing amounts of CA are added to determine the amount necessary to yield a stable dispersion. Results are gathered in **Table 2-12** and **Table 2-13**.

Table 2-12: copolymerization of 33% of AETAC and 67% of AM in presence of P(AA_{0.66}-co-AMPS_{0.33}).

	Moles CA	pH	η (Pa.s)	Solids content (%)	Aspect
D31	0.003	4.5	7.8	5.1	Transparent liquid
D32	0.005	4.2	5.3	4.8	Whitish liquid
D33	0.01	3.3	1.9	5.1	Whitish liquid
D34	0.03	3.1	0.9	5.0	Milky dispersion
D35	0.05	2.8	-	1.3	Transparent Matrix + Coagulate

When the CA contains only one third of permanently charged anionic groups, the dispersions exhibit characteristics which are close to the ones observed for homo PAA. Indeed, the three regimes described in paragraph 2.3.1., i.e. solution, dispersion and coagulation are also

observed. With this copolymer, the amount of complexing agent needed to form a dispersion is lower; this is due to the presence of AMPS which interacts more efficiently with AETAC.

Table 2-13: copolymerization of 33% AETAC and 67% AM in presence of P(AA_{0.33}-AMPS_{0.66}).

	Moles CA	pH	Aspect
D41	0.001	4.1	Transparent liquid
D42	0.003	4.2	Sedimentating dispersion
D43	0.005	3.7	Sedimentating dispersion
D44	0.01	3.0	Transparent Matrix + Coagulate
D45	0.03	2.5	Transparent Matrix + Coagulate
D46	0.05	2.7	Transparent Matrix + Coagulate

With P(AA_{0.33}-co-AMPS_{0.66}) no viscosities are measured as no dispersion with long-time stability is formed. Concerning the aspect of the products, the results follow the same evolution as previously: when large quantities of CA are used, i.e. for dispersions D44, D45 and D46 the dispersions are not stable and macroscopic phase separation occurs. D41 is a viscous solution. In between, a new case of figure is encountered. Dispersions are formed but they are stable only for some minutes. If not shaken regularly, phase separation occurs between a solid complex which sediments and a transparent supernatant. After several days without shaking, flocculation is irreversible probably due to aggregation of flocculated particles.

2.3.3.2. Characterization by NMR

Because of the poor stability observed for the dispersions synthesized with P(AA_{0.33}-co-AMPS_{0.66}) as complexing agent, which does not make them promising for potential further use, NMR measurements are performed only on D31, D32, D33 and D34. results are gathered in **Figure 2-13**.

Again, the trend observed with P(AA_{0.66}-co-AMPS_{0.33}) is similar to the two previous systems. The ratio of choline chloride to polymer increases from sample D31 to sample D35 and coupled with the decrease in viscosity, the lower solids content in case of D35 and the change in aspect, one can conclude that the encapsulation of the polymer is better when more complexing agent is present.

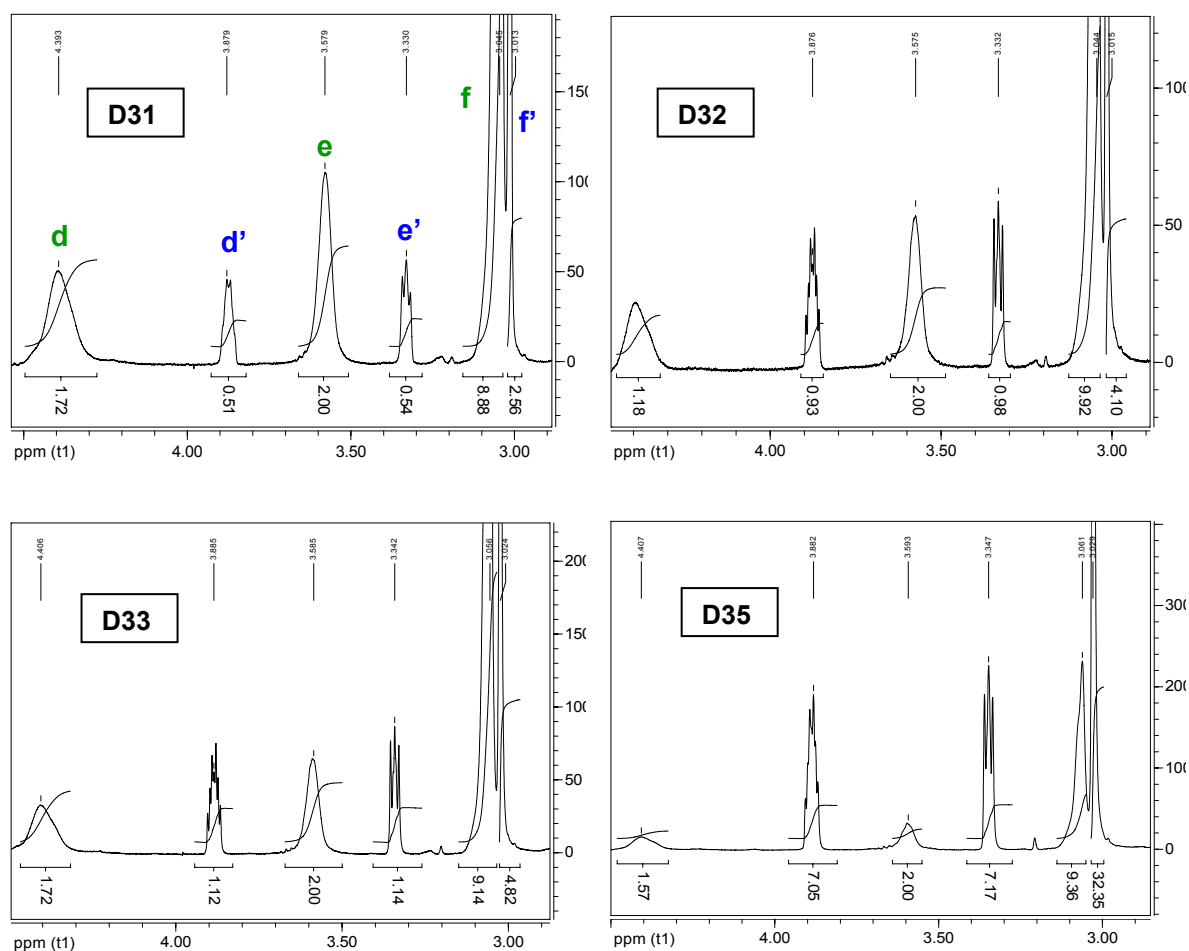


Figure 2-13: NMR spectra of dispersions D31, D32, D33 and D35

2.3.3.3. Characterization by cryo-TEM

D34 is characterized by cryo-TEM. The pictures at 2 magnifications are shown in **Figure 2-14**. The structure observed is similar to the one of D15: big particles are formed by the coalescence of smaller ones. The size of the “primary” particles is relatively homogeneous, in the order of a few dozen nanometres, while the size of the aggregates is more heterogeneous, ranging between 100nm and 400nm. The shape of small particles is almost spherical. The shape of aggregates is ill-defined with large discrepancies in aspect ratios.

On **Figure 2-15**, pictures of sedimentating dispersion D42 are shown. The thread-like structures are artefacts due to the freezing process and are not considered.

The structure of the particles is similar to the ones observed for other dispersions: polydisperse aggregates resulting from aggregation of small primary particles. In this case, aggregates are significantly bigger than the ones observed so far, having a size up to 1 μ m. This explains their tendency to sediment.

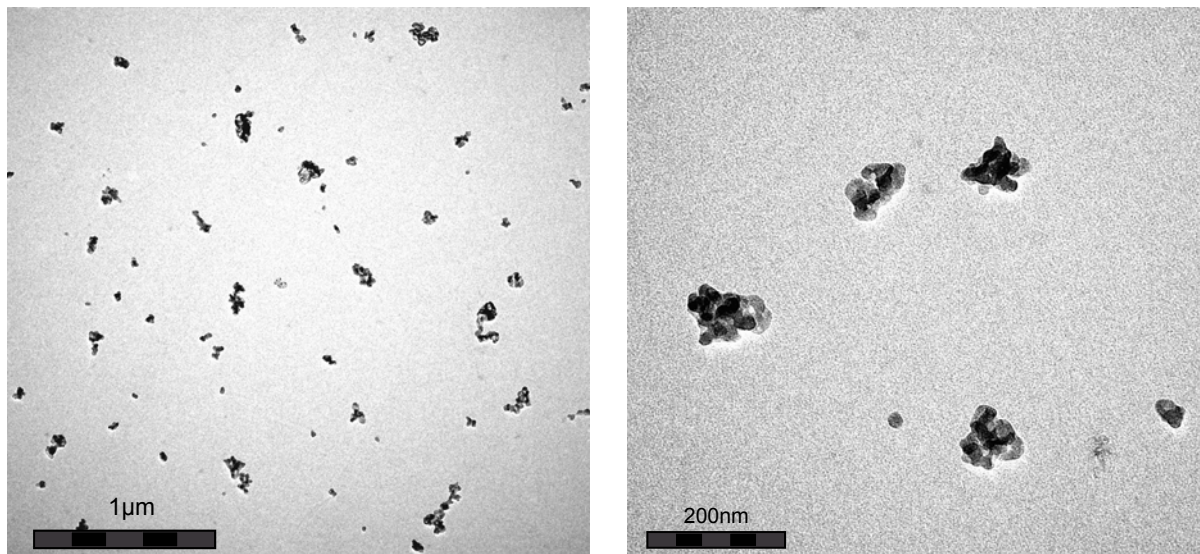


Figure 2-14: cryo-TEM imaging of dispersion D34.

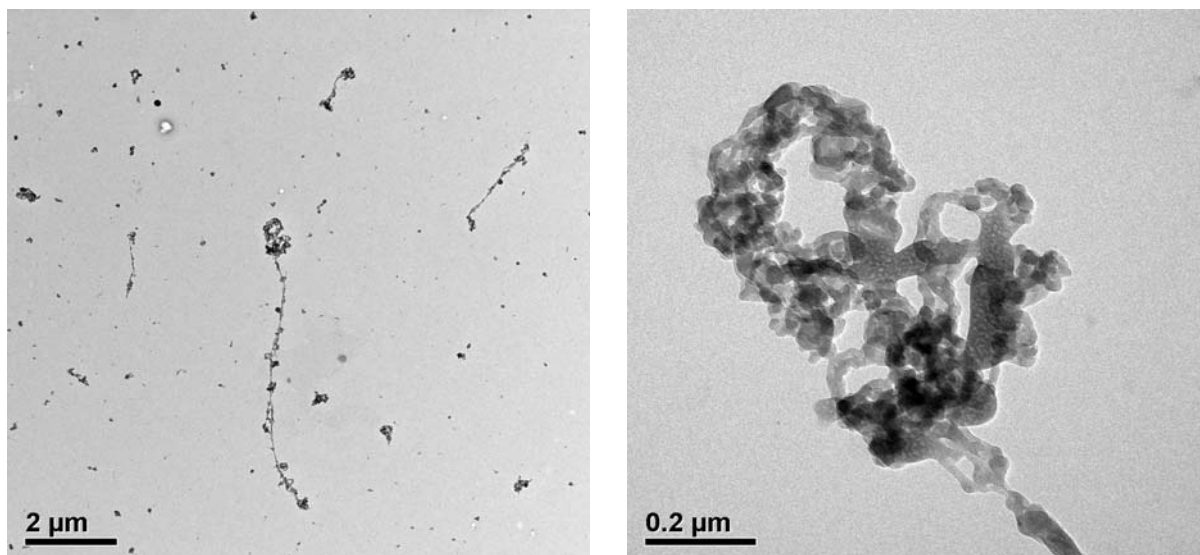


Figure 2-15: cryo-TEM imaging of dispersion D42.

2.3.4. Molar mass of the polymers

The molecular weights of the polymers of 6 dispersions have been measured by FFF at pH=11.3. The results obtained for D15, D19, D110, D33, D34 and D42 are gathered in **Figure 2-16**.

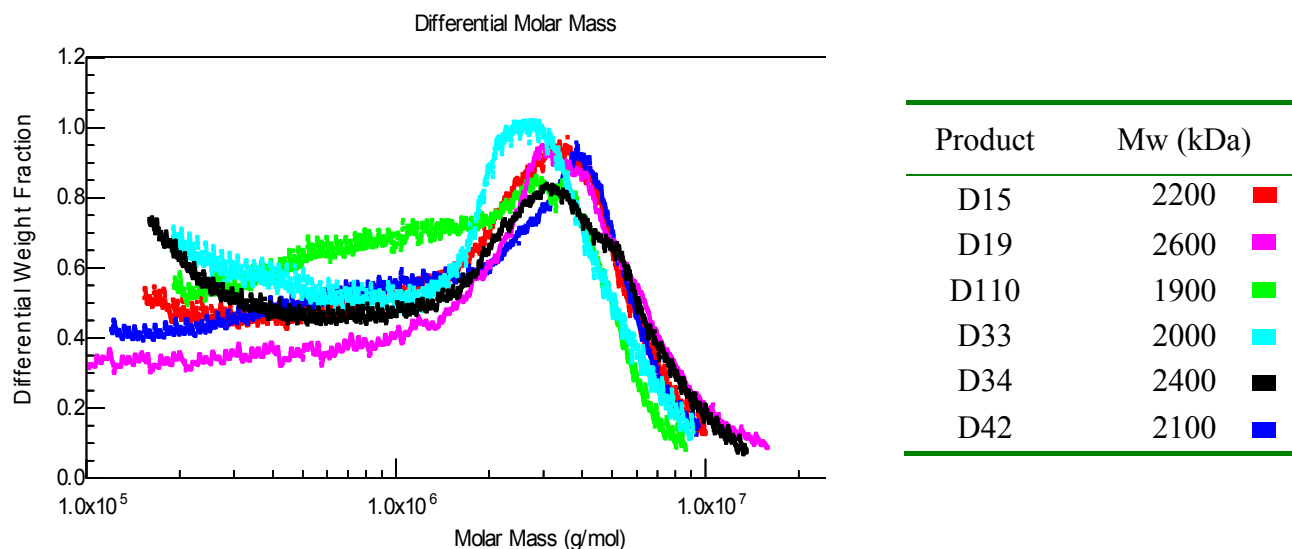


Figure 2-16: molar mass distribution of dispersions D15, D19, D110, D33, D34 and D42.

When poly(acrylic acid) is used as complexing agent, the molar masses lay in a narrow range. It is slightly larger for D19 and slightly smaller for D110 but this can be due to the presence of the complexing agent itself since its molar mass also accounts for the final value obtained for the dispersion. The molar mass of the products D33, D34 and D42 are also close to 2000 kDa and the distribution of the mass of the chains is similar.

Apparently, the structure and molecular weight of the complexing agent do not influence the molar mass of the copolymer; the assumption made in the beginning that CA does not act as template and that the interactions occur only between polyanion and fully grown polycation seems to be confirmed.

2.3.5. Discussion of the stability of the dispersions

The behavior of the different formulations investigated is somehow different from the behaviors typically described in literature. The charge compensation is of special interest in this respect. Indeed, in most articles published so far, the general statement is that an excess in charges, either positive or negative in the system leads to the formation of small particles which are electrostatically stabilized by the charges in excess, thus forming core-shell like particles. When

the isoelectric point (IP) is met and crossed, flocculation occurs leading to phase separation and sedimentation.

Dragan and Schwarz studied this phenomenon on PAMPS-PDADMAC systems by optical density measurements (Dragan 2004). In this work, very similar in approach to the pioneering work of Tsushida and Kabanov, the particle size is derived from the evolution of the turbidity of the mixtures. The aggregation occurs very close to the isoelectric point. After a sudden increase of the particles radius R_h , a plateau value is reached for OD_{500} indicating that the aggregates which are formed are stable and do not further grow or sediment (this would be indicated by either a further increase or a decrease of OD_{500}).

However, this is true only up to moderate concentrations, $\sim 0.1\%$. This has been shown first by both Tsushida and Kabanov and has been further demonstrated by several groups, amongst which the ones of Buchhammer, Dragan and Dautzenberg.

At higher concentrations, the situation differs from this ideal case and several factors have to be taken into account:

- The ionic strength plays an important part. An increase in ionic strength can essentially lead to 2 very different situations: either a swelling and eventually dissociation of formed complexes or a strengthening of the hydrophobic interactions leading to the salting out of the complexes (Mende 2002, Dautzenberg 1997). Concentration, chemistry, charges matching play a role in whether one or the other phenomenon is more relevant.
- The level of aggregation varies strongly with the concentration. For example, for the system PDADMAC/NaPSS, Dautzenberg showed that the variation of the molecular weight of the aggregates with the concentration follows the simple power law: $M_w \sim c^{2.47}$. This law is valid between 0.1wt% and 1wt%: it underlines the rapid growth of the aggregates with solids content.
- The stoichiometry of charge neutralization can differ from 1:1. This implicates that the structural density (reciprocal of the degree of swelling) can be influenced by the charge density of the polyelectrolytes. A better charge neutralization leads to more compact structures containing less water and prone to sedimentating (Dautzenberg 1997, 2002). Thus, sedimentation occurs at ratios far from isoelectric point. The process is governed by the kinetics of mixing not by the thermodynamics equilibriums, yielding almost instantaneously highly aggregated particles.

The 3 points cited above put in light some explanations for the discrepancies observed when using either PAA or PAMPS as complexing agent in the preparation of polyelectrolyte complexes. The last one is of special importance.

Indeed, the stable dispersions prepared with PAA are synthesized at pH comprised between 2.5 and 3.2 (cf. **Table 2-9**). At such low pH, only few acid groups are deprotonated and the charge density on the polyanion is low. At the same time, the geometric charge matching is poor, since the charges are much closer on the polycation than on the polyanion. Under these conditions, loose aggregates are formed which can be electrostatically stabilized. Besides the presence of uncomplexed polymer, the fact that aggregates are highly swollen also explains the viscosity of the dispersions, significantly higher than what would be expected for dispersions of compact particles in water.

On the contrary, when PAMPS is used, geometric charge matching and thus complexation is more favourable and structural density is higher. Because of the high concentration, large aggregates are formed almost instantaneously, which contain only little water and sediment. By mixing strong polyanions and strong polycations, “frozen” structures are obtained, which do not further rearrange over time: the excess charges present in the system can not potentially lead to the resolubilization of the precipitated aggregates.

When P(AA-co-AMPS) is used, stable aggregates can be obtained only when the amount of complexing agent is kept low. An increase of polyanion content quickly leads to large particles with a tendency to coalesce, i.e. to sediment.

2.4. Conclusion

By copolymerizing [2-(acryloyloxy)ethyl]-trimethylammonium chloride and acrylamide in presence of a polyanion, it is possible to produce stable dispersions in which particles are formed thanks to the interactions between opposite charges. The morphology of these particles barely depends on the system studied: they are always formed by aggregation of primary particles, which have a diameter of about 10nm. Depending on the complexing agent, the size of the aggregates is variable, from 100nm to almost 1 μ m. In this last case, the corresponding dispersion is not stable and has a tendency to macroscopically phase separate.

Stable dispersions are obtained only when the ratio between cationic and ionic species is suitable. If the amount of complexing agent is not sufficient, the product is a solution of polymer in water with a relatively high viscosity. If the amount of complexing agent is too high, phase separation occurs leading to the formation of a solid coagulate and a water-like supernatant. It is only between these extreme cases that stable milky dispersions are formed. The suitable quantity of polyanion does not depend on its molar mass but depends on the nature

of the charge. Permanent anionic charges are more efficient regarding complexation. However, using only strong polyelectrolytes does not permit to produce stable dispersions as phase separation is prominent. By using only weak anionic charges, dispersions can be obtained. The drawback in this case is that a lot of complexing agent is necessary. Therefore, copolymers of AA and AMPS containing less than 50% of permanent charges (to avoid sedimentation) seem to be the most promising complexing agents for the production of stable dispersions.

The chemistry of the system studied gives rise to additional issues as the [2-(acryloyloxy)ethyl]-trimethylammonium chloride can be hydrolyzed easily when the pH is higher than 5. If dispersions were to be stored for long periods, it is likely that the polymer would suffer degradation. For long-term storage, an alternative chemistry should be considered.

2.5. Perspectives

The synthetic work described in this chapter follows a “proof of concept” approach. It is clear that an appropriate charge balance ensures the electrostatic stabilization. However, the transition from stability to phase separation is not well understood. Especially, the factors controlling the aggregation process of the primary particles and the formation of a stable aggregate have to be further investigated. On the existing systems, a first approach could be to do an electrophoretic study, to correlate the stability of a dispersion with the charge of the particles. By changing the concentration and the pH, it should be possible to define a critical charge on the particles (having a suitable size) which prevents them from aggregating. In a second time, new systems could be investigated. Either comparable with the existing ones, based on AETAC and AM, by changing their ratio and using other copolymers of AA and AMPS. Or based on new chemistries and new reaction conditions: for example, some promising results have been obtained with a reverse system in which AA is polymerized in the presence of a copolymer of VP and VI. Stable dispersions can be obtained in this manner up to 15wt%. But again, this work is mostly empirical and requires better understanding of the phenomena occurring at the microscopic level.

3. Rheological properties of mixtures of positively charged polyelectrolytes with poly(acrylic acid)

3.1. Introduction

In the previous chapter, it has been shown that the in-situ polymerization of a cationic monomer in the presence of an anionic polymer enables to produce stable aqueous dispersions. These dispersions are obtained at low pH, similar to a number of commercial formulations. Indeed most thickeners are supplied either as powders, water in oil or oil in water dispersions. Within the latter, alkali swellable emulsions (ASE) are prominent. They are acrylic or methacrylic based highly concentrated, milky, formulations supplied at a pH usually comprised between 2 and 3.5. Upon neutralization the weak acrylic or methacrylic acid groups dissociate, thus solubilizing the polymer and developing their thickening properties (Siddiq et al. 1999).

A similar behavior could possibly be observed for inter-polyelectrolyte complexes as electrostatic interactions are highly sensitive to ionic strength and pH. With poly(acrylic acid) based IPEC, raising the pH from 3 to 7 results in the deprotonation of carboxylic groups of the PAA, ultimately leading to the swelling of polymer chains and possibly to decomplexation. The study of decomplexed systems, especially their rheological properties is of first interest for potential future applications.

The synthesis of an IPEC following the protocol described in chapter two is demanding regarding quantity of material and time of reaction. It is therefore difficult to imagine a vast systematic study which would consist first in synthesizing in-situ IPEC at low pH and second in diluting and neutralizing those IPEC for further analysis. A more rational approach is to mix oppositely charged polyelectrolytes under appropriate conditions and study these model mixtures. For the cationic species, using 2-[(Acryloxy)ethyl]trimethylammonium chloride has the major drawback that it is sensitive to pH and prone on hydrolyzing at pH=7. This would lead to a drastic modification of the chemistry of the system and the physical properties would subsequently also be changed. Therefore, other polycations are used, based on vinyl imidazole. This monomer is widely used in industry, especially in body care formulations and the corresponding polymers are stable, independent of the pH. The polyanions are still based on

poly(acrylic acid) or on poly(acrylic acid-co-2-acrylamido-2-methyl-1-propanesulfonic acid), polymers which are also not sensitive to hydrolyzes.

The pure polyanions are investigated first. Once their behavior is documented, mixtures of oppositely charged polyelectrolytes, based on polymers mentioned above, are measured.

3.2. Experimental

3.2.1. Materials

3.2.1.1. Polyanions

Poly(acrylic acid) is synthesized as follows. A one liter reactor equipped with two dropping funnels and a nitrogen inlet is filled with 400mL of water. Temperature is raised to 50°C. The system is mechanically stirred at 150 rpm using an anchor shaped stirrer and purged with nitrogen. After 30 minutes, the feeding of 93g of acrylic acid plus 107g of water in one dropping funnel and 0.35g of V50 in 10g of water in another dropping funnel is started. The feeding is done dropwise. All the reagents are introduced within ninety minutes. Then the reacting mixture is stirred under inert atmosphere for another four hours. The study carried out in the previous chapter showed that the use of this reacting procedure ensures full conversion of the monomer. The end product is a viscous, transparent solution having a solids content of 15 weight percent. This solution is diluted using deionized water in order to obtain a stock solution having a concentration of 10 weight %.

To produce the solutions which are used for rheological measurements, this stock solution is further diluted to the desired concentration with deionized water before being neutralized to the desired pH with 1N sodium hydroxide.

Field Flow Fractionation at pH=11 and 1g.L^{-1} yields average molecular weights of $M_w=1.6 \times 10^6$ g/mol. This poly(acrylic acid) is referred to as PAA1600.

The same protocol is used to synthesize other poly(acrylic acid). The only variable is the quantity of initiator: either 0.23 g, 0.525g or 1.05g are used. The end-product is always a transparent solution which viscosity decreases with increasing amount of V50. Field Flow Fractionation at pH=11 and 1g.L^{-1} yields average molecular weights of respectively $M_w=3.3 \times 10^6$ g/mol (PAA3300), $M_w=0.9 \times 10^6$ g/mol (PAA900) and $M_w=0.25 \times 10^6$ g/mol (PAA250) for the different initiator concentrations.

Table 3-1: quantity of initiator and molar mass of synthesized PAA.

Product	Molar ratio Initiator/AA (%)	Mw (kDa)
PAA250	0.3	250
PAA900	0.15	900
PAA1600	0.1	1600
PAA3300	0.07	3300

3.2.1.2. Polycation

Poly(vinyl pyrrolidone-co-chlorine quaternized vinyl imidazole) containing 30 molar percent of charged repeating units is provided by BASF SE (Ludwigshafen Germany) as a 38 weight % solution in water. Field Flow Fractionation at pH=11 and 1g.L⁻¹ yields and average molecular weight $M_w=1.1 \times 10^5$ g/mol.

Poly(vinyl pyrrolidone_{0.5}-co-vinyl imidazole_{0.5}) (P(VP_{0.5}-VI_{0.5}) or simply P(VP-VI)) is provided by BASF SE (Ludwigshafen Germany) as a 20 weight % solution in water. Field Flow Fractionation at pH=11 and 1g.L⁻¹ yields and average molecular weight $M_w=1.0 \times 10^5$ g/mol.

Table 3-2: composition and molar mass of the polycations used in rheology investigations.

Product	mol % of VP	mol % of QVI / VI	Mw (kDa)
P(VP _{0.7} -QVI _{0.3})	70	30	110
P(VP _{0.5} -VI _{0.5})	50	50	100

3.2.2. Methods

3.2.2.1. Sample Preparation

Prior to the preparation of the mixtures which are to be measured, intermediate stock solutions of polyanions and polycations at different pH and concentrations are prepared. As mentioned before, the rheological properties of the mixings are investigated under technically relevant conditions. The total concentration of polymer in the mixtures is 2%, 1% or 0.5%. The pH of the diluted stock solutions is usually varied between 5.5 and 9. To assess the modifications induced by the presence of the polycation, the solution of the pure polyanion having the same

concentration as in the mixture is used as a reference. Therefore, stock solutions at 0.25wt% are also prepared (reference of 0.5wt% mixtures).

The samples are prepared by slowly pouring a solution of the polycation into a solution of the polyanion. The concentration and pH of both solutions are equal to the desired final value. For example, to prepare a one to one in weight mixture of PAA1600 and P(VP-VI) with a final concentration of 2wt%, 2g of PAA1600 at 2wt% and pH=7 are mixed with 2g of P(VP-VI) at 2wt%. After mixing, the samples are shaken vigorously for some seconds and left to equilibrate at room temperature for at least 48h. The homogeneous mixtures are then subjected to rheological measurements.

3.2.2.2. Measurements

- **Rotational rheometry**

A rotational rheometer MARS (Modular Advanced Rheometer System) (Thermo Fischer Scientific) equipped with a cone-plate fixture (diameter $d = 60$ mm, cone angle $\alpha = 1^\circ$) is used to perform steady shear as well as small amplitude oscillatory shear experiments. The measurements are performed at room temperature, i.e. $20^\circ\text{C} \pm 0.5^\circ\text{C}$. For lengthy measurements (> 2 hours), the sample is placed in a humidity saturated chamber, to prevent excessive evaporation.

All dynamic measurements are carried out in the linear viscoelastic regimes of the polymers, determined for every polymer by dynamic stress sweep default test.

- **Oscillatory squeeze flow**

Oscillatory squeeze flow experiments were performed using a piezo-driven axial vibrator (Crassous et al. 2005, Kirschenmann 2003) customized at the Institute for Dynamic Material Testing (Ulm, Germany). The instrument operates at constant force amplitude and from the ratio of the dynamic displacement of the lower plate (amplitude ~ 5 nm) with and without fluid the complex squeeze stiffness K^* of the fluid is obtained which is directly related to the complex shear modulus G^* (Kirschenmann 2003):

$$K^* = \frac{3\pi R^4}{2d^3} G^* / (1 + \frac{\rho\omega^2 d^2}{10G^*} + \dots) \quad (3.1)$$

where ρ is the fluid density, R (here 10 mm) is the radius and d is the height of the gap. The determination of G^* strongly depends on the exact knowledge of d , which is determined by calibration using Newtonian liquids with viscosities between 10^{-3} and 2 Pas. Gap heights

between 15 and 100 μm have been used here. Moduli G' or G'' in the range from 0.1 Pa to 10kPa are accessible with this set-up at frequencies between 1 Hz and 10 kHz.

3.3. Results and Discussion

3.3.1. Rheology of pure polyanions

To understand how the addition of low molar mass polycation affects the rheological behavior of high molar mass polyanion, their behavior alone is investigated first. Four concentrations are studied (2%, 1%, 0.5% and 0.25% in weight). The pH is varied in the range 5.5 to 9.

Results obtained for pure PAA1600 are gathered in **Figure 3-1**: a similar pattern is observed for all concentrations. G'' curves (open symbols) are parallel one to each other as well as G' curves (closed symbols). For the former, the slope in a double logarithmic plot versus ω is always close to 1 and for the latter, the slope is always close to 2. Moreover, G'' is always larger than G' . This regime is the typical terminal regime of viscoelastic fluids. Results obtained when measuring solutions at 0.5wt% and 0.25wt% are poor. Only the viscous modulus is measurable accurately with the geometry used. In this case, the viscosity is almost independent of frequency and the solution has a Newtonian behavior.

The crossover frequency, corresponding to the intersection of G' and G'' , is not visible in the frequency range investigated. Taking into account that the moduli depend only slightly on the pH, the crossover, if it exists, should be essentially independent of the pH at a given concentration.

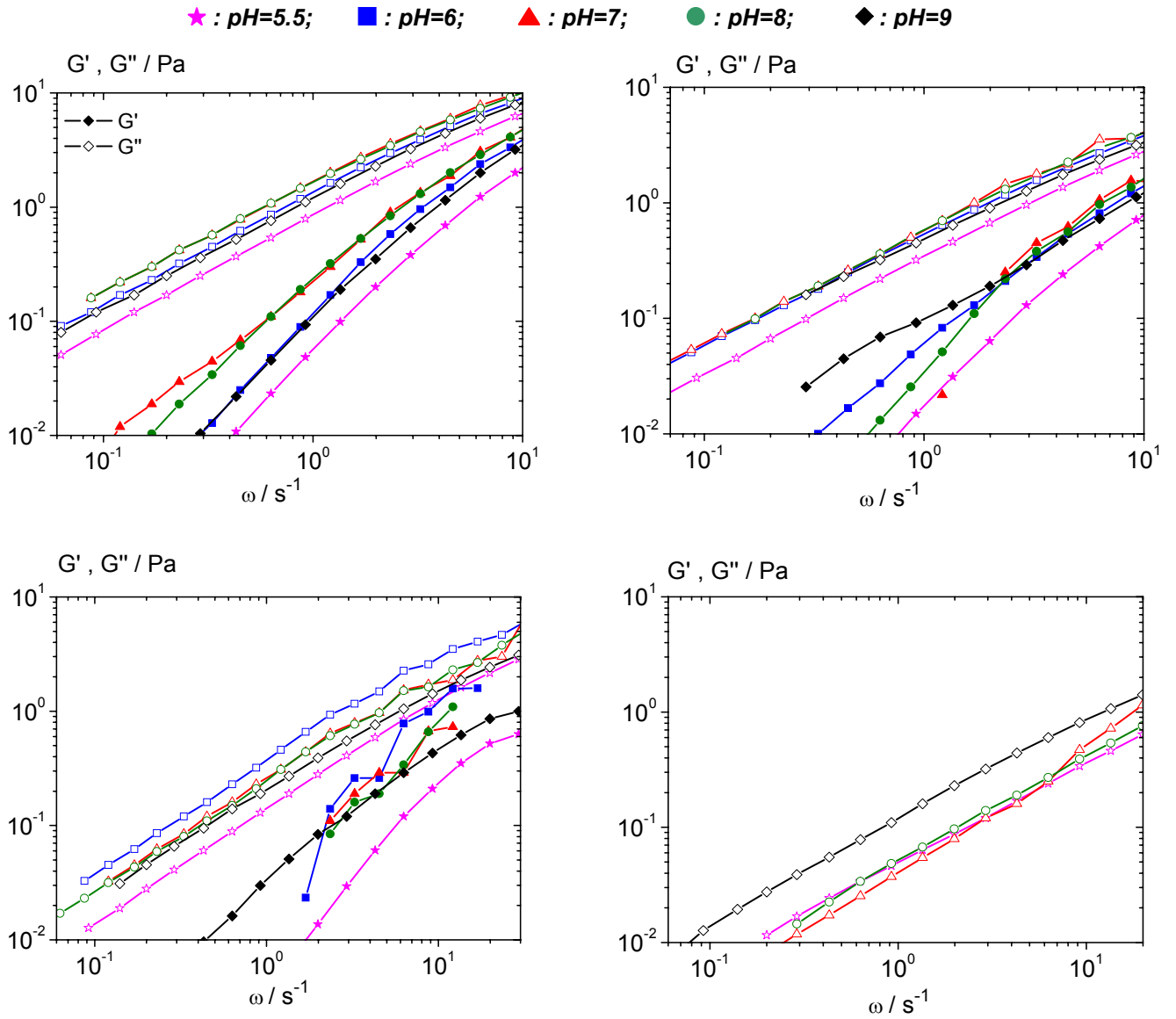


Figure 3-1: storage (full symbols) & loss (open symbols) moduli of PAA1600 at 2wt% (top left), 1wt% (top right), 0.5wt% (bottom left), 0.25wt% (bottom right).

The complex viscosities $|\eta^*|$ have been calculated from G' and G'' according to 3.2.

$$\eta^* = \frac{\sqrt{G'^2 + G''^2}}{\omega} \quad (3.2)$$

As an example, the evolution of the viscosity versus frequency for 2wt% solutions at different pH is shown in **Figure 3-2**.

★ : pH=5.5; ■ : pH=6; ▲ : pH=7; ● : pH=8; ◆ : pH=9

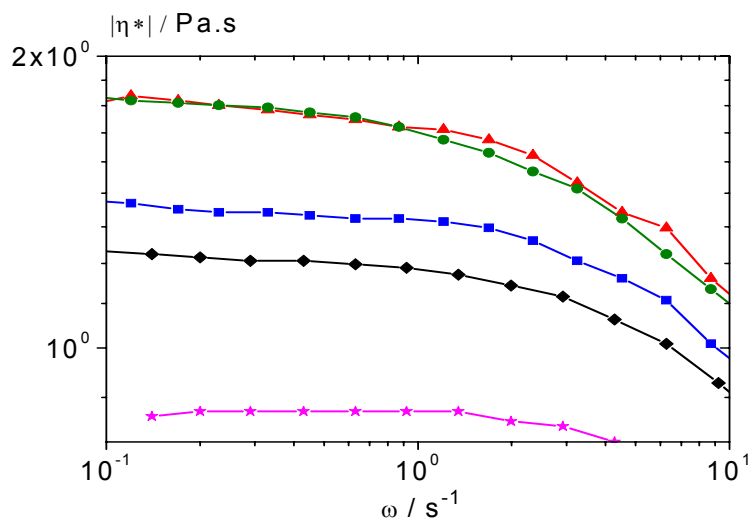


Figure 3-2: complex viscosity vs frequency of PAA1600 at 2wt% depending on pH.

Figure 3-2 shows that solutions at 2wt% are shear thinning, with a decrease in viscosity starting around 1 rad^{-1} . When ω is lower than 1 rad^{-1} , the viscosity remains constant. This value is the zero shear viscosity (η_0 or $|\eta^*|_0$) which from now on is used to compare the different samples. The zero shear viscosity of PAA1600 has been determined for 4 concentrations (referred to as Solids Content (SC) in all the subsequent graphs) and 5pH. All values are gathered in **Table 3-3** and **Figure 3-3**.

Table 3-3: zero shear viscosity in Pa.s of PAA1600 as a function of pH and concentration.

Concentration	pH=5.5	pH=6	pH=7	pH=8	pH=9
2wt%	0,86	1,38	1,75	1,76	1,25
1wt%	0,34	0,58	0,61	0,57	0,50
0.5wt%	0,14	0,27	0,26	0,24	0,23
0.25wt%	0,06	0,05	0,04	0,05	0,13

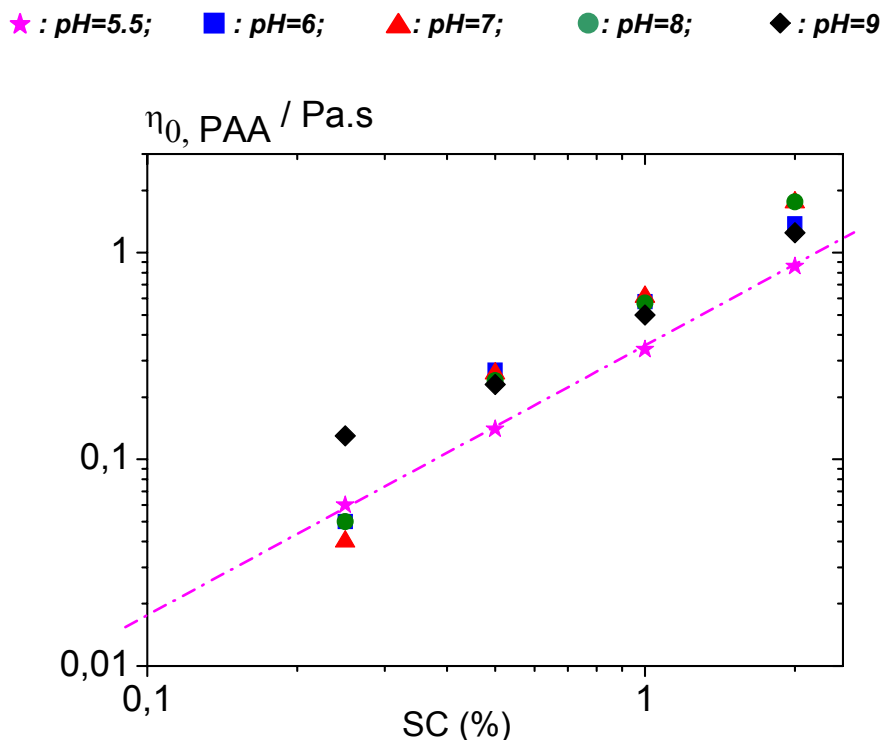


Figure 3-3: zero shear viscosity of PAA1600 as a function of pH and concentration.

The evolution versus pH and concentration of the zero shear viscosity depicted in **Figure 3-3** is typical for non-charged polymers at pH=5.5. Under such conditions, the viscosity increases with concentration following a power law, $|\eta^*|_0 \sim c^\alpha$, with $\alpha=1.28$. This is in good agreement with predictions for unentangled, semidilute solutions of neutral polymers (Colby 1994). Indeed, at pH=5.5, not all carboxylic groups are dissociated and the polymer still behaves as if it were neutral. At pH=9, the behavior is roughly the same, which is in good agreement with predictions for polyelectrolytes in the high salt limit (Dobrynin 1995); the addition of NaOH required to neutralize the polymer to pH=9 leads to a high ionic strength. At intermediate pH, (6, 7 and 8), the increase of viscosity with concentrations follows a power law, α being the same as for pH=5.5 only above 0.5wt%. At lower concentrations (0.25wt% here), the viscosities are smaller than expected. At such low polymer concentration, the quantity of base necessary to neutralize the samples is small, and therefore the system remains in the low salt limit. For polyelectrolytes in the low salt limit, a weaker concentration dependence of viscosity is observed, approaching $\eta_0 \sim c^{0.5}$ (Fuoss 1951, Dobrynin 1995). Accordingly, the viscosity at low concentration at intermediate pH is lower than the one at substantially higher pH or concentration.

3.3.2. Rheology of mixtures of PAA and polycation depending on mixing ratio

The pioneering works of Tsuchida(1974) and Kabanov(1982) have shown that charge matching is a feature of paramount importance when dealing with mixtures of oppositely charged polyelectrolytes. Therefore, the behavior of mixtures at different mixing ratios might be variable. More recently, Liu et al. (2001) have also studied the rheological behavior of mixtures of oppositely charged polyelectrolytes at different mixing ratios and shown that large discrepancies are induced by this ratio. Therefore, the viscosity of mixtures of polycation, either permanent or non-permanent, with poly(acrylic acid) at several mixing ratios are measured.

3.3.2.1. Permanent polycation

The evolution of the zero shear viscosity of mixtures of PAA1600 with P(VP_{0.7}-QVI_{0.3}) are determined at different mixing ratios. Mixtures at pH=6 are never stable as they always macroscopically phase separate.

At pH=7, this phenomenon of phase separation is also observed, but not at all mixing ratios. When a majority of polyanion or a large majority of polycation is present in the mixture, the system is stable. Values of zero shear viscosities for sample measured at pH=7, 2wt% are gathered in **Figure 3-4**.

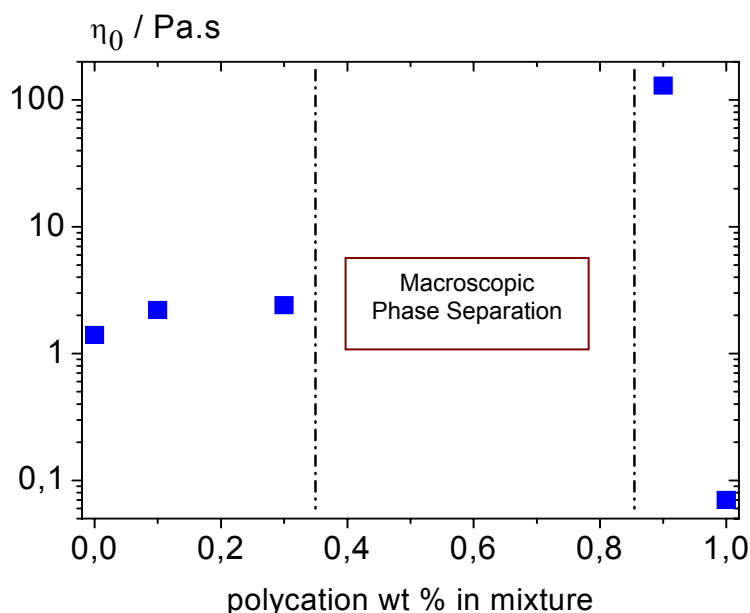


Figure 3-4: zero shear viscosity of mixtures of PAA1600 and P(VP_{0.7}-QVI_{0.3}) as a function of mixing ratio at 2wt% and pH=7.

The zero shear viscosity of pure PAA1600, the point on the left hand side in **Figure 3-4** is approximately 1.7 Pa.s under the conditions of study. The viscosity of the pure polycation is

almost independent of shear rate and has a constant value of approximately 0.07Pa.s, corresponding to the point on the right hand side in **Figure 3-4**.

If the two polymers are mixed at ratios at which no precipitation occurs, two very different behaviors are observed. When polyanion is present in majority in the system, the viscosity changes only slightly. Over the three decades investigated, the behavior is almost Newtonian. The second behavior, observed when there is 90wt% of polyanion in the system, is characterized by a sharp increase in viscosity, as the zero shear viscosity reaches 130Pa.s. To determine if this increase in viscosity goes along with a modification of the dynamic features, this sample is measured in small amplitude oscillary shear experiments. The elastic and loss moduli as well as the complex viscosity are shown in **Figure 3-5**.

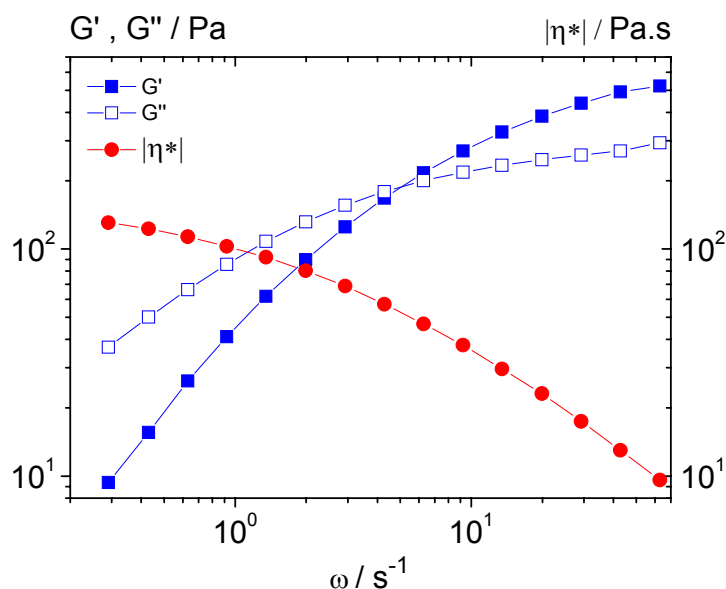


Figure 3-5: complex viscosity, storage and loss moduli of 1:9 mixtures of PAA1600 with P(VP_{0.7}-QVI_{0.3}).

Compared to the pattern of pure PAA1600 at 2wt%, not only is the absolute value of the moduli higher, but the crossover of G' and G'' and the onset of a rubbery plateau are visible, indicating that entanglements are present in this mixed solution resulting in a slower relaxation due to interactions between oppositely charged polyelectrolytes.

When the polyanion and polycation are mixed at ratios between 7 to 3 and 1 to 9, the system macroscopically phase separates: a solid complex is formed surrounded by a water-like supernatant. This has already been described in chapter 2 when polymers carrying strong charges are mixed (AMPS + AETAC).

To try to circumvent this problem of phase separation, one of the possibilities is to decrease the charge density on one of the polymers. PAA being an interesting model weak polyanion for this

study, the charge density on the polycation is decreased. Instead of decreasing the amount of QVI in the copolymer, a copolymer of VP and VI is used instead. Thus, the amount of positive charges on the polymer can be tuned by changing pH.

3.3.2.2. Non permanent polycation

Mixtures of PAA1600 and P(VP_{0.5}-VI_{0.5}) at different mixing ratios are studied. The total concentration in polymer is always 2wt%. The pH value is set at 6. At this pH, contrary to what was measured with P(VP_{0.7}-QVI_{0.3}), no macroscopic phase separation is visible. In weight, the ratios PAA to P(VP-VI) are: 9 to 1, 7 to 3, 5 to 5, 4 to 6, 3 to 7 and 1 to 9.

The values of zero shear viscosity and G'/G'' crossover frequency are gathered in **Table 3-4**. The frequency dependence of the complex viscosity and dynamic moduli depending on mixing ratio are gathered respectively in **Figure 3-6** and **Figure 3-7**.

Table 3-4: zero shear viscosity and crossover frequency of mixtures of PAA1600 with P(VP-VI) depending on mixing ratio.

Mixing	PAA (wt%)	P(VP-VI) (wt%)	$ \eta^* _0 / \text{Pa.s}$	Crossover / s ⁻¹
M91	90	10	0.93	-
M73	70	30	13.5	9
M55	50	50	120	0.6
M46	40	60	60	1.2
M37	30	70	41	2
M19	10	90	10	13

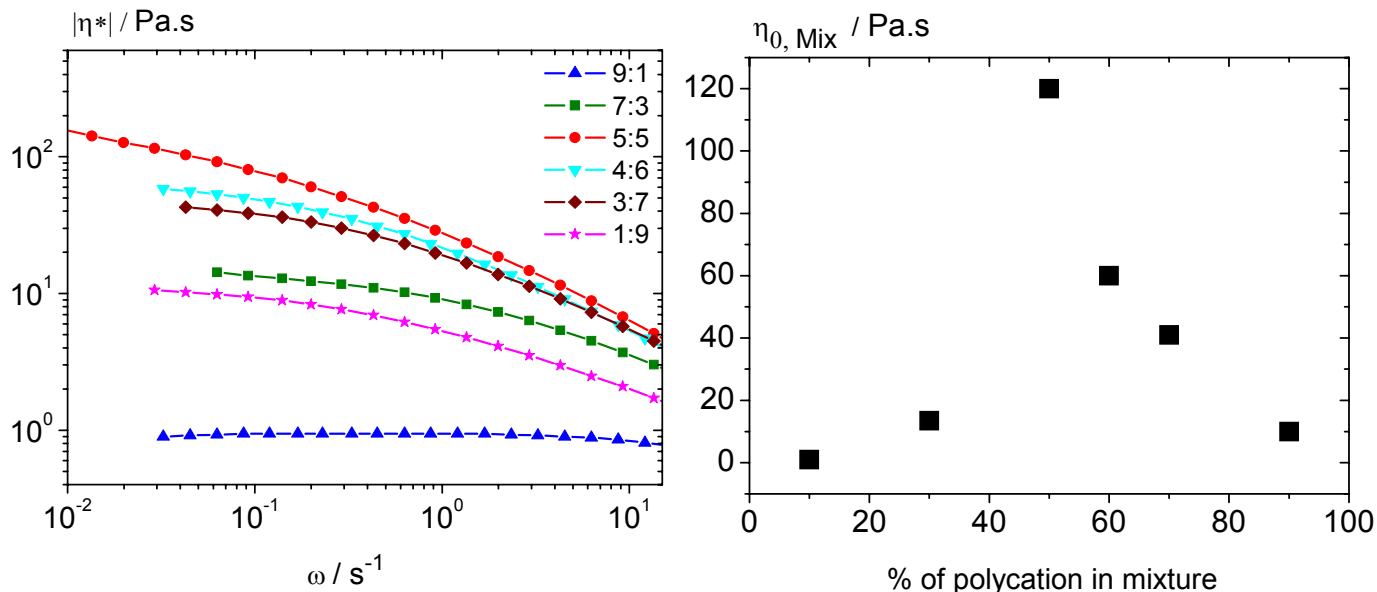


Figure 3-6: complex viscosity of mixtures of PAA1600 with P(VP-VI) depending on mixing ratio.

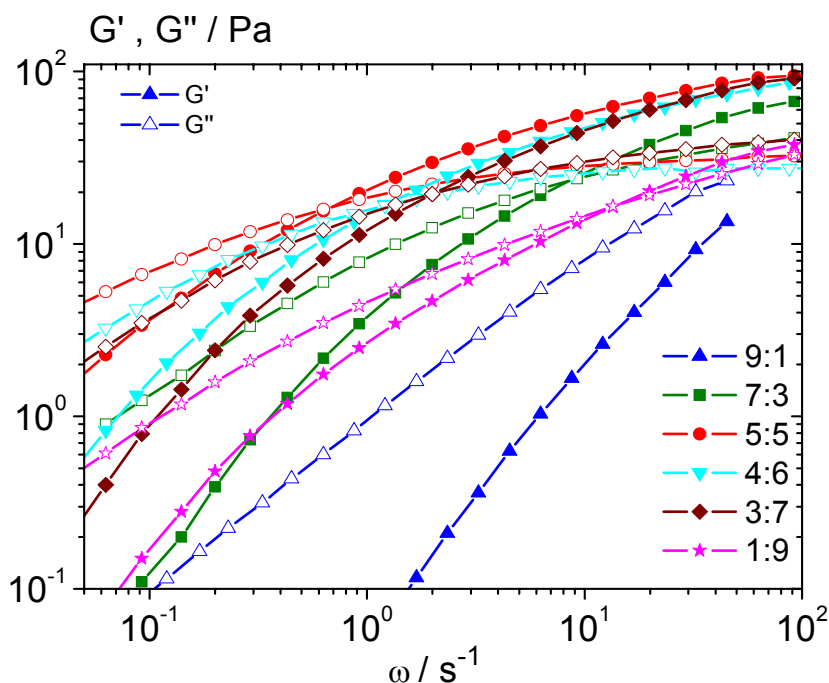


Figure 3-7: storage (closed symbols) and loss (open symbols) moduli of mixtures of PAA1600 with P(VP-VI) depending on mixing ratio.

The behavior of mixture M91 is similar to pure PAA1600, with $G' \sim \omega^2$ and $G'' \sim \omega$. For the other mixing ratios, both an increase in the absolute value of the moduli and a shift of the crossover frequency towards lower values is observed. Parallel to this shift of frequency, an increase of viscosity and a more pronounced shear thinning are recorded. The highest viscosity and the

lowest crossover frequency are found for a one to one mixture (in weight). The obvious question of the charge ratio especially depending on pH is discussed in more details in Chapter 6.

The next mixtures investigated hereafter always have a one to one weight ratio between polyanion and polycation as it appears that this ratio yields the highest viscosity enhancement.

3.3.3. Rheology of Mixtures of PAA and P(VP-VI)

One to one mixings of PAA1600 and P(VP-VI) have been studied at different concentrations: 2wt%, 1wt% and 0.5wt%. The pure polyanion having the same concentration as in the mixing is usually used as a reference to quantify the change in rheological properties since the polycation itself does not contribute significantly to either $|\eta^*|$ or $|G^*|$.

3.3.3.1. Mixtures at an overall concentration of 2wt%

The complex viscosity versus frequency at different pHs is represented in **Figure 3-8**. The dynamic moduli G' and G'' are represented in **Figure 3-9**.

★ : pH=5.5; ■ : pH=6; ▲ : pH=7; ● : pH=8; ◆ : pH=9; ☆ : PAA at pH=9

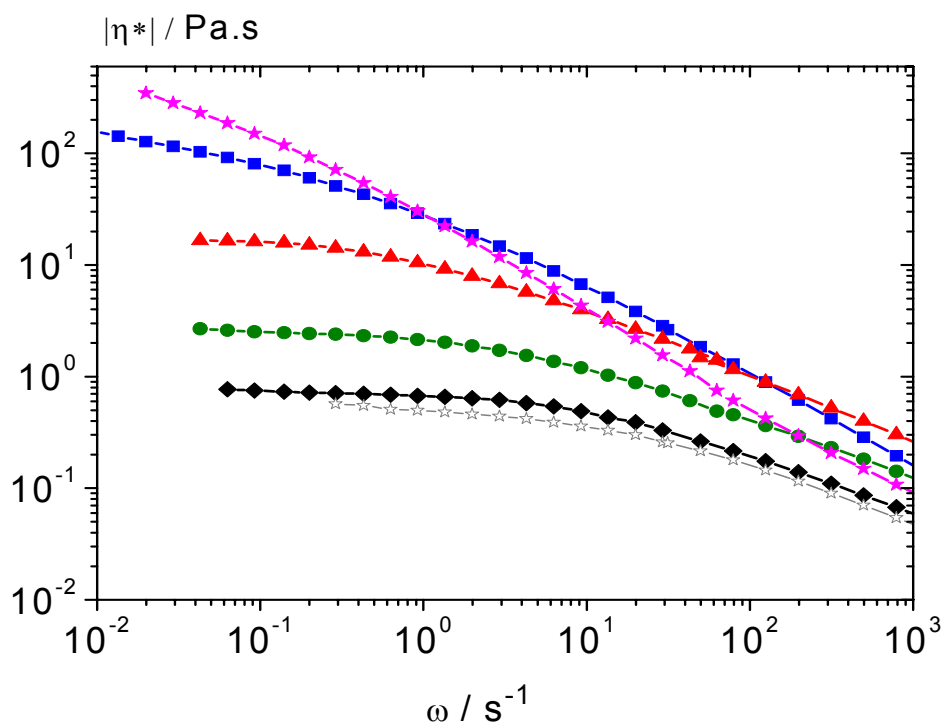


Figure 3-8: complex viscosity vs ω of mixtures of PAA1600 with P(VP-VI) at 2wt% depending on pH.

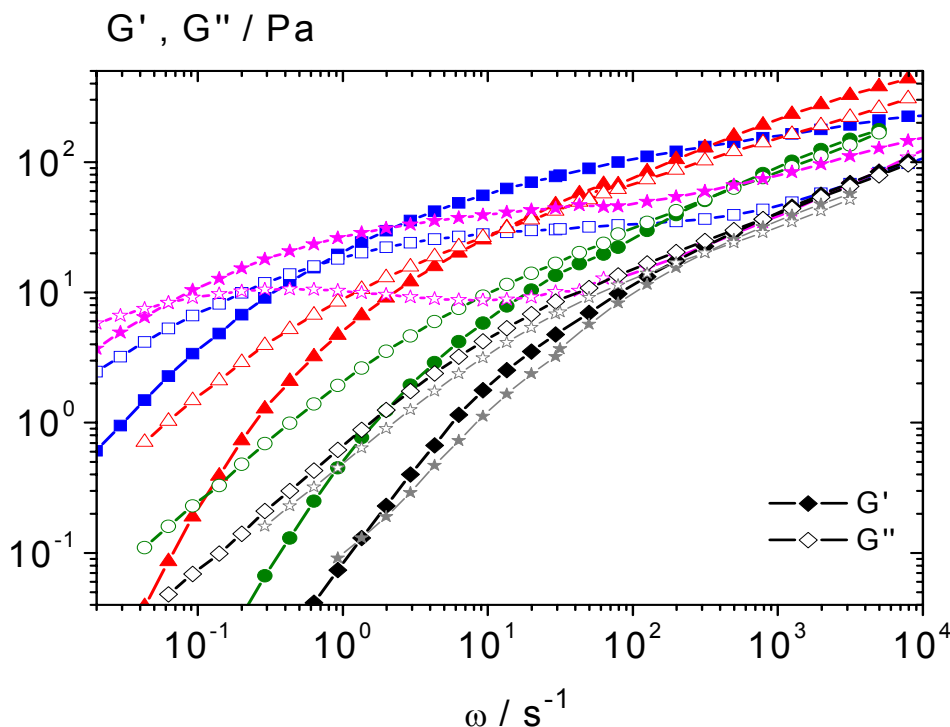


Figure 3-9: storage (closed symbols) and loss (open symbols) moduli vs ω of mixtures of PAA1600 with P(VP-VI) at 2wt% depending on pH.

At pH = 9 there is essentially no difference in viscosity between the pure PAA and the PAA/P(VP-VI) mixture. As mentioned before, the viscosity of a 1wt% solution of pure P(VP-VI) is $\eta = 4.7 \cdot 10^{-3}$ Pa.s (also independent of pH), it does not contribute to the viscosity of the mixture. From pH=9, a drop in pH leads to an increase in the zero shear viscosity of the PAA/P(VP-VI) mixtures. At pH=6 and 5.5, the viscosity is enhanced by more than two orders of magnitude. The dependency of viscosity versus frequency is also modified as the curves are no longer parallel to the ones at pH=7, 8 and 9 but are more strongly shear thinning.

At all pH, the relaxation spectra exhibit a terminal regime with $G' \sim \omega^2$, $G'' \sim \omega$, and $G'' > G'$ as well as a rubbery plateau zone, where G' is essentially independent of ω and $G' > G''$. This is not fully true at pH=5.5: relaxation is slow and measurements do not permit to document the terminal regime under these conditions.

Both regimes are separated by a critical crossover frequency ω_c at which $G' = G''$. This critical crossover depends also strongly on pH. Again, at pH=9, the PAA/P(VP-VI) mixture has a similar behavior as pure PAA with a crossover frequency ω_c around $300 \text{ rad} \cdot \text{s}^{-1}$. When the pH is decreased, the crossover frequency is shifted towards lower values, reaching 0.05 rad^{-1} at pH=5.5. At the same time, the shear moduli in the high frequency range (plateau zone) of the spectra do not vary much with pH (except at pH=5.5).

To summarize, these first results show that mixtures of PAA1600 with P(VP-VI) at 2wt% exhibit unique rheological features which depend strongly on pH. At pH=9, the viscosity and dynamic moduli of the mixtures are similar to the ones of pure PAA but as the pH is decreased, the rheological pattern is modified. These findings can be interpreted in terms of a simple linear chain model. Then the shift in ω_c corresponds to an increase in effective chain length or molecular weight. Assuming that, as predicted by the reptation model of Doi and Edwards for the stress relaxation in entangled polymer solutions or melts, $1/\omega_c \sim M_w^3$, the effective molecular weight of these complexes can be estimated. For example, the 500fold shift in ω_c observed at pH=6 corresponds to an 8fold increase in molecular weight resulting in an effective molecular weight of the complex of $M_{w,eff}=10^7$ g/mol. Moreover, the entanglement density (corresponding to the plateau modulus G') remains essentially constant.

Assuming $1/\omega_c \sim M_w^3$, **Table 3-5** summarizes the apparent increase of molar mass at different pH values. It is maximum at pH=5.5, for which the molar mass of aggregates formed appears to be 17 times larger than the one of pure PAA;

Table 3-5: apparent molar mass of mixtures of PAA1600 with P(VP-VI) at 2wt% depending on pH.

	PAA pH=9	Mix pH=9	Mix pH=8	Mix pH=7	Mix pH=6	Mix pH=5.5
ω_c (rad.s ⁻¹)	300	300	100	6	0.6	0.06
ω_c / ω_c (PAA)	1	1	$3.3 \cdot 10^{-1}$	$2 \cdot 10^{-2}$	$2 \cdot 10^{-3}$	$2 \cdot 10^{-4}$
MW_{app} / MW_{PAA}	1	1	1.4	3.7	8	17

3.3.3.2. Mixtures at an overall concentration of 1wt%

A similar study is realized for mixtures of PAA1600 and P(VP-VI) at a total concentration of 1wt%. Results for the viscosity and dynamic moduli dependency on frequency are shown in **Figure 3-10** and **Figure 3-11** respectively.

3. Rheological properties of mixtures of positively charged polyelectrolytes with poly(acrylic acid)

★ : pH=5.5; ■ : pH=6; ▲ : pH=7; ● : pH=8; ◆ : pH=9; ☆ : PAA at pH=9

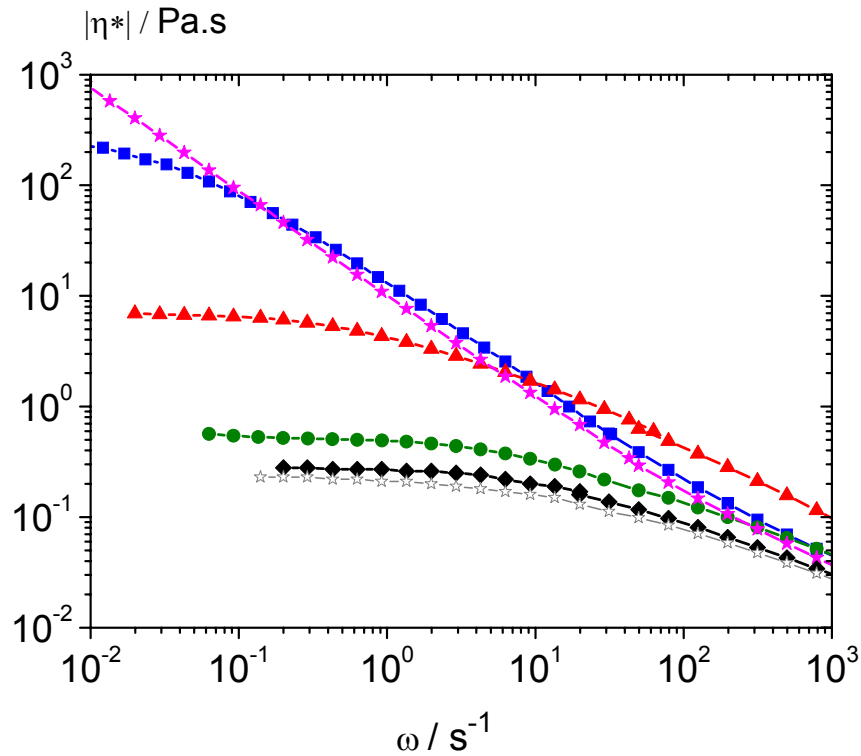


Figure 3-10: complex viscosity vs ω of mixtures of PAA1600 with P(VP-VI) at 1wt% depending on pH.

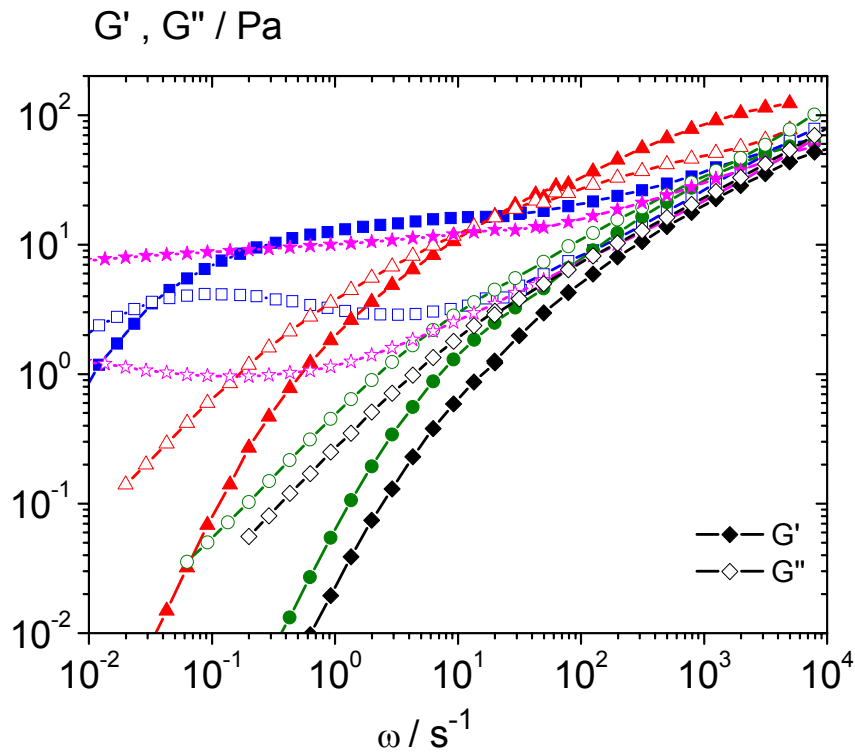


Figure 3-11: storage and loss moduli vs ω of mixtures of PAA1600 with P(VP-VI) at 1wt% depending on pH.

The same features as previously are observed. The viscosity at PH=9 for the pure PAA and the mixture of PAA and P(VP-VI) is approximately the same. A slight increase is observed at pH=8, a more pronounced one at pH=7 and a drastic one at pH=6 and pH=5.5. For this last curve, no zero shear viscosity can be measured. The sample is shear thinning over the entire frequency range.

The study of the dynamic moduli confirms these observations. At pH=5.5, G' and G'' are essentially independent of pH and no crossover can be measured. At pH=6, G' and G'' cross at $3 \cdot 10^{-2} \text{ rad} \cdot \text{s}^{-1}$. Compared to the 2wt% solution, the crossover frequency is shifted by more than a decade towards lower values.

Assuming again that $1/\omega_c \sim M_w^3$ and taking into account that pure PAA has a crossover frequency ω_c around $300 \text{ rad} \cdot \text{s}^{-1}$, the apparent molar mass at pH=7 is multiplied by almost three ($\omega_c / \omega_c(\text{PAA}) = 5 \cdot 10^{-2}$) and the apparent molar mass at pH=6 is multiplied by twenty ($\omega_c / \omega_c(\text{PAA}) = 10^{-4}$), i.e. more than the one at pH=5.5 at 2wt%.

Apparently, when concentration is decreased from 2wt% to 1wt%, relaxation becomes slower.

3.3.3.3. Mixtures at an overall concentration of 0.5wt%

Mixtures of PAA1600 and P(VP-VI) are studied at a total concentration of 0.5wt%. The complex viscosity and dynamic moduli are gathered in **Figure 3-12** and **Figure 3-13** respectively. At pH=9 and pH=8, PAA/P(VP-VI) and PAA do not differ significantly. At pH=7, the viscosity of the mixtures is again enhanced by a factor of ten. At lower pH, the mixtures do not exhibit a zero shear viscosity and are shear thinning over the entire range of frequency. The evolution of the viscosity and dynamic moduli are essentially the same at pH=5.5 and pH=6. Both the elastic and loss modulus are almost independent of the frequency and the former is one order of magnitude larger than the latter.

These features reflect the transition to a gel-like behavior in which the terminal relaxation is too slow to be measured. This phenomenon occurs while the modulus curves at different pH merge in a narrow band at high frequencies, showing that entanglement density remains essentially constant. However, the plateau value of G' are significantly different at pH=5.5 and pH=6, indicating discrepancies in the microstructure of both mixtures.

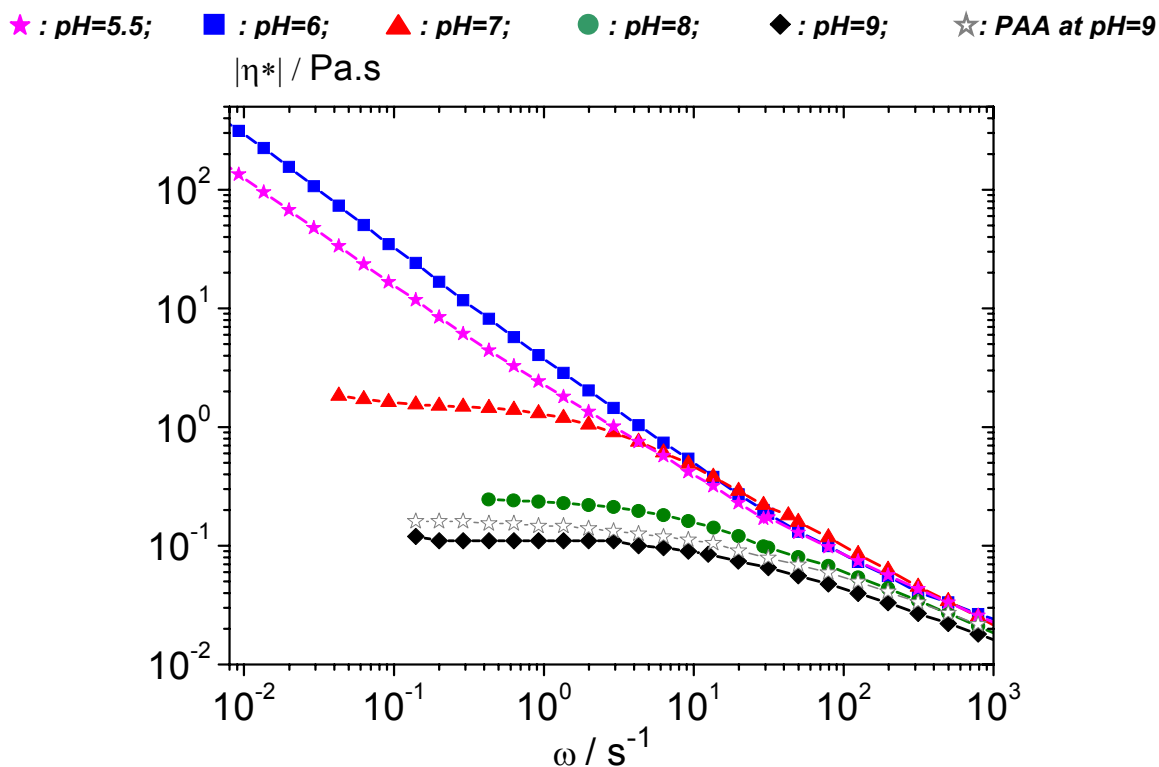


Figure 3-12: complex viscosity vs ω of mixtures of PAA1600 with P(VP-VI) at 0.5wt% depending on pH.

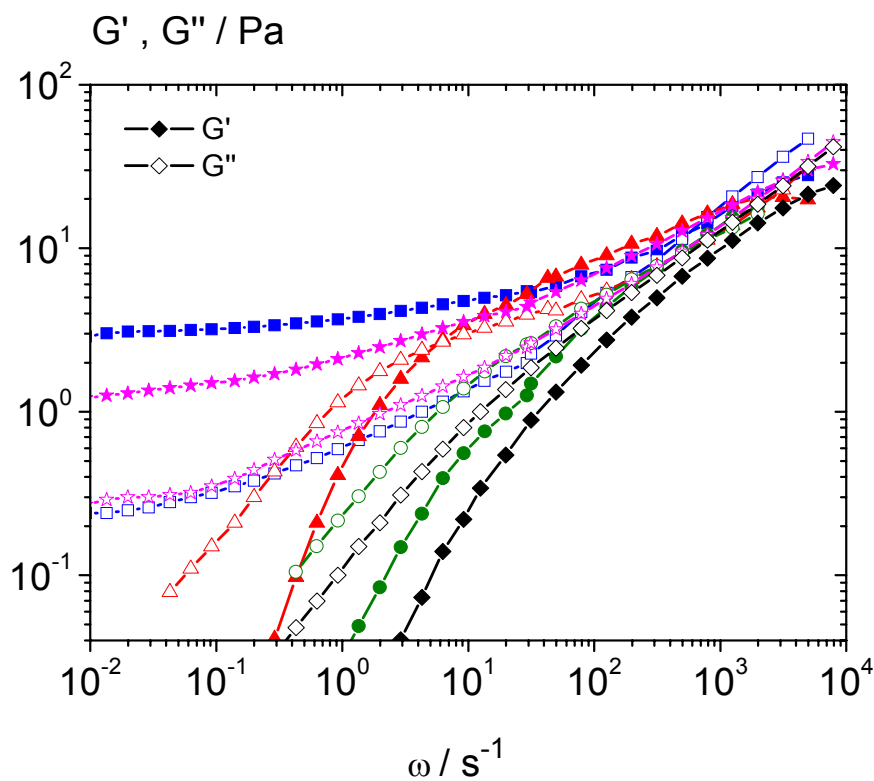


Figure 3-13: storage (closed symbols) and loss (open symbols) moduli vs ω of mixtures of PAA1600 with P(VP-VI) at 0.5wt% depending on pH.

3.3.3.4. Summary

The pH and concentration dependency of one to one PAA/P(VP-VI) mixtures exhibit unusual and unexpected features. At pH=9, the behavior of the mixtures is essentially the same as the pure polyanion. When the pH is lowered, an enhancement of the viscosity is observed as well as a decrease in the crossover frequency, while the moduli in the plateau region and high frequency scalling regime remain almost constant. These observations suggest that there must be an interaction between the polyanions and the polycations. This interaction results in an apparent increase of molecular weight of the polymers, while the entanglement density, which in the apparent linear chain model is inversely proportional to the plateau modulus, is essentially not changed. Thus, assessing a linear chain model, the molar mass increases up to 20 times. At lower concentrations and low pH, the crossover frequency and the zero shear viscosity are out of measuring range and the rheological measurements indicate a transition towards gel structures. The association of the molecules seems to be favored when the concentration is lowered. This is probably due to the unique microstructure of these mixtures, as further discussed in chapter 6.

Table 3-6: viscosity enhancement for mixtures of PAA1600 with P(VP-VI) depending on concentration and pH.

Concentration	pH=5.5	pH=6	pH=7	pH=8	pH=9
2wt%	1200	100	30	4.4	1.3
1wt%	-	650	25	2.6	1.1
0.5wt%	-	-	45	4.9	0.9

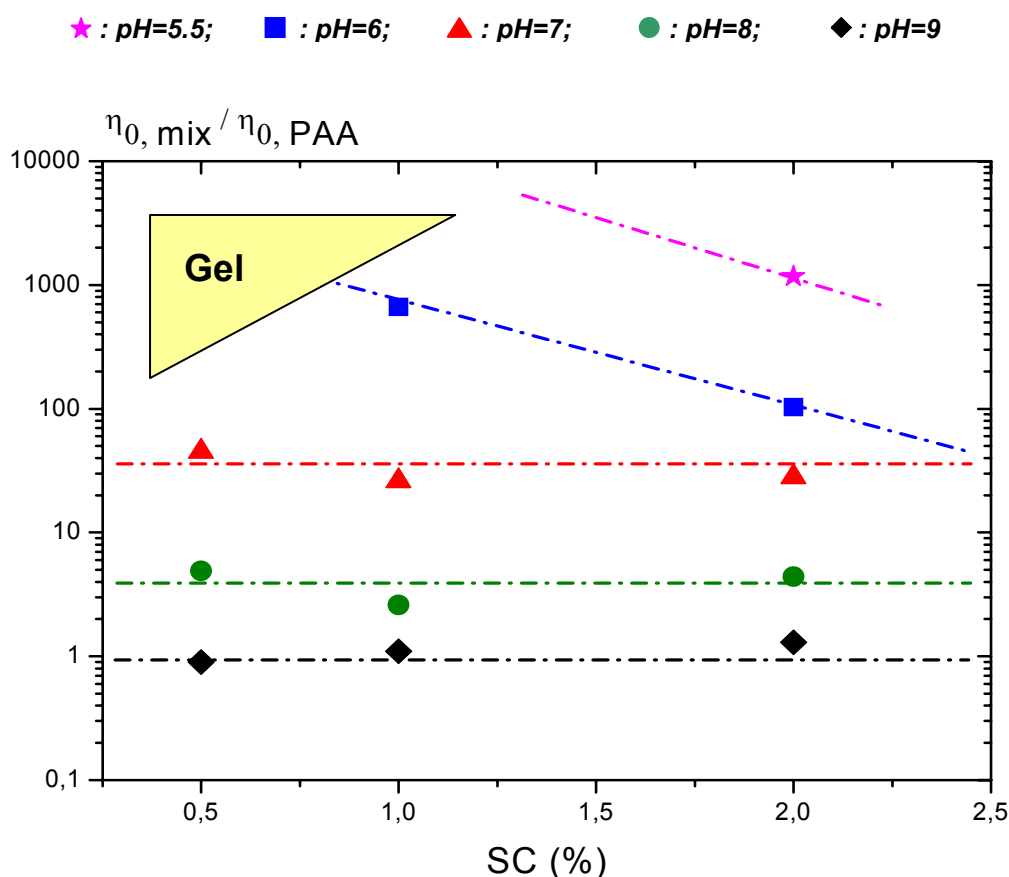


Figure 3-14: viscosity enhancement for mixtures of PAA1600 with P(VP-VI) depending on concentration and pH.

Table 3-6 and **Figure 3-14** summarize the viscosity enhancement (zero shear viscosity of mixtures over the zero shear viscosity of the pure PAA at half the concentration) for the three concentrations and the five pH studied. A different regime is observed for each pH.

- pH=9: no enhancement of the viscosity
- pH=8: moderate enhancement, less than five times
- pH=7: clear increase, up to 50 times. Relaxation is slower.

For these three pH, the increase does not depend on concentration.

- pH=6: huge increase, more than two orders of magnitude. At 0.5wt%, no zero shear viscosity can be measured and the sample exhibits a gel-like behavior.
- pH=5.5: increase in viscosity by three order of magnitudes at 2wt%. At lower concentrations, gel-like structures are also observed and no relaxation time can be determined.

3.3.4. Influence of the molar mass of poly(acrylic acid)

To assess the influence of the molar mass on the unexpected behavior described in the previous paragraph, one to one (in weight) mixtures of P(VP-VI) with 3 PAA of different molar masses have been studied. The molar masses are: 250kDa (PAA250), 900kDa (PAA900), 3300kDa (PAA3300).

3.3.4.1. Mixtures of P(VP-VI) with PAA250

The solution of PAA250 at pH=6, 7 or 8 turn out to be of very low viscosity and dynamic measurements are difficult to perform. As the behavior of the solutions can be assumed to be Newtonian, static measurements are done on the 2wt% and 1wt% solutions at pH=6.

The zero shear viscosity is 10mPa.s for the pure PAA250 at 2wt% and 13mPa.s for a one to one P(VP-VI)/PAA250 mixture having a same concentration in polyanion. No viscosity increase takes place. The 1wt% mixture is water-like and not measured.

These results show that below a critical molecular weight of the polyanion, the mixtures of PAA and P(VP-VI) do not exhibit any thickening effect at pH=6. Apparently a critical molar mass, higher than 250kDa is necessary for the formation of extended structures responsible for the increase in viscosity.

3.3.4.2. Mixtures of P(VP-VI) with PAA900

First, in order to be able to calculate a viscosity enhancement, the zero shear viscosity of the pure PAA900 (which is the viscosity over the entire frequency range for the pure polymers since it is basically Newtonian) at various pH and concentrations is measured (**Table 3-7**).

Table 3-7: zero shear viscosity in Pa.s of PAA900 depending on concentration and pH.

Concentration	pH=6	pH=7	pH=8
2wt%	0.29	0.32	0.31
1wt%	0.12	0.13	0.12
0.5wt%	0.062	0.058	0.057
0.25wt%	0.025	0.023	0.021

The rheological behavior of one to one mixtures of PAA900 and P(VP-VI) in weight at concentrations 0.5wt%, 1wt% and 2wt% and pH=6, 7 or 8 is determined subsequently. The aim

of this study is to determine if 900kDa is a sufficient molar mass to observe the same viscosity increase as in previous paragraphs using PAA1600.

Results obtained for complex viscosity and dynamic moduli measurements are gathered in **Figure 3-15**, respectively in the first and second columns. The upper row corresponds to mixtures at 2wt%, the middle row to mixtures at 1wt% and the lower row to mixtures at 0.5wt%.

For the 2wt% mixtures at pH=8, the behavior is almost Newtonian as the sample has a constant viscosity over the entire frequency range. No crossover can be determined in this case and G' and G'' exhibit the terminal regime of viscoelastic fluids, for which $G' \sim \omega^2$, $G'' \sim \omega$. As the pH is lowered, the viscosity increases and the mixtures become shear thinning. The G' and G'' crossover frequency is also shifted towards lower values.

At 0.5wt% and pH=6, a transition towards a gel-like behavior is observed. Nevertheless, G' and G'' differ only by a factor of two and not by an order of magnitude like it was the case with PAA1600. This indicates a less defined network due to a poorer bridging, probably because of the shorter negative chains.

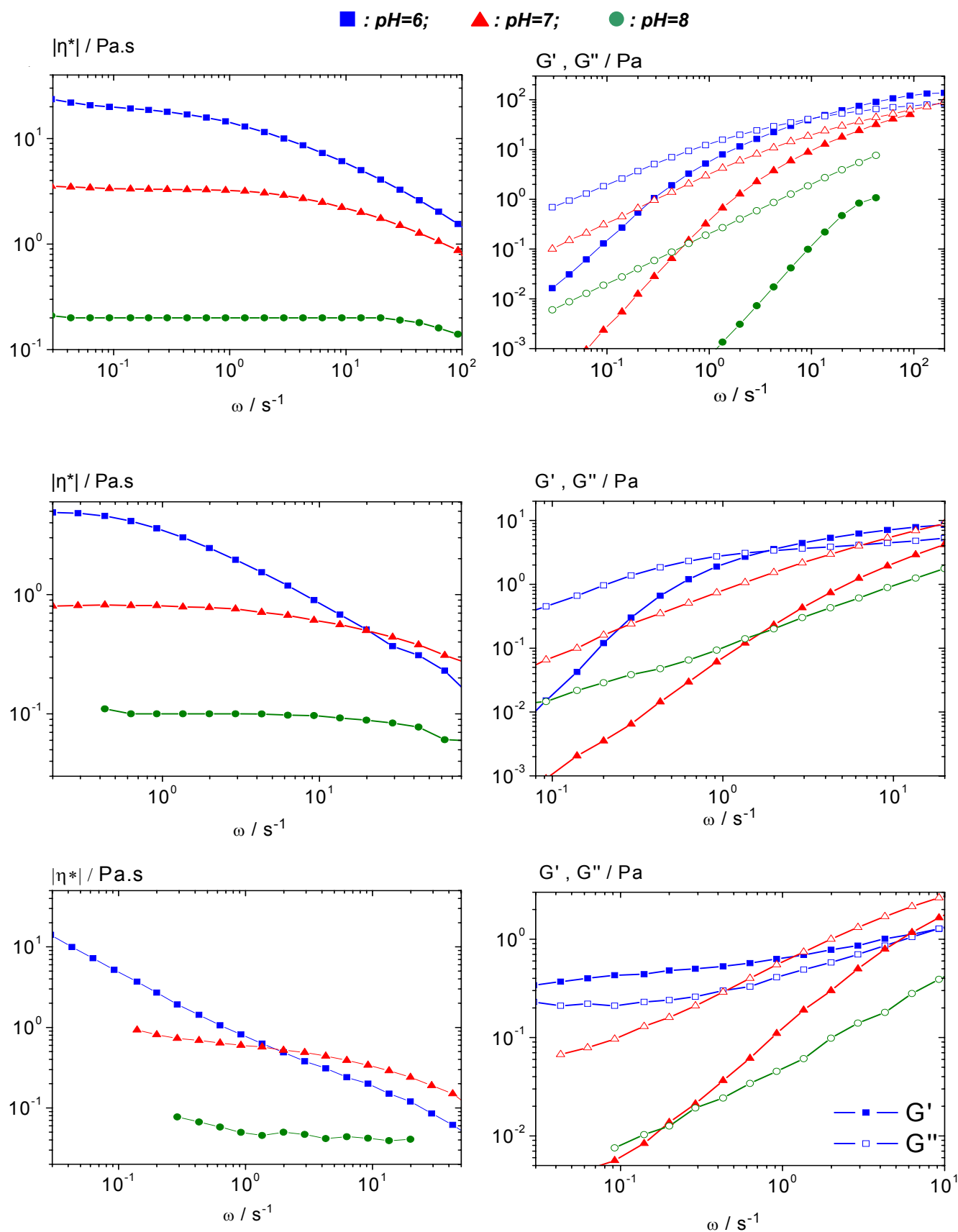


Figure 3-15: complex viscosity, storage (closed) and loss (open symbols) moduli vs ω for 1:1 mixtures of P(VP-VI) + PAA900 at 2wt% (upper row), 1wt% (middle row) and 0.5wt% (lower row).

Using the values of zero shear viscosities measured for pure PAA900 and mixtures of PAA with P(VP-VI), the viscosity enhancement ($|\eta^*|_0(\text{mix}) / |\eta^*|_0(\text{PAA})$) can be calculated; results are shown in **Figure 3-16**.

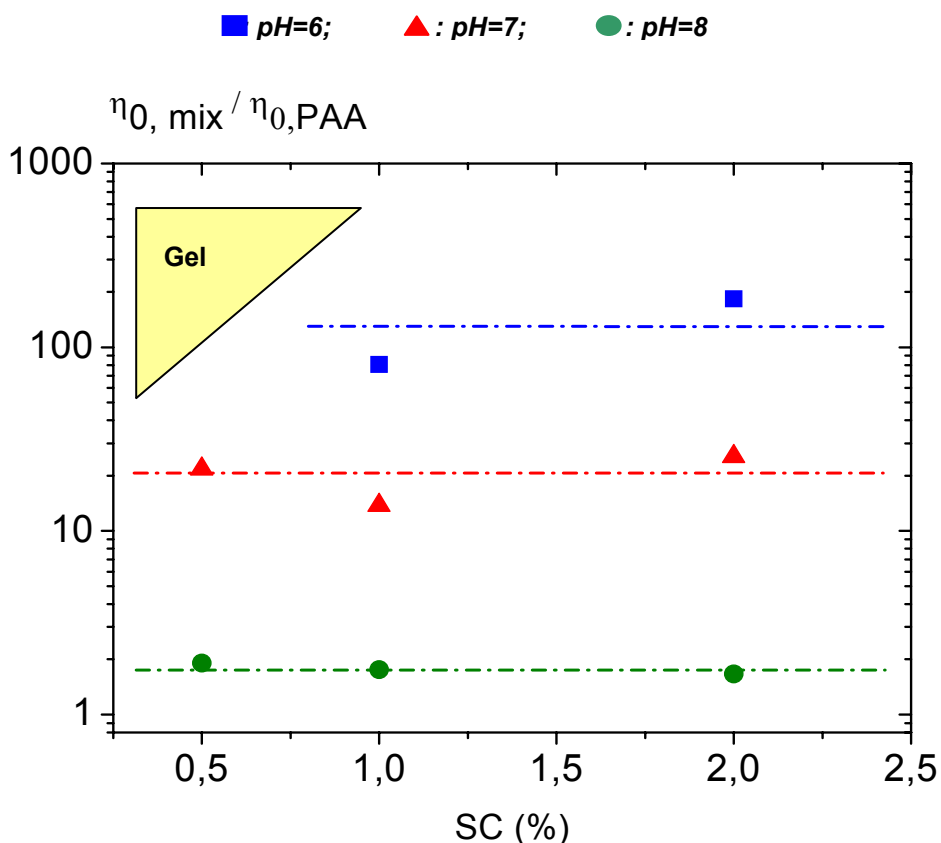


Figure 3-16: viscosity enhancement for mixtures of PAA900 with P(VP-VI) depending on concentration and pH.

Three regimes are clearly visible again, represented by the green, red and blue lines: only a marginal change in viscosity at pH=8, a tenfold increase at pH=7 and an increase by two order of magnitude at pH=6 for a concentration of 2wt% and 1wt%. At pH=6 and 0.5wt%, a gel-like structure is observed, but the dynamic moduli shown in **Figure 3-15** (bottom right) seem to indicate that such a structure is not as well defined as for PAA1600. At 2wt% and 1wt%, it seems that the plateau modulus is essentially independent of the pH, again indicating that the entanglement density is essentially not modified.

3.3.4.3. Mixtures of P(VP-VI) with PAA3300

After using a polyanion with a lower molar mass compared to PAA1600, the next set of experiments is carried out with a higher molar mass PAA. The dynamic zero shear viscosity of PAA3300 is determined first, in order to subsequently assess the viscosity enhancement. Results are gathered in **Table 3-8**.

Table 3-8: zero shear viscosity in Pa.s of PAA3300 depending on concentration and pH.

Concentration	pH=6	pH=7	pH=8
1wt%	2.6	4.1	2.1
0.5wt%	1.4	1.7	1.1
0.25wt%	0.6	0.9	0.5

The rheological behavior of one to one mixtures of PAA3300 and P(VP-VI) at concentrations 0.5wt% and 2wt% and pH=6, 7 or 8 is then measured. Results are shown in **Figure 3-17**.

At 2wt%, an increase in viscosity is observed when the pH is lowered. Again at pH=6, this increase goes along with a shift of the G' and G'' crossover frequency towards lower values. However, this shift is not very marked compared to what has been measured with PAA900 and PAA1600: less than & order of magnitude here compared to more than 2 with lower Mw PAA. At pH=7 and pH=8, no difference in the crossover frequency appears.

At 0.5wt%, the same phenomenon is observed: increase in viscosity and shift in crossover frequency. From 8 rad.s^{-1} at pH=8, the crossover is shifted to 2 rad.s^{-1} at pH=7 and $7 \cdot 10^{-2} \text{ rad.s}^{-1}$ at pH=6. Again, the variations with decreasing pH are minor: only 2 orders of magnitude between pH=8 and pH=6. Furthermore, no gel-like behavior is observed for these mixtures as G' and G'' still exhibit characteristics of visco-elastic fluids. It seems that using a polyanion with a very high molar mass does not favor the formation of extended structures, but limits it on the contrary. This observation is further commented in the conclusion of this chapter.

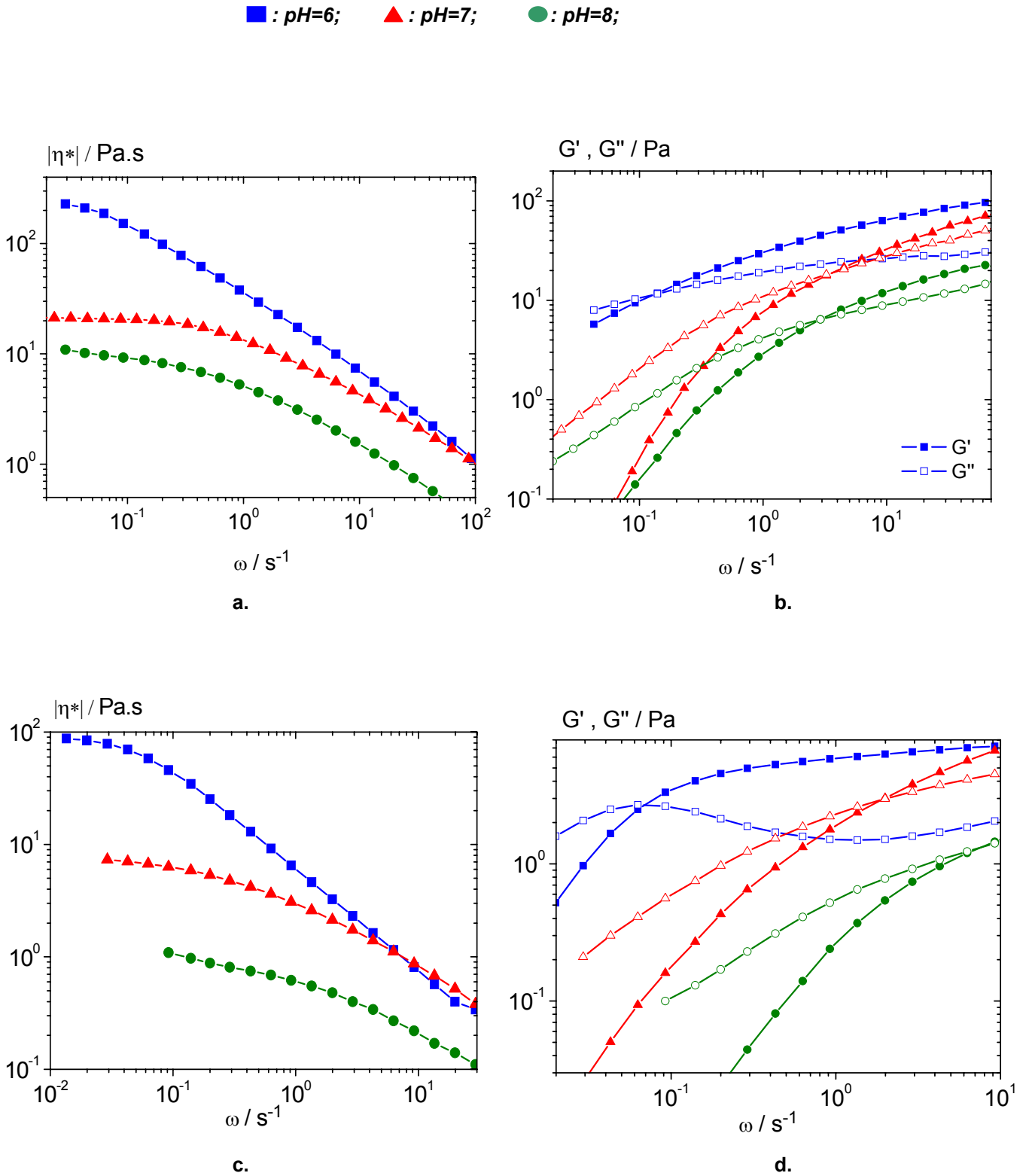


Figure 3-17: complex viscosity, storage (closed symbols) and loss (open symbols) moduli vs ω for 1:1 mixtures of P(VP-VI) + PAA3300 at 2wt% (upper row) and 0.5wt% (lower row) depending on pH.

Using the zero shear viscosity measured for pure PAA3300 (cf. **Table 3-8**), the viscosity enhancement is calculated (cf. **Figure 3-18**).

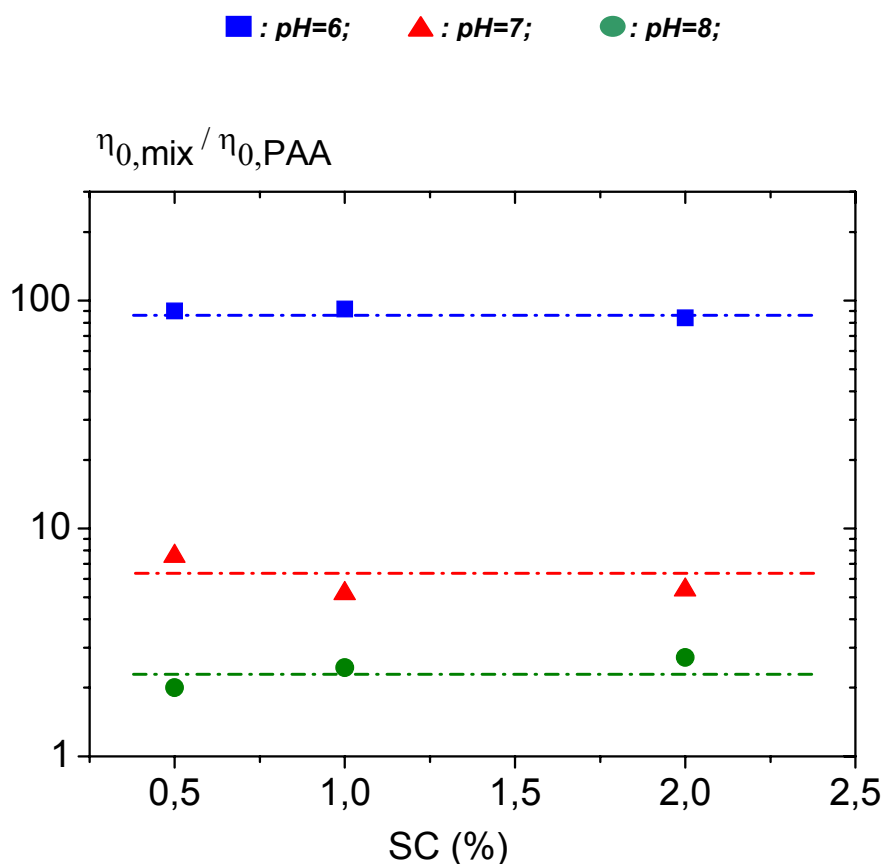


Figure 3-18: viscosity enhancement for mixtures of PAA3300 with P(VP-VI) depending on concentration and pH.

Again 3 regimes can be pointed out corresponding to the three pH investigated. If the crossover at pH=8 is taken as a reference and assuming again that $1/\omega_c \sim M_w^3$, the apparent molar mass is then increased by a factor of 1.6 at pH=7 and by a factor of 5 at pH=6. These values are significantly lower than the ones measured for PAA1600 and even PAA900.

As a consequence, viscosity enhancement for PAA3300 is less pronounced compared to PAA1600 and PAA900. Moreover, there is no transition in the thickening effect from “linear chains” to a “gel-like structure” like in the other cases.

3.4. Conclusion

To compare the thickening efficiency of the different PAA depending on pH and concentration, the value of the ratio $|\eta^*|_0(\text{mix}) / |\eta^*|_0(\text{PAA})$ for all mixtures investigated is plotted in **Figure 3-19**. The colors refer to different polymers and the change in symbols to different pH.

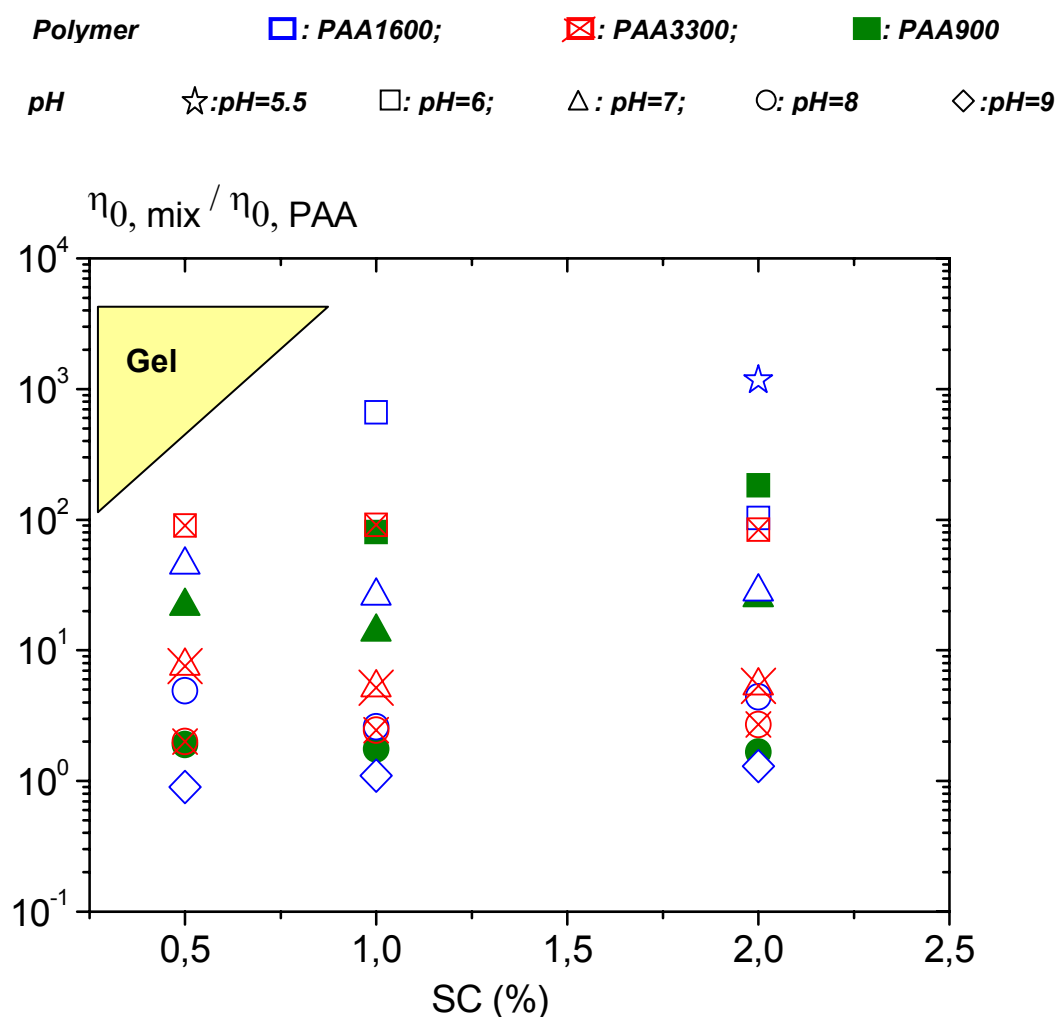


Figure 3-19: viscosity enhancement for mixtures of PAA with P(VP-VI) depending on concentration and pH.

In all cases, similar characteristics features of one to one mixtures of PAA and P(VP-VI) are:

- Viscosity increases as pH is lowered.
- Viscosity enhancement is essentially independent of concentration except at 0.5wt%.
- A transition from a linear chain behavior towards a gel-like behavior occurs when concentration is decreased from 1wt% to 0.5wt% at pH=6 (and pH=5.5).

By changing the molecular weight of the PAA, some additional features can be pointed out:

- A minimum Mw is necessary so that thickening phenomenon occurs, with $250\text{kDa} < M_{w,crit} < 900\text{kDa}$.
- Highest absolute viscosities are measured using the highest Mw PAA. However, the highest viscosity enhancement ($\eta_{0,mix}/\eta_{0,PAA}$) is recorded with the intermediate PAA Mw. This is clearly visible in **Figure 3-20**, in which the concentration is always 1wt% (trends are similar at other concentrations). In the right hand side graph, viscosity enhancement at different pH is plotted versus Mw of PAA; in the left hand side one, viscosity enhancement for different Mw is plotted versus pH.

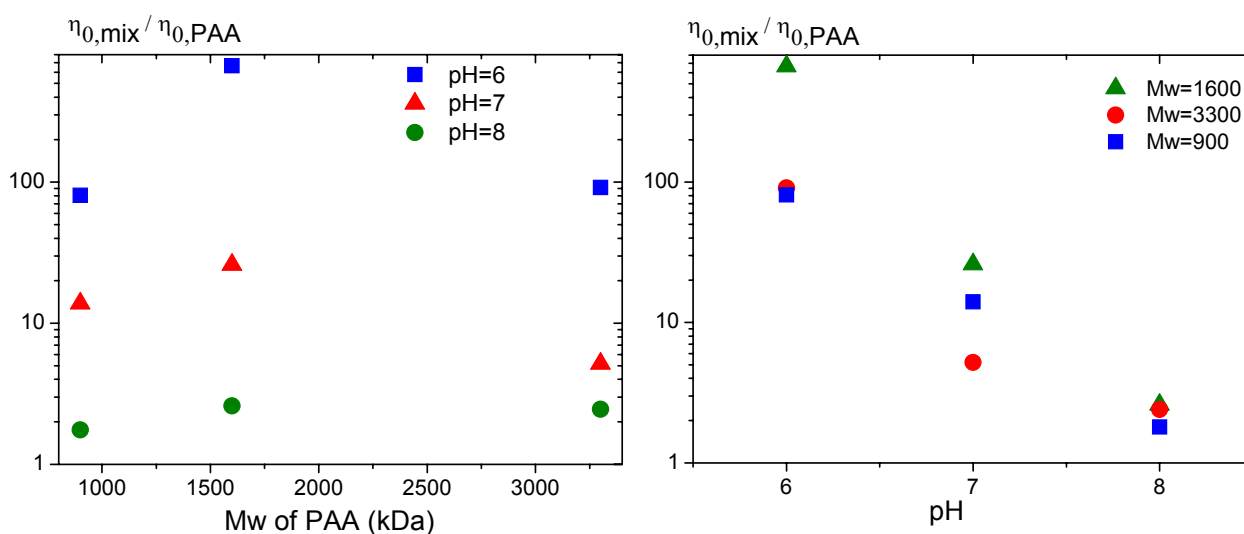


Figure 3-20: viscosity enhancement for mixtures of PAA and P(VP-VI) at SC=1%, depending on Mw of PAA and pH.

The reason why the increase in viscosity is more pronounced when intermediate molar mass PAA are used may lie in the microstructures which are formed when the oppositely charged polyelectrolytes are mixed. Studying mixtures of high molar mass positively charged rigid polysaccharides with low molar mass polyanions and hydrophobically modified polyanions, Liu et al. observed an increase in viscosity comparable with the one depicted in this chapter (Liu 2001 and 2003). They attributed this effect to the formation of networks which characteristics depend mainly on concentration, charges and molar mass. Regarding this last parameter, they assumed that a higher molar mass of the polysaccharides leads to more likely complexation of several short polyanions with one long polycation.

The same phenomenon is probably occurring here when PAA3300 is used: small P(VP-VI) chains more likely stick to a single PAA chain rather than bridging several ones, thus leading to

an increase in viscosity less marked than with PAA1600. It is likely that larger structures are formed but not infinite (or very extended) structures which would lead to a “freezing” of the system.

On the contrary, when PAA900 is used, the chains are too small to allow for the formation of structures extended enough to increase the viscosity as much as when PAA1600 is used.

4. Influence of the nature of the negative charge

4.1. Introduction

Mixing oppositely charged aqueous polyelectrolytes usually leads to the formation of polyelectrolyte complexes. The resulting complexes can be water soluble; however, they are usually present as dispersed colloids or macroscopic precipitates. This was shown in chapter 2, in which the importance of the mixing ratio between positive and negative charges has been demonstrated. These in-situ complexation experiments also showed the importance of the nature of the charge, as the charge balance is modified if either AA (weak acid) or AMPS (strong acid) is used as polyanion.

From a fundamental perspective, there has been interest in understanding the detailed structures of polyelectrolyte complexes, composition, degrees of swelling, and the concentration of ionic crosslinks depending on the chemistry and nature of the charge used. A number of approach has been used to determine especially the variation of stoichiometry for various systems (Michaels 1965, Tsuchida 1982, Dautzenberg 1989).

Concerning the difference between weak and strong polyelectrolytes, studies, especially theoretical, have been undertaken which revealed how complex this issue is. Indeed, pK_a values of ionizable groups in macromolecules can be significantly different from those of the isolated groups in solution because of interactions between neighboring ionizable groups, solvation effects, and conformational changes (Mafé 2004). End-group effects can also play a role (Limbach 2001).

Weak acid and basic groups are of particular importance because the charge balance (and then the ionic selectivity of the system) can be controlled by the pH and salt concentration of the external solution (English 1996, Jimbo 2000, Rmaile 2002). Therefore, the theoretical estimation of the apparent dissociation constant of a weak polyacid in the vicinity of a basic group has been of great interest in recent years. But as the effective pK_a of an acid group i.e. the effective charge density on a weak polyelectrolyte can be changed due to several factors (Haines 1983), the best way to study a particular system is mainly empirical.

Therefore, to complete the study carried out on the influence of the nature of the charge at low pH in chapter 2, the influence of the nature of the charge at higher pH was also investigated.

Copolymers of AA and AMPS have been synthesized and mixed with P(VP-VI) in 1 to 1 (w/w) mixtures.

4.2. Experimental

4.2.1. Materials and methods

4.2.1.1. Polyanions

The polyanions are statistical copolymers of acrylic acid and 2-acrylamido-2-methyl-1-propanesulfonic acid containing either 20 molar % or 40 molar % of AMPS in the copolymer (named respectively P(AA_{0.8}-AMPS_{0.2}) and P(AA_{0.6}-AMPS_{0.4})). Both copolymers are synthesized following the recipe described in the experimental section.

Field Flow Fractionation at pH=11 and 1g.L⁻¹ yields an average molecular weight of M_w=1.8 x10⁶ g/mol for both polymers.

After synthesis, the polymers are stored as low pH stock solutions (depending on AMPS content) having a concentration of 10wt %. Before direct measurement or preparation of mixtures, these stock solutions are diluted to the desired concentration with deionized water and neutralized to the desired pH with 1N sodium hydroxide.

4.2.1.2. Polycation

Poly(vinyl imidazole-co-vinyl pyrrolidone) is provided by BASF SE (Ludwigshafen Germany) as a 20 weight % solution in water. Field Flow Fractionation at pH=11 and 1g.L⁻¹ yields an average molecular weight M_w=1,0 x10⁵ g/mol. This stock solution is diluted to the desired concentration using distilled water.

4.2.1.3. Sample preparation

The rheometer and measuring procedure are as described in chapter 3.

The pure P(AA_{0.8}-AMPS_{0.2}) and P(AA_{0.6}-AMPS_{0.4}) are diluted to 4 different concentrations: 2wt%, 1wt%, 0.5wt% and 0.25wt%. These solutions are neutralized to 5 pH: 5.5, 6, 7, 8 and 9. The viscosity measured at a given pH and concentration serves as a reference for the calculation of viscosity enhancement at the same pH and double concentration. Mixtures are investigated in a narrower frequency range than PAA. Based on the results obtained for PAA using a PAV, it is assumed that at high frequency all G' curves merge in a narrow window.

4.3. Results and discussions

4.3.1. Rheology of pure polyanions

The frequency dependence of complex viscosity and dynamic moduli are measured for pure polyanions at various pH and concentrations.

As examples, the frequency dependence of G' and G'' at different pH for 2wt% solutions of P(AA_{0.8}-AMPS_{0.2}) (left hand side) and P(AA_{0.6}-AMPS_{0.4}) (right hand side) are plotted in **Figure 4-1**.

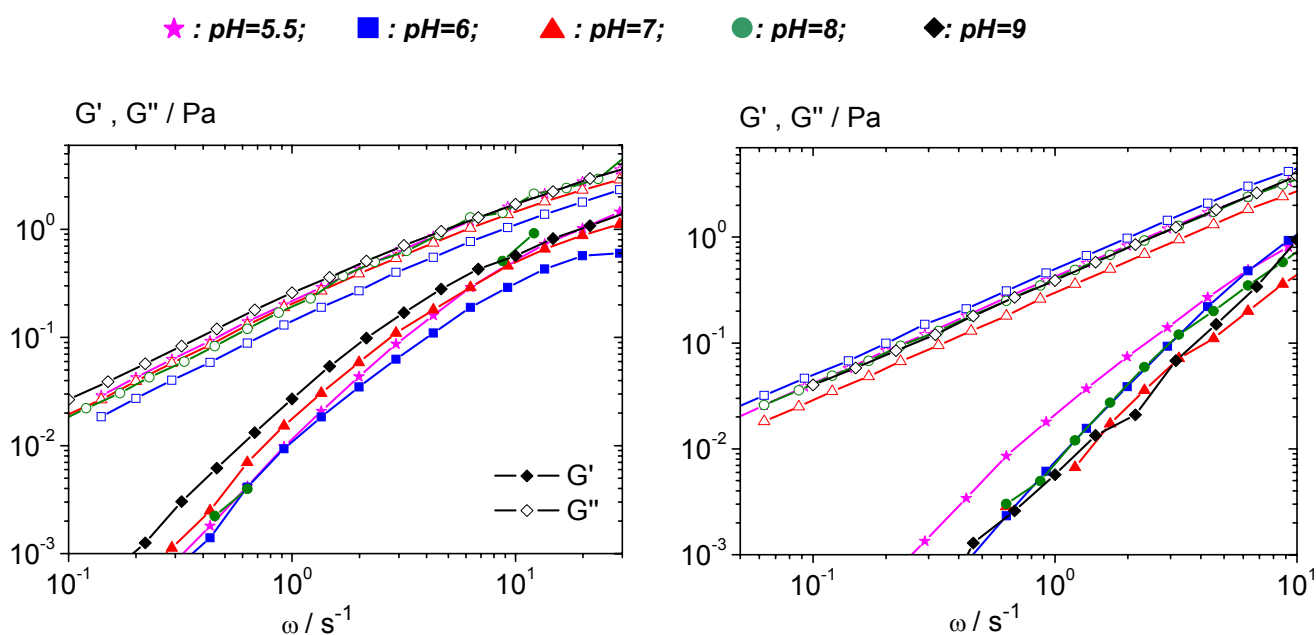


Figure 4-1: frequency dependence of storage (closed symbols) & loss (open symbols) moduli of P(AA_{0.8}-AMPS_{0.2}) (left hand side) and P(AA_{0.6}-AMPS_{0.4}) (right hand side) at 2wt% depending on pH.

Results are comparable to the ones gathered in **Figure 3-1** obtained for pure PAA. The terminal regime of viscoelastic fluids in which G' and G'' exhibit slopes of respectively 2 and 1 is observed over most of the frequency range investigated. The pH dependency is minor for both polyanions and there is no clear trend concerning the evolution of the dynamic moduli with pH. The zero shear viscosities are gathered in **Table 4-1**. For each pH, results corresponding to P(AA_{0.8}-AMPS_{0.2}) are gathered in column “AA_{0.8}” and results corresponding to P(AA_{0.6}-AMPS_{0.4}) in column “AA_{0.6}”.

4. Influence of the nature of the charge

Table 4-1: $|\eta^*|_0$ of $P(AA_{0.8}\text{-}AMPS_{0.2})$ & $P(AA_{0.6}\text{-}AMPS_{0.4})$ depending on concentration and pH.

	pH=5.5		pH=6		pH=7		pH=8		pH=9	
Concentration	AA _{0.8}	AA _{0.6}	AA _{0.8}	AA _{0.6}	AA _{0.8}	AA _{0.6}	AA _{0.8}	AA _{0.6}	AA _{0.8}	AA _{0.6}
2wt%	1,41	0,43	1.12	0,45	1.18	0,38	1,15	0,41	1,6	0,39
1wt%	0,54	0,19	0,46	0,13	0,42	0,144	0,4	0,157	0,6	0,19
0.5wt%	0,22	0,087	0,18	0,073	0,19	0,08	0,18	0,097	0,26	0,09
0.25wt%	0,04	0,017	0,023	0,019	0,027	0,012	0,026	0,025	0,13	0,05

A sharp viscosity decrease with decreasing concentration is measured for both polyanions, independent of pH.

The absolute values are lower for $P(AA_{0.6}\text{-}AMPS_{0.4})$ compared to $P(AA_{0.8}\text{-}AMPS_{0.2})$. This is clearly visible in **Figure 4-2** in which zero shear viscosity for both polyanions are plotted using the same logarithmic scale.

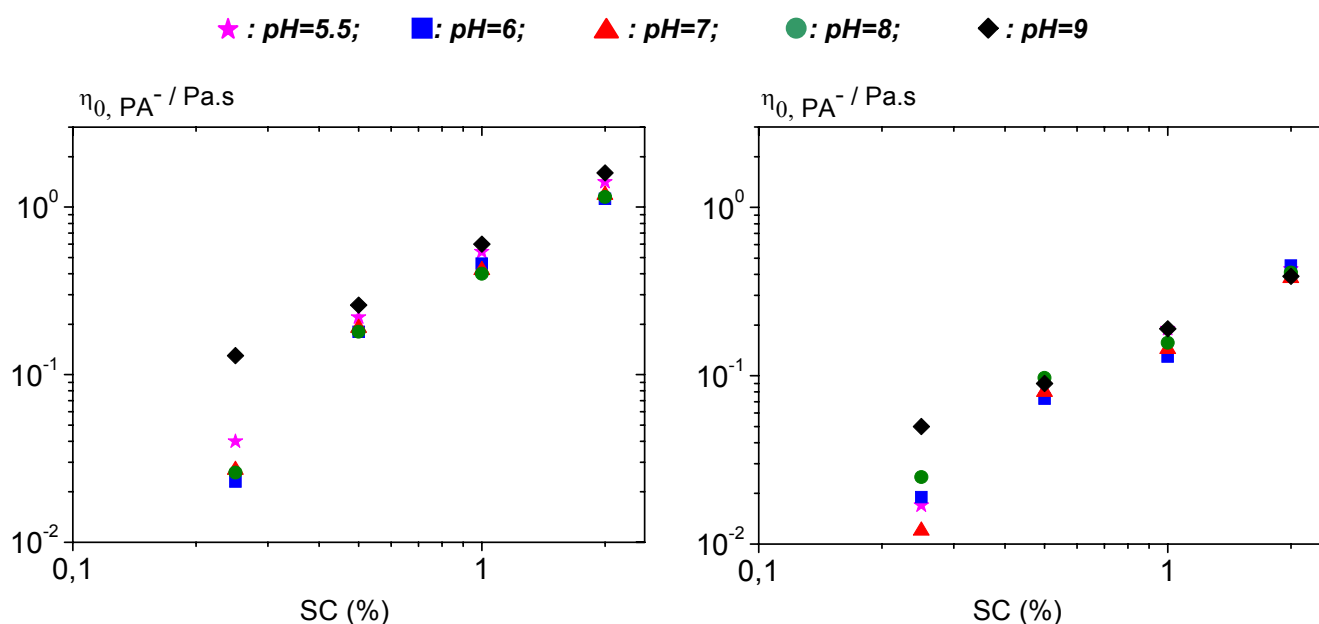


Figure 4-2: $|\eta^*|_0$ of $P(AA_{0.8}\text{-}AMPS_{0.2})$ (left hand side) & $P(AA_{0.6}\text{-}AMPS_{0.4})$ (right hand side) depending on concentration and pH.

This difference in absolute value of viscosity may be related to the differences in molar mass of AA ($72\text{g}\cdot\text{mol}^{-1}$) and AMPS ($207\text{g}\cdot\text{mol}^{-1}$). Indeed, from the molecular weight of the polyanions determined by FFF, it is possible to deduce the average degree of polymerization which is respectively 22200, 18100 and 14300 for PAA ($M_w=1.6\text{MDa}$),

P(AA_{0.8}-AMPS_{0.2}) (Mw=1.8MDa) and P(AA_{0.6}-AMPS_{0.4}) (Mw=1.8MDa). The difference in degree of polymerization means that the contour length of the polyanion chain decreases with increasing amount of AMPS, leading to lower zero shear viscosities.

Concerning the evolution of the viscosity with concentration, similar to what has been observed with pure PAA (cf. page 78 of this manuscript), $\eta_0 \sim c^\alpha$ at 0.5wt% and higher concentrations with $\alpha=1.34$ for P(AA_{0.8}-AMPS_{0.2}) and $\alpha=1.15$ for P(AA_{0.6}-AMPS_{0.4}): this is in good agreement with predictions for polyelectrolytes in the high salt limit. At 0.25wt%, such a power-law dependency is observed only at pH=9, where the ionic strength is highest. At lower pH, the viscosities are lower: this is expected for polyelectrolytes in the low salt limit for which $\eta_0 \sim c^{0.5}$.

Pure P(AA_{0.8}-AMPS_{0.2}) and P(AA_{0.6}-AMPS_{0.4}), similar to what has been measured for PAA, exhibit the terminal regime typical for viscoelastic fluids, for which $G' \sim \omega^2$ and $G'' \sim \omega$. Viscosity decreases along with the concentration and no significant and systematic influence of pH is visible.

4.3.2. Rheology of Mixtures

4.3.2.1. P(AA_{0.8}-AMPS_{0.2}) + P(VP-VI)

One to one mixtures (in weight) of P(AA_{0.8}-AMPS_{0.2}) and P(VP-VI) have been studied at different concentrations (2wt%, 1wt% and 0.5wt%) and different pH (5.5, 6, 7, 8 and 9) using the same standard procedure already used for PAA. For all experiments described in this chapter, the mixtures at pH=9 are taken as references as it was shown in the previous chapter that the behavior of pure polymers and mixtures at pH=9 (double concentration) are essentially similar.

Results are gathered in **Figure 4-3**. At pH=8 and pH=9, the zero shear viscosities values are strictly the same and so is the frequency dependence of G' and G'' . A regime is reached in which G'' is always greater than G' and their slopes are respectively 2 and 1, typical for the terminal regime of viscoelastic fluids, like solutions of polymers. At different concentrations, only the value of the dynamic moduli are affected, not their frequency dependence. Generally, the values of the moduli decrease accordingly to decreasing concentrations.

At pH=7, zero shear viscosity is increased by a factor of 10, raising from 0.3Pa.s to 3Pa.s. In parallel, a modification of G' and G'' pattern is observed, as the crossover frequency is shifted

towards lower values. Again, this shift is comparable at 2wt%, 1wt% and 0.5wt% ($\sim 30s^{-1}$). Only the value of the dynamic moduli and the zero shear viscosity decrease as the concentration is lowered.

As the pH is further decreased to pH=6, the relaxation behavior of the samples changes. At 2wt% and 1wt%, the crossover is again shifted to lower value. This shift is more pronounced at 1wt%. At 0.5wt%, the relaxation is so slow that no crossover can be measured, G' and G'' are parallel, essentially pH independent and G' is approximately one order of magnitude greater than G'' . These features are typical for gel-like structures. Therefore, no zero shear viscosity can be measured as the sample is shear thinning over the entire frequency range.

At pH=5.5, a similar slowing down of the relaxation similar to the one at pH=6 is observed. The more acute shear thinning visible when measuring the zero shear viscosities goes along with a shift in the G' and G'' crossover frequency, more pronounced as the concentration decreases. At 0.5wt%, G' and G'' are again frequency independent indicating that the systems evolves toward a gel-like structure. Interestingly, the value of the G' plateau is significantly lower at pH=5.5, 0.5wt% compared to the mixtures at other pH for which they merge into a narrow range. This further supports the idea that significant structural changes occur within the sample, as the system evolves from free chains towards grafted chains and finally towards more extended structures. Similarly to the results gathered in chapter 3 for mixtures of PAA with P(VP-VI), distinction between the mixtures at pH=9 and pH=8, the mixture at pH=7 and the mixtures at pH=6 and pH=5.5 is clear. A 10fold increase in viscosity is observed when pH is lowered from 8 to 7, followed by a transition towards a gel-like behavior characterized by a further increase in viscosity and by G' and G'' being essentially frequency independent at pH=5.5. In **Table 4-2**, the viscosity enhancements, $\eta_{0, \text{mix}} / \eta_{0, \text{PA}^-}$ are gathered depending on pH and concentrations. For the mixtures for which no value is indicated, the samples are shear thinning over the entire frequency range and η_0 is not defined. Results are discussed in the next paragraph.

Table 4-2: viscosity enhancement of $P(AA_{0.8}\text{-}AMPS_{0.2})+P(VP\text{-}VI)$ depending on concentration and pH

Concentration	pH=5.5	pH=6	pH=7	pH=8	pH=9
2wt%	-	211	20	2.2	1.5
1wt%	-	-	17	1.7	1.2
0.5wt%	-	-	63	3.6	1.0

4. Influence of the nature of the charge

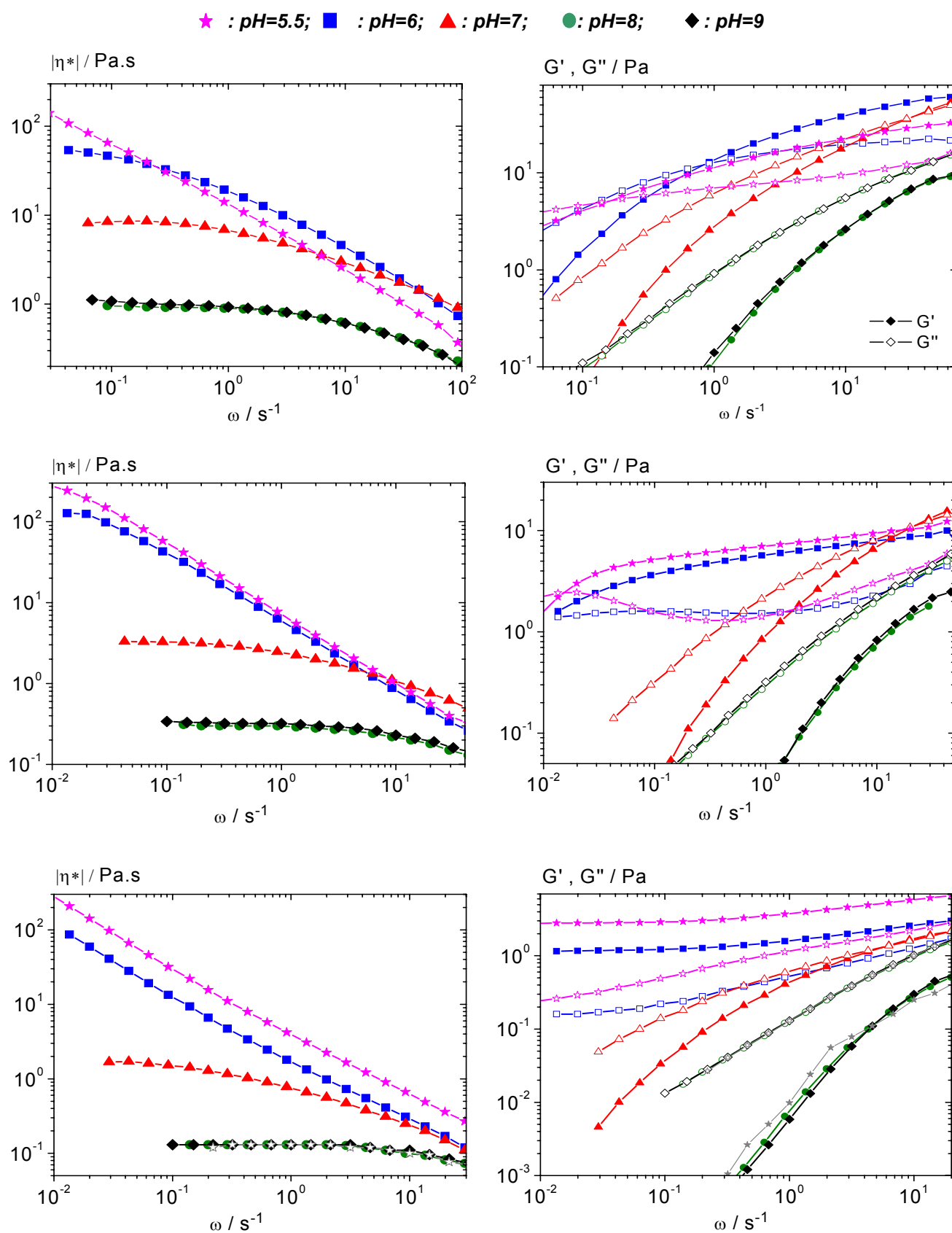


Figure 4-3: $|\eta^*|_0$ (left hand side) & dynamic moduli (right hand side) of $P(AA_{0.8}\text{-}AMPS_{0.2})+P(VP\text{-}VI)$ depending on pH at 2wt% (top row), 1wt% (middle row) and 0.5wt% (bottom row).

4.3.2.2. P(AA_{0.6}-AMPS_{0.4}) + P(VP-VI)

The rheological behavior of mixtures of P(AA_{0.6}-AMPS_{0.4}) with P(VP-VI) is essentially similar to what has been described in chapter 3 concerning PAA and in the first paragraphs of this chapter concerning P(AA_{0.8}-AMPS_{0.2}). Indeed, both the complex viscosity and dynamic moduli in **Figure 3-11** to **Figure 3-17** and **Figure 4-3** exhibit the same typical patterns: an increase in viscosity with decreasing pH at all concentrations coupled with a slowing down of relaxation phenomena. At low concentration, relaxation becomes extremely slow and a transition towards gel-like structures is observed.

For the sake of clarity, all these characteristics are summarized in the conclusion (**Table 4-4**).

The major differences of mixtures of P(AA_{0.6}-AMPS_{0.4}) with P(VP-VI) (cf. **Figure 4-4**) compared to the mixtures of P(AA_{0.8}-AMPS_{0.2}) and PAA with P(VP-VI) are twofold.

First, the shift in ω_c is more pronounced at 2wt% pH=5.5 compared to the shift measured with PAA and P(AA_{0.8}-AMPS_{0.2}). Indeed, the crossover frequency is 3 orders of magnitude lower at pH=5.5 than the one at pH=7 (10^{-2}s^{-1} and 10s^{-1} respectively). With the polyanions having a lower charge density, the shift ω_c in when the pH is decreased from 7 to 5.5 is only 2 orders of magnitude. This means that more polymer chains are bridged, suggesting stronger interactions between the polyanion and P(VP-VI).

Second, there are only minor discrepancies between mixtures at pH=5.5 and pH=6 at 1wt% and 2wt%. The relaxation patterns are almost superimposed. This suggests that the structures at the microscopic level are similar. A weaker pH dependency can be explained by the higher AMPS content in the polyanion: since it is pH independent, a slight decrease in pH from 6 to 5.5 does not modify the charge density on the polymer significantly. Thus the physical crosslinking density is essentially not modified. The issue of charge compensation depending on pH is further discussed in chapter 6.

In **Table 4-3**, the viscosity enhancements are gathered. Results are discussed in the next paragraph.

Table 4-3: viscosity enhancement of P(AA_{0.6}-AMPS_{0.4})+P(VP-VI) depending on concentration and pH.

Concentration	pH=5.5	pH=6	pH=7	pH=8	pH=9
2wt%	-	846	60	2.7	2.0
1wt%	-	-	49	2.1	1.9
0.5wt%	-	-	167	3.8	1.7

4. Influence of the nature of the charge

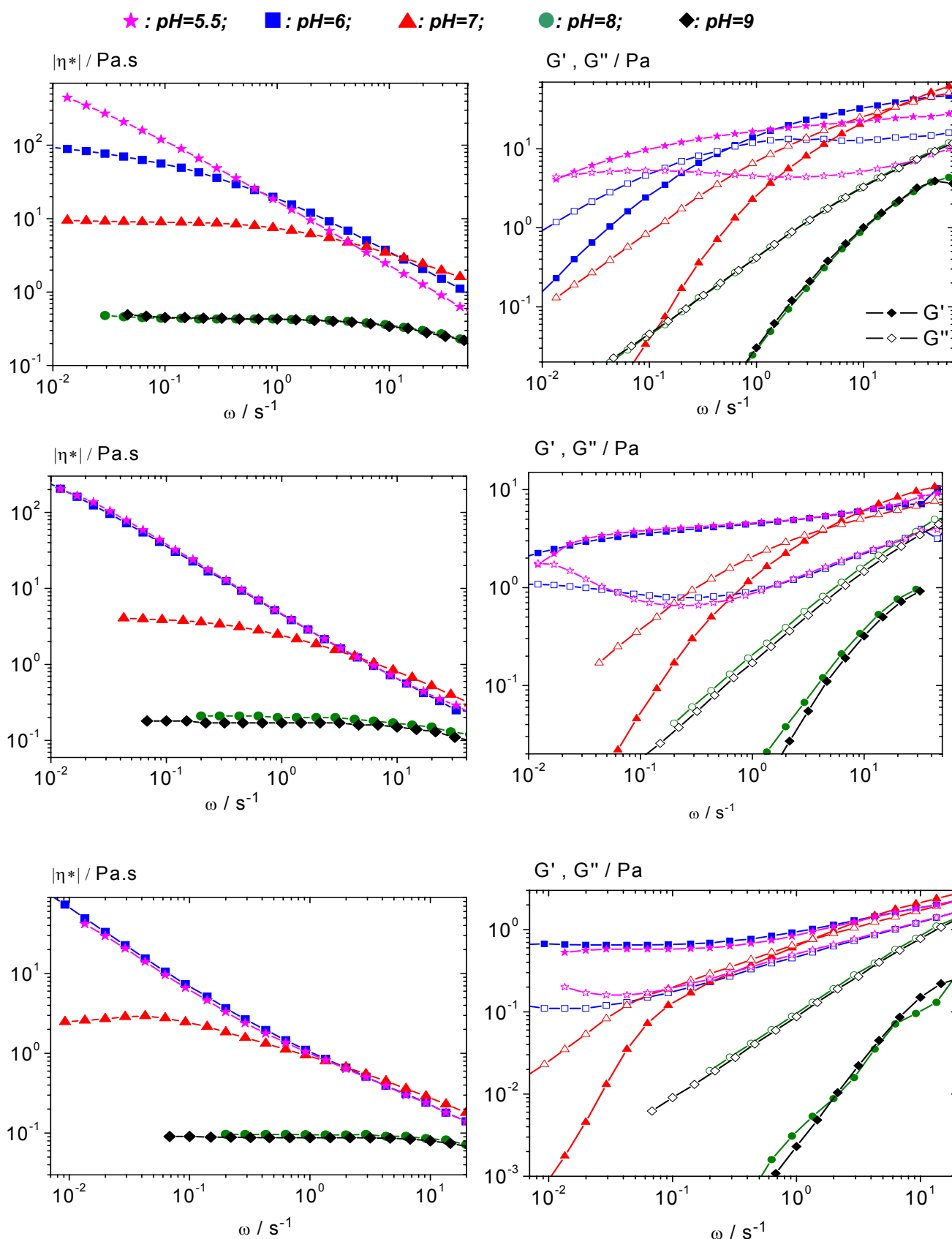


Figure 4-4: $|\eta^*|_0$ (left hand side) & dynamic moduli (right hand side) of $P(AA_{0.6}-AMPS_{0.4})+P(VP-VI)$ depending on pH at 2wt% (top row), 1wt% (middle row) and 0.5wt% (bottom row).

4.3.3. Thickening efficiency of PAA, P(AA_{0,8}-AMPS_{0,2}) and P(AA_{0,6}-AMPS_{0,4})

The viscosity enhancement for the mixtures for PAA, P(AA_{0,8}-AMPS_{0,2}) and P(AA_{0,6}-AMPS_{0,4}) with P(VP-VI) depending on the concentration of solution (SC, expressed in wt%) are gathered in **Figure 4-5**. The different colours correspond to the three copolymers studied and the shape of the symbols account for the pH value.

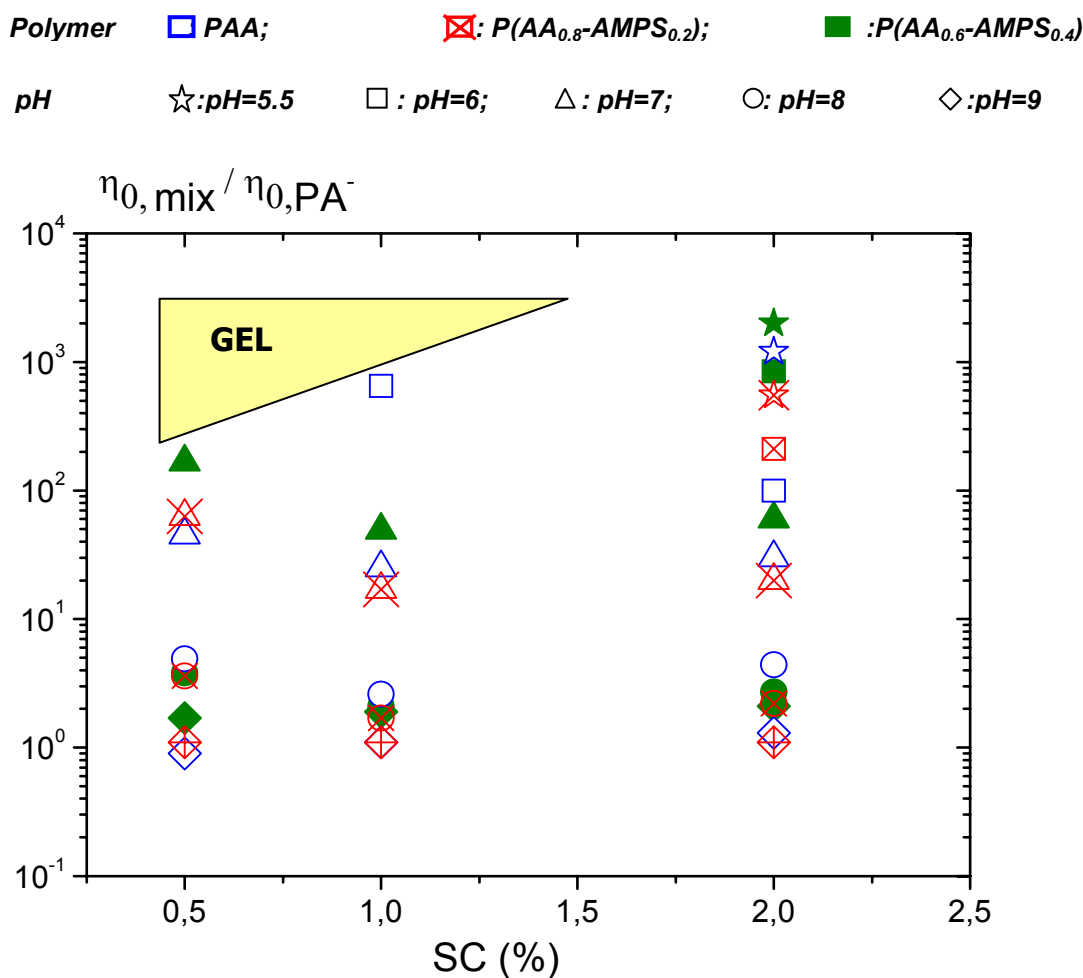


Figure 4-5: viscosity enhancement for mixtures of PAA, P(AA_{0,8}-AMPS_{0,2}), P(AA_{0,6}-AMPS_{0,4})+P(VP-VI) depending on concentration and pH.

There is essentially no difference in the enhancement observed for PAA, P(AA_{0,8}-AMPS_{0,2}) and P(AA_{0,6}-AMPS_{0,4}) at pH=9 for which it is always less than 2. At pH=8, the viscosity enhancement is always less than 5 and PAA exhibits a slightly larger increase in viscosity but the difference is not large enough to be considered as significant. At lower pH, the discrepancies between the different polyanions become more pronounced.

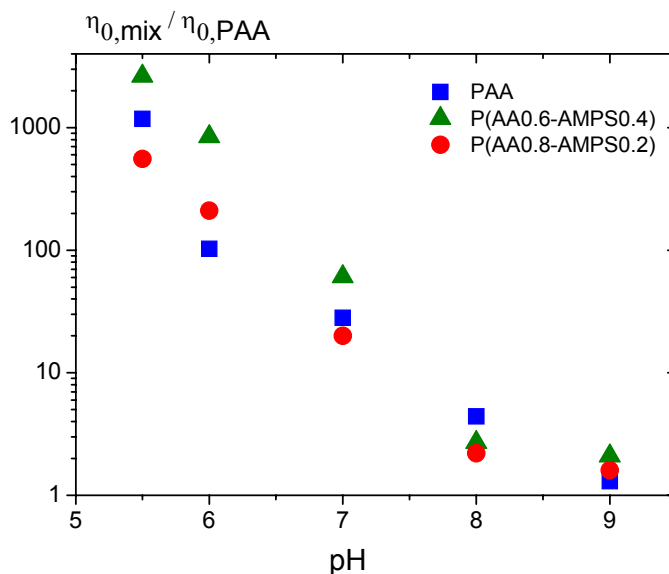


Figure 4-6: viscosity enhancement for mixtures of PAA, $P(AA_{0.8}\text{-}AMPS_{0.2})$, $P(AA_{0.6}\text{-}AMPS_{0.4})+P(VP\text{-}VI)$ at 2wt% depending on pH.

This is clearly visible in **Figure 4-6** in which $\eta_{0,mix}/\eta_{0,PAA}$ at 2wt% is plotted versus pH for the 3 different polyanions. Between pH=5.5 and 7, the use of $P(AA_{0.6}\text{-}AMPS_{0.4})$ leads to more pronounced viscosity increase than the polyanions containing less AMPS. At pH=7, the increase in viscosity is at least double for $P(AA_{0.6}\text{-}AMPS_{0.4})$ compared to PAA and $P(AA_{0.8}\text{-}AMPS_{0.2})$, at a concentration of 2wt% but also at lower ones. At 2wt%, for pH=5.5 and pH=6, same results are observed.

These results suggest that permanent polyanions lead to slightly larger viscosity increase. However, in absolute values, PAA leads to the highest viscosities since the zero shear viscosity of the pure polymer is slightly larger than the one of $P(AA_{0.8}\text{-}AMPS_{0.2})$ and significantly larger than the one of $P(AA_{0.6}\text{-}AMPS_{0.4})$, due to the difference in DP_n .

These results support the assumption that the thickening effect is due to electrostatic interactions between negative charges (either permanent on AMPS or depending on pH for the carboxylic group on PAA) and positive protonated imidazole groups. This issue will be further discussed in chapter 6.

4.4. Conclusion

Small amplitude oscillatory shear measurements carried out on 1 to 1 mixtures of polyanions with P(VP-VI) have unveiled typical features which are similar for all polyanions studied. Modifying pH and concentration leads to radical changes in the viscosity and relaxation patterns of the samples. These patterns are summarized in **Table 4-4**.

Table 4-4: summary of typical behavior observed for mixtures of PA⁻+P(VP-VI) depending on concentration.

2wt%	<ul style="list-style-type: none"> • pH=8 and 9, $G' \sim \omega^2$ and $G'' \sim \omega$. Crossover cannot be measured with rotational rheometry. Viscosity is similar to pure PA⁻ with half concentration. • pH=7, viscosity is increased by 1 order of magnitude. G'/G'' crossover is shifted to lower frequencies. $G' \sim \omega^2$ and $G'' \sim \omega$ at low frequencies • pH=6, viscosity further increases while crossover frequency further decreases. Shear thinning is more pronounced. • pH=5.5, no Newtonian plateau measurable for viscosity and crossover shifter by more than 4 decades compared to pure PA⁻.
1wt%	<ul style="list-style-type: none"> • pH=8 and 9, $G' \sim \omega^2$ and $G'' \sim \omega$. Crossover cannot be measured with rotational rheometry. Viscosity is similar to pure PA⁻ with half concentration. • pH=7, viscosity is increased by more than 1 order of magnitude. G'/G'' crossover is shifted to lower frequencies. $G' \sim \omega^2$ and $G'' \sim \omega$ at low frequencies • pH=5.5 and 6, crossover frequency further decreases. Sample shear thinning over whole frequency range. Almost no difference between both pH.
0.5wt%	<ul style="list-style-type: none"> • pH=8 and 9, $G' \sim \omega^2$ and $G'' \sim \omega$. Crossover cannot be measured with rotational rheometry. Viscosity is similar to pure PA⁻ with half concentration. • pH=7, viscosity is increased by more than 1 order of magnitude. G'/G'' crossover is shifted to lower frequencies. $G' \sim \omega^2$ and $G'' \sim \omega$ at low frequencies • pH=5.5 and 6, no crossover frequency. Sample shear thinning over whole frequency range. Almost no difference between both pH.

A more pronounced increase in viscosity results from the presence of AMPS in the polyanion. This is coupled with a smaller pH dependency of the thickening phenomenon. This supports the

explanation for these features already discussed in the conclusion of chapter 3. As the pH decreases, polyanion and polycation chains electrostatically interact one with each other, forming extended structures. The chains are physically weakly crosslinked. The viscosity and relaxation times increase as the crosslinking density increases, i.e. as the pH decreases. The relationship between pH and charge neutralization in the mixtures are discussed more thoroughly in chapter 6. It is anyway clear that pH influences the charge density on the polyanions most in those polymers in which the portion of AMPS is the lowest.

5. Behavior of Mixtures of Oppositely Charged Polyelectrolytes under Extensional Flow

5.1. Introduction

Most rheological studies, both in industry and academics, emphasize on the rheological behavior under shear. However, in many applications, even though the behavior under shear is important, it may be less important than the stretching behavior. This is particularly true in various technical processes. Accordingly, not only shear but also extensional flow properties of the corresponding complex formulations have been investigated intensively with respect to processing or application properties, e.g. by Fernando et al. (2000), Stelter et al. (2002), Agarwal and Gupta (2002) or Tuladhar and Macklay (2007). Another field of interest is to understand the relationship between molecular properties and extensional flow properties. The dependence of extensional viscosity on polymer concentration, molecular weight, molecular stiffness or solution elasticity has been studied for various synthetic and natural polymers, e.g. by Kennedy et al. (1995), Dexter (1996), Ng et al. (1996), Solomon et al. (1996), Stelter et al. (2002) or Plog et al. (2005).

So far, synthetic as well as natural polymers and polyelectrolytes are predominately used as thickeners for water-based formulations (Braun and Rosen 2000) and have therefore been studied most intensively.

In the experiments discussed in this chapter, a Capillary Break-up Extensional Rheometer (CaBER) (Entov and Hinch 1997; Bazilevsky et al. 2001) is used in order to characterize the elongational flow properties of mixtures of polyanions based on acrylic acid and 2-acrylamido-2-methyl-1-propanesulfonic acid with P(VP-VI). In a CaBER experiment a fluid drop is exposed to an extensional step strain, thus forming a liquid filament. Subsequent necking of that liquid bridge is controlled by the balance of capillary and viscoelastic forces. Large extensional strains are attained as the filament undergoes thinning and finally breaks. The only measured quantity is usually the change in the midpoint diameter with time. The advantage of this method is its wide applicability to various kinds of fluids. However neither strain rate nor stress can be controlled externally. But these measurements enable to determine an extensional relaxation time λ_E which can be ultimately compared to the relaxation behavior observed in shear measurements.

The CaBER used in the experiments described hereafter is equipped with a high-speed camera (Fastcam 1024 PCI Photron) taking 1000 images/s at a resolution of 1024 x 512 pixels featuring a macro zoom objective (Eneo Verifokal B 45 Z03 MV-MP, focal length: 45-160 mm). Illumination is done with a white LED from the back. The value of the diameter of the filament is derived from the images recorded with the camera. To do so, a software has been developed within our group which enables to determine the diameter of the filament. This software is based on the difference of brightness between the edge of the filament which appears black when illuminated from the back and the background which is light grey. An example is given in **Figure 5-1**: the red line corresponds to the middle of the gap and on the right the evolution of the brightness (in arbitrary units) along this red line is shown. The distance between the two minima in brightness is the diameter of the filament.

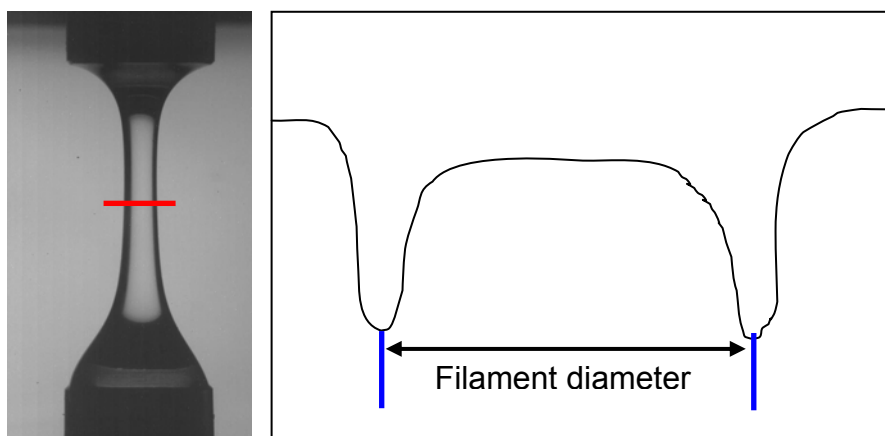


Figure 5-1: brightness profile used for diameter calculation.

All CaBER experiments are performed at room temperature on mixtures which have already been characterized in shear flow, to ensure better comparability between the two techniques. The diameter of the filament is measured in the middle of the gap, i.e. approximately in the middle of the filament, the region where breaking occurs.

Some solutions of pure polyanions, studied in chapter 3 are also investigated using CaBER. The results exposed previously show that pH has only a minor effect on pure polyanions: the zero-shear viscosity at a given concentration as well as the rheological behavior are essentially similar at pH=6, 7 and 8. Moreover, at the four concentrations studied (2%, 1%, 0.5% and 0.25% in weight), G' and G'' are proportional respectively to ω^2 and ω up to high frequencies, indicating that pure polyanions are present in solution as free chains. Hence, only a few

polyanions are studied, which give a reasonable overview of the behavior under extensional flow.

5.2. Extensional Rheology of pure polyanions

All materials used hereafter have been used in the shear experiments described in chapter 3 and chapter 4.

All measurements are performed at room temperature. The aspect ratio between the initial and final position is 4 (from a gap of 4mm to 16mm) and stretching time is 40ms. The filling of the gap is done in a reproducible way, with the same quantity of material (around 1mL)

5.2.1. Poly(acrylic acid)

Measurements realized in chapter 3 on pure poly(acrylic acid) show that at pH=7 zero shear viscosity are respectively 1.76, 0.57 and 0.24 Pa.s for 2wt%, 1wt% and 0.5wt% solutions. At other pH, these values differ only slightly. In CaBER experiments, this renders the measurements at 1% and 0.5% difficult with the geometry and set-up used. Indeed, the lifetime of the filament is too short to allow accurate recording of the filament diameter. Therefore, only solutions of PAA at 2% are measured. The diameter D_0 measured just after the upper and lower plate are fully separated is used as reference to normalize the filament's diameter $D(t)$ decay. Typical curves $D(t)/D_0$ resulting from a CaBER measurement on pure PAA are shown in **Figure 5-2**. Such curves can be separated into 3 regimes:

- 1: the filament has just formed and is not fully equilibrated. Vibrations propagate in the filament due to the choc of the upper plate reaching its final position.
- 2: the decay of the filament can be fitted by an exponential in a linear plot (on the left) or by a straight line in a semi-logarithmic plot (on the right). This is the typical behavior observed for polymer solutions.
- 3: the decay becomes faster as the filament comes close to rupture. This is typical for weakly viscoelastic polymer solutions and has been attributed to finite extensibility of the polymer chains.

The curves in **Figure 5-2** correspond to three measurements of the same sample, at pH=7 and 2wt%. Results of $D(t)/D_0$ are plotted in linear and semi-logarithmic plot. These three measurements are similar one to each other, showing that reproducibility is good for

measurements performed on pure polyanions. This is true provided that the filling of the gap is always similar, as this parameter is of high relevance for the final result of a measurement.

Under these conditions, the error is typically less than 10% for the filament lifetime, the value of the diameter at a given time and the slope in regime 2 from which the extensional relaxation time can subsequently be calculated.

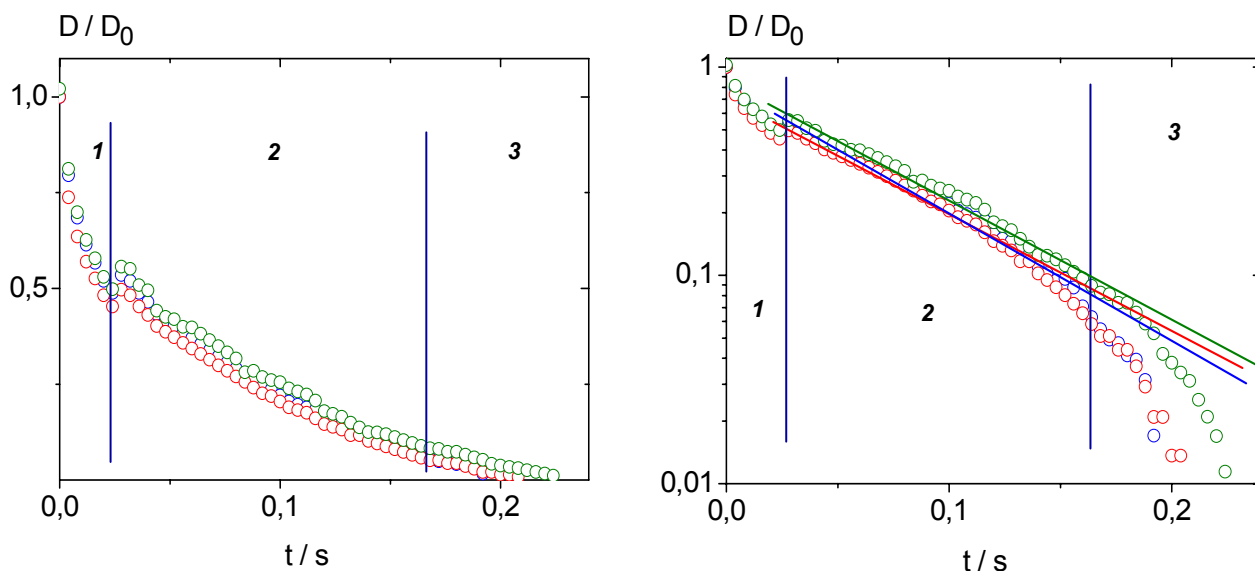


Figure 5-2: filament decay of PAA1600 at 2wt% pH=7.

Figure 5-3 shows results obtained for a 2wt% solution of PAA investigated at three different pH: six, seven and eight. The 3 regions described above can clearly be identified. The decay pattern is similar for the three measurements, as well as the characteristics features already mentioned: filament lifetime and slope in region 2 measured in a semi-logarithmic plot. These features are characteristics of homogeneous weakly elastic fluids (Kheirandish 2008).

Hereafter, the pictures are represented in a matrix in which the columns represent different pH and lines different times within a given experiment. The first picture is taken just after the filament is formed i.e. just after t_0 . When there are three rows of pictures, they correspond (from top to bottom) to $\{0.1, 0.5, 0.9\} * t_F$ (the total duration of the experiment, from formation of the filament until its rupture). When four pictures are shown, they correspond to $\{0.1, 0.25, 0.5, 0.9\} * t_F$.

The pictures gathered in **Figure 5-4** confirm that a similar decay is observed for the three pH investigated: the shape of the filament at a given time is identical. The homogeneity of the filaments is also visible in these pictures.

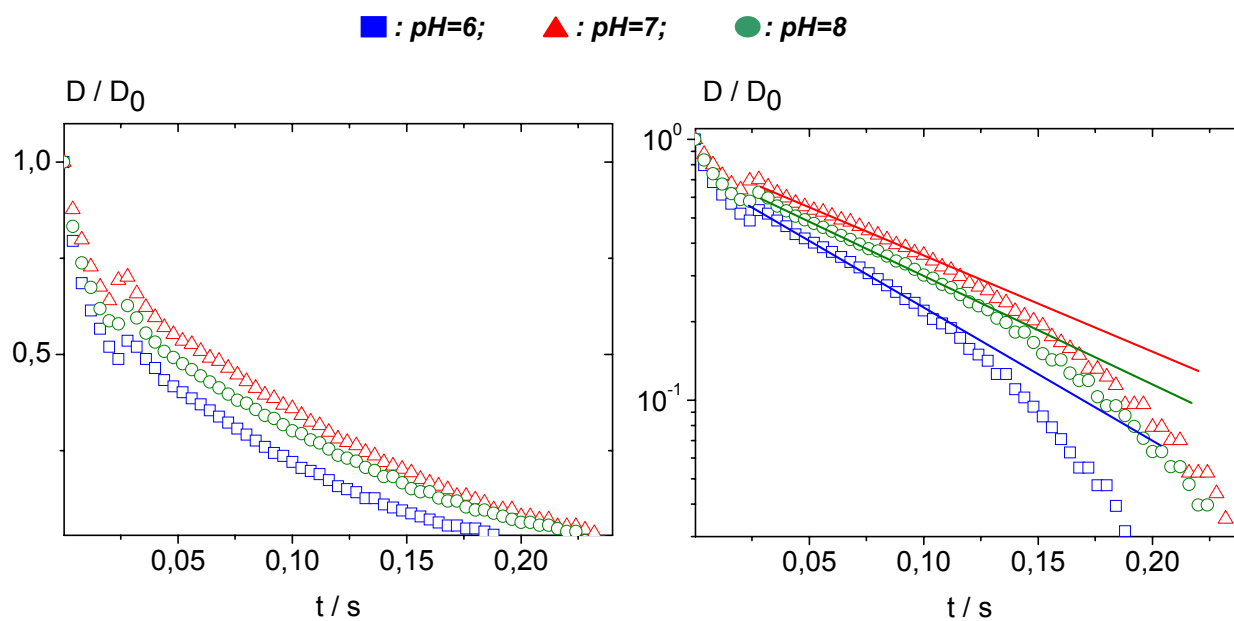


Figure 5-3: filament decay of PAA1600 at 2wt% depending on pH.

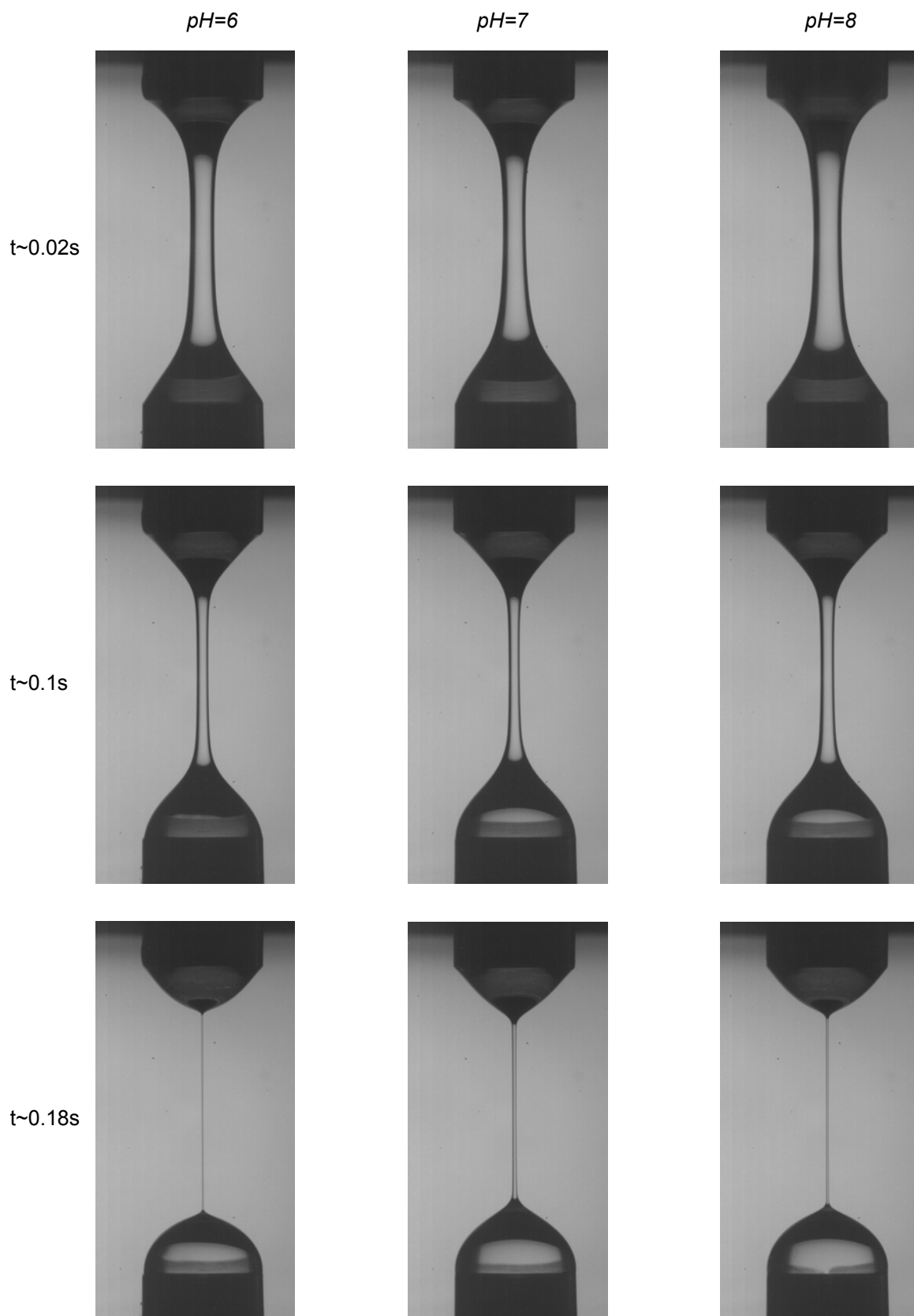


Figure 5-4: time-evolution (rows) of the filament formed by PAA at pH=6, pH=7 and pH=8 (columns).

5.2.2. Poly(acrylic acid-co-2-acrylamido-2-methyl-1-propanesulfonic acid)

Same experiments are carried out on pure $P(AA_{0.8}\text{-}AMPS_{0.2})$ at 2wt% at pH=6, 7 and 8. Results of $D(t)/D_0$ are shown in **Figure 5-5**. The behavior is exactly the same as the one observed for PAA: an initial sagging followed by an exponential decay and finally a faster decay close to rupture. The typical error is again close to $\pm 10\%$, for the filament lifetime and the slope of the linear part of the curves in semi-logarithmic plot (**Figure 5-5 b**).

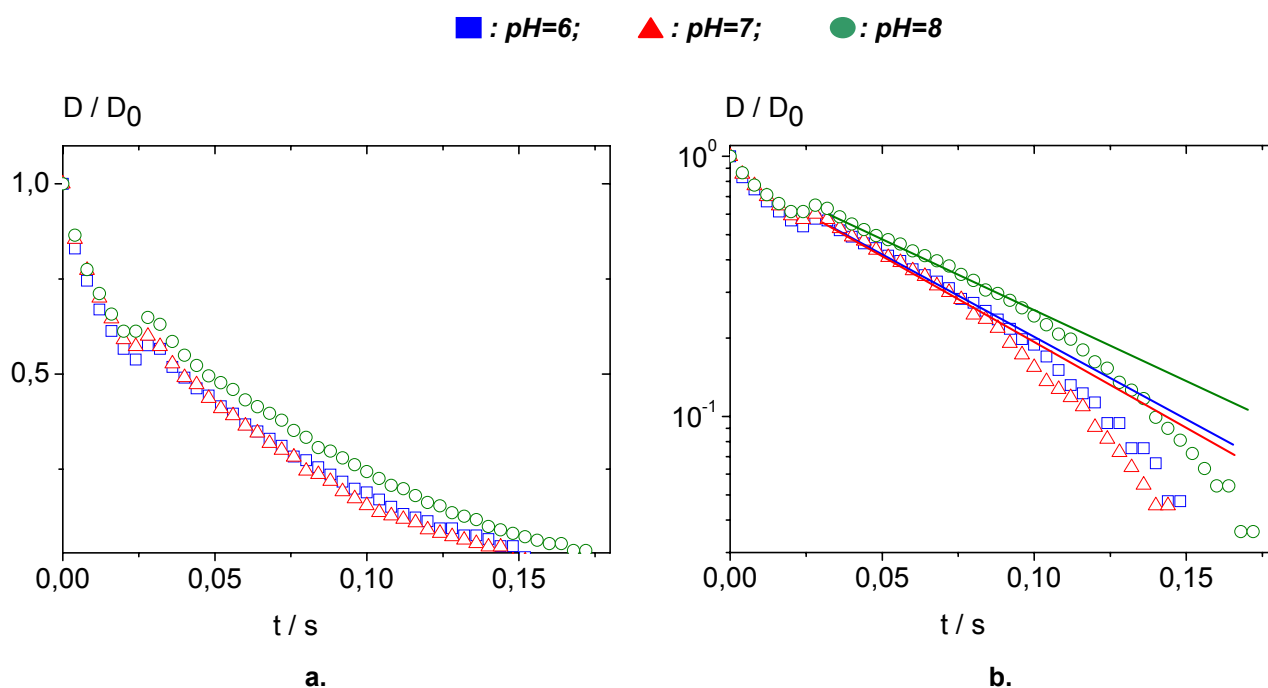


Figure 5-5: filament decay of $P(AA_{0.8}\text{-}AMPS_{0.2})$ at 2wt% depending on pH.

The pictures in **Figure 5-6** show that the filaments are uniform and homogeneous at any time during the experiment and the decay pattern is similar for all of them. All these features are typical for low viscosity solutions of viscoelastic fluid.

When comparing the filament lifetimes, the values obtained for the copolymer is slightly lower than the ones for pure PAA. This can be directly related to the zero shear viscosity of these solutions, which are respectively around 1.7Pa.s for PAA and around 1.2Pa.s for the copolymer, almost independent of pH.

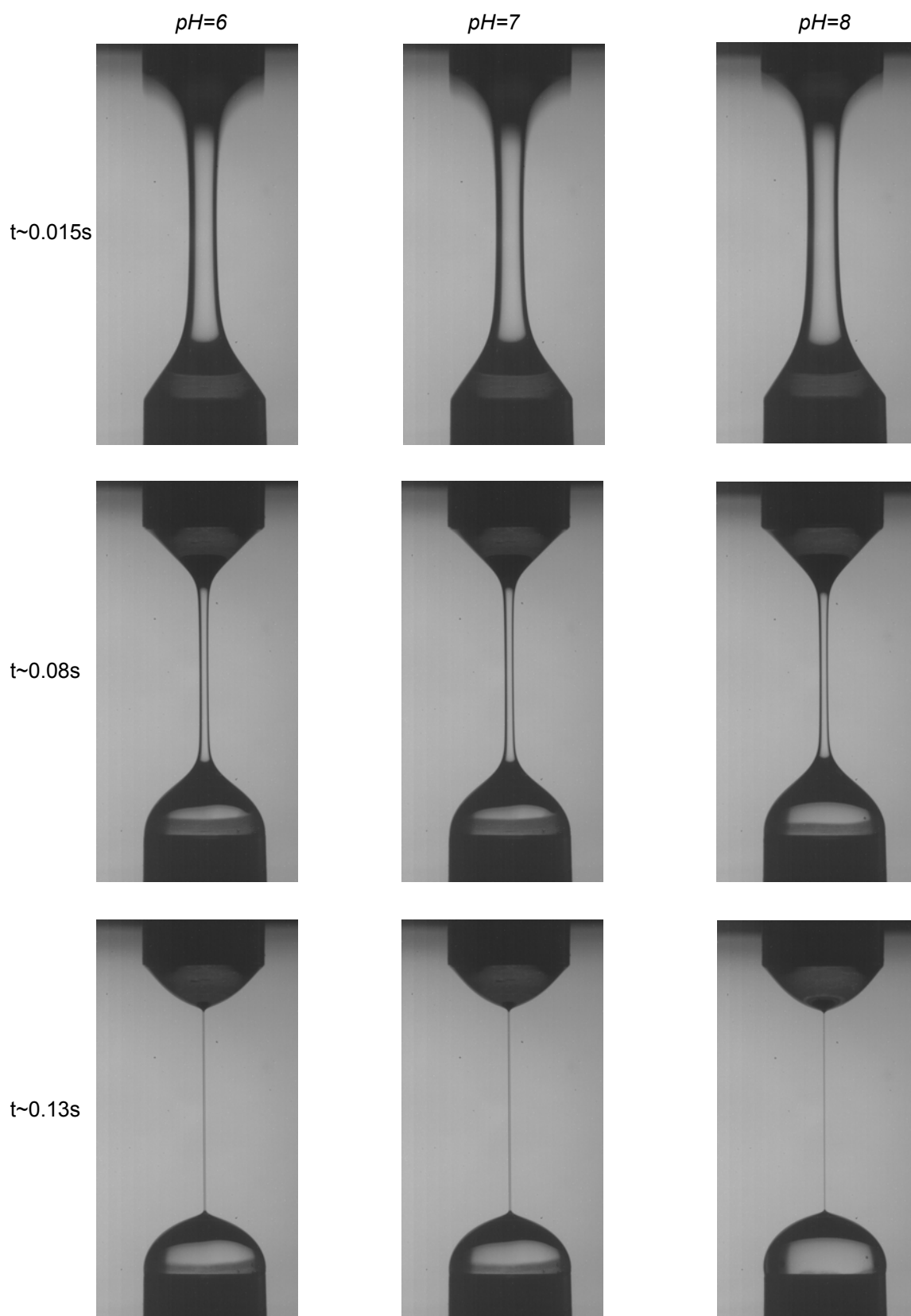


Figure 5-6: time-evolution of the filament formed by $P(AA_{0.8}\text{-}AMPS_{0.2})$ at $\text{pH}=6$, $\text{pH}=7$ and $\text{pH}=8$.

5.2.3. Extensional relaxation times of pure polyanions

To determine the longest relaxation time in extensional experiments (λ_e), the semi-logarithmic plots $D(t)/D_0=f(t)$ are used.

$$\lambda_e \text{ can be determined using the equation } \frac{D(t)}{D_0} = \exp\left(-\frac{t}{3\lambda_E}\right) \quad (5.1)$$

This simple model is valid only when the decay of the diameter of the filament follows a classical exponential decay, which is the case for pure polyanions (only regime 2 is considered). As an example, in **Figure 5-3** and **Figure 5-5**, the slope considered to determine λ_e would be the red, blue and green straight lines corresponding to the slope within the exponential regime.

For pure poly(acrylic acid) and poly(AMPS-co-AA), the results obtained are gathered in table 1. Solutions at 0.5wt% can not be measured as their viscosity is too low for a homogeneous, reproducible filament to form. The error, as determined in previous paragraph, is 10%.

Table 5-1: relaxation features of pure PA^- depending on pH and concentration.

pH	C. (wt%)	PAA		$P(AA_{0.8}\text{-}AMPS_{0.2})$		$P(AA_{0.6}\text{-}AMPS_{0.4})$	
		t_F (ms)	λ_E (ms)	t_F (ms)	λ_E (ms)	t_F (ms)	λ_E (ms)
6	2.0	200 ± 20	42 ± 4	170 ± 17	35 ± 3.5	100 ± 10	22 ± 2.2
	1.0	90 ± 9	27 ± 2	70 ± 7	16 ± 1.6	-	-
7	2.0	240 ± 24	48 ± 5	140 ± 14	29 ± 3	80 ± 8	16 ± 1.6
	1.0	100 ± 10	28 ± 3	80 ± 8	18 ± 2	-	-
8	2.0	210 ± 21	46 ± 5	180 ± 18	36 ± 3.6	90 ± 9	18 ± 1.8
	1.0	110 ± 11	29 ± 3	80 ± 8	19 ± 2	-	-

The value of filament lifetime t_F and the extensional relaxation time λ_E are directly correlated and a longer filament lifetime corresponds to a slower relaxation. Both t_F and λ_E decrease with increasing amount of AMPS in the copolymer; again this can be related to the degree of polymerization which is lower for $P(AA_{0.8}\text{-}AMPS_{0.2})$ compared to PAA and even lower for $P(AA_{0.6}\text{-}AMPS_{0.4})$ which leads to smaller viscosities in shear flow and shorter filament lifetime in extensional flow.

5.3 Extensional rheology of mixtures of polyanions with P(VP-VI)

5.3.1. Reproducibility of the measurements

Mixtures of PAA and P(VP-VI) are studied using the same geometry and the same protocol as the one used for the pure polymers.

Reproducibility of the measurements is assessed first. At pH=7 and pH=8, the behavior is similar to the one observed for pure polyanions. The stretching of the polymer solution leads to the formation of a homogeneous filament, which thins in a homogeneous way with time as shown in **Figure 5-7**.

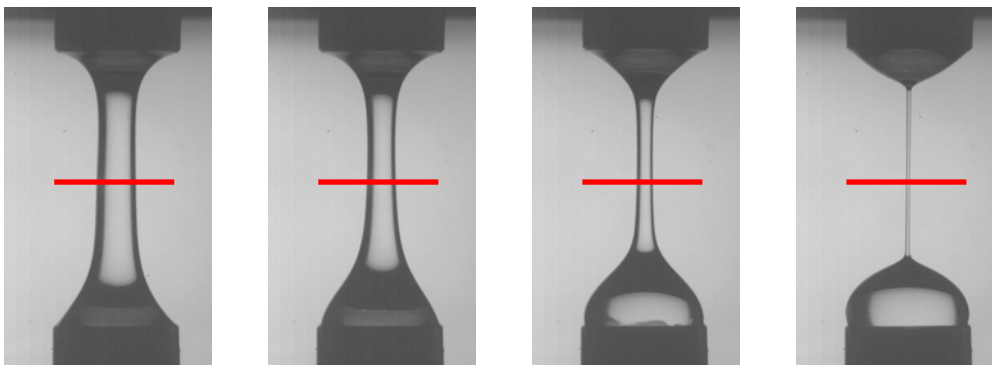


Figure 5-7: time-evolution of the filament formed by PAA+P(VP-VI) 2wt% pH=7.

A mixture of PAA and P(VP-VI) at 1wt%, pH=7 is measured three times under the same conditions. The 3 filaments decay curves plotted in **Figure 5-8** show that the reproducibility of the measurement is excellent. Both the shape of the curve and the value of the filament lifetime are almost similar for the three measurements (ranging from 1.96s to 2.02s). A value of $\pm 10\%$ for the error, similar to the one for pure polyanions, is considered hereafter, slightly higher than the one of 3% which can be extracted from the filament lifetime mentioned before.

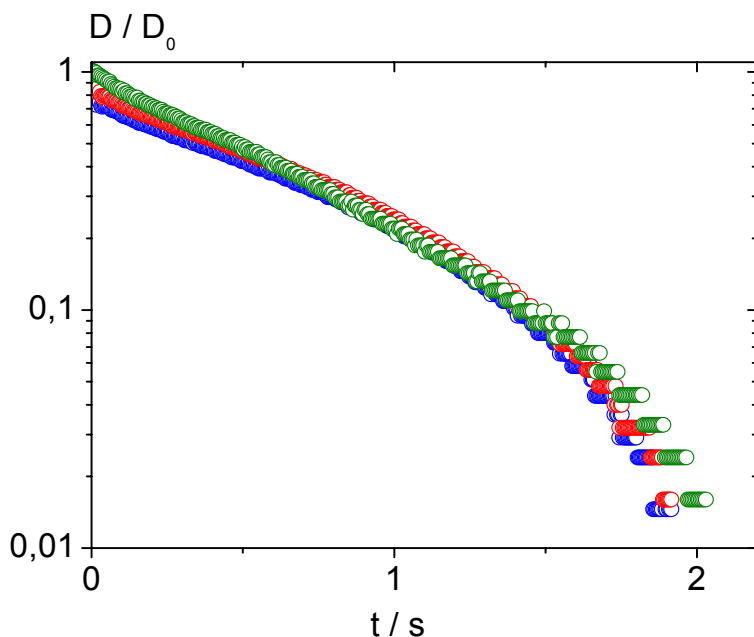


Figure 5-8: time-evolution of the filament formed by PAA+P(VP-VI) 2wt% pH=7.

Contrary to what was observed for pure polyanions, the behavior depends highly on pH. Thus, at pH=5.5 and 6, the stretching of a polymer solution droplet leads to the formation of non-homogeneous filaments. The decay is also non-homogeneous mainly because of the presence of heterogeneities in the vicinity of the surface of the filament. **Figure 5-9** shows the evolution of a 1wt% mixture of PAA and P(VP-VI) at pH=5.5 versus time. The red lines correspond to the middle of the gap, height at which the diameter of the filament is measured. Circled in yellow, an example of the movement of an heterogeneity, towards the lower plate, responsible for the non linearity in the decay curves of the diameter of the filament. Indeed, when the heterogeneity crosses the red line, it reflects as a sharp decrease on the $D(t)/D_0$ curve.

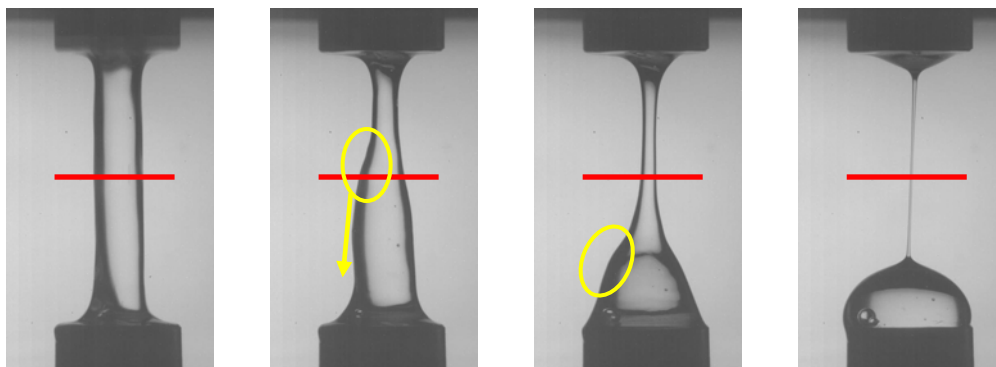


Figure 5-9: time-evolution of the filament formed by PAA+P(VP-VI) 2wt% pH=5.5.

The same mixture is measured three times to get information about the reproducibility of measurements at low pH. Results obtained for PAA+P(VP-VI) at 1wt%, pH=5.5 are shown in **Figure 5-10**.

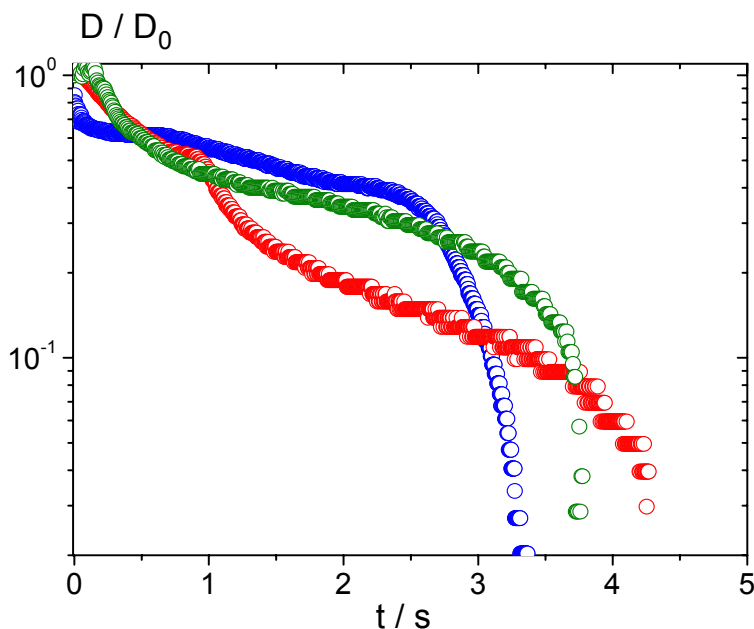


Figure 5-10: time-evolution of the filament formed by PAA+P(VP-VI) 2wt% pH=5.5.

Contrary to pure polyanions or mixtures at pH=7 and pH=8, the curves showing the evolution of the filaments diameter versus time do not superimpose. The decay pattern depends on the initial filling, and especially on the presence or the absence of heterogeneities within the volume of sample filled in. The “size” of these heterogeneities also plays a role on the decay pattern: large ones have a tendency to move towards the lower plate faster than small ones, leading to faster thinning of the filament and to shorter filament lifetime.

This leads to a much lower reproducibility under such pH conditions. For the filament lifetime, the example shown in **Figure 5-10** is characteristic of the behavior usually observed. The filament lifetime varies between 3.4 and 4.3 seconds. To be on the safe side, an error of $\pm 20\%$, higher than what can be calculated from **Figure 5-10**, is considered for measurements under such conditions: results of CaBER measurements for mixtures at low pH are more qualitative than quantitative.

5.3.2. Poly(acrylic acid) + P(VP-VI)

CaBER measurements for mixtures of PAA with P(VP-VI) are carried out at 3 concentrations (2wt%, 1wt% and 0.5wt%) and 4 pH (pH=5.5, 6, 7 and 8). In **Figure 5-11** (**a** and **b** correspond to solutions at 2wt%, **c** at 1wt% and **d** at 0.5wt%), results showing the evolution of the normalized diameter versus time are gathered.

Similarly to what has been observed in the previous paragraph, two different behaviors are generally observed.

The shape of the curves $D(t)/D_0 = f(t)$ for the mixtures at pH=7 and pH=8 is similar to what is observed for pure polyanions, i.e. three regimes appear successively

- an equilibrating period.
- an exponential decrease of the diameter of the filament which appear as a linear decay in a semi-logarithmic plot.
- a faster decay as the rupture of the filament is closer.

Comparatively to pure polymer solutions, the exponential decay is longer compared to the other two regimes. In parallel, the filament lifetime for pure polyanions is typically 0.2s and such small values are observed only for mixtures at 0.5wt% whatever the pH and for mixtures at 2wt% and 1wt% at pH=8. At pH=7, the decay pattern is similar to pure polyanions but filament lifetime is much longer, respectively close to 2s and 1s at 2wt% and 1wt%.

The shape of the curves $D(t)/D_0 = f(t)$ for the mixtures at pH=5.5 and pH=6 does not exhibit the three regimes observed at higher pH values. Especially, no exponential decay appears, replaced by a more irregular behavior. Again, the filament lifetime is longer than what is measured for pure polymers, attaining for example, $40s \pm 8s$ for the mixture at 2wt% and pH=5.5. This case is unique but the trend of higher filament lifetime is observed for all mixtures at pH lower than eight.

In **Figure 5-12** pictures are shown which can explain some of the features observed in **Figure 5-11**. Indeed, at pH=8 and pH=7, the filaments look uniform and homogeneous during their whole decay. No necking or sagging appears. On the contrary, at pH=6 and pH=5.5, the filament are not uniform and it seems that they are not homogeneous as a pronounced sagging is observed. The peculiar decay observed in **Figure 5-11** can be explained by these local heterogeneities, which look like aggregates pointing out of the filament. Moreover, the high viscosity of the solutions implies that the regime at which capillary forces are predominant is attained only after several seconds; gravity forces are not negligible during the major part of the experiments and explain for instance the fast decay of the curve at pH=6 in **Figure 5-11 b**. The measurements of

the solutions at 1wt% and 0.5wt% do not differ significantly from the one at 2wt%. The unexpected features, bumps or sudden drops in the curves in **Figure 5-11 c.** and **d.** are again attributed to heterogeneities present in the filament at pH=5.5 and pH=6. At pH=8 and pH=7, the filaments are homogeneous and the diameter shrinkage can approximately be fitted with an exponential.

At 0.5%, the behavior is peculiar, as the filament lifetime does not increase with decreasing pH like for the other two concentrations. This feature is explained by the non homogeneity in the filaments: aggregates have a tendency to move very fast to the bottom plate and this movement is not hindered by the viscosity of the surrounding media.

Two dissimilar behaviors are observed when mixtures of P(VP-VI) and PAA are elongated extensionally. At pH=7 and 8, a homogeneous filament is formed and its diameter thins uniformly following an exponential law. Filament lifetime increases compared to pure polymers. At pH=5.5 and 6, inhomogeneities appear in the filament, leading to a more heterogeneous decay. Filament lifetime is dramatically increased at 2wt% and 1wt%, not at 0.5wt%.

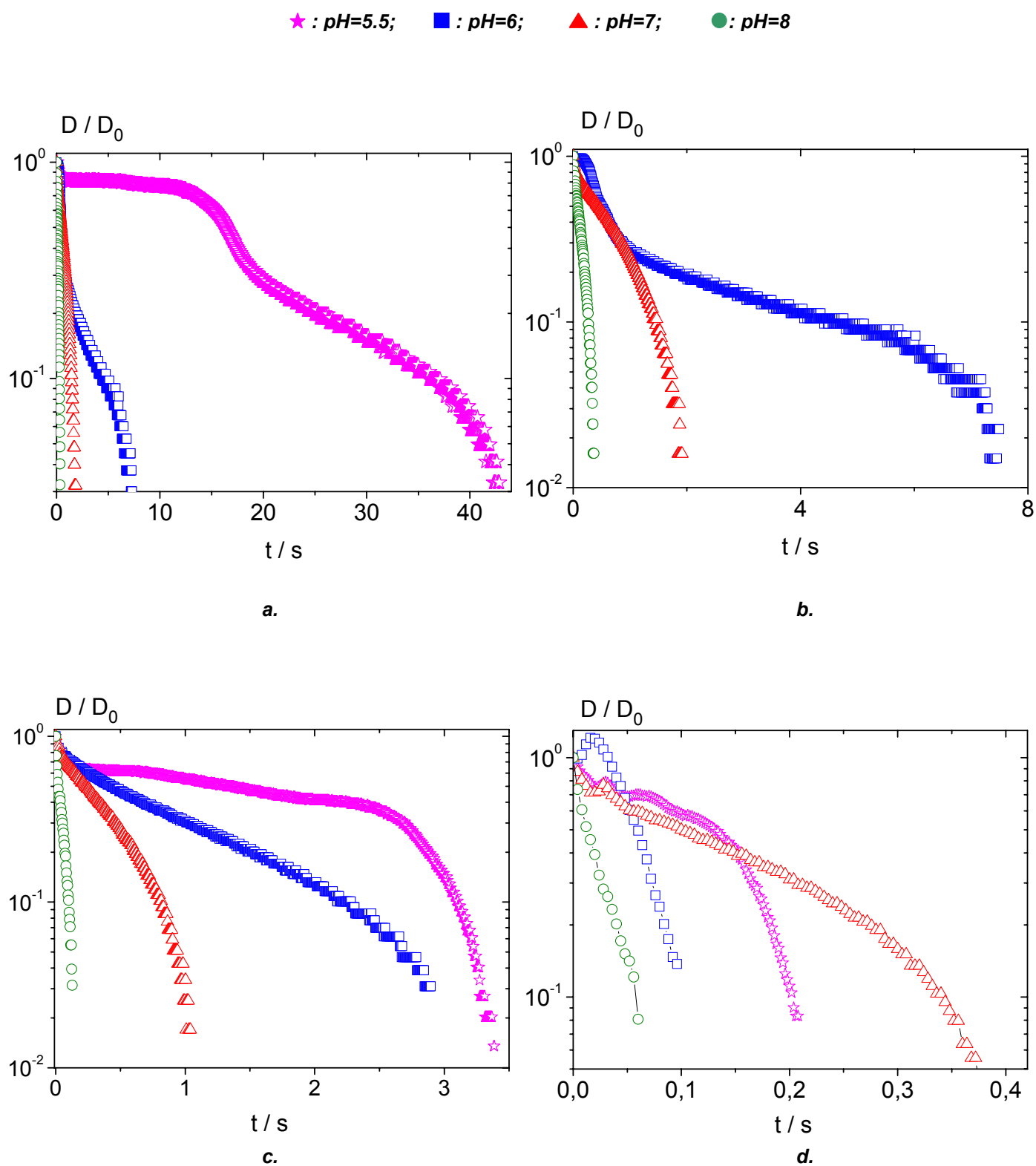


Figure 5-11: time-evolution of normalized diameter of PAA+P(VP-VI) depending on pH
 a and b: 2wt% ; c: 1wt% ; d: 0.5wt%

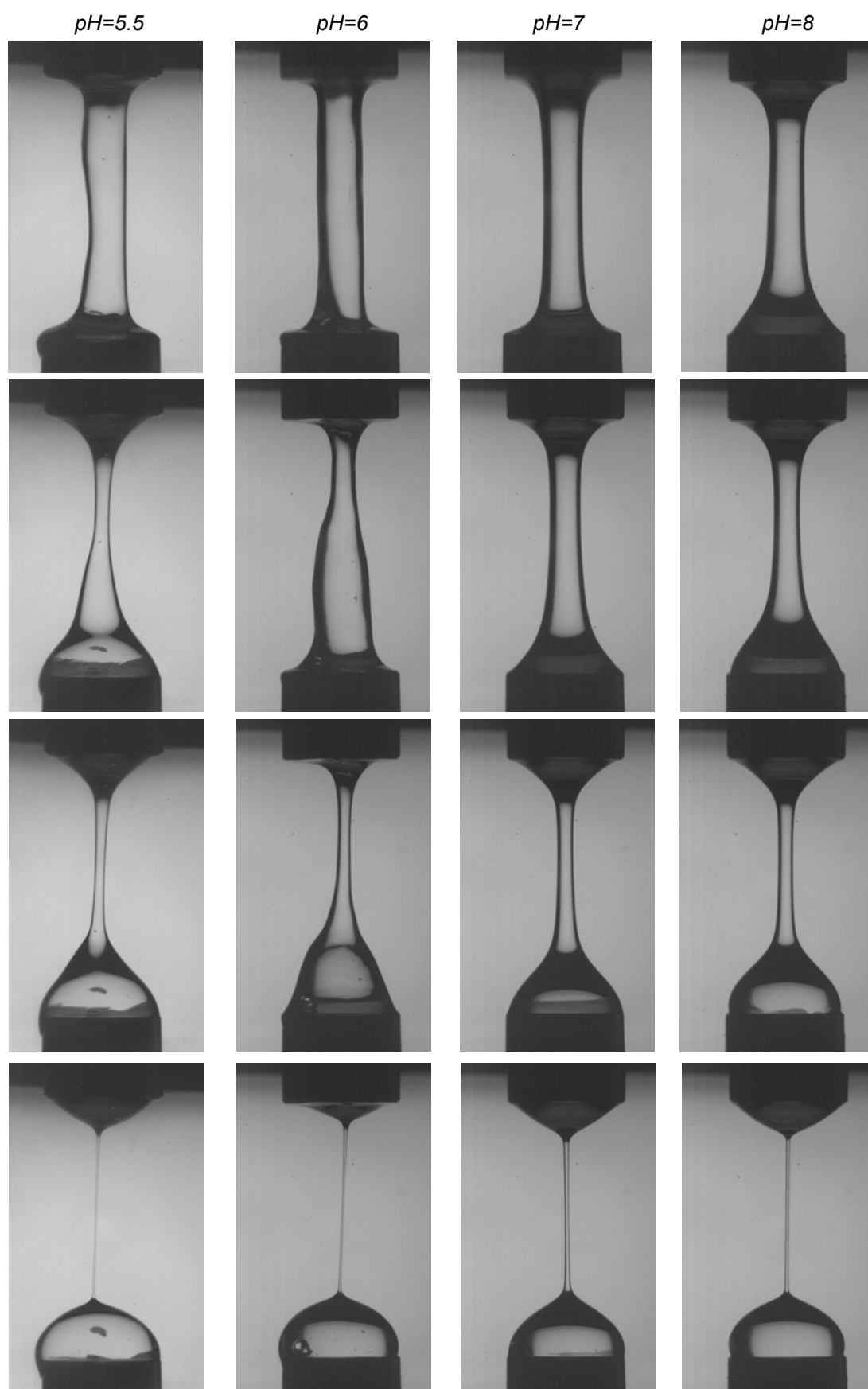


Figure 5-12: time-evolution of mixtures of PAA with P(VP-VI) at 2wt% depending on pH.

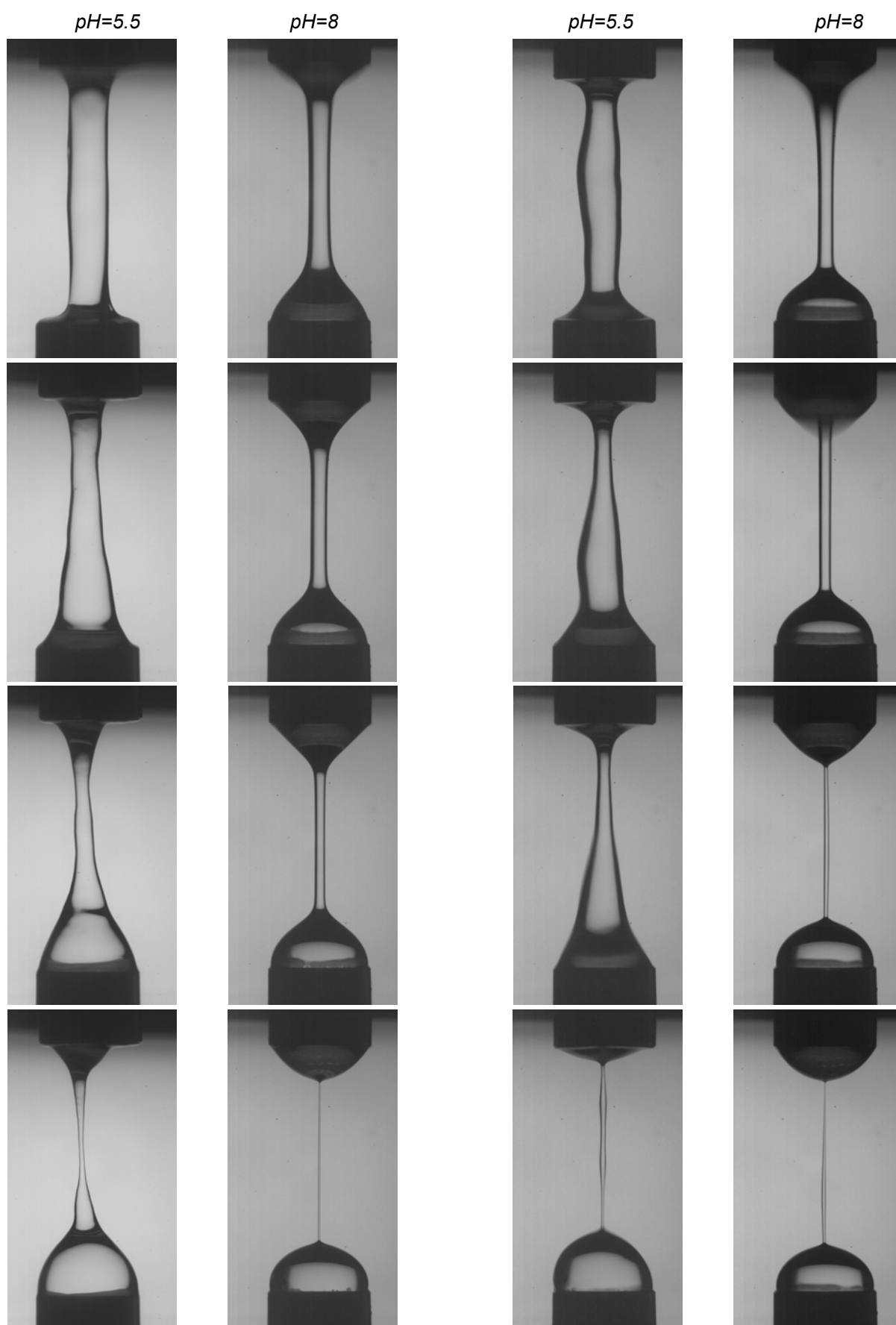


Figure 5-13: time-evolution of PAA+P(VP-VI) at 1wt%, pH=5.5 and pH=8 (first two columns respectively) and at 0.5wt%, pH=5.5 and pH=8 (third and fourth column respectively).

5.3.3. P(AA-co-AMPS) + P(VP-VI)

Similarly to what was undergone in the chapter on shear measurements, the same experiments are carried out with mixtures of copolymers of poly(acrylic acid) and poly(2-acrylamido-2-methyl-1-propanesulfonic acid) containing twenty percent and forty percent of permanently charged groups with P(VP-VI). The curves showing the evolution of the normalized diameter with time are gathered in **Figure 5-14**. The first column corresponds to mixtures of P(AA_{0.8}-co-AMPS_{0.2}) while the second one corresponds to P(AA_{0.6}-co-AMPS_{0.4}).

At pH=8 and at pH=7, the behavior is similar to what is expected as the decay of the normalized diameter of the filament appears linear in a semi-logarithmic plot over a wide portion of its lifetime. The decay curves are smooth indicating that the samples are homogeneous. Pictures in **Figure 5-15**, in which no aggregates are visible, confirm this.

The curves show a very irregular behavior at pH=5.5 at any concentration, with plateaus and sudden drops due to the pronounced inhomogeneity of the sample, with aggregates sticking out, which explains the relative maxima in diameter which are observed. The presence of several air bubbles within the filament, i.e. within the initial droplet of material placed in the gap is due to the difficulty of handling materials with high viscosities.

At pH=6, the observations are similar at 0.5wt% and 1wt%, where the decay curves are typical for inhomogeneous samples. At 2wt%, the decay curves are smoother, linear in a semi-logarithmic plot. Pictures in **Figure 5-16** confirm that the filament looks homogeneous. This is true for P(AA_{0.8}-co-AMPS_{0.2}) and P(AA_{0.6}-co-AMPS_{0.4}), suggesting that the transition from heterogeneous to homogeneous as the pH increases is sharper at 2wt% when AMPS is present in the polyanion.

The same general features as in the previous paragraph, especially regarding the discrepancies between pH=7 and 8 on one side and pH=5.5 and 6 on the other one, are observed for mixtures of P(VP-VI) with P(AA-AMPS). The sole difference appears at pH=6, 2wt%, conditions under which the presence of AMPS leads to less heterogeneous mixtures.

5. Behavior of mixtures of oppositely charged polyelectrolytes under extensional flow

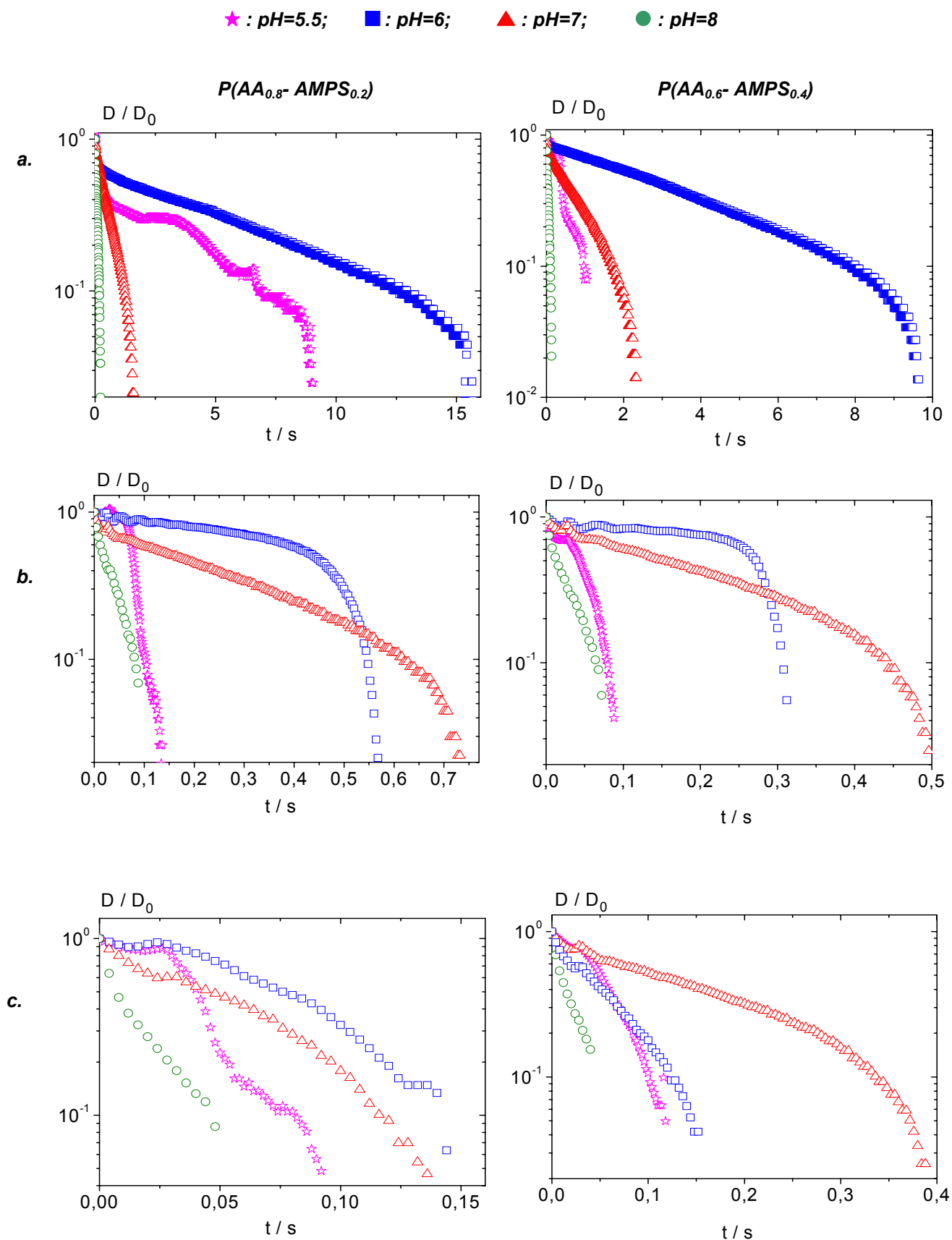


Figure 5-14: time-evolution of normalized diameter of $P(AA_{0.8}\text{-}co\text{-}AMPS_{0.2})$ (1st column) and of $P(AA_{0.6}\text{-}co\text{-}AMPS_{0.4})$ (2^d column) + $P(VP\text{-}VI)$, a: 2wt%; b: 1wt%; c: 0.5wt%, depending on pH.

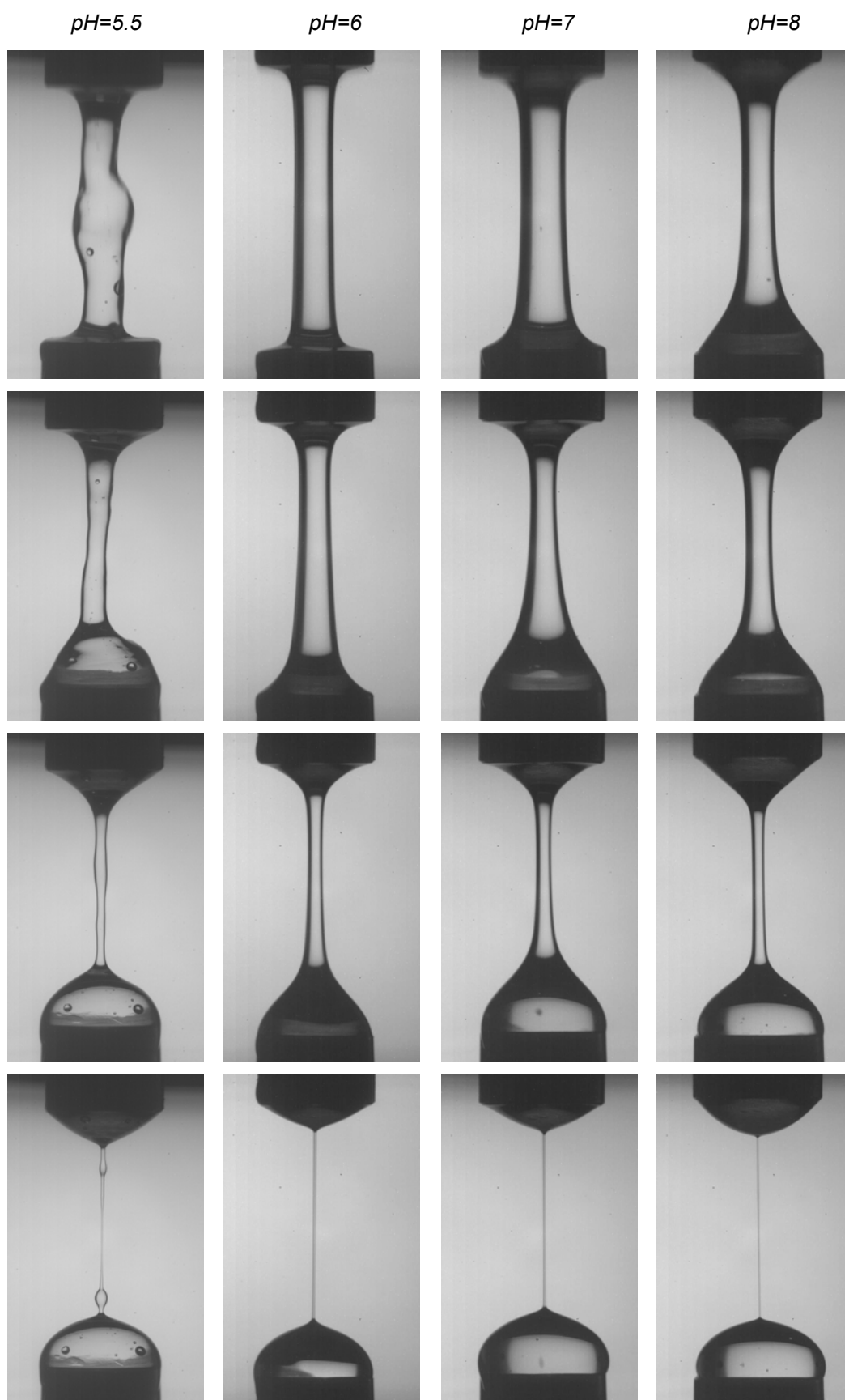


Figure 5-15: time-evolution of $P(AA_{0.8}\text{-co-AMPS}_{0.2}) + P(VP\text{-VI})$ at 2wt% at depending on pH.

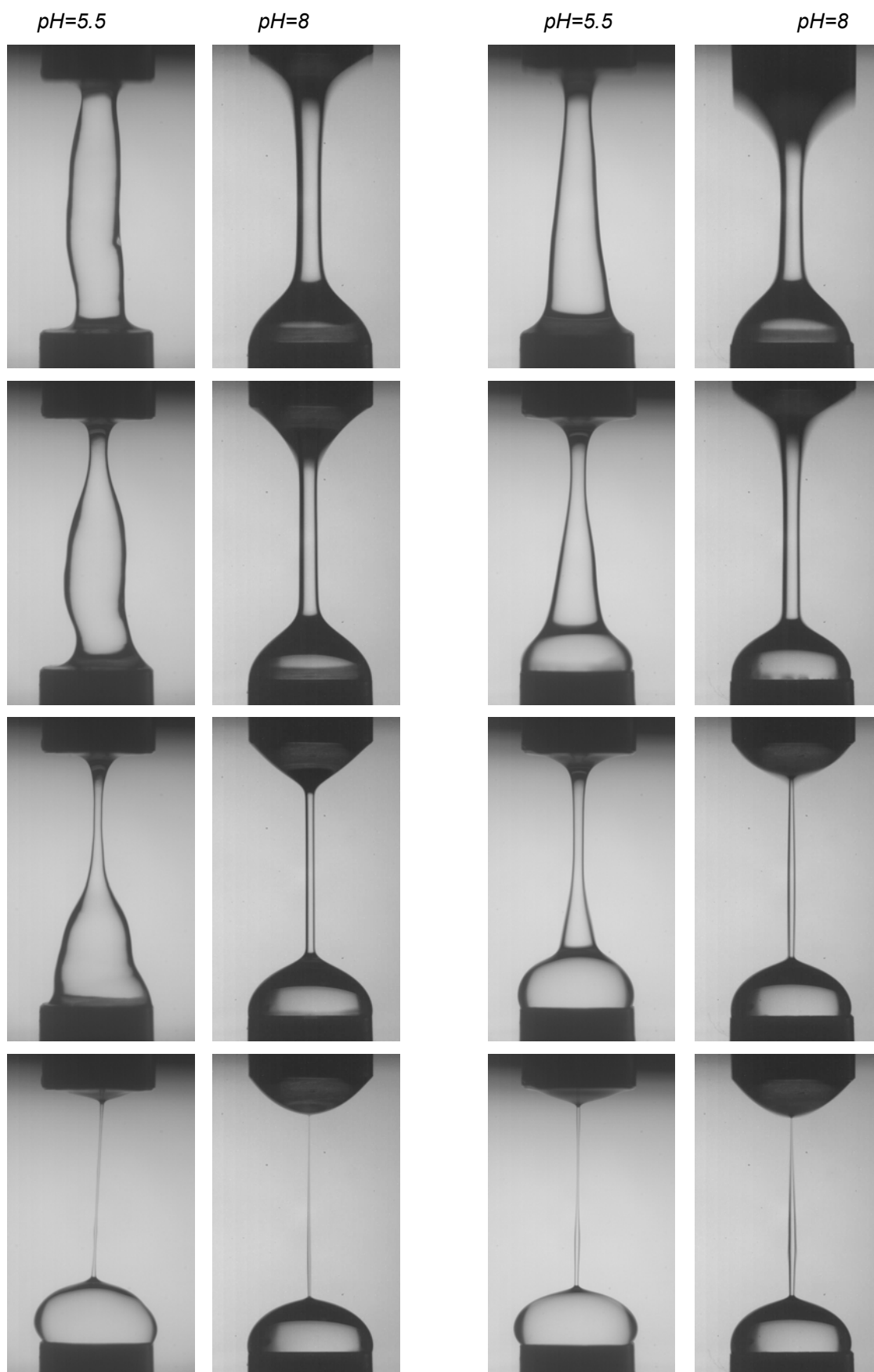


Figure 5-16: time-evolution of $P(AA_{0.8}\text{-co-AMPS}_{0.2}) + P(VP\text{-VI})$ at 1wt%, pH=5.5 and pH=8 (first two columns respectively) and at 0.5wt%, pH=5.5 and pH=8 (third and fourth column respectively).

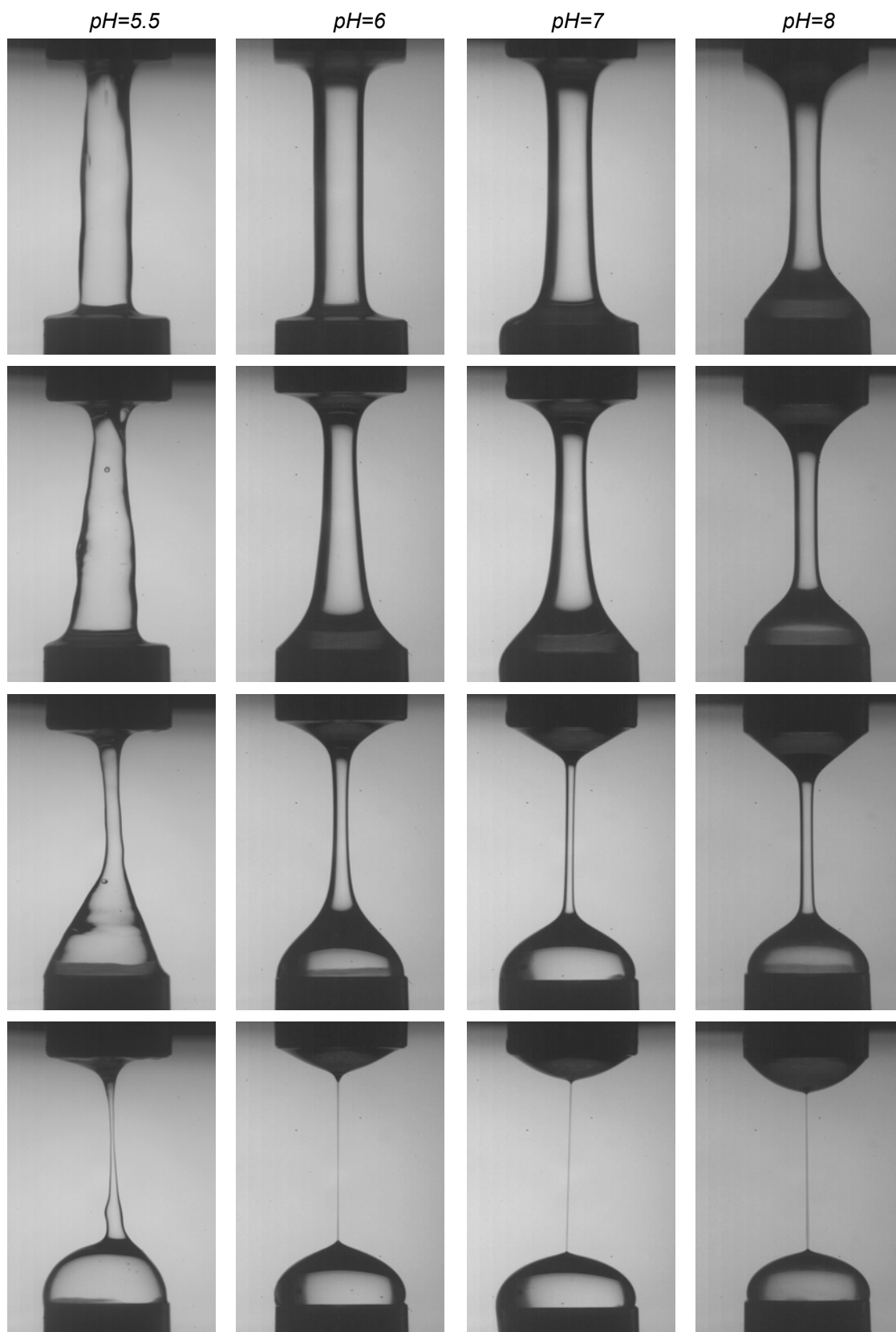


Figure 5-17: time-evolution of $P(AA_{0.6}\text{-co-AMPS}_{0.4}) + P(VP\text{-VI})$ at 2wt% depending on pH.

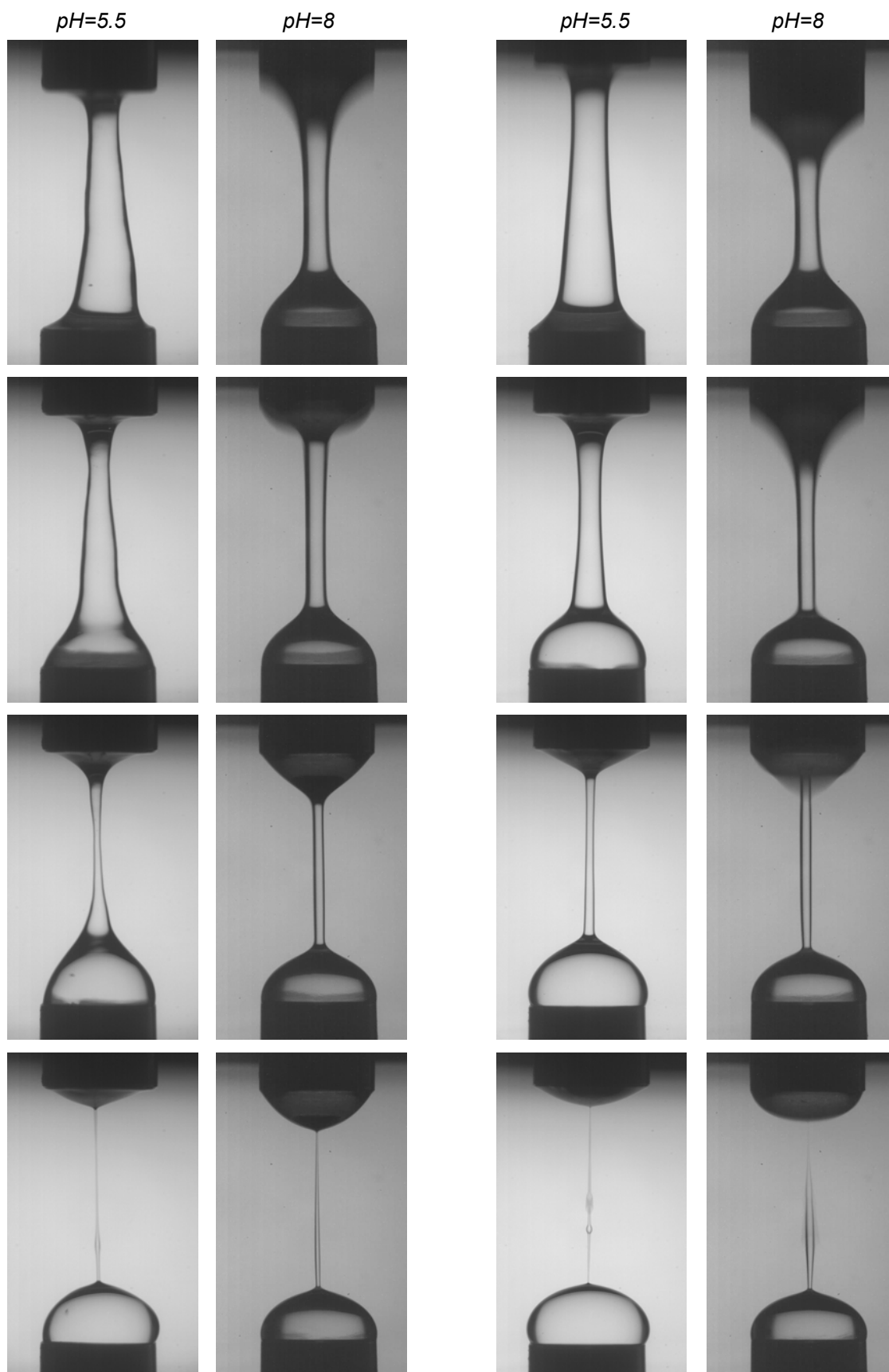


Figure 5-18: time-evolution of $P(AA_{0.6}\text{-co-AMPS}_{0.4}) + P(VP\text{-VI})$ at 1wt%, pH=5.5 and pH=8 (first two columns respectively) and at 0.5wt%, pH=5.5 and pH=8 (third and fourth column respectively).

5.3.4. Extensional relaxation times of mixtures polyanions+P(VP-VI)

Again, λ_E is determined using the equation $D(t)/D_0 = \exp\left(-t/3\lambda_E\right)$ (5.2)

As mentioned in the previous paragraph, only mixtures at pH=7 and pH=8 appear perfectly homogeneous and exhibit an exponential decay. Therefore, extensional relaxation times are calculated only for these mixtures.

Concerning mixtures at pH=5.5 and pH=6, which are essentially inhomogeneous, only filament lifetimes (t_F) are considered hereafter.

Table 5-2: relaxation features for mixtures of $PA^- + P(VP-VI)$ at pH=7 & 8 depending on concentration.

pH	C. (wt%)	PAA		P(AA _{0.8} -AMPS _{0.2})		P(AA _{0.6} -AMPS _{0.4})	
		t_F (s)	λ_E (s)	t_F (s)	λ_E (s)	t_F (s)	λ_E (s)
7	2.0	1.94±0.2	0.31±0.03	1.62±0.2	0.22±0.03	2.53±0.26	0.40±0.04
	1.0	1.04±0.1	0.18±0.02	0.74±0.08	0.14±0.014	0.50±0.05	0.09±0.009
	0.5	0.39±0.04	0.08±0.01	0.14±0.02	0.02±0.002	0.39±0.04	0.08±0.008
8	2.0	0.36±0.04	0.06±0.06	0.23±0.03	0.04±0.004	0.13±0.013	0.03±0.003
	1.0	0.13±0.02	0.03±0.003	0.10±0.01	0.03±0.003	0.07±0.007	0.02±0.002
	0.5	0.06±0.01	0.02±0.002	0.05±0.005	0.01±0.001	0.04±0.004	0.01±0.001

The evolution of the filament lifetimes for all polyanions follows the same trend as solutions of pure polyanions. A regular decrease when the concentration is lowered from 2wt% to 1wt% and then to 0.5wt%. Logically, the same decrease is observed for the extensional relaxation time.

As summarized in **Figure 5-19**, at pH=7, the values of λ_E for mixtures are significantly higher than the ones measured for pure polyanions. The same is true for t_F . The increase is close to 1 order of magnitude for PAA and P(AA_{0.8}-AMPS_{0.2}) while it is more than 2 orders of magnitude for P(AA_{0.6}-AMPS_{0.4}). At pH=8, t_F and λ_E for the mixtures are close to the ones measured for the pure corresponding polymer. This tends to indicate that the interactions responsible for the slower relaxation in shear play the same role in CaBER experiments at pH=7 and pH=8.

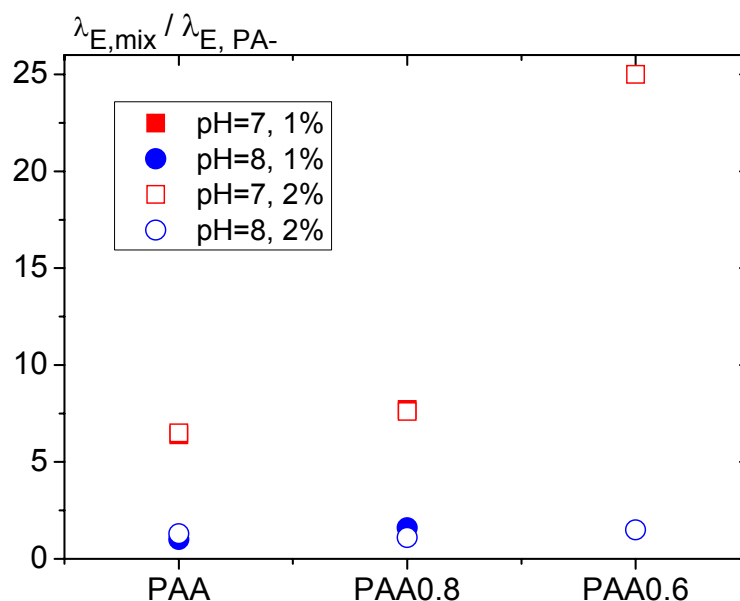


Figure 5-19: ratio extensional relaxation times of mixtures of polyanions with $P(VP-VI)$.

At pH=5.5 and pH=6, pictures in **Figure 5-11** and **Figure 5-14** indicate that because of the heterogeneous character of the mixtures, the filament decay patterns are completely different compared to higher pH. This is coupled with huge differences in filament lifetime depending on concentration, as shown in **Table 5-3**.

Table 5-3: filament lifetimes for mixtures of $PA^- + P(VP-VI)$ at pH=5.5 & 6 depending on concentration.

		PAA	$P(AA_{0.8}-AMPS_{0.2})$	$P(AA_{0.6}-AMPS_{0.4})$
pH	SC (wt%)	FL (s)	FL (s)	FL (s)
	2.0	42.8 ± 8.6	9.04 ± 1.8	1.05 ± 0.21
5.5	1.0	3.38 ± 0.68	0.54 ± 1.1	0.10 ± 0.02
	0.5	0.22 ± 0.044	0.10 ± 0.02	0.12 ± 0.024
	2.0	7.43 ± 1.5	15.50 ± 3.1	9.63 ± 1.92
6	1.0	0.50 ± 0.1	0.57 ± 0.11	0.31 ± 0.06
	0.5	0.12 ± 0.024	0.06 ± 0.012	0.16 ± 0.032

At 0.5wt%, filament lifetime is close to what is observed for pure polymers. This indicates that relaxation is fast within the filament.

At 1wt%, pH=6, t_F is increased but remains in the same order of magnitude as mixtures at pH=7. At pH=5.5, the nature of the polyanion has an influence as the t_F decreases with

increasing amount of AMPS in the copolymer. Same behavior is observed at 2wt%, concentration for which the t_F ranges between ~ 40 s for PAA and ~ 1 s for P(AA_{0.6}-AMPS_{0.4}). The very short lifetime measured for this sample may result from the stronger electrostatic interactions due to the higher content in strong anionic sites (as discussed in chapter 4). These stronger interactions may result in a more “brittle” rupture of the filament as the chains do not have the freedom to move one pass the other. The presence of larger or denser aggregates may also play a role in the shorter t_F measured at pH=5.5 for P(AA_{0.2}-AMPS_{0.8}) and P(AA_{0.6}-AMPS_{0.4}) compared to PAA.

5.4. Conclusion

Extensional flow behavior of polyelectrolyte solutions has been characterized using the CaBER technique. Behavior of pure polyanions is essentially independent of pH and is similar for PAA, P(AA_{0.8}-AMPS_{0.2}) and P(AA_{0.6}-AMPS_{0.4}). Three regimes can be distinguished in filament thinning experiments: first an equilibration period; second an exponential decay of the filament diameter; last an increase of the decay speed as the filament thins due to the finite elasticity of the chains. The lifetime of the filament is always short, less than 0.3s for 2wt% solutions and the relaxation times are also short, typically less than 0.05s for 2wt% solutions and less than 0.03s for 1wt% solutions. Pictures of CaBER experiments show that these low viscosity solutions are always homogeneous.

Extensional behavior of mixtures of polyanions with P(VP-VI) does not significantly depend on the nature of the negative polymer. But it is highly dependent on the pH and the concentration and this dependency can be summarized as follows:

- pH=8 and pH=7: three regimes can be distinguished, similar to the pure polyanion solutions, featuring an extended exponential decay which enables to calculate an extensional relaxation time. Filaments are homogeneous and always thin uniformly. Reproducibility of the measurements is good. Relaxation times decrease with decreasing concentration and with increasing pH.
- pH=5.5 and pH=6: decay pattern is irregular and governed mainly by the presence of aggregates within the sample. Filament lifetime is long at 2wt% but rapidly drops as the concentration decreases. This drop is significantly more pronounced than what is observed at higher pH. No relaxation times can be calculated but qualitatively,

relaxation appears to be faster as pH increases and concentration decreases. Especially, a spectacular drop of filament lifetime is observed from 1wt% solution to 0.5wt%, when large gel-like aggregates rapidly sag in the surrounding low viscosity liquid.

In a word, it appears that the increase in apparent molar mass leading to slower relaxation in shear measurements has the same effect in extensional measurements, at high pH and concentration. When pH and concentration are lowered, the behavior is essentially controlled by the movement of heterogeneities present within the sample. These features enable to assess a structure of these mixtures, which is discussed in the next chapter.

6. Origin of the Thickening Mechanism

6.1. Introduction

In recent years, a series of articles focused on comparing the behavior of different systems under shear and extensional flow. A straightforward way to do so is to compare the relaxation times in both processes, i.e. calculate λ_E/λ_S . For dilute solutions of linear, flexible polymers like polystyrene and poly(ethylene oxide) (PEO), it has been demonstrated that $\lambda_E/\lambda_S \approx 1$ (Anna and McKinley 2001; Oliveira et al. 2006). For solutions of PEO above c^* , $\lambda_E/\lambda_S < 1$ and this ratio decreases with increasing concentration (Arnolds 2009). In the case of entangled wormlike micellar solutions, smaller values of λ_E/λ_S , close to 0.3 have been reported. This low value is attributed to the dynamic nature of breaking and reforming micelles, also referred to as living polymers (Yesilata et al. 2006). Tan et al. studied solutions of hydrophobically modified HASE-type acrylate thickener (Tan et al. 2000). They observed a decrease in the extensional viscosity at high elongation rates. This phenomenon was attributed to a break-up of intermolecular clusters which are not able to withstand strong extensional flows. Same conclusion was drawn by Kheirandish et al. when they recorded low values of λ_E/λ_S (typically < 0.1) for solutions of sterocoll FD. This commercially available polymer is a statistical copolymer of methacrylic acid (MAA) and ethylacrylate (EA). These co-polymers are known to form intermolecular aggregates in aqueous solution due to the hydrophobic nature of statistically occurring EA-sequences. Time evolution of the filament diameter could be described by a single Maxwell-model. The corresponding relaxation time λ_E is always at least one order of magnitude lower than the longest shear relaxation time λ_S . It is not yet clear whether these aggregates break in elongational flow or whether they are too stiff to deform due to associative sites within the aggregates.

The studies carried out in chapter 3 and 4 on the one hand and in chapter 5 on the other one permit to collect information on respectively the shear and extensional behavior of pure polyanions and mixtures of polyanions with P(VP-VI). They show clearly that solutions of pure polyanions always exhibit a classical viscoelastic behavior, their viscosity and relaxation times depending essentially on concentration (both $|\eta^*|_0$ and λ_S decreasing with decreasing concentration), but only weakly on pH. On the contrary, the behavior of mixtures depends strongly both on concentration and on pH. Under shear flow, highest viscosity increase and slowest relaxation are measured at low pH and low concentration. Under extensional flow,

lowering the pH leads to increased relaxation times only at 1wt% and 2wt%. On the contrary, at low pH and 0.5wt%, filament lifetime is very short. To get a better insight into these discrepancies, λ_E/λ_S at pH=7 and 8 and filament lifetimes at lower pH are compared.

6.2. Microstructure of mixtures of polyanions with P(VP-VI)

6.2.1. Shear versus extensional rheology of pure polyanions

Using the equations 6.1 and 6.2, the shear and extensional relaxation times have been calculated for pure polyanions.

$$D(t)/D_0 = \exp\left(-t/3\lambda_E\right) \quad (6.1)$$

$$\lambda_s = \lim_{\omega \rightarrow 0} \frac{G'}{G''(\omega)}, \quad (6.2)$$

Hence, value of the ratios λ_E/λ_S can be calculated. These values will later serve as a reference to discuss the values calculated for the mixtures. As relaxation times of the mixtures can only be calculated at pH=7 and pH=8, the study of the pure polyanions is deliberately limited to these two pH. Two concentrations are considered: 1wt% and 2wt%. Results are gathered in **Table 6-1**.

Table 6-1: relaxation features of polyanions at pH=7 and 8 at 1wt% and 2wt%.

C. (wt%)	PAA			P(AA _{0.8} -AMPS _{0.2})			P(AA _{0.6} -AMPS _{0.4})			
	λ_S (s)	λ_E (s)	λ_E / λ_S	λ_S (s)	λ_E (s)	λ_E / λ_S	λ_S (s)	λ_E (s)	λ_E / λ_S	
pH=7	2.0	0.35	0.048	0.14	0.15	0.029	0.19	0.06	0.016	0.27
	1.0	0.31	0.028	0.09	0.11	0.018	0.16	0.03	-	-
pH=8	2.0	0.24	0.046	0.19	0.09	0.036	0.28	0.09	0.018	0.20
	1.0	0.17	0.029	0.17	0.06	0.019	0.31	0.04	-	-

The ratios λ_E/λ_S are not significantly different for the three polyanions studied. The dependency on pH is minor and no clear trend appears as λ_E/λ_S is slightly higher at pH=8 compared to pH=7 for PAA and P(AA_{0.8}-AMPS_{0.2}) but lower for P(AA_{0.6}-AMPS_{0.4}). At a given pH, decreasing the concentration leads to a slight decrease in λ_E/λ_S .

The values of the ratios are always comprised between 0.1 and 0.3. These values are significantly lower than what is expected for dilute solutions of flexible polymers ($\lambda_E/\lambda_S \approx 1$) (Anna and McKinley 2001) but agree well with values reported for PEO solutions above c^* (Arnolds 2009). This could be due to the presence of charges on the side chains of these polymers which leads to more stretched conformation of the polymers compared to neutral ones. This is particularly true at the pH investigated here, for which most acrylic groups are dissociated. Expanded chains are less capable of stretching in extensional flow, and therefore exhibit smaller λ_E/λ_S . These calculated ratios are empirical findings and serve as references to compare the results obtained for the mixtures which are gathered in the next paragraph.

6.2.2. Shear versus extensional rheology of mixtures of polyanions with P(VP-VI)

6.2.2.1. Mixtures at pH=7 and pH=8

At pH=7 and pH=8, λ_E/λ_S can be numerically calculated using the values collected in chapter 3, 4 and 5. Results are summarized in **Table 6-2** and **Figure 6-1**.

Table 6-2: relaxation features of mixtures of $PA^- + P(VP-VI)$ at pH=7 & 8 depending on concentration.

	PAA			$P(AA_{0.8}-AMPS_{0.2})$			$P(AA_{0.6}-AMPS_{0.4})$			
	CS(wt%)	λ_S (s)	λ_E (s)	λ_E/λ_S	λ_S (s)	λ_E (s)	λ_E/λ_S	λ_S (s)	λ_E (s)	λ_E/λ_S
pH=7	2.0	1.28	0.31	0.25	0.8	0.22	0.27	0.35	0.40	1.14
	1.0	1.21	0.18	0.15	0.9	0.14	0.15	1.4	0.09	0.06
	0.5	3.2	0.08	0.025	2.9	0.03	0.01	1.9	0.08	0.04
pH=8	2.0	0.38	0.06	0.16	0.11	0.04	0.36	0.05	0.03	0.6
	1.0	0.12	0.04	0.3	0.09	0.03	0.33	0.07	0.02	0.28
	0.5	0.08	0.02	0.25	0.05	0.015	0.3	0.03	0.01	0.33

All mixtures considered here are transparent and homogeneous. Nevertheless, several case of figure can be distinguished.

At pH=8, λ_E/λ_S depends only slightly on the concentration. For the three polyanions studied, the value of this ratio is roughly comprised between 0.2 and 0.6, comparable with what is recorded for pure polyanions. This supports the results obtained so far, which indicate that the

interactions existing between oppositely charged polymers at pH=8 and above are weak and do not significantly modify the rheology of the polyanions. The sole exception is P(AA_{0.6}-AMPS_{0.4}) at 2wt%. This may be due to the larger content of AMPS, which gives rise to slightly stronger interactions compare to AA and modifies slightly the behavior under extensional flow, as already mentioned in the previous chapters.

At pH=7, λ_E/λ_S values similar to the ones measured for pure polyanions are obtained only for 2wt% and 1wt% solutions of PAA and P(AA_{0.8}-AMPS_{0.2}). Only these mixtures exhibit relaxation phenomena similar to free polyelectrolyte chains. For P(AA_{0.6}-AMPS_{0.4}), the ratio is again significantly higher at 2wt%, the explanation for this observation being the same as previously.

Polymer ■ : PAA; ▲ : P(AA_{0.8}-AMPS_{0.2}); ● : P(AA_{0.6}-AMPS_{0.4})

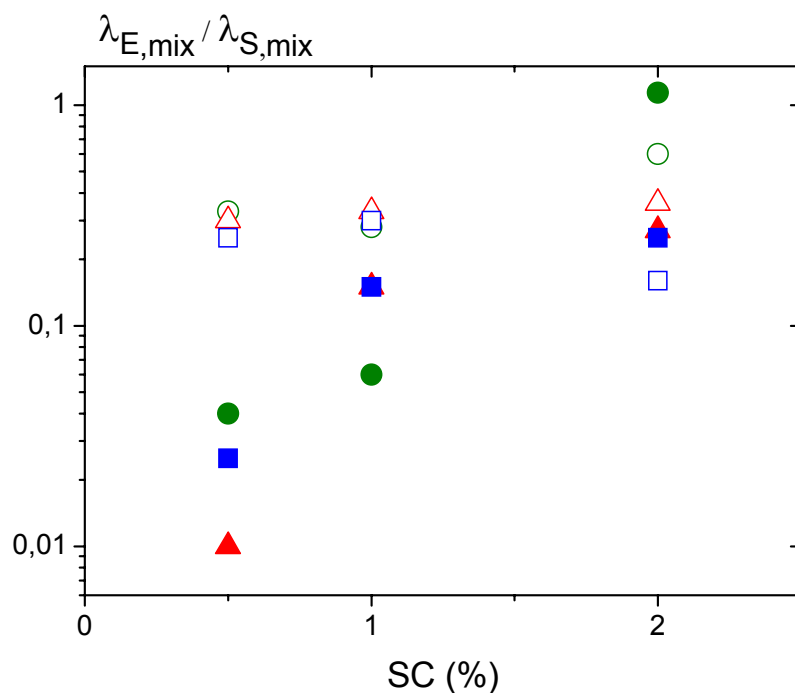


Figure 6-1: ratio of extensional and shear relaxation times at pH=7 (closed symbols) and pH=8 (open symbols).

The same general trend is observed for all polyanions as the concentration decreases: a fast decrease of λ_E/λ_S . Thus, at 0.5wt%, the relaxation times ratio is approximately one order of magnitude smaller than for pure polyanions. In the case of acrylate thickeners, this observation is explained by the presence of inhomogeneities/aggregates within the sample. Same explanation accounts for the present evolution of λ_E/λ_S , as CaBER experiments show that the mixtures undergo a transition from homogeneous to inhomogeneous as the pH is decreased

from 7 to 6. Thus, some inhomogeneities may also be present at pH=7 and influence the flow/relaxation properties. These inhomogeneities, as mentioned in the previous chapter, play a dramatic role for the behavior of the mixtures.

6.2.2.2. Mixtures at pH=5.5 and pH=6

At pH=5.5 and 6, only the filament lifetimes of the mixtures can be measured, as the decay of the filament is not exponential, which would allow for a straightforward definition of a relaxation time. As explained in the previous chapter, this particular behavior is due to the presence of large aggregates in the solutions which modify dramatically the behavior under extensional flow at low pH;

Table 6-3: filaments lifetime of mixtures of PA⁻ with P(VP-VI) at pH=5.5 & 6 depending on concentration.

		<i>PAA</i>	<i>P(AA_{0.8}-AMPS_{0.2})</i>	<i>P(AA_{0.6}-AMPS_{0.4})</i>
	SC. (wt%)	t _F (s)	t _F (s)	t _F (s)
pH=5.5	2.0	42.82	9.04	1.05
	1.0	3.38	0.54	0.09
	0.5	0.22	0.10	0.12
pH=6	2.0	7.43	15.50	9.63
	1.0	0.50	0.57	0.31
	0.5	0.12	0.06	0.16

In the set of results summarized in **Table 6-3**, the exact values of filament lifetimes are less meaningful than the order of magnitude and the variations as it should be kept in mind that an error of 20% is to be considered (cf. **Table 5-5**).

However, an increase of filament lifetime by one or two orders of magnitude compared to the pure polyanions indicates clearly a slowing down of the chain relaxation. Slower relaxation phenomena are observed at 2wt% for all polyanions, except P(AA_{0.6}-AMPS_{0.4}) at pH=5.5, mixture for which t_F is only 1s. For this mixture and one at pH=5.5 at 1wt%, because of stronger electrostatic interactions, the rupture is more “brittle” compared to mixtures with more weakly charged polyanions, and subsequently t_F is drastically smaller.

At lower concentrations, the filament lifetimes are always orders of magnitude lower. It appears that the AMPS content plays a role: the more AMPS in the polyanion, the shorter the filament lifetime. This result can be put in parallel with the higher values of λ_E/λ_S obtained for P(AA_{0.6}-

AMPS_{0.4}) and with the viscosity increases calculated in chapter 3 and 4, which showed that more AMPS in the polyanion leads to slightly higher values for viscosity enhancement.

For mixtures at pH=6, a general trend indicating that a decrease in concentration by a factor of 2 leads to a decrease of filament lifetime by roughly an order of magnitude is observed. Thus, at 0.5wt%, filament lifetimes are comparable with the ones of pure polyanions (but at 1wt%).

Comparing shear and extensional measurements, huge discrepancies between the relaxation phenomena under both kind of flow appear. These discrepancies are schematically summarized in **Table 6-4**. The term homogeneous or heterogeneous which are used to describe the samples do refer to the observations made during CaBER experiments (cf. pictures in chapter 5). If macroscopic gelly lumps are visible on the pictures taken during the decay of the filament, the sample is called heterogeneous; if no gel is visible and the decrease of the diameter of the filament follows an exponential law, the sample is called homogeneous. Whether the structure at the microscopic level is homogeneous or inhomogeneous is not elucidated.

6.2.2.3. Possible microstructure of mixtures of polyanions with P(VP-VI)

Table 6-4: relaxation features for mixtures of PA⁻ with P(VP-VI) depending on pH and concentration.

	pH=5.5 and pH=6	pH=7 and pH=8
2wt%	<ul style="list-style-type: none"> • Heterogeneous • Slow shear relaxation • Very long FL i.e. very slow elongational relaxation <p><i>NB: P(AA_{0.6}-AMPS_{0.4}) too heterogeneous</i></p>	<ul style="list-style-type: none"> • Homogeneous • pH=8: $\lambda_E / \lambda_S \sim$ similar to pure polyanions • pH=7: $\lambda_E / \lambda_S \sim$ similar to pure polyanions at 2wt% and 1wt%. One order of magnitude lower at 0.5wt%
1wt%	<ul style="list-style-type: none"> • Heterogeneous • Very slow shear relaxation • Short FL i.e. fast elongational relaxation 	
0.5wt%	<ul style="list-style-type: none"> • Heterogeneous • Extremely slow shear relaxation • Very short FL i.e. very fast elongational relaxation 	

In this schematic summary, the striking opposite variation of relaxation times at low pH with concentration is pointed out: while shear experiments show a transition towards gel-like structures when concentration decreases from 2wt% to 0.5wt%, in CaBER experiments the filament lifetime decreases by two orders of magnitude. This means that while shear relaxation becomes much slower, extensional relaxation becomes much faster.

The microstructure of the system is responsible for this behavior. Indeed, shear experiments show that an increase of the average apparent molar mass is observed when pH is lowered. The pictures taken during CaBER experiments provide the additional information that macroscopic phase separation takes place at pH=5.5 and pH=6, which leads to an inhomogeneous deformation of fluid filaments.

To the best of our knowledge, no work specifically deals with the microstructure of networks formed by oppositely charged polyelectrolytes. However, a lot of work has been carried out on electrostatic interactions arising between polyelectrolytes and oppositely charged proteins, because of potential applications in the field of biotechnologies. Some of this work focuses more precisely on the structures of these complexes. For example, the group of F. Boué has published a serie of articles on their work on the interactions between poly(styrene sulfonate sodium) (PSSNa) and lysozymes (positively charged proteins). The main conclusions of these articles is that long enough PSSNa chains can be crosslinked by lysozymes and can yield various structures depending on the conditions. In particular, gel-like structures can be formed, provided that the PSSNa is under semi-dilute conditions and that the ratio between the negative charges of the polymer and the positive charges present on the protein is close enough to 1. Utilizing small angle neutron scattering measurements, they got some insight into the microstructure of these gels and were able to prove that the gels are inhomogeneous on a microscopic level, some regions being denser than others.

A schematic representation of a plausible microstructure is reproduced in **Figure 6-2** (Gummel 2003).

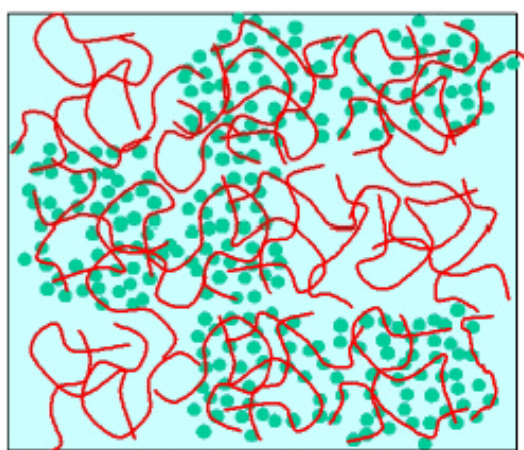


Figure 6-2: schematic representation of gels formed by mixtures of PSSNa with lysosomes.

The heterogeneous repartition of the crosslinking points had been calculated by Monte-Carlo simulation by Carlsson et al. in 2003. It is related to the complex equilibrium existing between attractive interactions between opposite charges and repulsion between similar charges.

Taken the conclusions of Boué et al. into account, the results obtained by shear and CaBER experiments can reasonably be interpreted as resulting from a balance between extended structures (resulting from the grafting of several chains of polyanions by polycations which still behave as flexible chains but with an increased molar mass) and large aggregates or gelly lumps (resulting from the association of many chains and behave as discrete gel-like areas):

- **Extended structures**, account for increase in shear and extensional viscosity/filament lifetime. These structures resulting from the bridging between oppositely charged polyelectrolytes are capable of withstanding strong extensional flow and lead to long filament lifetime. They govern the behavior of the mixtures at 2wt%: aggregates are present but they are “trapped” in a surrounding high viscosity matrix of entangled polymer chains having a high apparent molar mass. When the concentration is decreased, the entanglement density decreases and the behavior is controlled by the aggregates.
- **Aggregates** result from the strengthening of electrostatic interactions upon pH decrease (cf. next paragraph). At low pH, they are present at 2wt%, 1wt% and 0.5wt% but account differently on the rheological behavior of the samples. At 2wt%, they are entrapped in the surrounding highly viscous matrix and do not play a major role. As the viscosity of the matrix decreases upon dilution, they are freer to move and interact/overlap one with each other. The decrease of ionic strength and overall concentration may also lead to a swelling of these aggregates. The overlap and interactions between aggregates leads to an apparent “freezing” of the system under small amplitude oscillatory measurements. However, the aggregates are not entangled one with each other and under extensional deformation, they move freely one past the other, not contributing to the extensional viscosity. The viscosity of the surrounding media is fast decreasing with concentration and this leads to dramatic shortening of filament lifetime at 0.5wt%. The fact that filament lifetime is even shorter than for pure polyanions may be due to the fact that the density in polymer is higher in the aggregates, meaning that the polymer concentration in the surrounding media is lower than 0.5wt% and that t_F is therefore shorter.

Such a structure accounts for the experimental results obtained in shear and extensional flow experiments but is only speculative and scattering or other structural investigations would be necessary to further elucidate the origin of the observed rheological features.

6.3. Origin of cooperative interactions

6.3.1. Introduction

So far in this work, it has been assumed that the formation of extended structures and of large aggregates results only from electrostatic interactions between deprotonated carboxylic groups from poly(acrylic acid) and protonated imidazole group from poly(vinyl imidazole). Indeed, it is known that PAA and PVI can interact to form strong complexes (Kreuer 1998). Such complexes have for instance recently been used to form conducting polymer electrolyte which exhibit excellent temperature stability (Arslan 2006).

However, several works have also proved that poly(acrylic acid) can interact with poly(vinyl pyrrolidone) via hydrogen bonds. Depending on the conditions, these interactions can be strong enough to induce phase separation. Most studies focus either on determining the stoichiometry of the complex (Argüelles-Monal 1998) or on studying the properties of the complex once it is dried (Lau 2002). Khutoryanskiy et al. (2003, 2004) published several articles describing the complexation of PAA with hydrogen-bond acceptors. They could determine that depending on the polymer used, weak or strong complexes can be formed and that complexation occurs only below a critical value of the pH (pH_{crit}). With PVP, pH_{crit} is close to 4.7. This value can change slightly with concentration, temperature etc but generally, above $pH=4.7$, no H-bond based complexes are formed. This roughly corresponds to the pK_a of PAA, meaning that above there are not enough carboxylic groups which are protonated for efficient H-bond interactions.

These results indicate that in the work presented in this manuscript, for which the pH is 5.5 or above, interactions between poly(acrylic acid) and poly(vinylpyrrolidone-co-vinylimidazole) are only electrostatic.

To support this assumption, mixings of PAA, $P(AA_{0.8}-AMPS_{0.2})$, $P(AA_{0.6}-AMPS_{0.4})$ with a homopolymer of VP having a molar mass of 100kDa, similar to the one of P(VP-VI) are realized. The mixtures have a composition of one to one in weight and the procedure to prepare the mixtures and carry out the measurements is similar to the one used in chapter 3, 4 and 5.

6.3.2. Rheological behavior of mixtures polyanions + PVP

Similar to what was undertaken with mixtures of AA/AMPS copolymers with P(VP-VI), the dynamic viscosities and rheological features of mixtures of AA/AMPS copolymers with PVP are measured. Measured concentrations are 2wt%, 1wt % and 0.5wt%. Measured pH are 5.5, 6 and 7; pH=8 is not investigated as H-bonds are less likely to form as pH increases. To determine if the rheology of the mixtures differs significantly from the one of the pure polymers, the viscosity enhancement $|\eta^*|_0(\text{mixture}) / |\eta^*|_0(\text{polyanion})$ is calculated and the dynamic moduli G' and G'' measured versus frequency.

These moduli are shown in **Figure 6-3** at 2 concentrations (left-end side column corresponds to 2wt% and right-end side to 1wt%) depending on pH for mixtures of PAA, P(AA_{0.8}-AMPS_{0.2}) and P(AA_{0.6}-AMPS_{0.4}) with PVP (respectively from top row to bottom row in **Figure 6-3**). Mixtures at 0.5wt% are not shown but they always exhibit the typical terminal regime of viscoelastic fluids for which $G' \sim \omega^2$ and $G'' \sim \omega$. Such a terminal regime is also observed for all mixtures both at 2wt% and 1wt%. The reference, i.e. the same polyanion at pH=8 and half concentration is displayed as grey stars in **Figure 6-3**. For all polyanions, both G' and G'' curves do essentially not depend on pH and superimpose with G' and G'' curves from the reference. This result is very different from what was measured for polyanions mixtures with P(VP-VI) and proves that the relaxation pattern of the polyanions molecules is not modified by the addition of a hydrogen bond acceptor like PVP.

This is confirmed by the results obtained for the calculation of viscosity enhancement $|\eta^*|_0(\text{mixture}) / |\eta^*|_0(\text{polyanion})$, summarized in **Figure 6-4**. For all polyanions, viscosity enhancement is comprised between 0.7 and 1.4, meaning that the viscosity of the polyanions is essentially not affected by the addition of PVP. No systematic trend appears depending on pH and concentrations.

With a pH ranging from 5.5 to 7 and a concentration ranging from 0.5wt% to 2wt%, addition of PVP does not affect the viscosity and rheological behavior of polyanions based on AA and AMPS. H-bonds do not play a role in the thickening effect described in the previous chapters, which are solely due to electrostatic interactions between carboxylate and imidazolium.

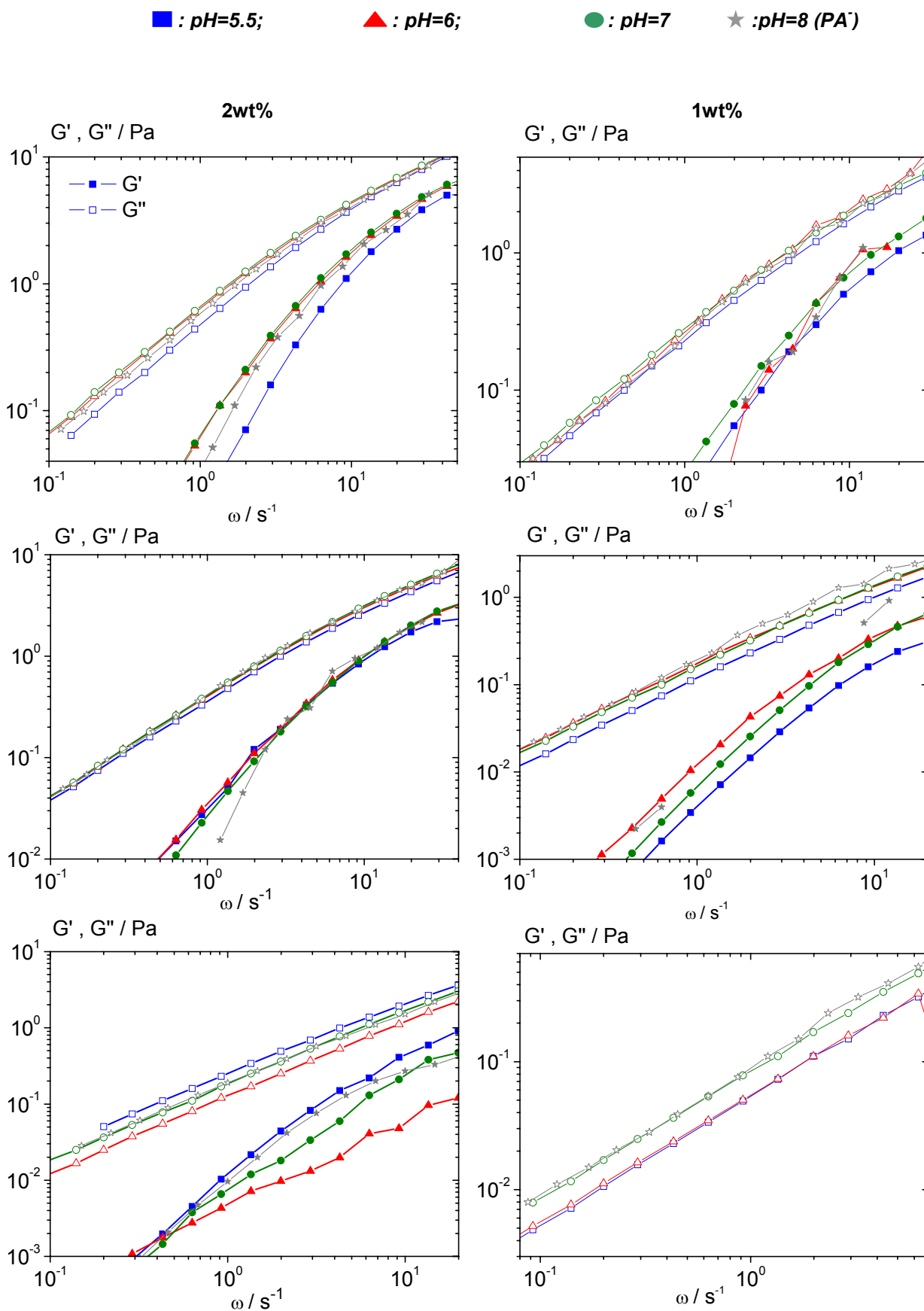


Figure 6-3: dynamic moduli for mixtures of PAA, $P(AA_{0.8}\text{-}AMPS_{0.2})$ and $P(AA_{0.6}\text{-}AMPS_{0.4})$ (1st, 2d & 3rd rows respectively) with PVP at 2wt % & 1wt % (1st & 2d column respectively) depending on pH.

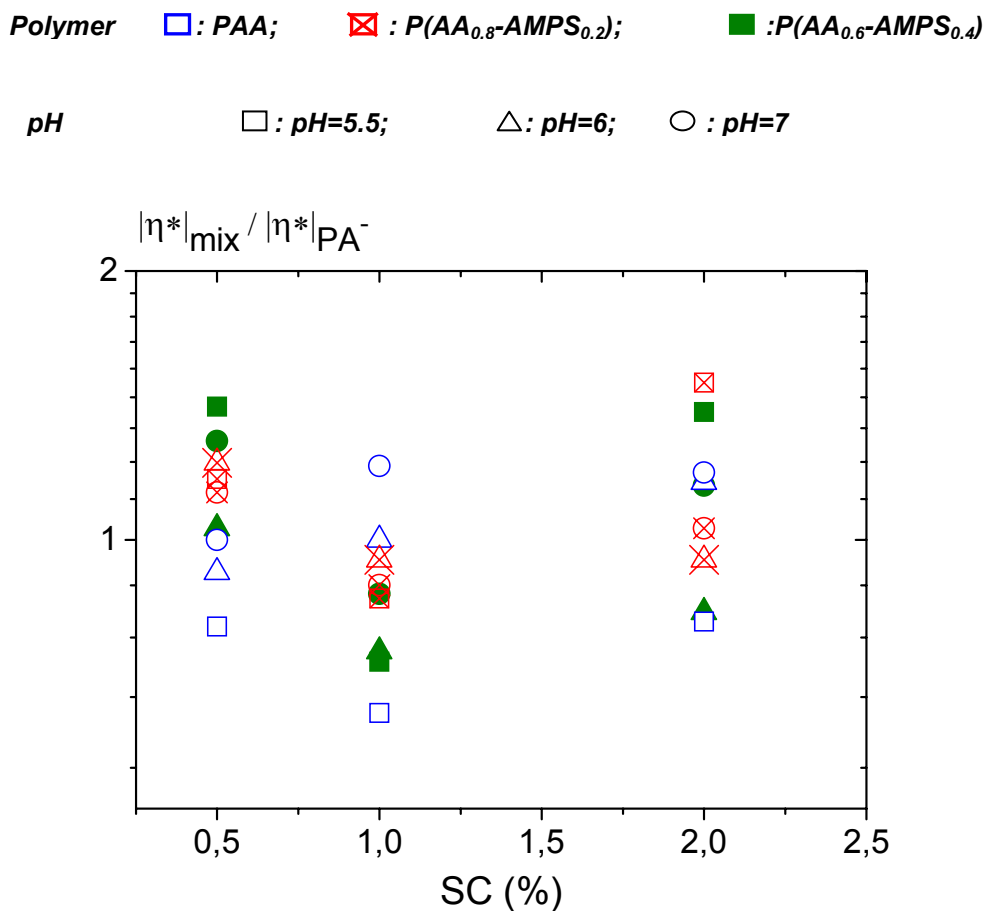


Figure 6-4: viscosity enhancement for mixtures of PA⁻ and PVP depending on concentration and pH.

6.3.3. Balance between positive and negative charges

The results described in the previous paragraph prove that electrostatic interactions are responsible for the increase in viscosity discussed so far. The strength of these interactions resulting in the bridging of polyanions by short polycations, formation of extended structures, aggregates and finally phase separation are directly related to the charge compensation, which is related to the charge density on the positive and negative species. This complex equilibrium depends on the species mixed together, and in the case discussed here, mostly on the pK_a of the carboxylic group and of the imidazole group. Above its pK_a, a weak acid is mostly dissociated into A⁻ and H⁺. Below its pK_a, a weak base is mostly present as its protonated form BH⁺. Thus, the charge density on each weak polyelectrolyte can be estimated roughly depending on pH using the Hendersen-Hasselbach equation:

$$\text{pH} = \text{pK}_a + \log \frac{[\text{A}^-]}{[\text{AH}]} \quad (6.3)$$

If the system in which PAA and P(VP-VI) are mixed is considered, the relationship between the pH and the charge density for each species can be written:

$$\text{pH}_1 = \text{pK}_a(\text{PAA}) + \log \frac{[\text{COO}^-]}{[\text{COOH}]} \quad (6.4)$$

$$\text{pH}_2 = \text{pK}_a(\text{VI}) - \log \frac{[\text{VI}^+]}{[\text{VI}]} \quad (6.5)$$

As in a mixture, pH_1 and pH_2 are of course similar, this can be summarized:

$$\frac{[\text{COO}^-]}{[\text{COOH}]} \cdot \frac{[\text{VI}^+]}{[\text{VI}]} = \text{Constant value} \quad (6.6)$$

There is a balance between charged acid groups and charged vinyl imidazole groups. Whether one or the other is preponderant in the system is directly related to the value of the pH.

Figure 6-5 shows the evolution of the charges present in the system depending on pH, keeping in mind that the pK_a of PAA is 4.6 while the pK_a of PVI is close to 6.

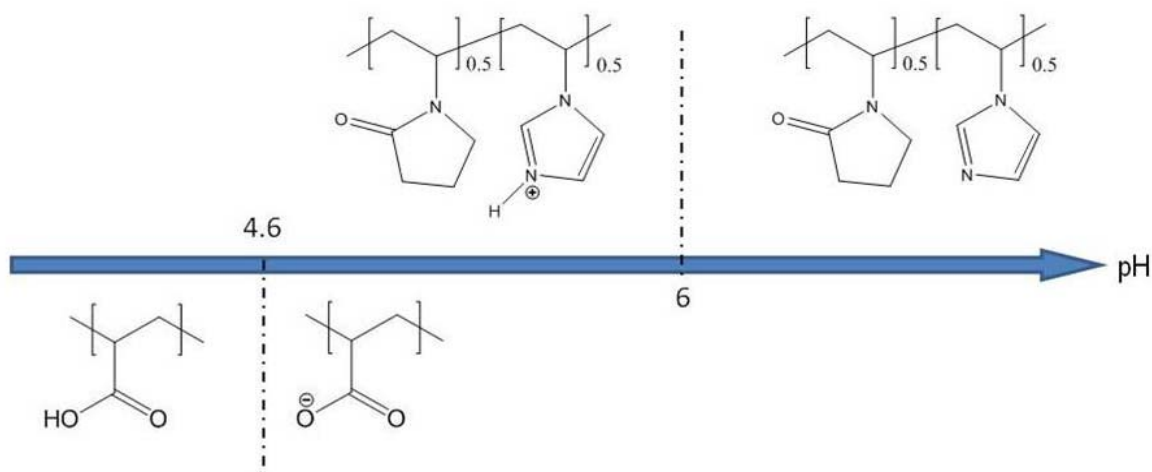


Figure 6-5: preponderant species in a mixture of PAA with P(VP-VI) depending on pH.

In all mixtures studied in this manuscript, the mass ratio between polyanions and polycation is one to one. Hence, it is possible to calculate the molar ratio between constitutive repeating

units. The molar mass of acrylic acid is $72\text{g}\cdot\text{mol}^{-1}$, the molar mass of a repeating unit composed half of VP, half of VI is $102.6\text{g}\cdot\text{mol}^{-1}$. This means that at a one to one ratio in mass, there is 1.4 times more acid repeating units than $(\text{VP}_{0.5}\text{-VI}_{0.5})$ repeating units. Only half of the latter can be charged (VP is always neutral), and therefore the ratio of negative to positive ionizable groups becomes 2.8. This simple calculation coupled with Hendersen-Hasselbach equations for the polybase and polyacid enables to assess the charge balance in the system as a function of pH.

The same simple calculation can be used with $\text{P}(\text{AA}_{0.8}\text{-AMPS}_{0.2})$ and $\text{P}(\text{AA}_{0.6}\text{-AMPS}_{0.4})$, taking into account that the molar mass of AMPS is $207\text{g}\cdot\text{mol}^{-1}$ which changes the molar mass of the repeating unit, and also that AMPS is charged whatever the pH.

The charge balance versus pH for the three polyanions is shown in **Figure 6-6**.

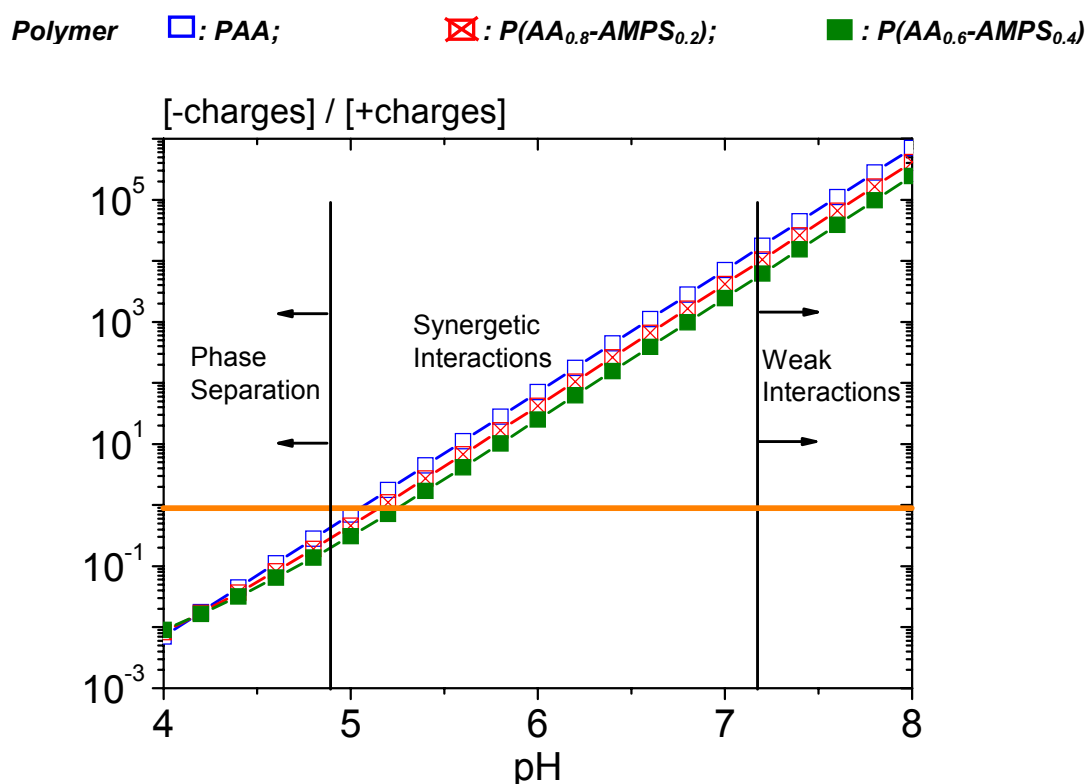


Figure 6-6: negative to positive charge ratio in a 1:1 mixture of PA^- with $\text{P}(\text{VP-VI})$ depending on pH.

First, it appears that the dependency of the charge balance on the nature of the negative charge is minor. The isoelectric point (IEP), pH at which positive and negative charges are balanced, is almost similar for PAA, $\text{P}(\text{AA}_{0.8}\text{-AMPS}_{0.2})$ and $\text{P}(\text{AA}_{0.6}\text{-AMPS}_{0.4})$. The fact that AMPS is a strong polyanion is counterbalanced by its higher molar mass, as mixtures are always prepared in terms of mass ratio.

Concerning the charge neutralization, at pH below 4.5, positive charges are present in large majority while at pH above 5.5 a large majority of negative charges are present in the system for all polyanions. In between, the charges are more or less balanced.

The results obtained so far regarding viscosity enhancement, enable to correlate the charge matching with the increase in viscosity:

- When negative charges are present in large excess, no viscosity enhancement is detected and the behavior of the mixture is similar to pure polyanion. Polyanion chains, which are highly charged, can not be bridged by P(VP-VI) as this cationic species are not charged.
- When the charge ratio gets closer to one, oppositely charged groups can interact to form super-structures which lead to an increase in viscosity. The physical crosslinking density is low so that structures formed are loose and remain soluble.
- When positive charges become more numerous, more P(VP-VI) crosslink the polyanionic macromolecules, leading to the formation of large aggregates with internal physical crosslinks. The system finally macroscopically phase separates between a solid complex and a water-like supernatant.
- Trials to further decrease the pH show that this does not lead to resolubilization of the complex. On the contrary, lower pH values seem to lead to complexes that are stronger and more compact. This is also true for PAA. In this case, H-bonds probably play a greater role in the complexation phenomenon.

It is necessary to point out that **Figure 6-6** is only a very coarse estimation of charge evolution which does not take into account the ionic strength, the shielding effects, the potentially concerted interactions, and all the other factors which are likely to modify the acido/basic equilibriums. Moreover, as just mentioned, at pH below 5, H-bonds due to the interactions between VP and protonated AA probably start to play an important part, as the pH is lower than $\text{pH}_{\text{critical}}$ determined by Khutoryanskiy (2003, 2004).

6.4. Conclusion

Results obtained in shear and extensional rheology exhibit similarities as well as pronounced discrepancies. At high pH, a decrease in concentration leads to faster relaxation both in shear and under extensional flow. On the contrary, at low pH, while a decrease in concentration results in a shorter filament lifetime in a CaBER experiments, it results in much longer relaxation times in shear, where a transition towards gel-like behavior is observed.

These very different behaviors are explained by differences in microstructure. At pH=8, polymers are essentially present as free chains some of them being grafted with oppositely charged ones. As the pH decreases, this grafting evolves to bridging, resulting in flexible complexes with an apparent molecular weight several times larger than that of the pure polyanions, and then to the formation of gel-like aggregates. All these structures coexist and are in equilibrium one with each other.

To determine if hydrogen-bonds which may arise between carboxylic and pyrrolidone groups play a role in the formation of these structures, PAA and P(AA-co-AMPS) are mixed with PVP at different pH and the viscosity of these mixtures measured. No viscosity enhancement is observed, meaning that when these polyanions are mixed with P(VP-VI), the increase in viscosity arises from interactions with VI: the electrostatic interactions are predominant. The viscosity enhancement can be correlated to the charge matching between polyanions and polycations, roughly calculated using the Hendersen-Hasselbach equation: it appears that the increase in viscosity is the most pronounced just before a charge ratio of 1 to 1, i.e. just before macroscopic phase separation of the system.

6.5. Perspectives

Using both shear and extensional rheology, I was able to point out some of the modifications occurring at the microscopic level when 2 oppositely charged polyelectrolytes interact to form larger structures. However, the “model” I came up with, in which aggregates, free chains, grafted chains etc... coexist only result from macroscopic measurements. To get a better understanding of the phenomena occurring at the microscopic level, new characterization techniques have to be considered in the future:

Microrheology: multiple particles tracking (MPT) is a technique in which monodisperse beads (polystyrene for example) are injected in a sample and their motion is subsequently recorded with a fast camera. Assuming movements of the particles are only due to Brownian motion, it is possible to calculate the viscosity of the sample, its dynamic moduli and also to get an estimation of the homogeneity of the sample. Some preliminary tests have been carried out on mixtures of PAA with P(VP-VI) at 0.5wt% and pH=5.5 but yielded poor results. The viscosity measured with MPT was much lower than the value obtained in shear. An explanation could be that particles are not homogeneously distributed within the sample and especially that they cannot penetrate aggregates present in the mixtures. Thus only the viscosity of the continuous low density phase is measured.

Small angle neutron scattering (SANS): neutron scattering is a powerful tool to get information about the organization at the microscopic level. Especially, if a periodic network is formed, a structure factor, related to the mesh-size should be visible on the scattering spectrum and a physical crosslinking density could be calculated.

To get a better understanding of the complexation phenomenon, the same system could be studied under different conditions, of ionic strength and temperature to start with. Other systems could also be considered. Based on the same chemistry, other copolymers of VP and VI, differing in their composition or molar mass could be studied. This could lead to an even finer control of the gelation with pH, since it should occur at a pH closer to 7 for PVI and possibly at a much lower pH for PVP. Indeed, some tests have shown that by mixing PAA and PVP at pH~3, phase separation occurs. No gelation was observed so far when the pH is increased, only a redissolution of the precipitate...

It is difficult to extrapolate to potential applications for mixtures of P(VP-VI) with PAA based polyanions, as no time, temperature or salt stability has been determined. However, the possibility to modify the rheology of a low viscosity commercial oil in water emulsion has been assessed by mixing such an emulsion (solids content is 23wt% and oil droplets average size is 17 μ m) with a 1:1 mixture of PAA with P(VP-VI) (noted PAA/P(VP-VI)). The emulsion and the already homogenized mixture PAA/P(VP-VI) are mixed in a 1:1 ratio in weight. Stock solutions of two PAA (PAA1600 and PAA3300) and P(VP-VI) at concentrations 2wt%, pH=6 and pH=7 have been used. Hence, the final concentration of both PAA and P(VP-VI) in the final mixtures with the emulsions is 1wt%. These final mixtures have been measured in static shear measurements (from 10^{-3} to 10^2 s $^{-1}$ in 10 minutes), using the same cone-plate geometry used in chapter 3 and 4.

In **Figure 6-7**, viscosity of the mixtures of PAA/P(VP-VI)+emulsion in which the concentration of polymer is 1wt% are shown respectively at pH=6 and pH=7 in the left-hand side graph and in the right-hand side graph. In these graphs, the viscosity of the pure emulsion, measured using a Couette geometry, is shown in black.

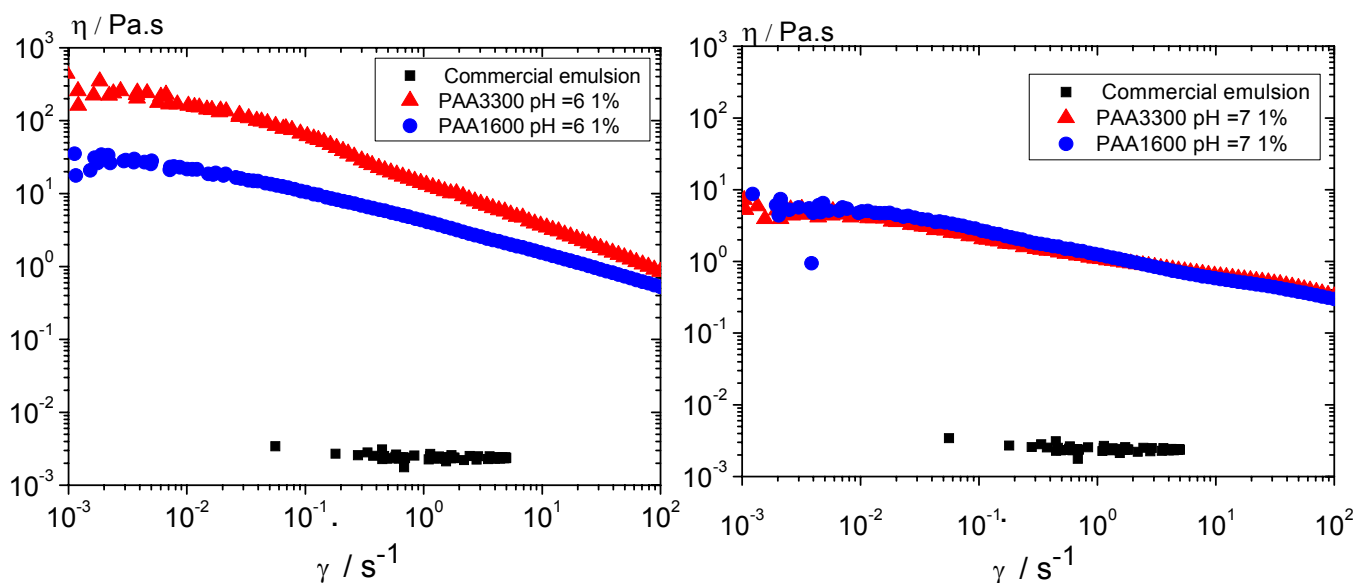


Figure 6-7: viscosity vs shear rate of mixtures of a commercial emulsion with PAA/P(VP-VI) at 1wt% depending on pH.

At both pH=6 and pH=7, the viscosity of the emulsion is dramatically increased by the addition of PAA/P(VP-VI).

At pH=7, PAA1600 and PAA3300 based complexes exhibit the same efficiency regarding viscosity enhancement: from $2 \cdot 10^{-3}$, the viscosity increases to almost 10 Pa.s. The shear thinning pattern is similar for both polymers.

At pH=6, the zero shear viscosity increases up to 30 Pa.s using PAA1600 based complexes and up to 200 Pa.s using PAA3300 based complex. Compared to the zero shear viscosity of the polyanion/polycation mixtures without the emulsion, which are close to 200 Pa.s and 350 Pa.s for the 2 polyanions respectively, a severe drop is recorded for PAA1600 due to the presence of the emulsion and only a minor drop for PAA3300. This observation is not explained yet but it seems that a higher molar mass PAA based complex/network is less disrupted by the presence of the o/w emulsion. It is important to note that all samples were stable over time and no phase separation was visible even after several weeks.

Mixtures of oppositely charged polyelectrolytes, especially when a high molar mass polyanion is used, seem to be promising systems to modify the rheology of simple waterborne formulations. How the presence of salt, pigments, other polymers will modify these preliminary results is amongst the next questions to be answered.

Summary

This PhD work deals with polyelectrolyte complexes under two very different regimes. First, I was able to show that, at low pH and at a concentration of 5wt%, it is possible to produce stable dispersions by copolymerizing [2-(acryloyloxy)ethyl] trimethylammonium chloride (AETAC) with acrylamide (AM) in the presence of a weak polyanion. The initial step was to determine suitable conditions (stirring, initiation, temperature etc) to synthesize this copolymer. Then, by systematically varying the amount of polyanion, a suitable ratio polycation/polyanion has been determined. This ratio cannot easily be translated into a charge ratio: the amount of positive charges is known precisely but the negative charge density depends on the pH and on the potential deprotonation induced by the presence of the polycation. However, it is clear that a large excess of positive charges is present in all systems exhibiting time stability.

Through TEM analysis it was found that the dispersion particles being mostly non-spherical and having an average particle diameter of 100nm to 1 μ m consist of primary particles of about 10nm diameter. When AETAC and AM are copolymerized in the presence of PAA stable dispersions were obtained in a given stoichiometric ratio and pH. It was found that increasing the AMPS content in the polyanion complexing agent allows to reduce the ratio of complexing agent vs. polycation which can be attributed to the permanent charge character of AMPS vs. AA. On the other hand all AMPS containing dispersions showed poor colloidal stability which is likely due to the fast (non-reversible) complexation of permanent polycations by AMPS containing copolymers.

To produce colloidal stable dispersions in an effective way, a balance has to be found between strong and weak charges.

In a second part, the rheology of mixtures of different polycations with PAA was investigated at (semi)dilute conditions in order to explore potential benefits e.g. as rheology modifiers. First, mixtures of a quarternary polycation with PAA were prepared. Due to significant hydrolysis of AETAC into choline chloride under the given pH conditions the more stable quaternary vinylimidazole containing polycations were chosen subsequently for PAA complexation. In this system, on the other hand, per strong charge interaction at low ionic strength precipitation phenomena dominate at pH>5.5. The most interesting system turned out to be the combination of PAA with P(VP-VI), i.e. the non-quaternized weak polycation. This polymer besides being

insensitive to hydrolysis has the additional advantage that its charge density can be tuned by varying the pH. When P(VP-VI) and PAA are mixed at pH=6 at different ratios, a strong viscosity increase is observed which is maximum at a weight ratio of 1:1. This specific mixture has been studied systematically varying the pH and concentration: small amplitude oscillatory measurements were carried out using a cone-plate rheometer and a longest shear relaxation time $\lambda_S \sim \omega_c^{-1}$ (with $(G' = G''(\omega_c))$) was estimated. For 1:1 mixtures of PAA with P(VP-VI) the general trend is an increase of the viscosity as the pH is decreased. At pH=7 and 8, this increase in viscosity does not depend on the concentration. On the contrary, at pH=5.5 and 6, the increase becomes more pronounced as the concentration is decreased. The increase in viscosity goes along with a modification of the dynamic rheology pattern.

- At pH=8 and 9, the terminal regime of viscoelastic fluids, in which $G' \sim \omega^2$ and $G'' \sim \omega$, is reached. The behavior of the mixtures and the pure polyanions at these pH is essentially the same.
- At pH=7, the terminal regime is on the verge of the frequency range investigated. ω_c is shifted towards lower values indicating a slowing down of the relaxation of the polymeric chains while the G' plateau modulus is almost constant indicating that the entanglement density is essentially not modified. The slower relaxation has been interpreted as an increase of the apparent molar mass of the polymer in solution, due to the bridging of long polyanions by short polycation chains, forming extended structures.
- At pH=5.5 and 6, the behavior depends strongly on the concentration. At 2wt%, ω_c is further shifted towards low frequencies, indicating that more chains are interconnected. As the concentration is lowered to 0.5wt%, the relaxation is further slowed down and the systems become gel-like, as G' and G'' are frequency independent, G' being one order of magnitude higher than G'' .

A similar study was carried out on 1:1 mixtures of PAA with PVP, a neutral polymer, and no viscosity enhancement was visible. VI is necessary to get an increase in viscosity as it results from the bridging of polymer chains due to electrostatic interactions between deprotonated AA and protonated VI. By assessing the charge ratio using Hendersen-Hasselbach equation, it was shown that the bridging is more efficient when the charge ratio approaches 1, which is also the ratio at which macroscopic phase separation occurs. Non-neutralized negative charges play an important role as they induce repulsive interactions within the formed structures and ensure their stability.

The same behavior is observed when P(AA_{0.8}-co-AMPS_{0.2}) and P(AA_{0.6}-co-AMPS_{0.4}) are mixed with P(VP-VI). The only discrepancy is that the viscosity enhancement is slightly more pronounced when more permanent charges are present in the polyanion, probably arising from stronger electrostatic interactions.

To get a better idea of potential applicability of the increase in viscosity observed under shear and also to get a better insight into the microstructure of the mixtures, a Capillary Break-up Extensional Rheometer (CaBER) has been used to study 1:1 PAA-P(VP-VI) mixtures. In this technique, a filament is formed and its decay pattern gives valuable information about the relaxation phenomena within the polymer solution. Provided that the decay of the filament follows an exponential law, an extensional relaxation time λ_E can be assessed with $D(t)/D_0 = \exp(-t/3\lambda_E)$. Again the pH and the concentration play a dramatic role on the filaments behavior.

- At pH=8, the behavior of the mixtures is similar to pure polyanions. The filament looks homogeneous and its diameter follows an exponential decay with time, behavior typical for solutions of entangled polymers.
- At pH=7, the decay of the filament still follows an exponential decay, but the filament lifetime, hence the extensional relaxation time is longer compared to pure polyanions.
- At pH=5.5 and pH=6, the filaments appear inhomogeneous and the decay pattern is hardly reproducible. It is controlled mainly by the presence of large aggregates present in the mixtures. Filament lifetime can be very long at 2wt% but decreases quickly with decreasing concentration.

Measurements under shear and extensional flow yield complementary data. At sufficiently low pH, both techniques show an increase in relaxation times, i.e. in apparent molar mass at high concentration. But at lower concentration, shear experiments show a transition towards gel-like structures while the filament lifetime under CaBER is extremely short. These “opposite” behavior indicate that the aggregates present in the mixtures overlap in the cone-plate geometry, thus “freezing” the system, while they are free to move one past the other in a thin matrix under extensional flow. The results depicted in this work results from the variety of structures present in the system when polyanions are mixed with P(VP-VI): free chains, bridged chains, bridged aggregates, free aggregates, swollen aggregates, which all account for the rheology of these systems. For example, the unusual gelation observed upon dilution is due to a modification of

the balance between aggregates and its surrounding media, which viscosity decreases sharply with decreasing concentration. Whether one or the other structure is preponderant depends essentially on the pH and concentration and can give rise to very different rheology, both under shear and extensional flow. This simple system, consisting only in the mixture of two readily available polymers, is a good example of a smart system.

Experimental part

1. Synthesis of polyanions, polycations and their in-situ complexation

For all synthesis of pure polyanions, pure polycations and for the in-situ formation of interpolyelectrolyte complexes (IPEC), a 1l glass reactor is used. This reactor is equipped with mechanical stirring (anchor type), nitrogen inlet and temperature sensor (cf. **Figure 7-1**). For efficient stirring, at least 150mL of product have to be synthesized per batch. Therefore, in each experiment, 300mL of polymer solution or dispersion are synthesized.



Figure 7-1: reactor used for the synthesis of polyanions, polycations and IPEC

The reagents which are used in the different synthesis described in chapter 2 are summarized in **Table 7-1**. All reagents are liquids except V50 which is a powder.

Table 7-1: reagents used for the synthesis of polyanions, polycations and IPEC

Reagent	Abbreviation	Provider	Purity (wt %)
Acrylic acid	AA	BASF	>99.9
2-acrylamido-2-methyl-1-propanesulfonic acid	AMPS	Aldrich	>99
Acrylamide	AM	Fluka	>99
[2-(Acryloyloxy)ethyl]trimethylammonium chloride	AETAC	BASF	>98
2,2'-azobis (2-amidinopropane) dihydrochloride	V50	Fluka	>99.9

1.1. Synthesis of polyanions

Initially, 250mL of water are placed in the reactor and heated up to 50°C under nitrogen bubbling for 30minutes. As explained in chapter 2, stirring speed is set at an optimal value of 150 rpm. Depending on which complexing agent is synthesized, the reactor is equipped with either 2 or 3 dropping funnels: one contains the initiator (V50) diluted in a small quantity of water, the other one(s), the monomer(s) (AA and AMPS) diluted in distilled water so that the concentration of the final solution is 10wt% and that the ratio of the copolymer is as wished (i.e. containing either 1/3 or 2/3 of AMPS). Feeding of all reagents is done dropwise over 2 hours. When feeding is over, reaction is continued for another 3 hours and the solution is then stored as obtained in polyethylene containers.

As an example, a typical recipe used to synthesize P(AA-co-AMPS) is given in **Table 7-2**.

Table 7-2: quantities of reagents used to synthesis P(AA_{0.66}-co-AMPS_{0.33})

Reagent	V50	AA	AMPS
Quantity (g)	0.135	23.76	34.15
Quantity (molar %)	0.1	66	33
Additional water in funnel (ml)	5	51	41

1.2. In-situ synthesis of inter-polyelectrolyte complexes

The reactor is the same as described in the first paragraph. 200mL of distilled water are placed in the reactor as initial charge, degassed with nitrogen and heated to 50°C. The reactor is equipped with a supplementary dropping funnel which contains the polyanion/complexing agent solution. The other 3 dropping funnels contain respectively V50, AETAC and AM. Feeding time is again 2 hours and reaction is carried out for another 3 hours to ensure full monomer conversion. The final dispersion (stable, sedimentating or phase separated) is stored as synthesized for further characterization.

1.3. Characterization

- **Solids content:** is measured with a Mettler Toledo HB43 halogen moisture analyser. Approximately 3 g of polymer solution or dispersion is placed on an aluminium plate and heated at 110°C until the variation of mass over a period of 30s is less than 0.1%. The sample is then considered to be dry. Provided that monomer fraction is small, the solids

content corresponds to the fraction of polymer in the sample. Generally, samples are homogenised i.e. shaken before measurements to prevent errors due to slow sedimentation. On the contrary, for analysis of supernatants, attention is paid on the fact that only the water-like part is analysed.

- **pH**: is measured using a Handylab 1 pH-meter (Schott Geräte). A glass electrode is used. The pH is measured at least 48h after the end of the reaction, so that slow complexation processes are essentially finished. Samples are homogenised before measurement, except supernatants.
- **Proton Nuclear Magnetic Resonance spectroscopy ($^1\text{H-NMR}$)**: is measured using a Bruker Avance 400 MHz NMR spectrometer. Prior to measurement, samples to be analyzed are dried either using Mettler Toledo HB43 or a vacuum oven. The quantity of solution/dispersion to be dried is calculated so that approximately 10mg of dry product is obtained. It is then diluted in approximately 1mL of D_2O and then analyzed.
- **Brookfield viscosity**: is measured using a Brookfield DV-III rheometer equipped with a spindle 06. Measurement is performed at least 48h after synthesis of the product. Only homogeneous products can be measured; supernatants are not viscous enough.
- **Field-Flow Fractionation (FFF)**: is used to assess the molar mass of synthesized polymers. First, pH is increased to 11 and 0.1 mol/L of NaNO_3 is added. The resulting solution is filtered through a $1.2\mu\text{m}$ cellulose membrane. The average molar mass (M_w , g/mol) of the prepared polymer is then determined using double detection. The first detector is a MALLS Wyatt DAWN EOS and the second detector is a Wyatt Optilab DSP refractometer. For full fractionation of the polyelectrolytes, a gentle crossflow of 0.2 ml/min is reduced linearly to zero towards the end of the 30min elution time, while maintaining the detector flow constant at 0.5 ml/min.
- **Cryo-Transmission Electronic Microscopy (cryo-TEM)**: is used to assess the size and morphology of the particles present in polymer dispersions. Dispersion is diluted to ~1 wt% with distilled water and then vitrified by plunging the thin liquid specimen into liquid ethane using a Vitrobot vitrification device. The micrographs are recorded on a Philips FEI CM120.

2. Rheological investigation of pure polyanions and polyelectrolyte mixtures

2.1. Materials

Polyanions

The polyanions are pure Poly(acrylic acid) (PAA) or copolymers of AMPS containing either 20 or 40 percent of permanent charges (i.e. 20 or 40 molar % of AMPS in the copolymer).

Poly(acrylic acid) is typically synthesized as described in the previous paragraph. The stock solutions have a concentration of 10 weight % and are diluted to the desired concentration with deionized water before being neutralized to the desired pH with 1N sodium hydroxide. Three different PAA are synthesized. Field Flow Fractionation at pH=11 and 1g.L⁻¹ yields average molecular weights of $M_w=1.6 \times 10^6$ g/mol (PAA1600), $M_w=3.3 \times 10^6$ g/mol (PAA3300) and $M_w=0.9 \times 10^6$ g/mol (PAA900).

Poly(AA_x-co-AMPS_{1-x}) is also synthesized as described in the previous chapter. The stock solutions have a concentration of 10 weight % and are diluted to the desired concentration with deionized water before being neutralized to the desired pH with 1N sodium hydroxide.

For Field Flow Fractionation at pH=11 and 1g.L⁻¹ yields average molecular weights of $M_w=1.8 \times 10^6$ g/mol and $M_w=1.7 \times 10^6$ g/mol respectively for P(AA_{0.8}-AMPS_{0.2}) and P(AA_{0.6}-co-AMPS_{0.4}).

Polycation

Poly(vinyl imidazole_{0.5}-co-vinyl pyrrolidone_{0.5}) is provided by BASF SE (Ludwigshafen Germany) as a 20 weight % solution in water and is diluted to the desired concentration with deionized water. Field Flow Fractionation at pH=11 and 1g.L⁻¹ yields and average molecular weight $M_w=1.5 \times 10^5$ g/mol.

Mixtures

Prior to the preparation of the mixtures which are to be measured, intermediate stock solutions of polyanions and polycations at different pH and concentrations are prepared. The total concentration of polymer in the mixtures is 2%, 1% or 0.5%. The pH of the diluted stock solutions is usually varied between 5.5 and 9.

The samples are prepared by slowly pouring a solution of the polycation into a solution of the polyanion. The concentration and pH of both solutions are equal to the desired final value. For example, to prepare a one to one in weight mixture of PAA1600 and P(VP-VI) with a final

concentration of 2wt%, 2g of PAA1600 at 2wt% and pH=7 are mixed with 2g of P(VP-VI) at 2wt%. After mixing, the samples are shaken vigorously for some seconds and left to equilibrate at room temperature for at least 48h. The homogeneous mixtures are then subjected to rheological measurements.

2.2. Methods

Cone-plate rheometers

In chapter 3 and 4, all the measurements are carried out using cone-plate geometry. Such a set-up has the double advantage that only little material is needed and that the range of viscosities which can be measured accurately is broad.

All rotational rheometers are built on the same principle: the sample to be measured is squeezed between a plate which is fixed and cone which can rotate (cf. **Figure 7-2**).

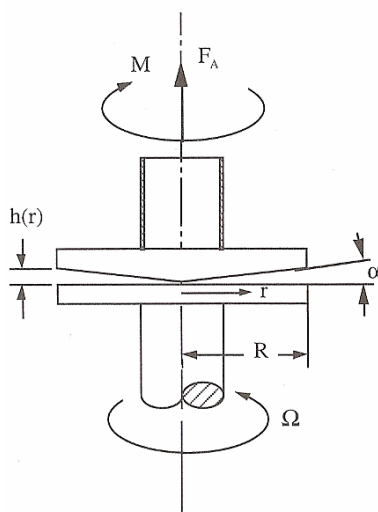


Figure 7-2: principle of a cone-plate rheometer

Relevant parameters, identical for all measurements carried out, are:

- Angle of the cone $\alpha=1^\circ$
- Radius of the cone $R=6\text{cm}$
- Gap between the upper and lower plate, depending on r

$$h(r) = r \cdot \tan\alpha \approx r \cdot \alpha$$

In the middle of the plates, the gap is $45\mu\text{m}$ for all measurements.

A rotational rheometer MARS (Modular Advanced Rheometer System) (Thermo Fischer Scientific) equipped with the cone-plate fixture described above is used to perform small amplitude oscillatory shear experiments.

Measurements are typically carried out as follows. Approximately 1 mL of equilibrated sample is placed carefully on the lower plate, paying attention that no air bubble is trapped and that filling is sufficient when the upper plate is brought down. Prior to the actual measurement, the “history” of the sample is erased by applying steady shear at 1 s^{-1} for 2 minutes and leaving the sample to rest for 3 minutes. Then the dynamic measurement is performed starting from high frequency to low frequency. Controlled Stress (CS) is used, the value of the stress depending on the viscosity of the measured sample. For measurements lasting more than 3 hours, the sample is isolated from its surrounding medium to minimize evaporation.

Oscillatory squeeze flow

Oscillatory squeeze flow experiments were performed using a piezo-driven axial vibrator (Crassous et al. 2005, Kirschenmann 2003) customized at the Institute for Dynamic Material Testing (Ulm, Germany). The instrument operates at constant force amplitude and from the ratio of the dynamic displacement of the lower plate (amplitude $\sim 5\text{ nm}$) with and without fluid the complex squeeze stiffness K^* of the fluid is obtained which is directly related to the complex shear modulus G^* (Kirschenmann 2003):

$$K^* = \frac{3\pi R^4}{2d^3} G^* / \left(1 + \frac{\rho\omega^2 d^2}{10G^*} + \dots\right) \quad (1)$$

where ρ is the fluid density, R (here 10 mm) is the radius and d is the height of the gap. The determination of G^* strongly depends on the exact knowledge of d , which is determined by calibration using Newtonian liquids with viscosities between 10^{-3} and 2 Pa.s. Gap height is 50 μm . Moduli G' or G'' in the range from 0.1 Pa to 10 kPa are accessible with this set-up at frequencies between 1 Hz and 10 kHz.

Capillary Break-up Extensional Rheology

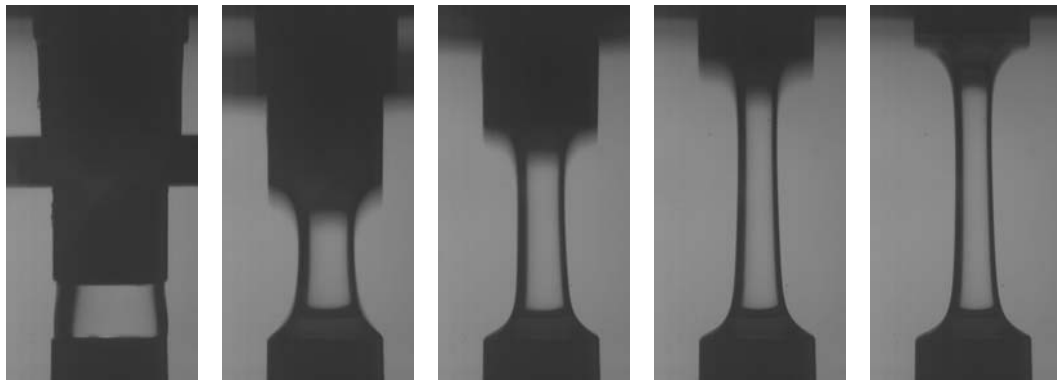


Figure 7-3: formation of a filament in a CaBER experiment

In a CaBER experiment, a fluid drop is placed between two plates and subsequently exposed to an extensional step strain thus forming a liquid filament. As an example, in **Figure 7-3**, the formation of a filament using a drop of pure PAA at 2wt% is shown; the 5 pictures correspond to initial set-up, $t=10\text{ms}$ (after separation of the plates), $t=20\text{ms}$, $t=30\text{ms}$, $t=40\text{ms}$ and $t=50\text{ms}$ (also referred to as t_0). A CaBER 1 (Thermo Electron) extensional rheometer is used with plates diameter $d_c = 6\text{ mm}$. The sample droplet is filled in a reproducible way, trying to avoid the presence of air bubbles. After filling, the sample is left to rest for 2 minutes. Plate separation time is 40ms. The gap is varied from $L_{\text{initial}} = 4\text{ mm}$ to $L_{\text{final}} = 16\text{ mm}$. This choice of parameters ensures that the initial filament diameter directly after plate separation (t_0) is always around 1.5 to 2 mm.

The decay of the filament is recorded using a CCD-camera and the diameter of the filament versus time in the middle of the gap (i.e. approximately in the middle of the filament) is assessed. The measurement stops after breaking of the filament.

References

- Agarwal, S.; Gupta, R.K., *Rheol Acta*, **2002**, 45, p.456-460.
- Akiyoshi, K.; Nagai, K.; Nishikawa, T.; Sunamoto, J., *Chem. Lett.*, **1992**, 21(9), p.1727-1730.
- Alberts; Bray; Johnson; Lewis; Raff; Roberts; Walter, *Essential cell biology*, Garland Publishing, USA, **1998**.
- Almgren, M.; Hansson, P.; Mukhtar, E.; van Stam, J., *Langmuir*, **1992**, 23, p.2405 - 2412.
- Anna, S.; McKinley, G.H., *J. Rheol.*, **2001**, 45, p.115-138.
- Annable, T.; Buscall, R.; Ettelaie, R.; Whittlestone, D., *Journal of Rheology*, **1993**, 37(4), p.695-726.
- Anthony, O.; Zana. R., *Langmuir*, **1996**, 12, p.1967 - 1975.
- Arguelles-Monal, W.; Perez-Gramatges, A.; Peniche-Covas, C.; Desbrieres, J.; Rinaudo, M., *European Polymer Journal*, **1998**, 34(5/6), p.809-814.
- Arslan, A.; Kiralp, S.; Toppare, L.; Bozkurt, A., *Langmuir*, **2006**, 22(6), p.2912-2915.
- Aubry, T.; Moan, M., *J. Rheol.*, **1994**, 38(6), p.1681-1692.
- Ballauff, M., *Macromol. Chem. Phys.*, **2003**, 204, p.220.
- Baranovsky, V.Y.; Kazarin, L.A.; Litmanovich, A.A.; Papisov, I.M., *Eur. Polym. J.*, **1984**, 20, p.191.
- Bazilevskii, A.V.; Entov, V.M.; Rozhkov, A.N., *Polym. Sci.*, **2001**, 43, p.716-726.
- Berth, G.; Voigt, A.; Dautzenberg, H.; Donath, E.; Mohwald, H., *Biomacromolecules*, **2002**, 3(3), p.579-90.
- Bevington, J.C, *Radical Polymerization*, Academic Press, New York, **1961**.
- Bhatia, S.R.; Mourchid, A.; Joanicot, M., *Curr. Opin. Colloid Interface Sci.*, **2001**, 6, p.471.
- Bixler, H.J.; Michaels, A.S., *Encycl. Polym. Sci. Technol.*, **1969**, 10, p.765-80.
- Blumstein, A.; Kakivaya, S., *Polymerization of organized systems*, Gordon and Breach, New York, **1977**.
- Bock, J.; Siano, D.B.; Valint Jr., P. L.; Pace, S. J., *Polymers in aqueous media*, Glass, J. E., Ed.; American Chemical Society: Washington DC, Vol. 223, **1989**.
- Bossard, F.; Tsitsilianis, C.; Yannopoulos, S.N.; Petekidis, G.; Sfika, V., *Macromolecules*, **2005**, 38, p.2883-2888.

- Boussif, O.; Lezoualch, F.; Zanta, M.A.; Mergny, M.D.; Scherman, D.; Demeneix, B.; Behr, J.P., *Proc. Natl. Acad. Sci. U. S. A.*, **1995**, 92, p.7297–7301.
- Braun, D.B.; Rosen, M.R., *Rheology Modifiers Handbook, Practical Use & Application*, William Andrew Publishing, Norwich, NY, US, **2000**.
- Bungenberg de Jong, H.G.; Dekker, W.A.L., *Kolloidbehefte*, **1936**, 43, p.143-212.
- Cabane, B.; Duplessix, R., *J. Phys.*, **1987**, 48, p.651.
- Cabestany, J.; Trouve, C. FR 2471391 19810619 **1981**.
- Cameron, N. S.; Corbierre, M. K.; Eisenberg, A., *Can. J. Chem.*, **1999**, 77, p.1311
- Cerrai, P.; Guerra, G.D.; Maltini, S.; Tricoli, M., *Macromol. Rapid. Commun.*, **1994**, 15, p.983.
- Cerrai, P.; Guerra, G.D.; Maltini, S.; Tricoli, M.; Barbani, N.; Petarca, L., *Macromol. Chem. Phys.*, **1996**, 1, p.197.
- Chanana, M.; Gliozzi, A.; Diaspro, A.; Chodnevskaja, I.; Huewel, S.; Moskalenko, V.; Ulrichs, K.; Galla, H.-J.; Krol, S., *Nano Letters*, **2005**, 5(12), p.2605-2612.
- Chodanowski, P., Stoll, S., *Macromolecules*, **2001**, 34, p.2320-2328.
- Choi, Y.H.; Liu, F.; Kim, J.S.; Choi, Y.K.; Park, J.S.; Kim, S.W., *J. Control. Release*, **1998**, 54, p.39-48.
- Colby, R.H.; Rubinstein, M.; Daoud, M., *J. Phys*, **1994**, 4(8), p.1299-1310.
- Cousin, F.; Gummel, J.; Ung, D.; Boue, F., *Langmuir*, **2005**, 21(21), p.9675-9688.
- Crassous, J.J.; Régisser, R.; Ballauff, M.; Willenbacher, N., *J. Rheol.*, **2005**, 49, p.851-863.
- Dai, S.; Tam, K. C.; Jenkins, R. D., *Macromolecular Chemistry and Physics*, **2001**, 202(2), p.335-342.
- Dautzenberg, H.; Jaeger, W.; Kotz, J.; Philipp, B.; Stscherbina, D., *Characterization and Application*, **1994**, 343p.
- Dautzenberg, H.; Rother, G., *J. Polym. Sci.*, **1988**, Part B, 76, p.353.
- Dautzenberg, H.; Rother, G.; Linow, K. J.; Philipp, B., *Acta Polym.*, **1988**, 39 (4), p.157.
- Decher, G., *Science*, **1997**, 277(5330), p.1232-1237.
- Demeneix, B.; Behr, J.; Boussif, O.; Zanta, M.A.; Abdallah, B.; Remy, J., *Adv. Drug Deliv. Rev.*, **1998**, 30, p.85–95.
- Desbrières, J.; Rinaudo, M.; Chtcheglova, L., *Macromol. Symp.*, **1997**, 113, p. 135-149.
- Dexter, R.W., *Atomization and Sprays*, **1996**, 6, p.167-191.

- Diaspro, A.; Silvano, D.; Krol, S.; Cavalleri, O.; Gliozzi, A., *Langmuir*, **2002**, 18, p.5047.
- Dole, M., *The radiation Chemistry of Macromolecules*, Academic Press, New York, **1972**.
- Donath, E.; Sukhorukov, G.B.; Caruso, F.; Davis, S.A.; Mohwald, H., *Angew. Chem.*, **1998**, 37, p.2202.
- Duhamel, J.; Yekta, A.; Hu, Y.Z.; Winnik, M.A., *Macromolecules*, **1992**, 25(25), p.7024-7030.
- Entov, V.M.; Hinch, E.J., *J. Non-Newtonian Fluid Mech.*, **1997**, 72, p.31-53.
- Euranto, E.K., *Chem. Carboxylic Acids Esters*, Esterification and ester hydrolysis, Univ. Turku, Turku, Finland, **1969**.
- Ferguson J.; Alawi S.A.; Granmayeh R., *Eur. Polym. J.*, **1983**, 19, p.475.
- Fernando, R.H.; Xing, L.L.; Glass, J.E., *Progress in Organic Coatings*, **2000**, 40, p.35-38.
- Ferrari, S.; Moro, E.; Pettenazzo, A.; Behr, J.P.; Zacchello, F.; Scarpa, M., *Gene Ther.*, **1997**, 4, p.1100–1106.
- Fuoss R.M.; Sadek, H., *Sciences*, **1949**, 110, p.552-554.
- Gelman, R. A., *International dissolving Pulps Conference*, TAPPI, Ed. Geneva, **1987**.
- Glass, E.J., *Coatings Technology*, **2001**, 73, p.79-98.
- Gonzalez G.G.; Kreft, T.; Alb, A.M.; de la Cal, J.C.; Asua, J.M.; Reed, W.F., *Journal of Physical Chemistry*, **2009**.
- Goula, D.; Remy, J.S.; Erbacher, P.; Wasowicz, M.; Levi, G.; Abdallah, B.; Demeneix, B.A., *Gene Ther.*, **1998**, 5, p.712–717.
- Griebel, T.; Kulicke, W.M., *Makromolekulare Chemie*, Molecular characterization of water-soluble, cationic polyelectrolytes, 193(3), **1992**.
- Gummel, J.; Boue, F.; Deme, B.; Cousin, F., *The journal of physical chemistry. B*, **2006**, 110(49), p.24837-46.
- Gummel, J.; Cousin F.; Verbavatz, J.-M.; Boue, F., *The journal of physical chemistry. B*, **2007**, 111(29), p.8540-6.
- Gummel, J.; Cousin, F.; Boue, F., *Macromolecules*, **2008**, 41(8), p.2898-2907.
- Hansson, P.; Almgren, M., *J. Phys. Chem.*, **1995**, 99, p.16694-16703.
- Hansson, P.; Almgren, M., *Langmuir*, **1994**, 10, p.2115-2124.
- Harada-Shiba, M.; Yamauchi, K.; Harada, A.; Takamisawa, I.; Shimokado, K.; Kataoka, K., *Gene Ther.*, **2002**, 9, p.407-414.
- Hill, A.; Candau, F.; Selb, J., *Progress in Colloid & Polymer Science*, **1991**, 84(5), p.61-65.

- Hu, Y.Z.; Zhao, C.L.; Winnik, M.A.; Sundararajan, P.R., *Langmuir*, **1990**, 6(4), p.880-883.
- Hwang, F.S.; Hogen-Esch, T.E., *Macromolecules*, **1995**, 28(9), p.3328-3335.
- Ito, T., *J. Polym. Sci.*, **1966**, Part B, 4, p.81
- Jenkins, R.D.; Sinha, B.R.; Bassett, D.R., *Polymeric Materials Science and Engineering*, **1991**, 65, p.72-73.
- Jiang, X.; Hammond, P.T., *Langmuir*, **2000**, 16, p.8501.
- Jimbo, T.; Ramirez, P.; Tanioka, A.; Mafe, S.; Minoura, N., *Journal of Colloid and Interface Science*, **2000**, 225(2), p.447-454.
- Kabanov, V.A.; Kargina, O.V.; Mishustina, L.A.; Lubov, S.Y.; Kaluzunski, K.; Penczek, S., *Makromol. Chem. Rapid. Commun.*, **1981**, 2, p.343.
- Kabanov, V.A.; Zezin, A.B., *Pure Appl. Chem.*, **1984**, 56, 3, p.343-354.
- Kästner, U.; Hoffmann, H.; Dönges, R.; Ehrler, R., *Colloid Surface A*, **1994**, 82(3), p.279-297.
- Katsampas, I.; Tsitsilianis, C., *Macromolecules*, **2005**, 38, p.1307.
- Kennedy, J.C.; Meadows, J.; Williams, P., *J. Chem. Soc. Faraday Trans.*, **1995**, 91, p.911-916.
- Khutoryanskiy, V.V.; Nurkeeva, Z.S.; Mun, G.A.; Sergaziyev, A.D.; Ryskalieva, Z.; Rosiak, J.M., *European Polymer Journal*, **2003**, 39(4), p.761-766.
- Khutoryanskiy, V.V.; Dubolazov, A.V.; Nurkeeva, Z.S.; Mun, G.A., *Langmuir*, **2004**, 20(9), p.3785-3790.
- Khutoryanskiy, V.V.; Nurkeeva, Z.S.; Mun, G.A.; Dubolazov, A.V., *Journal of Applied Polymer Science*, **2004**, 93(4), p.1946-1950.
- Kikushi Y.; Kubota N., *Makromol. Chem.*, **1985**, p.387-390.
- Kirschenmann, L., *PhD Thesis Institut für Dynamische Materialprüfung*, University of Ulm, **2003**.
- Koetz, J.; Kosmella, S.; Beitz, T., *Prog. polym. sci.*, **2001**, 26, p.1199-1232.
- Koetz, J.; Kunze, J.; Linow, K. J.; Phillipp, B., *Polymer Bulletin*, **1986**, 15(3), p.247-52.
- Kohler, K.; Shchukin, D.G.; Mohwald, H.; Sukhorukov, G.B., *The journal of physical chemistry. B*, **2005**, 109(39), p.18250-9.
- Konop, A.J.; Colby, R.H., *Macromolecules*, **1999**, 32(8), p.2803-2805.
- Korobko, A.V.; Jesse, W.; Lapp, A.; Egelhaaf, S.U.; van der Maarel, J.R.C., *J. Chem. Phys.*, **2005**, 122, p.24902.
- Kossel, A., *The Protamines and Histones*, Longmans Green and co, London, **1928**.

- Kriz, J.; Dautzenberg, H., *Journal of Physical Chemistry A*, **2001**, 105(15), p.3846-3854.
- Kunze, K.K.; Netz, R.R., *Phys. Rev. Lett.*, **2000**, 85, p.4389.
- Landoll, L.M., US 4352916 A 19821005, **1982**.
- Lau, C.; Mi, Y., *Polymer*, **2001**, 43(3), p.823-829.
- Lee, M.K.; Chun, S.K.; Choi, W.J.; Kim, J.K.; Choi, S.H.; Kim, A.; Oungbho, K.; Park, J.S.; Ahn, W.S.; Kim, C.K., *Biomaterials*, **2005**, 26, p.2147–2156.
- Limbach, H.J.; Holm, C., *Journal of Chemical Physics*, **2001**, 114(21), p.9674-9682.
- Liu, R.C.W.; Morishima, Y.; Winnik, F.M., *Macromolecules*, **2001**, 34(26), p.9117-9124.
- Liu, R.C.W.; Morishima, Y.; Winnik, F.M., *Macromolecules*, **2003**, 36(13), p.4967-4975.
- Liua, X.; Howarda, K.A.; Donga, M.; Andersena, M.O.; Rahbeka, U.L.; Johnsen, M.G.; Hansenc, O.C.; Besenbachera, F.; Kjems, J., *Biomaterials*, **2007**, 28, p.1280–1288.
- Loesche, M.; Schmitt, J.; Decher, G.; Bouwman, W.G.; Kjaer, K., *Macromolecules*, **1998**, 31(25), p.8893-8906.
- Mafe, S.; Garcia-Morales, V.; Ramirez, P., *Chemical Physics*, **2004**, 296(1), p.29-35.
- Mageli, O.L.; Kolcynski, J.R., *Encyclopedia of polymer science and Technology*, Vol.9, "Peroxy compounds", Wiley Interscience, New York, **1968**.
- McCormick, C.L.; Nonaka, T.; Johnson, C.B., *Polymer*, **1988**, 29(4), p. 731-739.
- McKinley, G.H.; Tripathi, A., *J. Rheol.*, **2000**, 44, p.653-670.
- Mende, Mandy; Petzold, Gudrun; Buchhammer, Heide-Marie., *Colloid and Polymer Science*, **2002**, 280(4), p.342-351.
- Meyer, K.; Palmer, J.W., *Journal of Biological Chemistry*, **1934**, 107, p.629-34.
- Michaels A.S.; Mir L.; Schneider N.S., *J. Phys. Chem.*, **1961**, 65, 10, p.1765-1773.
- Michaels, A.S.; Miekka, R.G., *Journal of Physical Chemistry*, **1961**, 65, p.1765-73.
- Michaels, A.S., *Journal of Industrial and Engineering Chemistry*, **1965**, 57(10), p.32-40.
- Michaels, A. S.; Bixler, H. J., *Encyclopedia of Chemical Technology*, Polyelectrolyte complexes, 2nd Edition, 16, Kirk-Othmer, **1968**.
- Moriguchi, R.; Kogure, K.; Akita, H.; Futaki, S.; Miyagishi, M.; Taira, K.; Harashima, H., *Int. J. Pharm.*, **2005**, 301, p.277–285.
- Nakajima, A.; Sato, H., *Biopolymers*, **1972**, 10, p.1345.

- Netz, R.R.; Joanny, J.-F., *Macromolecules*, **1999**, 32, p.9026.
- Ng, S.L.; Mun, R.P.; Boger, D.V.; James, D.F., *J. Non-Newtonian Fluid Mech.*, **1996**, 65, p.291-298.
- O'Driscoll, K.F., *Structure and Mechanism in Vinyl Polymerization*, Initiation in Free Radical Polymerization, Chapter 3, Marcel Dekker, New York, **1969**.
- Oliveira, M.S.N.; Yeh, R.; McKinley, G.H., *J. Non-Newtonian Fluid Mech.*, **2006**, 137, p.137-148.
- Oupicky, D.; Konak, C.; Ulbrich, K.; Wolfert, M.A.; Seymour, L.W., *J. Control. Release*, **2000**, 65, p.149-171.
- Patnaik, S.; Aggarwal, A.; Nimesh, S.; Goel, A.; Ganguli, M.; Saini, N.; Singh, Y.; Gupta, K.C., *J. Control. Release*, **2006**, 114, p. 398–409.
- Philipp, B.; Dautzenberg, H.; Linow, K.; Koetz, J.; Dawydoff, W., *Pro. Polym. Sci.*, **1989**, Vol.14, p.91-172.
- Plog, J.P.; Kulicke, W.M.; Clasen, C., *Appl. Rheol.*, **2005**, 15, p.28-37.
- Polowinski, S., *The Encyclopedia of Advanced Materials*, Oxford: Pergamon Press, **1994**.
- Polowinski, S., *Template Polymerization*, Toronto-Scarborough: Chem-Tec Pub, **1997**.
- Polowinski, S., *Progress in Polymer Science*, **2002**, 27(3), p.537-577.
- Rempp, P.; Merrill, E.W., *Polymer Synthesis*, Chap. 4, Huethig & Wepf Vlg., Basel, Heidelberg, New York, **1986**.
- Rio, F.; Jose, R.; Ochoa, G.; Sasia, P.M.; Escudero, F.J.; Diaz de Apodaca, E.; Nieto, J.; Katime, I., *e-Polymers*, **2007**.
- Rmaile, H.H.; Schlenoff, J.B., *Polymeric Materials Science and Engineering*, **2001**, 84, p.678-679.
- Rmaile, H.H.; Schlenoff, J.B., *Langmuir*, **2002**, 18(22), p.8263-8265.
- Roberts, G.A.F., *The Macmillan Press*, Chitin chemistry, Basingstoke, Great Britain, **1992**.
- Romoren, K.; Thu, B.J.; Bols, N.C.; Evensen, O., *Biochim. Biophys. Acta*, **2004**, 1663, p.127–134.
- Semenov, A.N.; Joanny, J.F.; Khokhlov, A.R., *Macromolecules*, **1995**, 28, p.1066.
- Semenov, A.N.; Nykrova, I.A.; Khokhlov, A.R., *Macromolecules*, **1995**, 28, p.7491.
- Seng, W.P.; Tam, K.C.; Jenkins, R.D.; Bassett, D.R., *Langmuir*, **2000**, 16(5), p.2151-2156.
- Sfika, V.; Tsitsilianis, C., *Macromolecules*, **2003**, 36, p.4983-4988.
- Shu, X.Z.; Zhu, K.J., *Eur. J. Pharm. Biopharm.*, **2002**, 54, p.235–243.

- Siddiq, M.; Tam, K.C.; Jenkins, R.D., *Colloid Polym. Sci.*, **1999**, 277, p.1172-1178.
- Sinquin, A.; Hubert, P.; Dellacherie, E., *Langmuir*, **1993**, 9(12), p.3334-3337.
- Solomon, M.J.; Muller, S.J., *J. Rheol.*, **1996**, 40, p.837-856.
- Stelter, M.; Brenn, G.; Yarin, A.L.; Singh, R.P.; Durst, F., *J. Rheol.*, **2002**, 46, p.507-527.
- Strauss, U.P., *Polymers in aqueous media*, Vol. 223, Glass, J. E., Ed., American Chemical Society, Washington, **1989**.
- Szwarc, M., *J. Polym. Sci.*, **1954**, 13, p.317.
- Tam, K.C.; Farmer, M.L.; Jenkins, R.D.; Bassett, D.R., *J. Polym. Sci. B: Polym. Phys.*, **1998**, 36, p.2275-2290.
- Tam, K.C.; Jenkins, R.D.; Winnik, M.A.; Bassett, D.R., *Macromolecules*, **1998**, 31(13), p.4149-4159.
- Tam, K.C.; Seng, W.P.; Jenkins, R.D.; Bassett, D.R., *Journal of Polymer Science, Part B: Polymer Physics*, **2000**, 38(15), p.2019-2032.
- Tan, H.; Tam, K.C.; Jenkins, R.D., *Journal of Applied Polymer Science*, **2001**, 79(8), p.1486-1496.
- Tan, H.; Tam, K.C.; Tirtaamadja, V.; Jenkins, R.D.; Bassett, D.R., *J. Non-Newtonian Fluid Mech.*, **2000**, 92, p.167-185.
- Tan, Y.Y., *Comprehensive polymer science*, **1989**, vol.3, p.245.
- Tan, Y.Y.; Challa, G., *Macromol Chem Macromol Symp*, **1987**, 10/11, p.215.
- Tanaka, F.; Edwards, S. F., *J. Non-Newtonian Fluids Mech.*, **1992**, 43, p.247.
- Tan, Y.Y., *Prog. Polym. Sci.*, **1994**, vol.3, 19, p.561.
- Tanaka, R.; Meadows, J.; Phillips, G.O.; Williams, P. A., *Carbohydrate Polymers*, **1990**, 12, p.443-459.
- Thuenemann, A.F.; Mueller, M.; Dautzenberg, H.; Joanny, J.-F.; Loewen, H., *Advances in Polymer Science*, **2004**, 166, p.113-171.
- Thuresson, K.; Karlström, G.; Lindman, B., *J. Phys. Chem.*, **1995**, 99, p.3823-3831.
- Tirrell, D.A., *Comprehensive Polymer Science*, Vol. 3, Part I, Chap. 15, Eastmond, G. C., Ledwith, A., Russo, S., Sigwalt, P. (Ed.s), Pergamon Press, Oxford, **1989**.
- Tong, W.; Dong, W.; Gao, C.; Mohwald, H., *Macromolecular Chemistry and Physics*, **2005**, 206(17), p.1784-1790.
- Tsitsilianis, C.; Iliopoulos, I.; Ducouret, G., *Macromolecules*, **2000**, 33, p.2936.
- Tsitsilianis, C.; Katsampas, I.; Sfika, V., *Macromolecules*, **2000**, 33, p.9054.

- Tsitsilianis, C.; Iliopoulos, I., *Macromolecule*, **2002**, 35, p.3662.
- Tsuchida E., Abe K., *Interaction between macromolecules in solution and intermacromolecular complexes*, Springer-Verlag, **1982**.
- Tsuchida, E.; Osada, Y.; Sanada, K. J., *Polym. Sci.*, **1972**, 10, p.3397.
- Tsuchida, E., *Makromol. Chem.*, **1974**, 175, p.603-611.
- Tsuchida, E.; Osada, Y., *J. Polym. Sci.*, **1975**, 13, p.559.
- Tsuchida, E.; Abe, K.; Honma, M., *Macromolecules*, **1976**, vol.9, No 1.
- Tsuchida E., *Pure Appl.Chem.*, **1994**, A31(1), p.1-15.
- Tsuruta, T., *Makromol. Chem.*, **1978**, 179, p.1121.
- Tsutsumi, T.; Hirayama, F.; Uekama, K.; Arima, H., *J. Control. Release*, **2007**, 119, p.349–359.
- Tuladhar, T.R.; Mackley, M.R., *Filament stretching rheometry and break-up behavior of low viscosity polymer solutions and inkjet fluids*, Submitted to J NNFM, **2007**.
- Uemura, Y.; McNulty, J.; Macdonald, P.M., *Macromolecules*, **1995**, 28(12), p. 4150-4158.
- Vollmert, B., *Grundriss der Makromolekularen Chemie*, Vol. I, E. Vollmert Vlg, Karlsruhe, **1988**.
- Volodkin, D.; Mohwald, H.; Voegel, J.-C.; Ball, V., *Journal of Controlled Release*, **2007**, 117(1), p.111-120.
- Wallin, T.; Linse, P., *Langmuir*, **1996**, 12, p.305-314.
- Wang, Y.; Winnik, M.A., *Langmuir*, **1990**, 6, p.1437.
- Xie, X.; Hogen-Esch, T.E., *Macromolecules*, **1996**, 29(5), p.1734-1745.
- Yekta, A.; Duhamel, J.; Adiwidjaja, H.; Brochard, P.; Winnik, M.A., *Langmuir*, **1993**,9(4), p.881-883.
- Yekta, A.; Xu, B.; Duhamel, J.; Adiwidjaja, H.; Winnik, M.A, *Macromolecules*, **1995**, 28, p.956.
- Yesilata, B.; Clasen, C.; McKinley, G.H., *J. Non-Newtonian Fluid Mech.*, **2006**, 133, p.73-90.
- Zand, R., *Encyclopedia of polymer science and Technology*, Vol.2, "Azo catalyst", Wiley Interscience, New York, **1965**.
- Zhang, L.F.; Eisenberg, A., *Science*, **1995**, 268, p.1728.

Acknowledgments

First, I would like to express my sincere gratitude to my Doktorvater, Prof. Dr. Norbert Willenbacher, for his support, help and guidance during these four years. It has been a wonderful, enriching experience.

In Karlsruhe, I would also like to express my thanks to Dr. Bernhard Hochstein, Beate Oremek and Dietmar Paul for all the technical and administrative support.

Special thanks also to (random order) Michael for IT and MARS support, Oliver and Katarzyna for CaBER discussions (it looks a lot more fancy now), Claude for MPT trials (and summary of Champions League matches on Thursday morning) and all the other group members. The atmosphere was great throughout the years thanks to them.

In Strasbourg, I am indebted to Dr. Volker Schaedler who offered lab-space, office-space, funding, enthusiasm and all the support I asked for or needed. Thanks also for the careful reading of this manuscript.

I would also like to thank Dr. Thomas Breiner for his help during the last part of my PhD (not the easiest one). J'espère que tu te plais en France!

Thanks also to Dr. Esteban Aramendia, Dr. Xinyuan Zhu, Dr. SuNee Tan and Dr. Michel Awkal with whom I collaborated and from whom I learned a lot, about science and life.

In Ludwigshafen, I would like to thank all GKD members for input and feedback on this work; Dr. Horst Schuch and Dr. Wendel Wohlleben for the field flow fractionation measurements; Dr. Thomas Frechen for the cryo-TEM measurements.

BASF SE for financial support.

Enfin, je voudrais remercier toute ma famille. Mes grand-parents qui ne sont plus là (Roger, Alfred, Yvonne et Charlotte que je n'ai pas connue), qui je pense auraient été fiers de moi ainsi que Marie-Ina, qui je le sais est fière de son petit-fils.

Mes parents, qui m'ont toujours encouragé et m'ont enseigné la valeur du travail et de l'instruction : ils m'ont permis d'être la personne que je suis aujourd'hui. Et enfin Rébecca, pour sa présence, sa patience et son soutien permanent.

MERCI à tous !!!

Curriculum Vitae

Personal Data

Name	Yves Matter
Date of birth	12. January 1979
Place of birth	Strasbourg, France
Nationality	French

Undergraduate studies

1985-1997	Primary School in Illkirch, France High school “Les Pontonniers” in Strasbourg, France Baccalauréat, 7 July 1997
9 / 1997-7 / 2000	Classe Préparatoire aux Grandes Ecoles, Lycée Kléber, Strasbourg
9 / 2000-8 / 2003	Ecole Européenne de Chimie, Polymères et Matériaux, Strasbourg, major in Chemistry
10 / 2003	Diplôme d’Ingénieur in Chemistry, specialized in Polymer Science
9 / 2003-9 / 2004	Master degree in Material Science (Techniques d’Elaboration et de Caractérisation de Matériaux en Couches Minces) at “Université Louis Pasteur”, Strasbourg

Graduate studies

1 / 2005- 03 / 2008	PhD at the Institut für Mechanische Verfahrenstechnik und Mechanik der Universität Karlsruhe (TH), Germany, under the supervision of Prof. Dr. Norbert Willenbacher untitled: „Towards new thickeners based on inter-polyelectrolyte complexes“
---------------------	---